frontiers | Research Topics

Greenhouse gas emissions and mitigation: Microbes, mechanisms and modeling

Edited by
Baoli Zhu, Yong Li, Zengming Chen,
Hangwei Hu and Adrian-Stefan Andrei

Published in
Frontiers in Microbiology

ISSN 1664-8714
ISBN 978-2-8325-4967-4
DOI 10.3389/978-2-8325-4967-4

About Frontiers

Frontiers is more than just an open access publisher of scholarly articles: it is a pioneering approach to the world of academia, radically improving the way scholarly research is managed. The grand vision of Frontiers is a world where all people have an equal opportunity to seek, share and generate knowledge. Frontiers provides immediate and permanent online open access to all its publications, but this alone is not enough to realize our grand goals.

Frontiers journal series

The Frontiers journal series is a multi-tier and interdisciplinary set of open-access, online journals, promising a paradigm shift from the current review, selection and dissemination processes in academic publishing. All Frontiers journals are driven by researchers for researchers; therefore, they constitute a service to the scholarly community. At the same time, the *Frontiers journal series* operates on a revolutionary invention, the tiered publishing system, initially addressing specific communities of scholars, and gradually climbing up to broader public understanding, thus serving the interests of the lay society, too.

Dedication to quality

Each Frontiers article is a landmark of the highest quality, thanks to genuinely collaborative interactions between authors and review editors, who include some of the world's best academicians. Research must be certified by peers before entering a stream of knowledge that may eventually reach the public - and shape society; therefore, Frontiers only applies the most rigorous and unbiased reviews. Frontiers revolutionizes research publishing by freely delivering the most outstanding research, evaluated with no bias from both the academic and social point of view. By applying the most advanced information technologies, Frontiers is catapulting scholarly publishing into a new generation.

What are Frontiers Research Topics?

Frontiers Research Topics are very popular trademarks of the *Frontiers journals series*: they are collections of at least ten articles, all centered on a particular subject. With their unique mix of varied contributions from Original Research to Review Articles, Frontiers Research Topics unify the most influential researchers, the latest key findings and historical advances in a hot research area.

Find out more on how to host your own Frontiers Research Topic or contribute to one as an author by contacting the Frontiers editorial office: frontiersin.org/about/contact

Greenhouse gas emissions and mitigation: Microbes, mechanisms and modeling

Topic editors

Baoli Zhu — Institute of Subtropical Agriculture, Chinese Academy of Sciences (CAS), China

Yong Li — Zhejiang University, China

Zengming Chen — Institute of Soil Science, Chinese Academy of Sciences (CAS), China

Hangwei Hu — The University of Melbourne, Australia

Adrian-Stefan Andrei — University of Zurich, Switzerland

Citation

Zhu, B., Li, Y., Chen, Z., Hu, H., Andrei, A.-S., eds. (2024). *Greenhouse gas emissions and mitigation: Microbes, mechanisms and modeling*. Lausanne: Frontiers Media SA. doi: 10.3389/978-2-8325-4967-4

Table of contents

frontiers | Frontiers in Microbiology

TYPE Editorial
PUBLISHED 18 January 2024
DOI 10.3389/fmicb.2024.1363814

OPEN ACCESS

EDITED AND REVIEWED BY
Paola Grenni,
National Research Council, Italy

*CORRESPONDENCE
Yong Li
liyong@zju.edu.cn

RECEIVED 31 December 2023
ACCEPTED 08 January 2024
PUBLISHED 18 January 2024

CITATION
Zhu B, Chen Z, Hu H, Andrei A-S and Li Y (2024) Editorial: Greenhouse gas emissions and mitigation: microbes, mechanisms and modeling. *Front. Microbiol.* 15:1363814. doi: 10.3389/fmicb.2024.1363814

Editorial: Greenhouse gas emissions and mitigation: microbes, mechanisms and modeling

Baoli Zhu[1], Zengming Chen[2], Hangwei Hu[3], Adrain-Stefan Andrei[4] and Yong Li[5]*

[1]Key Laboratory of Agro-Ecological Processes in Subtropical Region, Institute of Subtropical Agriculture, Chinese Academy of Sciences (CAS), Changsha, China, [2]Institute of Soil Science, Chinese Academy of Sciences (CAS), Nanjing, China, [3]School of Agriculture, The University of Melbourne, Melbourne, VIC, Australia, [4]Department of Plant and Microbial Biology, University of Zurich, Zurich, Switzerland, [5]College of Environmental and Resource Sciences, Zhejiang University, Hangzhou, China

KEYWORDS

greenhouse gas (CH_4 N_2O, CO_2), climate change, nitrification, denitrification, ammonia oxidizing microorganisms

Editorial on the Research Topic
Greenhouse gas emissions and mitigation: microbes, mechanisms and modeling

The soil, holding ~1500 Pg of total carbon (C) and 136 Pg of total nitrogen (N), represents the largest terrestrial reservoirs of these elements (Nieder and Benbi, 2008). Yet, it also stands as a significant source of greenhouse gas (GHG) emissions, contributing over 350 Pg CO_2-equivalents annually and thereby significantly impacting global warming. Over the years, atmospheric N_2O concentrations have risen by more than 20%, and CH_4 concentrations have nearly tripled to 1900 ppb, primarily attributed to microbial activities (Schaefer et al., 2016). Understanding the microbial mechanisms alongside the production and reduction of GHGs is crucial. Recent discoveries, such as atypical nitrous oxide reductase (NosZ II), comammox, and novel processes like oxygenic denitrification and anaerobic oxidation of CH_4 linked to the reduction of nitrate, nitrite, iron, and manganese oxides, underscore the pivotal role of soil microbes in regulating the biogeochemical cycles of C and N, and highlight avenues for targeted strategies to reduce GHG emissions and mitigate global warming. This Research Topic comprises nine articles that offer insights on the factors that influencing the emission of GHGs, especially N_2O, and the potential roles of microorganisms.

Nitrification and denitrification are the main processes producing N_2O. Fertilizer applications, especially N-fertilizers, fuel the emission of this potent greenhouse gas. Thus, nitrification inhibition can be a potential approach to reduce N_2O emissions. In this Research Topic, Lei et al. analyzed over 200 datasets from 48 studies and found that application of nitrification inhibitors on average reduced about 60% of total N_2O emission, increased over 70% of soil ammonium concentration, and decreased about 50% of AOB abundances. The findings emphasize AOB's significant role in N_2O emissions, and can be a better indicator and target for N_2O mitigation. Xie et al. compared N_2O emissions from grasslands featuring a

tropical grass species *Brachiaria humidicola*, whose root exudates with the capacity of biological nitrification inhibition, and a native grass *Eremochloa ophiuroide*, in Hainan, China. Interestingly, the N_2O emission rate of the *B. humidicola* grassland was significantly higher, especially under N-fertilization treatment. Nevertheless, its yield-scaled N_2O emission was significantly lower than the native *E. ophiuroide* grassland.

Nitrogen fertilizer application is also critical in influencing soil organic carbon (SOC) stability. Song et al. reported that nitrate addition enhanced the abundance and activity of SOC decomposers, thus, stimulating SOC decomposition in deep soils (>1 m), particularly when nitrate presented as the dominant electron acceptor over oxygen. This suggests the link between above-ground anthropogenic N input and deep soil carbon dynamics. Xu et al. demonstrated that delayed N fertilizer application in pea and maize intercropping reduced soil respiration rates and altered soil microbial community structures, thereby decreasing carbon emissions. This shed lights on agriculture management strategies in achieving carbon neutrality goals.

In addition, moisture plays important role in influencing greenhouse gas emissions and soil organic carbon (SOC) stability. Through laboratory incubations and literature synthesis, Wang et al. quantified N_2O emission rates from nitrification and denitrification under different soil moisture levels (40% to 120% WFPS, water-filled pore space), and found that N_2O emitting rate peaked at 80%−95% WFPS, while the dominating process switched from nitrification to denitrification when moisture increased over about 60% WFPS. Moisture as a major driver controls the relative contribution of nitrification and denitrification to N_2O emissions was evident from synthesized 80 groups of data.

Han et al. investigated the responses of total microbial community and ammonium oxidizing microbes to short-term moisture level changes and nitrogen fertilizer application in paddy soils. Moisture influenced the abundance and composition of total soil microbes, and nitrogen fertilizer reduced the connectivity and complexity of the total bacteria network. The community structures of ammonium-oxidizing-bacteria (AOB) and -archaea (AOA) were largely influenced by ammonium and nitrate, respectively, which play crucial roles in nitrification, indicating a differential response of these microbes.

Qu et al. investigated the respiration rates of different layer soils of the Loess Plateau, and underscored soil temperature and moisture as critical factors influencing soil respiration rates, suggesting a positive feedback loop amplifying global warming. Yang et al. investigated the impact of maize and rice straw biochar on N_2O emissions during paddy soil freeze-thaw cycles via simulating microcosm incubations. Results showed that biochar application decreased 10% of AOB abundance and reduced about two thirds of the total N_2O emissions, revealing the application potential of biochar in decreasing soil N_2O emissions.

By employing ^{15}N tracing and N_2O isotopocule methods, Karlowsky et al. dissected the contribution of bacterial denitrification and nitrifier denitrification to N_2O emissions in hydroponic tomato cultivation system. Results indicated that bacterial denitrification, nitrifier denitrification and coupled nitrification and denitrification all contributed to the N_2O emissions in the system.

In essence, these studies collectively offer profound insights into microbial mechanisms governing GHG emissions, presenting avenues for targeted mitigation strategies. More comprehensive and large-scale investigations are necessary to understand the intricate microbial processes driving GHG emissions, including methane, and to devise effective approaches to combat climate change.

Author contributions

BZ: Writing – original draft, Writing – review & editing. ZC: Writing – original draft, Writing – review & editing. HH: Writing – original draft, Writing – review & editing. A-SA: Writing – original draft, Writing – review & editing. YL: Writing – original draft, Writing – review & editing.

Funding

The author(s) declare financial support was received for the research, authorship, and/or publication of this article. The research was supported by the National Natural Science Foundation of China (project no. 42177104).

Conflict of interest

The authors declare that the research was conducted in the absence of any commercial or financial relationships that could be construed as a potential conflict of interest.

The author(s) declared that they were an editorial board member of Frontiers, at the time of submission. This had no impact on the peer review process and the final decision.

Publisher's note

References

Nieder, R., and Benbi, D. K. (2008). *Carbon and Nitrogen in the Terrestrial Environment*. Cham: Springer Science and Business Media.

Schaefer, H., Fletcher, S. E. M., Veidt, C., Lassey, K. R., Brailsford, G. W., Bromley, T. M., et al. (2016). A 21st-century shift from fossil-fuel to biogenic methane emissions indicated by $^{13}CH_4$. *Science* 352, 80–84. doi: 10.1126/science.aad2705

frontiers | Frontiers in Microbiology

TYPE Original Research
PUBLISHED 19 July 2022
DOI 10.3389/fmicb.2022.962146

OPEN ACCESS

EDITED BY
Yong Li,
Zhejiang University, China

REVIEWED BY
Hong Pan,
Shandong Agricultural University, China
Xiaoping Fan,
Zhejiang University, China

*CORRESPONDENCE
Rui Liu
rliu@cau.edu.cn

†These authors have contributed equally to this work and share first authorship

SPECIALTY SECTION
This article was submitted to Terrestrial Microbiology, a section of the journal Frontiers in Microbiology

RECEIVED 06 June 2022
ACCEPTED 29 June 2022
PUBLISHED 19 July 2022

CITATION
Lei J, Fan Q, Yu J, Ma Y, Yin J and Liu R (2022) A meta-analysis to examine whether nitrification inhibitors work through selectively inhibiting ammonia-oxidizing bacteria. *Front. Microbiol.* 13:962146. doi: 10.3389/fmicb.2022.962146

A meta-analysis to examine whether nitrification inhibitors work through selectively inhibiting ammonia-oxidizing bacteria

Jilin Lei†, Qianyi Fan†, Jingyao Yu, Yan Ma, Junhui Yin and Rui Liu*

College of Resources and Environmental Sciences, China Agricultural University, Beijing, China

Nitrification inhibitor (NI) is often claimed to be efficient in mitigating nitrogen (N) losses from agricultural production systems by slowing down nitrification. Increasing evidence suggests that ammonia-oxidizing archaea (AOA) and ammonia-oxidizing bacteria (AOB) have the genetic potential to produce nitrous oxide (N_2O) and perform the first step of nitrification, but their contribution to N_2O and nitrification remains unclear. Furthermore, both AOA and AOB are probably targets for NIs, but a quantitative synthesis is lacking to identify the "indicator microbe" as the best predictor of NI efficiency under different environmental conditions. In this present study, a meta-analysis to assess the response characteristics of AOB and AOA to NI application was conducted and the relationship between NI efficiency and the AOA and AOB *amo*A genes response under different conditions was evaluated. The dataset consisted of 48 papers (214 observations). This study showed that NIs on average reduced 58.1% of N_2O emissions and increased 71.4% of soil NH_4^+ concentrations, respectively. When 3, 4-dimethylpyrazole phosphate (DMPP) was applied with both organic and inorganic fertilizers in alkaline medium soils, it had higher efficacy of decreasing N_2O emissions than in acidic soils. The abundance of AOB *amo*A genes was dramatically reduced by about 50% with NI application in most soil types. Decrease in N_2O emissions with NI addition was significantly correlated with AOB changes (R^2 = 0.135, n = 110, $P < 0.01$) rather than changes in AOA, and there was an obvious correlation between the changes in NH_4^+ concentration and AOB *amo*A gene abundance after NI application (R^2 = 0.037, n = 136, P = 0.014). The results indicated the principal role of AOB in nitrification, furthermore, AOB would be the best predictor of NI efficiency.

KEYWORDS

nitrous oxide, DMPP, ammoxidation, edaphic conditions, microorganism

Introduction

Nitrification is a crucial process in the nitrogen (N) cycle, involving the oxidization of ammonium (NH_4^+) to nitrate (NO_3^-) through nitrite (NO_2^-). The process supplies significant amounts of N to be taken up by growing crops. However, unabsorbed N is lost to the atmosphere or the soil below the root zone. These unwanted losses of N have significant implications for the environment, for example NO_3^- leaching and greenhouse gas emissions (GHG), particularly nitrous oxide (N_2O). N_2O is a potent GHG which greatly contributes to global climate change, it has a 265-fold higher global warming potential than CO_2 (IPCC, 2014) and it is involved in the destruction of the protective ozone layer (Ravishankara et al., 2009), which has become one of society's most important challenges (Desloover et al., 2012).

The application of nitrification inhibitor (NI) is a promising technology to reduce N losses in different kinds of soil systems. In agriculture, several chemical compounds were designed to delay the steps of microbial oxidation of NH_4^+ to NO_3^- in the soil to decrease N_2O emissions, such as 3, 4-dimethylpyrazole phosphate (DMPP), dicyandiamide (DCD), and 2-chloro-6-(trichloromethyl) pyridine (nitrapyrin). Of these, DMPP is the most efficient commercial compound, which is applied as dihydrogen phosphate salt to reduce its loss through evaporation. NIs target the first step, i.e., the enzyme ammonia monooxygenase (AMO) in the case of DMPP (and other N-containing inhibitors) presumably through reversible complexation of the enzyme's Cu center (McCarty, 1999; Beeckman et al., 2018). Ammonia-oxidizing archaea (AOA) and bacteria (AOB) both perform the first step of nitrification and are probably targets for NIs. The impact of NIs in delaying nitrification and reducing N_2O emissions has been widely reported (Huang et al., 2014; Cai and Akiyama, 2017; Xu et al., 2019). However, the effectiveness of NIs varies greatly within different soils (Shi et al., 2017; Zhu et al., 2019), fertilizers (Pereira et al., 2010), and moisture content (Chen et al., 2010; Hu et al., 2015a; Fan et al., 2019). Soil temperature is another key factor controlling NI efficiency, which can subside after 1 week at 35°C (Barth et al., 2008; Chen et al., 2015). Furthermore, many studies focused on the impact and contribution of soil microorganisms on N_2O emissions (Chen et al., 2019; Lazcano et al., 2021; Yang et al., 2021; You et al., 2022). However, there is still a lack of direct evidence on whether soil microbial community, especially AOA and AOB, affects NI efficacy (Chen et al., 2010; Guardia et al., 2018; Lam et al., 2018).

Within the major N-cycling microbes, AOA and AOB are important functional strains, and both carry the *amo*A gene which encodes AMO (Xia et al., 2018). Due to its strong conserved nature, the *amo*A gene is often used as a biomarker for exploring ammonia-oxidizing microorganisms (Schleper and Nicol, 2010). This has certain advantages in analyzing the genetic diversity of ammonia-oxidizing microorganisms. The differences in cellular biochemistry and physiology between AOA and AOB lead to their different ecological niches in different agroecosystems in terms of sensitivity to soil pH, soil texture, N forms, moisture, temperature and other conditions (Morimoto et al., 2011; Prosser and Nicol, 2012; Hu et al., 2015b). Hu et al. (2013) showed that the increase of nitrification activity in most acidic soils was positively correlated with the increase of AOA quantity, but not with AOB. In general, AOB dominates nitrification in neutral and alkaline soils, while AOA is more suitable to the acidic environment (Lu et al., 2012; Li et al., 2018). Increasing the NH_4^+ concentration will enhance the nitrification activity of AOB (Okano et al., 2014), while AOA prefers an environment with a lower NH_4^+ concentration. For example, a low pH environment is favorable for the formation of NH_4^+ and changes the utilization of NH_4^+ by AOB (Ying et al., 2017). Therefore, different edaphic and environmental conditions would influence AOA and AOB nitrification activity, and in turn affect the response of AOA and AOB to NI application.

To date, most studies on the inhibitory effect of NIs on AOA and AOB have focused either on the change of the *amo*A gene population (Prosser and Nicol, 2008; Kleineidam et al., 2011) or on the change of the AOA and AOB community (Zhang et al., 2012a; Liu et al., 2015). There is very little research available with respect to the "indicator microbe," AOA or AOB, as the best predictor of NI efficiency under different environmental conditions. In acidic soils, AOA played a dominant role in nitrification and N_2O production (Liu et al., 2016; Gu et al., 2019; Zhou et al., 2020), but NIs especially DMPP showed a lower inhibitory effect in acidic soils. Furthermore, many studies showed that NIs effectively decreased the AOB population, but not AOA (Gong et al., 2013; Liu et al., 2015, 2017; Dong et al., 2018; Yin et al., 2021). Hence, it was hypothesized that AOB are more sensitive to NIs than AOA and NIs would work through selectively inhibiting AOB.

Using a meta-analytical approach, results of 48 individual studies were combined to estimate the variations of NI efficiency in different edaphic and experimental conditions. Moreover, the general trends in the response of AOA and AOB abundance to NI addition were explored. Lastly, the efficiency of NIs was investigated by looking at the relationship among AOA or AOB *amo*A gene abundance and N_2O emissions. This approach will help to identify the "indicator microbe," AOA or AOB, as the best predictor of NI efficiency under different environmental conditions.

Materials and methods

Data compilation

The databases used for the data collection included Web of Science, WanFang digital database and China knowledge Resource Integrated to search for relevant studies

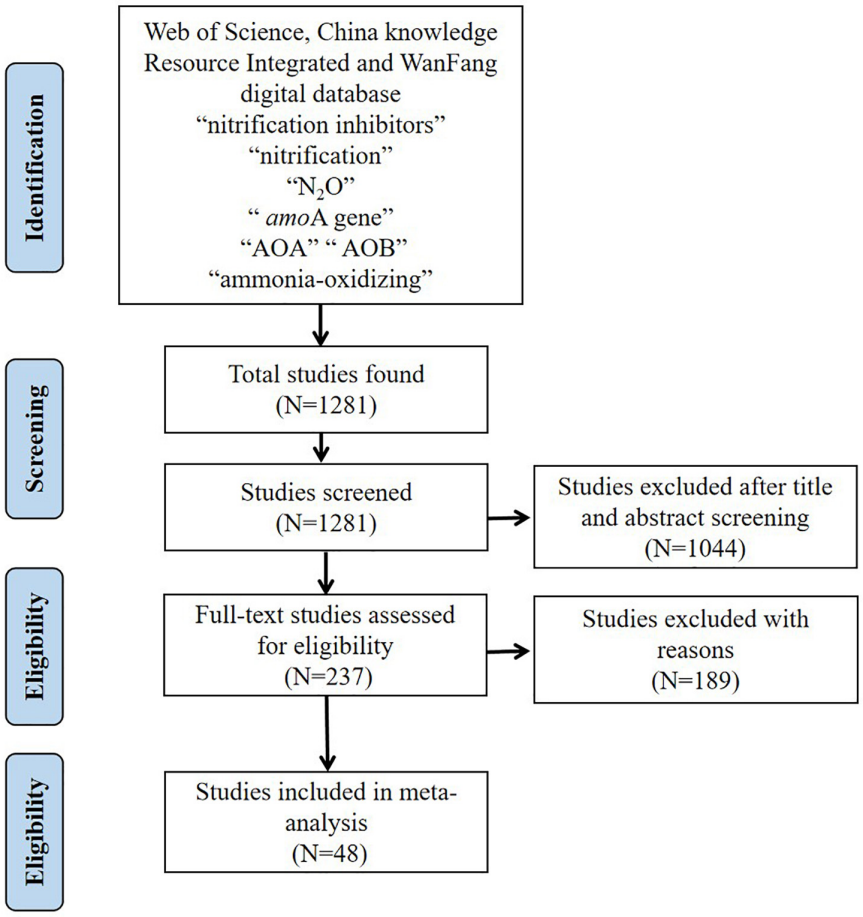

FIGURE 1
Selection of studies for inclusion in the meta-analysis.

published between 2010 and 2021. The key search terms were: nitrification inhibitors, nitrification, N_2O, *amo*A gene, AOA, AOB, ammonia-oxidizing. The number of studies selected at various stages is shown in the flow diagram in **Figure 1**. After screening the literature, the database consisted of 214 selected pairwise comparisons reported in 48 studies (**Supplementary Table 1**), which met predetermined quality criteria (studies with replication, with detailed information, and performed under greenhouse, field and controlled laboratory conditions) (Abalos et al., 2022). All the studies included pairwise comparisons in which treated soil (with NI addition) was compared to an untreated control (without NI addition). Furthermore, the collated observations which were screened should measure the abundance of the *amo*A functional gene for AOB and AOA and the studied ecosystem type belonged to pastoral or agricultural environments.

In these present analyses, to take full advantage of published results, multiple experimental treatments from the same study were included (e.g., treatments that varied by N fertilizer type). However, only one measurement from each experimental replicate was included to maximize independence among measurements (Carey et al., 2016). For instance, the highest NH_4^+ concentration was selected from the studies where NH_4^+ concentration was measured multiple times from the same treatment.

The mitigation of cumulative N_2O emissions and the changes in NH_4^+ concentrations were considered as the evaluation variables of the NI inhibitory effect. The change of *amo*A gene abundance was reflected as the influence of NIs on microorganisms. Of all the 214 observations in the present study, observations 155, 174, 166, 147 concerned N_2O yield, NH_4^+ concentration, AOB *amo*A and AOA *amo*A gene abundance, respectively. Data on soil physical and chemical properties and experimental conditions were also collected from the original literature to analyze their influence on NI efficacy. Soil pH, soil organic matter (SOM), soil texture, soil moisture content (water filled pore space, WFPS and water holding capacity, WHC), soil temperature (TEMP), N fertilizer type, N application rate (NR), and NIs type were chosen to assess how edaphic conditions and management measures influenced NI

efficacy. The following were the categorical variables classified into different groups:

- Soil pH: (1) soil pH ≤ 6, (2) 6 < soil pH < 8, (3) soil pH ≥ 8
- SOM (g kg^{-1}): (1) SOM ≤ 20, (2) 20 < SOM ≤ 40, (3) SOM > 40
- Soil texture: (1) coarse (sand, loamy sand, sandy loam, loam, silt loam, and silt), (2) medium (sandy clay loam, clay loam, and silty clay loam), (3) fine (sandy clay, silty clay, and clay)
- WFPS and WHC: (1) WFPS and WHC ≤ 40%, (2) 40% < WFPS and WHC ≤ 60%, (3) 60% < WFPS and WHC ≤ 80%, (4) WFPS and WHC > 80%
- TEMP (°C): (1) TEMP ≤ 20, (2) 20 < TEMP ≤ 25, (3) TEMP > 25
- N fertilizer type: (1) NH_4^+ based fertilizer (including ammonium chloride (NH_4Cl), ammonium nitrate (NH_4NO_3) and ammonium sulfate [$(NH_4)_2SO_4$)], (2) organic fertilizer (including livestock manure and urine), (3) urea, (4) both (combination of organic and inorganic fertilizer)
- NR (kg N ha^{-1}): (1) NR ≤ 100, (2) 100 < NR ≤ 150, (3) NR > 150
- NIs type: (1) DMPP, (2) DCD, (3) nitrapyrin and others

Data analysis

The natural logarithmic response ratio (ln*RR*) as an effect size for each observation was calculated as Equation (1) (Luo et al., 2006):

$$\ln RR = ln\frac{Xt}{Xc} = \ln Xt - \ln Xc \quad (1)$$

where *Xt* is the average value of index *X* from NIs treatments and *Xc* is the average from the control treatments.

The results were expressed by using the conversion equation according to Equation (2) as percentage change:

$$\%\ \text{change} = (e^{\ln RR} - 1) \times 100 \quad (2)$$

A positive percentage change indicated increases in N_2O yield, NH_4^+ concentration, and *amo*A gene abundance after NI addition, while a negative percentage change indicated decreases in these variables (Sha et al., 2020). Replication-based weighting was used to avoid the effect of extreme weightings, using the following Equation (3) (Groenigen et al., 2011):

$$W = \frac{n_t \times n_c}{n_t + n_c}, V = \frac{1}{W} = \frac{n_t + n_c}{n_t \times n_c} \quad (3)$$

where n_t and n_c were the number of replications in the treatment group and control group, respectively.

The mean effect size of environmental and management variables on NI efficacy was calculated by a random-effect model and 95% of confidence intervals (CIs) were produced by a bootstrapping procedure with 4,999 iterations (Sha et al., 2020). In the present meta-analysis, Metawin 2.1 software (Rosenberg et al., 2000) was applied to perform all the calculations. If the 95% CIs did not overlap zero, the effects of NIs on the evaluation variables were considered significant. When the 95% CIs of each categorical group did not overlap, there were significantly different from each other. For each categorical variable, total heterogeneity (Q_t) was segmented into within-group (Q_w) and between-group (Q_b). Q_b/Q_t describes the proportion of total variation explained by each modifier. The *P*-value is the probability value for randomization tests (999 permutations) with sample size as the weighting function, calculated only for the Q_b values. A particular categorical variable was considered to have a significant impact on the response ratio when Q_b was significant ($P < 0.05$) and was larger than the critical value (Carey et al., 2016). The heterogeneity in different categorical groups for each explanatory variable was also reported in **Tables 1**, **2**. Of all observations (from the 48 studies) included in this meta-analysis, 113 and 110 measured the effect of NIs on N_2O emissions, and AOA and AOB *amo*A gene abundance simultaneously. Of those, 133 and 136 measured NI effects on NH_4^+ concentration changes in addition to AOA and AOB *amo*A gene abundances, respectively. Based on these observations, a regression analysis was conducted in Origin 9.0 to explore the relationship between the effects of NIs on NH_4^+ concentration, N_2O emission and *amo*A gene abundance.

TABLE 1 Between-group heterogeneity (Q_b) illustrating the effects of NIs additions on N_2O emission and NH_4^+ concentration across categorical modifiers.

Explanatory variables	N_2O		NH_4^+	
	Q_b	Q_b/Q_t	Q_b	Q_b/Q_t
Soil pH	16.06**	0.09	3.11	0.02
Soil texture	24.82**	0.16	0.64	0.006
Soil organic matter	3.45	0.03	15.02**	0.11
Moisture	2.60	0.02	9.15*	0.06
Temperature	3.81	0.02	18.99**	0.10
N application rate	3.47	0.02	13.30**	0.08
Fertilizer type	9.71*	0.06	7.24	0.04
NIs type	2.63	0.02	6.28*	0.04

Q_b/Q_t describes the proportion of total variation explained by each modifier. The P-value is the probability value for randomization tests (999 permutations) with sample size as the weighting function, calculated only for the Q_b values; *$P < 0.05$; **$P < 0.01$.

Results

Inhibitory effect of nitrification inhibitors on nitrous oxide emissions

NIs effectively decreased N_2O emissions across all experimental and edaphic conditions. For the efficacy of

TABLE 2 Between-group heterogeneity (Q_b) illustrating the effects of NIs additions on ammonia oxidizer across categorical modifiers.

Explanatory variables	AOB		AOA	
	Q_b	Q_b/Q_t	Q_b	Q_b/Q_t
Soil Ph	3.53	0.03	0.16	0.002
Soil texture	1.37	0.01	5.99*	0.10
Soil organic matter	2.04	0.02	2.63	0.06
Moisture	3.31	0.02	1.39	0.02
Temperature	3.06	0.02	0.50	0.007
N application rate	0.89	0.006	3.00	0.04
Fertilizer type	43.76**	0.22	1.86	0.02
NIs type	0.80	0.01	0.17	0.002

Q_b/Q_t describes the proportion of total variation explained by each modifier. The P-value is the probability value for randomization tests (999 permutations) with sample size as the weighting function, calculated only for the Q_b values; *$P < 0.05$; **$P < 0.01$.

NIs, soil pH, soil texture and fertilizer type were the best explanatory variables (Table 1 and Figures 2A, 3A). N_2O emissions were reduced by 54.9, 51.4, 77.4% by NIs in acidic, neutral and alkaline soils, respectively (Figure 2A), indicating that NIs performed better in alkaline soils than in neutral and acidic soils. The efficacy of NIs on reducing N_2O emissions reached 75.2% in medium soil (Figure 2A, 95% CIs ranged 8.0–10.62%) while it only reached 46.9 and 47.7% in coarse and fine soils, respectively. The combined application of NIs with both organic and NH_4^+ fertilizer or urea (at a relatively high N rate above 100 kg N ha^{-1}) performed better (71.7%) than the combined application of NIs with organic or inorganic fertilizer alone (43.8 and 52.2%) (Figure 3A). Of all observations, DMPP was the best NI to mitigate N_2O emissions (63.3%).

Effect of nitrification inhibitors on NH_4^+ concentration

NH_4^+ concentration was increased by 71.4% on average with NI application across all experimental and edaphic conditions. NIs had a stronger ability to restrain the oxidization of NH_4^+ in soil with low SOM (below 20 g kg^{-1}) when the soil WHC/WFPS was lower than 40% (Figures 2B, 3B). The effect of NIs in slowing nitrification was better when the temperature was lower than 20°C (Figure 3B and Table 1, $P < 0.01$). Different NIs showed different efficacies in inhibiting nitrification, and DMPP was the most effective inhibitor compared with others (98.9% average change, 95% CIs range 36.5–48.8%, Figure 3B and Table 1, $P < 0.05$). The greater soil NH_4^+ retention by DMPP was associated with a lower N application rate (below 100 kg N ha^{-1}) (Figure 3B and Table 1, $P < 0.05$). In addition, NH_4^+ concentration in alkaline and neutral soils was more responsive to NI addition than in acid soils.

Effect of nitrification inhibitors on ammonia-oxidizing bacteria and archaea

AOB *amo*A gene abundance negatively responded to NI addition (Figures 2C, 3C). The response ratio was always lower than or equal to zero, the magnitude significantly depended on fertilizer type ($P < 0.01$; Table 2). The efficacy of NIs on reducing AOB *amo*A gene abundance reached up to 90.08% when NIs were applied with organic fertilizer, which was higher than in NI application combined with inorganic fertilizer alone and with both organic and inorganic fertilizers (Figure 3C). However, no significant differences were observed in the response of AOB gene abundance to NIs across most of the categorical variables ($P > 0.05$; Table 2), including soil pH, NI type, SOM, moisture, TEMP, and NR.

The response ratio of AOA *amo*A gene abundance was always slightly lower than or equal to zero. It was observed that only soil texture had significant impact on the responses of AOA to NIs ($P < 0.05$; Table 2). Under certain experimental and edaphic conditions, NIs increased AOA *amo*A gene abundances (Figures 2D, 3D). Notably, AOA *amo*A gene abundance positively responded to NIs in medium and fine soils ($P < 0.05$; Table 2). Furthermore, when soil moisture was between 60 and 80% WHC/WFPS or NR was below 100 kg N ha^{-1}, NIs could increase AOA *amo*A gene abundance (Figure 3D).

Relationship between nitrous oxide emissions, the efficiency of nitrification inhibitors and amoA gene response

The response ratio of AOB was significantly and positively correlated with N_2O emissions (N_2O emission[lnR] = 0.42 × AOB[lnR]−0.78, $R^2 = 0.14$, $P < 0.01$; Figure 4A). In contrast, there was no significant correlation observed between the response ratio of AOA and N_2O emissions (N_2O emission[lnR] = −0.06 × AOA[lnR]−1.05, $R^2 < 0.00$, $P = 0.71$; Figure 4A). There was an obvious correlation between the changes in NH_4^+ concentration and AOB *amo*A gene abundance after NI application (NH_4^+ concentration[lnR] = −0.17 × AOB[lnR] + 0.47, $R^2 = 0.04$, $P = 0.014$; Figure 4B).

Discussion

Effect of edaphic and experimental conditions on nitrification inhibitor efficacy

Soil pH was an important explanatory variable for NI efficacy in reducing N_2O emissions (Cui et al., 2021). The results

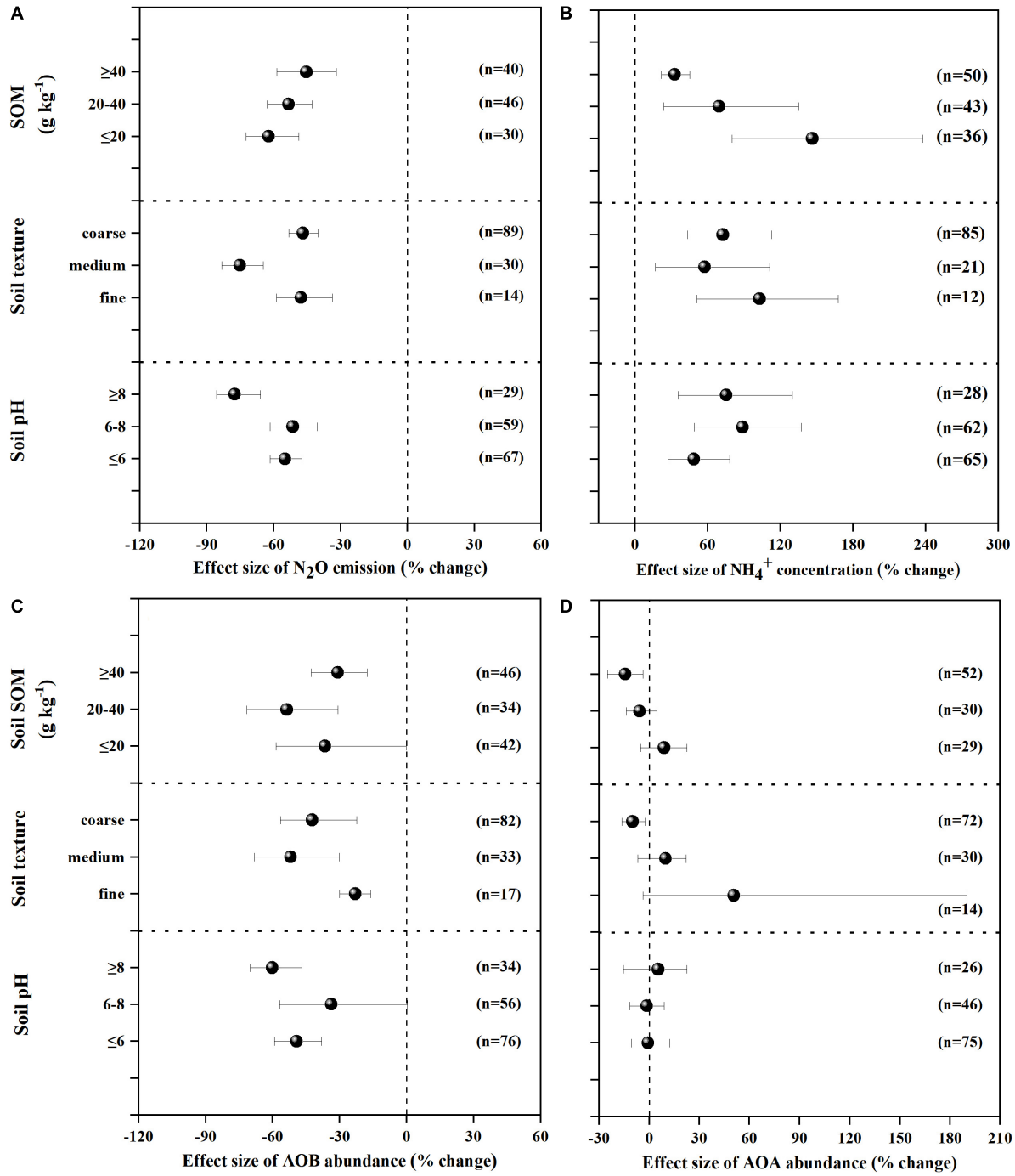

FIGURE 2
Mean response ratios (% change) and bootstrapped 95% Confidence Intervals (CI) for the effects of soil properties on the N_2O emissions **(A)**, NH_4^+ concentration **(B)**, AOB gene abundance **(C)** and AOA gene abundance **(D)** after NIs application. Values in parentheses represent the number of observations.

from the current meta-analysis showed that NIs had different effects on decreasing N_2O emissions under different soil pH (**Figure 2A** and **Table 1**, $P < 0.01$), and NIs efficacy had a positive response to soil pH. Firstly, it may be attributed to NIs being retained for longer in alkaline soils (pH $\geq$ 8). Soil pH has been considered as one of the most important factors controlling NI efficacy, because pH has potential to impact the degradation rate of the NIs in soils. Cui et al. (2021) showed that DMPP performed better in alkaline soil compared to acid soil conditions, which may be caused by the shorter half-life

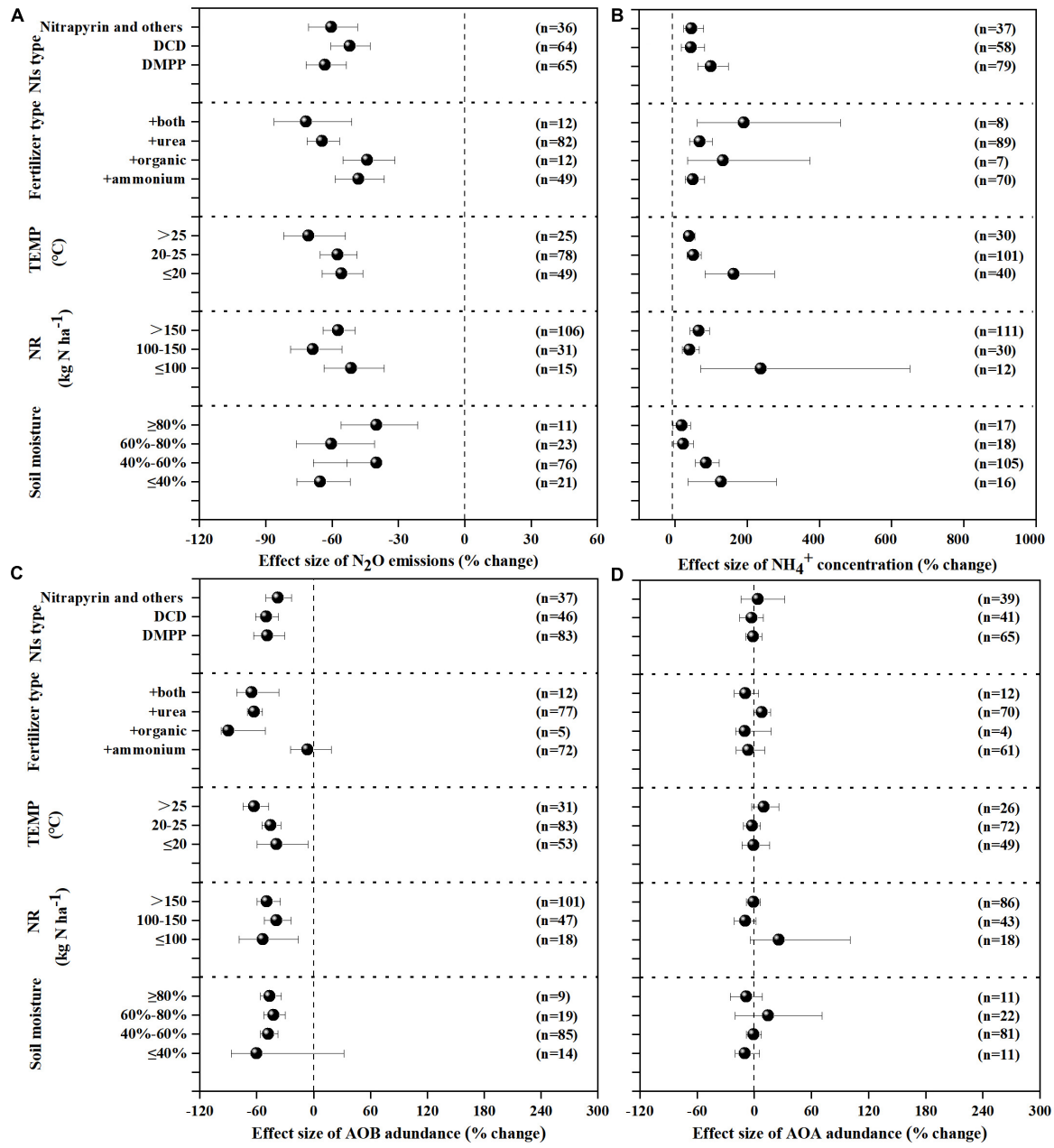

FIGURE 3
Mean response ratios (% change) and bootstrapped 95% Confidence Intervals (CI) for the effects of experiment conditions on the response of N_2O **(A)**, NH_4^+ **(B)**, AOB **(C)**, AOA **(D)** after NIs treatment. Values in parentheses represent the number of observations.

time of DMPP in acidic soil compared to alkaline soil. DMPP undergoes degradation in soil through chemical reaction steps, potentially involving reactive oxygen species (ROS) generated through abiotic and/or biotic processes (Sidhu et al., 2021), which would possibly be affected by pH. Secondly, soil pH played a vital role in controlling N_2O emissions from soils (Morkved et al., 2007). Wang Y. et al. (2018) demonstrated that soil pH was negatively correlated with N_2O emission, indicating less N_2O emission from alkaline soils. In the current research, the inhibition efficacy of NIs on reducing N_2O emissions increased with soil pH, indicating that NIs were more effective in alkaline soils. It may be also attributed to the less N_2O emissions from alkaline soils.

SOM and soil texture were also considered as main factors affecting NI performance (Jarvis et al., 2007). Previous studies have reported a negative correlation between NI efficacy and SOM and clay content (Barth et al., 2008; Zhu et al., 2019). High SOM and clay content could easily adsorb NIs, which

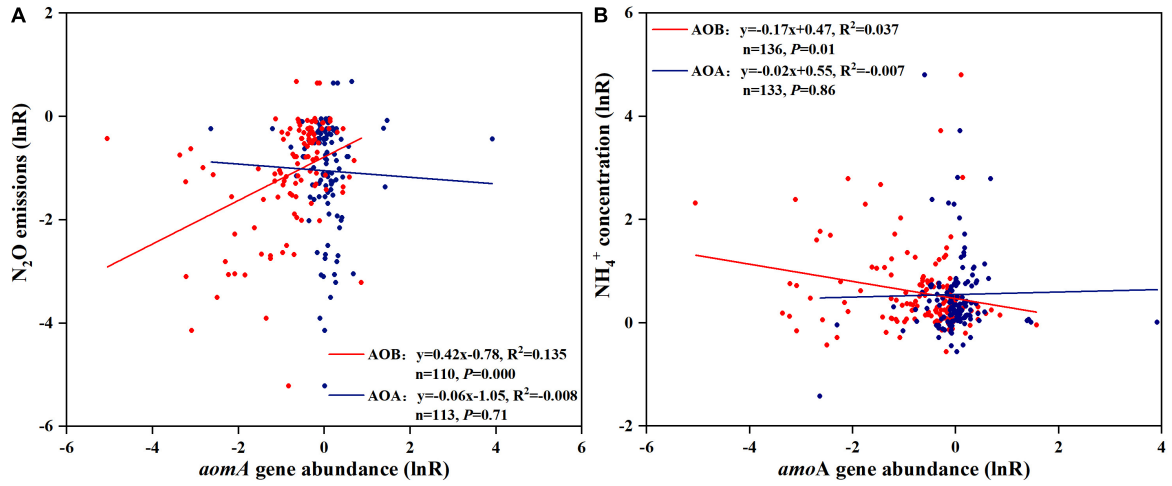

FIGURE 4
Relationship between effect size (lnR) of N_2O emissions **(A)** or NH_4^+ concentration **(B)** and effect size (lnR) of AOA and AOB *amo*A gene abundance. Line is the best-fit regression, where AOB-NIs effectiveness is the red line and AOA-NIs effectiveness is the blue line. Each symbol represents one observation; red point, AOB, blue point, AOA.

would influence their availability and effectiveness (Zhang et al., 2020; Cui et al., 2021). Furthermore, SOM could be used by soil microorganisms as energy, carbon (C), and N source, which improve microbial bioactivity, leading to accelerated biodegradation of NIs (Fisk et al., 2015). Clay had a protective effect on nitrifying oxidizers (Neufeld and Knowles, 1999). Higher clay content might make microorganisms less susceptible to being affected by inhibitors, thus weakening NIs inhibitory effects. Therefore, the current study found that NIs delayed ammonia oxidation and inhibited N_2O emissions more efficiently in medium soils with lower SOM.

Soil temperature had a significant effect on NIs inhibition on nitrification ($P < 0.01$). Temperature influenced the rate of nitrification, which might affect the inhibitory effect of NIs on nitrification and NH_4^+ retention (Mathieu et al., 2006). Irigoyen et al. (2003) reported that the nitrification rate accelerated at 20°C, but slowed down when the temperature reached up to 30°C. A lower temperature ($\leq$ 20°C) was favorable for improving the efficacy of NIs on delaying the nitrification rate, which may also be attributed to the rapid decomposition of NIs by microorganisms in high temperature (Irigoyen et al., 2003; Wang X. et al., 2018). Yu et al. (2015) found that the increased NH_4^+ concentration by DMPP at 15°C was 56 times higher than that at 25°C due to better persistence of the molecule of DMPP at 15°C. Hauser and Haselwandter (1990) also demonstrated that the degradation rate of DCD reached its highest between 25°C and 33°C. The above studies were consistent with the results in this study, in which the addition of NIs increased NH_4^+ concentration in temperatures below 20°C.

Kirschke et al. (2019) found that the effect of NIs on nitrification was negatively correlated with soil moisture, which was consistent with this study. The probable reason was that higher water content may increase the distance between NI and NH_4^+ because of faster diffusion of NH_4^+ than that of NIs (Azam et al., 2001). On the other hand, the soil was supposed to be hypoxic at high water content (80% WFPS), inducing denitrification occurrence and dominance (Menéndez et al., 2008). Nitrification dominated at 40% WFPS, which was conducive to the effect of NIs on NH_4^+ retention (Menéndez et al., 2012). This would also explain the negative correlation between the effect of NIs on NH_4^+ retention and soil moisture in the current study.

The combined application of NIs with the appropriate N fertilizers could improve their efficacy (Vinzent et al., 2018). The present results showed that the combined application of NIs with organic fertilizer could enhance NIs inhibitory effect on N_2O emissions. On the one hand, the application of organic fertilizer significantly improved soil pH, which could prolong the retention time of NIs and thus improve the efficacy of NIs in inhibiting N_2O emissions (Zhang et al., 2012b). On the other hand, as observed in the current study, the efficacy of NIs in reducing AOB *amo*A gene abundance was highest when NIs were applied with organic fertilizer, thus N_2O emission mitigation by NIs reaching its maximum. NR significantly influenced the effect size of NIs on NH_4^+ retention. Better NI efficacy in increasing NH_4^+ concentration could be observed at a lower N application rate ($\leq$100 kg N ha^{-1}). This is in accordance with previous findings by Rowlings et al. (2016), which revealed that N application which was less than the conventional rate could increase DMPP performance. Inappropriate N application rates may result in a large N surplus, providing adequate substrate of NH_4^+ for ammonia volatilization and thus reducing the efficacy of the NI in increasing NH_4^+ concentration (Nauer et al., 2018).

Response of ammonia oxidizers to nitrification inhibitors

AOB *amo*A gene abundance negatively responded to NI addition under different edaphic and experimental conditions. However, in contrast to AOB, AOA *amo*A gene abundance responded positively to NI addition in medium and fine soils. Fan et al. (2019) found an increase in AOA abundance after DMPP application in the tested soils, which was consistent with our results. Our results were also in good agreement with the study by Hink et al. (2018) and Fan et al. (2022), which reported that AOA growth were accelerated while AOB were inhibited with NIs. The growth of AOA might be promoted by organic compounds (Tourna et al., 2011; Ai et al., 2013), and it is possibly because that NIs such as acetylene and DMPP could be available C substrates for AOA (Florio et al., 2014; Hink et al., 2017). Compared to coarse soils, fine and medium soils showed a generally higher accumulation potential of SOM which provided sufficient C and N substrates for AOA proliferation (Kögel-Knabner et al., 2008; Dieckow et al., 2009). In line with results of this study, Shen et al. (2013) illustrated that most of the NIs appeared to have no effect on AOA in agricultural soils. Shi et al. (2016) also discovered that DMPP could strongly influence the metabolic activity of AOB by using DNA-stable isotope probing (SIP) but did not influence AOA. The potential physiological or metabolic differences between AOA and AOB (Prosser and Nicol, 2012) may explain the different responses of AOB and AOA to NIs. Furthermore, the most commonly used inhibitors suppressed microbial activity by chelating Cu active sites in AMO, and the periplasmic *Amo*B, a subunit of ammonia monooxygenase, presumably contains a copper-catalyzed active site (Monaghan et al., 2013; Beeckman et al., 2018). Lawton et al. (2014) found that archaea *Amo*B is a non-active enzyme and NIs tend to chelate on the active site of AOB to inhibit its activity, which indicated that the structural difference of the *Amo*B subunit and the ecophysiological differences also possibly lead to the variation in sensitivity among AOA and AOB to NIs (Tolar et al., 2017).

Fertilizer forms significantly affected the response of AOB to NIs, rather than the response of AOA (Tao et al., 2017). The results from the current study demonstrated that NIs showed the best performance in slowing down AOB growth in the case of organic fertilizer application, however, there was no difference observed on AOA abundance with NI application under different fertilizer forms. Wang et al. (2014) found an obvious stimulating effect of manure fertilization on the efficacy of NIs in reducing the population of AOB rather than AOA in a paddy soil, which was confirmed by the results of the current analysis. The application of organic fertilizer would provide an ideal alkaline environment for NIs to reduce AOB *amo*A gene abundance, which may be attributed to better activity and sensitivity of AOB to NI addition under alkaline conditions. But AOA adapted to low pH conditions (i.e., have a pH optima below 7; Hatzenpichler, 2012).

The best-fit regression in this study showed that N_2O mitigation and NH_4^+ concentration increase by NIs was positively correlated with the decrease of AOB-*amo*A gene abundance by NI application but not AOA-*amo*A. This supported the hypothesis that AOB are more sensitive to NIs than AOA and NIs would work through selectively inhibiting AOB. Previous studies illustrated that although the number of AOA far exceeds that of AOB in most terrestrial ecosystems, the N_2O production capacity of AOB was 10–1,000 times higher than that of AOA (Leininger et al., 2006; Jung et al., 2011; Xia et al., 2011; Gu et al., 2019). The main reason for that was that AOB-related N_2O was produced *via* nitrifier-denitrification and incomplete NH_2OH oxidation (Shaw et al., 2006; Wu et al., 2018), while the N_2O produced by AOA could not be attributed to nitrifier-denitrification, due to a lack of NO reductase (Tourna et al., 2011; Jung et al., 2014; Stieglmeier et al., 2014). Kozlowski et al. (2016) showed direct evidence that N_2O produced by AOA was attributed to abiotic reactions of released NO under anoxic conditions, in which Nitrososphaera viennensis EN76(T) (a Thaumarchaeon) was used as a test AOA. There was an obvious correlation between NH_4^+ and AOB ($P < 0.05$; **Figure 4B**), indicating the high inhibitory effect of NIs on nitrification through inhibiting AOB, which was consistent with the results reported by Zerulla et al. (2001) and Di and Cameron (2011). The obvious correlation between NH_4^+ concentration and AOB also revealed the dominate role of AOB in nitrification. Although the relationship between AOA *amo*A gene abundance and N_2O emissions, NH_4^+ concentration after NI application was found to be insignificant in this study, AOA was also important for nitrification in soils. AOA had been shown to play an integral role in soil nitrification of some unmanaged soils (Huang et al., 2011; Isobe et al., 2015), with the greatest contribution likely occurring in N-limited scenarios. As observed in this study, AOB was more sensitive to NIs than AOA, even in soils where AOA were more abundant.

Conclusion

Soil pH, soil texture, SOM, soil temperature, and N application rate were identified to be the factors most affecting the efficacy of NIs. There was a significant positive correlation between NIs efficacy on decreasing N_2O emissions, increasing NH_4^+ concentration and AOB *amo*A gene abundance reduction after NIs. Taken together, for both soil and experimental conditions, AOB plays a key role in nitrification and NIs specifically inhibit AOB rather than AOA, which indicates AOB would be the best predictor of NI efficiency. These results would provide a scientific basis for better modeling and N management strategies to reduce N_2O emissions and improve N use efficiency in agricultural systems.

Data availability statement

The original contributions presented in this study are included in the article/**Supplementary Material**, further inquiries can be directed to the corresponding author.

Author contributions

JL: data curation, writing – original draft preparation and review and editing, conceptualization, and validation. QF: methodology, software, and writing – original draft preparation. JiY: formal analysis, investigation, and resources. YM and JuY: writing – reviewing and editing. RL: supervision, project administration, funding acquisition, conceptualization, and writing – reviewing and editing. All authors contributed to manuscript revision, read, and approved the submitted version.

Funding

This research was supported by the National Natural Science Foundation of China (grant no. 42007031).

Conflict of interest

The authors declare that the research was conducted in the absence of any commercial or financial relationships that could be construed as a potential conflict of interest.

Publisher's note

All claims expressed in this article are solely those of the authors and do not necessarily represent those of their affiliated organizations, or those of the publisher, the editors and the reviewers. Any product that may be evaluated in this article, or claim that may be made by its manufacturer, is not guaranteed or endorsed by the publisher.

Supplementary material

The Supplementary Material for this article can be found online at: https://www.frontiersin.org/articles/10.3389/fmicb.2022.962146/full#supplementary-material

References

Abalos, D., Rittl, T. F., Recous, S., Thiébeau, P., Topp, C. F. E., Groenigen, K. J., et al. (2022). Predicting field N_2O emissions from crop residues based on their biochemical composition: a meta-analytical approach. *Sci. Total Environ.* 812:152532. doi: 10.1016/j.scitotenv.2021.152532

Ai, C., Liang, G., Sun, J., Wang, B., He, P., and Zhou, W. (2013). Different roles of rhizosphere effect and long-term fertilization in the activity and community structure of ammonia oxidizers in a calcareous fluvo-aquic soil. *Soil Biol. Biochem.* 57, 30–42. doi: 10.1016/j.soilbio.2012.08.003

Azam, F., Benckiser, G., Müller, C., and Ottow, J. C. G. (2001). Release, movement and recovery of 3, 4-dimethlpyrazole phosphate(DMPP), ammonium and nitrate from stabilized nitrogen fertilizer granules in a soil under laboratory conditions. *Biol. Fertil. Soils* 34, 118–125. doi: 10.1007/s003740100384

Barth, G., Tucher, S. V., and Schmidhalter, U. (2008). Effectiveness of 3, 4-dimethylpyrazole phosphate as nitrification inhibitor in soil as influenced by inhibitor content, application form, and soil matric potential. *Pedosphere* 18, 378–385. doi: 10.1016/S1002-0160(08)60028-4

Beeckman, F., Motte, H., and Beeckman, T. (2018). Nitrification in agricultural soils: impact, actors and mitigation. *Curr. Opin. Biotechnol.* 50, 166–173. doi: 10.1016/j.copbio.2018.01.014

Cai, Y., and Akiyama, H. (2017). Effects of inhibitors and biochar on nitrous oxide emissions, nitrate leaching, and plant nitrogen uptake from urine patches of grazing animals on grasslands: a meta-analysis. *Soil Sci. Plant Nutr.* 63, 405–414. doi: 10.1080/00380768.2017.1367627

Carey, C. J., Dove, N. C., Beman, J. M., Hart, S. C., and Aronson, E. L. (2016). Meta-analysis reveals ammonia-oxidizing bacteria respond more strongly to nitrogen addition than ammonia-oxidizing archaea. *Soil Biol. Biochem.* 99, 158–166. doi: 10.1016/j.soilbio.2016.05.014

Chen, D., Suter, H. C., Islam, A., and Edis, R. (2010). Influence of nitrification inhibitors on nitrification and nitrous oxide (N_2O) emission from a clay loam soil fertilized with urea. *Soil Biol. Biochem.* 42, 660–664. doi: 10.1016/j.soilbio.2009.12.014

Chen, H., Yin, C., Fan, X., Ye, M., Peng, H., Li, T., et al. (2019). Reduction of N_2O emission by biochar and/or 3,4-dimethylpyrazole phosphate (DMPP) is closely linked to soil ammonia oxidizing bacteria and *nos*ZI-N_2O reducer populations. *Sci. Total Environ.* 694:133658. doi: 10.1016/j.scitotenv.2019.133658

Chen, Q., Qi, L., Bi, Q., Dai, P., Sun, D., Sun, C., et al. (2015). Comparative effects of 3,4-dimethylpyrazole phosphate (DMPP) and dicyandiamide (DCD) on ammonia-oxidizing bacteria and archaeaina vegetable soil. *Appl. Microbiol. Biotechnol.* 99, 477–487. doi: 10.1007/s00253-014-6026-7

Cui, L., Li, D., Wu, Z., Xue, Y., Xiao, F., Zhang, L., et al. (2021). Effects of Nitrification inhibitors on soil nitrification and ammonia volatilization in three soils with different pH. *Agronomy* 11, 1674. doi: 10.3390/agronomy11081674

Desloover, J., Vlaeminck, S. E., Verstraete, W., and Boon, N. (2012). Strategies to mitigate N_2O emissions from biological nitrogen removal systems. *Curr. Opin. Biotechnol.* 23, 474–482. doi: 10.1016/j.copbio.2011.12.030

Di, H., and Cameron, K. C. (2011). Inhibition of ammonium oxidation by a liquid formulation of 3,4-Dimethylpyrazole phosphate (DMPP) compared with a dicyandiamide (DCD) solution in six new Zealand grazed grassland soils. *J. Soils Sediments* 11, 1032–1039. doi: 10.1007/s11368-011-0372-1

Dieckow, J., Bayer, C., Conceição, P. C., Zanatta, J. A., Martin-Neto, L., Milori, D. B. M., et al. (2009). Land use, tillage, texture and organic matter stock and composition in tropical and subtropical Brazilian soils. *Eur. J. Soil Sci.* 60, 240–249. doi: 10.1111/j.1365-2389.2008.01101.x

Dong, D., Kou, Y., Yang, W., Chen, G., and Xu, H. (2018). Effects of urease and nitrification inhibitors on nitrous oxide emissions and nitrifying/denitrifying microbial communities in a rainfed maize soil: a 6-year field observation. *Soil Tillage Res.* 180, 82–90. doi: 10.1016/j.still.2018.02.010

Fan, X., Chen, H., Yan, G., Ye, M., Yin, C., Li, T., et al. (2022). Niche Differentiation Among Canonical Nitrifiers and N2O Reducers Is Linked to Varying Effects of Nitrification Inhibitors DCD and DMPP in Two Arable Soils. *Microb. Ecol.* [Epub ahead of print]. doi: 10.1007/s00248-022-02006-8

Fan, X., Yin, C., Chen, H., Ye, M., Zhao, Y., Li, T., et al. (2019). The efficacy of 3, 4-dimethylpyrazole phosphate on N_2O emissions is linked to niche differentiation of ammonia oxidizing archaea and bacteria across four arable soils. *Soil Biol. Biochem.* 130, 82–93. doi: 10.1016/j.soilbio.2018.11.027

Fisk, L. M., Maccarone, L. D., Barton, L., and Murphy, D. V. (2015). Nitrapyrin decreased nitrification of nitrogen released from soil organic matter but not *amo*A gene abundance at high soil temperature. *Soil Biol. Biochem.* 88, 214–223. doi: 10.1016/j.soilbio.2015.05.029

Florio, A., Clark, I. M., Hirsch, P. R., Jhurreea, D., and Benedetti, A. (2014). Effects of the nitrification inhibitor 3,4-dimethylpyrazole phosphate (DMPP) on abundance and activity of ammonia oxidizers in soil. *Biol. Fertil. Soils* 50, 795–807. doi: 10.1007/s00374-014-0897-8

Gong, P., Zhang, L., Wu, Z., Chen, Z., and Chen, L. (2013). Responses of ammonia-oxidizing bacteria and archaea in two agricultural soils to nitrification inhibitors DCD and DMPP: a pot experiment. *Pedosphere* 23, 729–739. doi: 10.1016/S1002-0160(13)60065-X

Groenigen, K. J. V., Osenberg, C. W., and Hungate, B. A. (2011). Increased soil emissions of potent greenhouse gases under increased atmospheric CO_2. *Nature* 475, 214–216. doi: 10.1038/nature10176

Gu, Y., Mi, W., Xie, Y., Ma, Q., Wu, L., Hu, Z., et al. (2019). Nitrapyrin affects the abundance of ammonia oxidizers rather than community structure in a yellow clay paddy soil. *J. soils Sediments* 19, 872–882. doi: 10.1007/s11368-018-2075-3

Guardia, G., Marsden, K. A., Vallejo, A., Jones, D. L., and Chadwick, D. R. (2018). Determining the influence of environmental and edaphic factors on the fate of the nitrification inhibitors DCD and DMPP in soil. *Sci. Total Environ.* 624, 1202–1212. doi: 10.1016/j.scitotenv.2017.12.250

Hatzenpichler, R. (2012). Diversity, physiology, and niche differentiation of ammonia-oxidizing archaea. *Appl. Environ. Microbiol.* 78, 7501–7510. doi: 10.1128/aem.01960-12

Hauser, M., and Haselwandter, K. (1990). Degradation of dicyandiamide by soil bacteria. *Soil Biol. Biochem.* 22, 113–114. doi: 10.1016/0038-0717(90)90069-c

Hink, L., Gubry-Rangin, C., Nicol, G. W., and Prosser, J. I. (2018). The consequences of niche and physiological differentiation of archaeal and bacterial ammonia oxidisers for nitrous oxide emissions. *ISME J.* 12, 1084–1093. doi: 10.1038/s41396-017-0025-5

Hink, L., Nicol, G. W., and Prosser, J. I. (2017). Archaea produce lower yields of N_2O than bacteria during aerobic ammonia oxidation in soil. *Environ. Microbiol.* 19, 4829–4837. doi: 10.1111/1462-2920.13282

Hu, H., Chen, D., and He, J. (2015b). Microbial regulation of terrestrial nitrous oxide formation understanding the biological pathways for prediction of emission rates. *FEMS Microbiol. Rev.* 39, 729–749. doi: 10.1093/femsre/fuv021

Hu, H., Zhang, L., Dai, Y., Di, H., and He, J. (2013). pH-dependent distribution of soil ammonia oxidizers across a large geographical scale as revealed by high-throughput pyrosequencing. *J. Soils Sediments* 13, 1439–1449. doi: 10.1007/s11368-013-0726-y

Hu, H., Zhang, L., Yuan, C., Zheng, Y., Wang, J., Chen, D., et al. (2015a). The large-scale distribution of ammonia oxidizers in paddy soils is driven by soil pH, geographic distance, and climatic factors. *Front. Microbiol.* 6:938. doi: 10.3389/fmicb.2015.00938

Huang, R., Wu, Y., Zhang, J., Zhong, W., Jia, Z., and Cai, Z. (2011). Nitrification activity and putative ammonia-oxidizing archaea in acidic red soils. *J. Soils Sediments* 12, 420–428. doi: 10.1007/s11368-011-0450-4

Huang, T., Gao, B., Hu, X., Lu, X., Well, R., Christie, P., et al. (2014). Ammonia-oxidation as an engine to generate nitrous oxide in an intensively managed calcareous Fluvo-aquic soil. *Sci. Rep.* 4:3950. doi: 10.1038/srep03950

IPCC (2014). "Climate change 2014: synthesis report," in *Contribution of Working Groups I, II and III to the Fifth Assessment Report of the Intergovernmental Panel on Climate Change*, eds R. K. Pachauri and L. A. Meyer (Geneva: IPCC), 151.

Irigoyen, I., Muro, J., Azpilikueta, M., Aparicio-Tejo, P., and Lamsfus, C. (2003). Ammonium oxidation kinetics in the presence of nitrification inhibitors DCD and DMPP at various temperatures. *Soil Res.* 41, 1177–1183. doi: 10.1071/sr02144

Isobe, K., Ohte, N., Oda, T., Murabayashi, S., Wei, W., Senoo, K., et al. (2015). Microbial regulation of nitrogen dynamics along the hillslope of a natural forest. *Front. Environ. Sci.* 2:63. doi: 10.3389/fenvs.2014.00063

Jarvis, N., Larsbo, M., Roulier, S., Lindahl, A., and Persson, L. (2007). The role of soil properties in regulating non-equilibrium macropore flow and solute transport in agricultural topsoils. *Eur. J. Soil Sci.* 58, 282–292. doi: 10.1111/j.1365-2389.2006.00837.x

Jung, M. Y., Park, S. J., Min, D., Kim, J. S., Rijpstra, W. I. C., Damsté, J. S. S., et al. (2011). Enrichment and Characterization of an Autotrophic Ammonia-Oxidizing Archaeon of Mesophilic Crenarchaeal Group I.1a from an Agricultural Soil. *Appl. Environ. Microbiol.* 77, 8635–8647. doi: 10.1128/aem.05787-11

Jung, M. Y., Well, R., Min, D., Giesemann, A., Park, S. J., Kim, J. G., et al. (2014). Isotopic signatures of N_2O produced by ammonia-oxidizing archaea from soils. *ISME J.* 8, 1115–1125. doi: 10.1038/ismej.2013.205

Kirschke, T., Spott, O., and Vetterlein, D. (2019). Impact of urease and nitrification inhibitor on NH_4^+ and NO_3^- dynamic in soil after urea spring application under field conditions evaluated by soil extraction and soil solution sampling. *J. Plant Nutr. Soil Sci.* 182, 441–450. doi: 10.1002/jpln.201800513

Kleineidam, K., Kosmrlj, K., Kublik, S., Palmer, I., Pfab, H., Ruser, R., et al. (2011). Influence of the nitrification inhibitor 3, 4-dimethylpyrazole phosphate (DMPP) on ammonia-oxidizing bacteria and archaea in rhizosphere and bulk soil. *Chemosphere* 84, 182–186. doi: 10.1016/j.chemosphere.2011.02.086

Kögel-Knabner, I., Guggenberger, G., Kleber, M., Kandeler, E., Kalbitz, K., Scheu, S., et al. (2008). Organo-mineral associations in temperate soils: integrating biology, mineralogy, and organic matter chemistry. *J. Plant Nutr. Soil Sci.* 171, 61–82. doi: 10.1002/jpln.200700048

Kozlowski, J. A., Stieglmeier, M., Schleper, C., Klotz, M. G., and Stein, L. Y. (2016). Pathways and key intermediates required for obligate aerobic ammonia-dependent chemolithotrophy in bacteria and Thaumarchaeota. *ISME J.* 10, 1836–1845. doi: 10.1038/ismej.2016.2

Lam, S. K., Suter, S., Walker, C., Davies, R., Mosier, A. R., et al. (2018). Using urease and nitrification inhibitors to decrease ammonia and nitrous oxide emissions and improve productivity in a subtropical pasture. *Sci. Total Environ.* 644, 1531–1535. doi: 10.1016/j.scitotenv.2018.07.092

Lawton, T. J., Ham, J. W., Sun, T. L., and Rosenzweig, A. C. (2014). Structural conservation of the B subunit in the ammonia monooxygenase/particulate methane monooxygenase superfamily. *Proteins* 82, 2263–2267. doi: 10.1002/prot.24535

Lazcano, C., Zhu-Barker, X., and Decock, C. (2021). Effects of organic fertilizers on the soil microorganisms responsible for N_2O emissions: a review. *Microorganisms* 9:983. doi: 10.3390/microorganisms9050983

Leininger, S., Urich, T., Schloter, M., Schwark, L., Qi, J., Nicol, G. W., et al. (2006). Archaea predominate among ammonia-oxidizing prokaryotes in soils. *Nature* 442, 806–809. doi: 10.1038/nature04983

Li, Y., Chapman, S. J., Nicol, G. W., and Yao, H. (2018). Nitrification and nitrifiers in acidic soils. *Soil Biol. Biochem.* 116, 290–301. doi: 10.1016/j.soilbio.2017.10.023

Liu, R., Hayden, H. L., Hu, H., He, J., Suter, H., and Chen, D. (2017). Effects of the nitrification inhibitor acetylene on nitrous oxide emissions and ammonia-oxidizing microorganisms of different agricultural soils under laboratory incubation conditions. *Appl. Soil Ecol.* 119, 80–90. doi: 10.1016/j.apsoil.2017.05.034

Liu, R., Hayden, H., Suter, H., He, J., and Chen, D. (2015). The effect of nitrification inhibitors in reducing nitrification and the ammonia oxidizer population in three contrasting soils. *J. Soils Sediments* 15, 1113–1118. doi: 10.1007/s11368-015-1086-6

Liu, R., Hayden, H., Suter, H., Hu, H., Lam, S. K., He, J., et al. (2016). The effect of temperature and moisture on the source of N_2O and contributions from ammonia oxidizers in an agricultural soil. *Biol. Fertil. Soils* 53, 141–152. doi: 10.1007/s00374-016-1167-8

Lu, L., Han, W., Zhang, J., Wu, Y., Wang, B., Lin, X., et al. (2012). Nitrification of archaeal ammonia oxidizers in acid soils is supported by hydrolysis of urea. *ISME J.* 6, 1978–1984. doi: 10.1038/ismej.2012.45

Luo, Y., Hui, D., and Zhang, D. (2006). Elevated CO_2 stimulates net accumulations of carbon and nitrogen in land ecosystems: a meta-analysis. *Ecology* 87, 53–63. doi: 10.1890/04-1724

Mathieu, O., Hénault, C., Lévêque, J., Baujard, E., Milloux, M. J., and Andreux, F. (2006). Quantifying the contribution of nitrification and denitrification to the nitrous oxide flux using ^{15}N tracers. *Environ. Pollut.* 144, 933–940. doi: 10.1016/j.envpol.2006.02.005

McCarty, G. W. (1999). Modes of action of nitrification inhibitors. *Biol. Fertil. Soils* 29, 1–9. doi: 10.1007/s003740050518

Menéndez, S., Barrena, I., Setien, I., González-Murua, C., and Estavillo, J. M. (2012). Efficiency of nitrification inhibitor DMPP to reduce nitrous oxide emissions under different temperature and moisture conditions. *Soil Biol. Biochem.* 53, 82–89. doi: 10.1016/j.soilbio.2012.04.026

Menéndez, S., López-Bellido, R. J., Benítez-Vega, J., González-Murua, C., López-Bellido, L., and Estavillo, J. M. (2008). Long-term effect of tillage, crop rotation and N fertilization to wheat on gaseous emissions under rainfed Mediterranean conditions. *Eur. J. Agron.* 28, 559–569. doi: 10.1016/j.eja.2007.12.005

Monaghan, R. M., Smith, L. C., and de Klein, C. A. M. (2013). The effectiveness of the nitrification inhibitor dicyandiamide (DCD) in reducing nitrate leaching and nitrous oxide emissions from a grazed winter forage crop in southern New Zealand. *Agric. Ecosyst. Environ.* 175, 29–38. doi: 10.1016/j.agee.2013.04.019

Morimoto, S., Hayatsu, M., Hoshino, Y. T., Nagaoka, K., Yamazaki, M., Karasawa, T., et al. (2011). Quantitative analyses of ammonia-oxidizing archaea (AOA) and ammonia-oxidizing bacteria (AOB) in fields with different soil types. *Microbes Environ.* 26, 248–253. doi: 10.1264/jsme2.me11127

Morkved, P. T., Dorsch, P., and Bakken, L. R. (2007). The N_2O product ratio of nitrification and its dependence on long-term changes in soil pH. *Soil Biol. Biochem.* 39, 2048–2057. doi: 10.1016/j.soilbio.2007.03.006

Nauer, P. A., Fest, B. J., Visser, L., and Arndt, S. K. (2018). On-farm trial on the effectiveness of the nitrification inhibitor DMPP indicates no benefits under commercial Australian farming practices. *Agric. Ecosyst. Environ.* 253, 82–89. doi: 10.1016/j.agee.2017.10.022

Neufeld, J. D., and Knowles, R. (1999). Inhibition of nitrifiers and methanotrophs from an agricultural humisol by allylsulfide and its implications for environmental studies. *Appl. Environ. Microbiol.* 65, 2461–2465. doi: 10.1128/aem.65.6.2461-2465.1999

Okano, Y., Hristova, K. R., Leutenegger, C. M., Jackson, L. E., Denison, R. F., Gebreyesus, B., et al. (2014). Application of real-time PCR to study effects of ammonium on population size of ammonia-oxidizing bacteria in soil. *Appl. Environ. Microbiol.* 70, 1008–1016. doi: 10.1128/aem.70.2.1008-1016.2004

Pereira, J., Fangueiro, D., Chadwick, D. R., Misselbrook, T. H., Coutinho, J., and Trindade, H. (2010). Effect of cattle slurry pre-treatment by separation and addition of nitrification inhibitors on gaseous emissions and N dynamics: a laboratory study. *Chemosphere* 79, 620–627. doi: 10.1016/j.chemosphere.2010.02.029

Prosser, J. I., and Nicol, G. W. (2008). Relative contributions of archaea and bacteria to aerobic ammonia oxidation in the environment. *Environ. Microbiol.* 10, 2931–2941. doi: 10.1111/j.1462-2920.2008.01775.x

Prosser, J. I., and Nicol, G. W. (2012). Archaeal and bacterial ammonia-oxidisers in soil: the quest for niche specialisation and differentiation. *Trends Microbiol.* 20, 523–531. doi: 10.1016/j.tim.2012.08.001

Ravishankara, A. R., Daniel, J. S., and Portmann, R. W. (2009). Nitrous Oxide (N_2O): the Dominant Ozone-Depleting Substance Emitted in the 21st Century. *Science* 326, 123–125. doi: 10.1126/science.1176985

Rosenberg, M. S., Adams, D. C., and Gurevitch, J. (2000). *MetaWin (Version 2)*. Sunderland: Sinauer Associates.

Rowlings, D. W., Scheer, C., Liu, S., and Grace, P. R. (2016). Annual nitrogen dynamics and urea fertilizer recoveries from a dairy pasture using ^{15}N: effect of nitrification inhibitor DMPP and reduced application rates. *Agric. Ecosyst. Environ.* 216, 216–225. doi: 10.1016/j.agee.2015.09.025

Schleper, C., and Nicol, G. W. (2010). Ammonia-oxidising archaea: physiology, ecology and evolution. *Adv. Microb. Physiol.* 57, 1–41. doi: 10.1016/b978-0-12-381045-8.00001-1

Sha, Z., Ma, X., Wang, J., Lu, T., Li, Q., Misselbrook, T., et al. (2020). Effect of N stabilizer on fertilizer-N fate in soil-crop system: a meta-analysis. *Agric. Ecosyst. Environ.* 290:106763. doi: 10.1016/j.agee.2019.106763

Shaw, L. J., Nicol, G. W., Smith, Z., Fear, J., Prosser, J. I., and Baggs, E. M. (2006). Nitrosospira spp. can produce nitrous oxide via a nitrifier denitrification pathway. *Environ. Microbiol.* 8, 214–222. doi: 10.1111/j.1462-2920.2005.00882.x

Shen, T., Stieglmeier, M., Dai, J., Urich, T., and Schleper, C. (2013). Responses of the terrestrial ammonia-oxidizing archaeon Ca. Nitrososphaera viennensis and the ammonia-oxidizing bacterium Nitrosospira multiformis to nitrification inhibitors. *FEMS Microbiol. Lett.* 344, 121–129. doi: 10.1111/1574-6968.12164

Shi, X., Hu, H., Muller, C., He, J., Chen, D., and Suter, H. (2016). Effects of the nitrification inhibitor 3,4-dimethylpyrazole phosphate on nitrification and nitrifiers in two contrasting agricultural soils. *Appl. Environ. Microbiol.* 82, 5236–5248. doi: 10.1128/aem.01031-16

Shi, X., Hu, H., Zhu-Barker, X., Hayden, H., Wang, J., Suter, H., et al. (2017). Nitrifier-induced denitrification is an important source of soil nitrous oxide and can be inhibited by a nitrification inhibitor 3, 4-dimethylpyrazole phosphate. *Environ. Microbiol.* 19, 4851–4865. doi: 10.1111/1462-2920.13872

Sidhu, P. K., Taggert, B. I, Chen, D., and Wille, U. (2021). Degradation of the Nitrification Inhibitor 3,4-Dimethylpyrazole Phosphate in Soils: indication of Chemical Pathways. *Agric. Sci. Technol.* 1, 540–549. doi: 10.1021/acsagscitech.1c00150

Stieglmeier, M., Mooshammer, M., Kitzler, B., Wanek, W., Zechmeister-Boltenstern, S., Richter, A., et al. (2014). Aerobic nitrous oxide production through N-nitrosating hybrid formation in ammonia-oxidizing archaea. *ISME J.* 8, 1135–1146. doi: 10.1038/ismej.2013.220

Tao, R., Wakelin, S. A., Liang, Y., and Chu, G. (2017). Response of ammonia-oxidizing archaea and bacteria in calcareous soil to mineral and organic fertilizer application and their relative contribution to nitrification. *Soil Biol. Biochem.* 114, 20–30. doi: 10.1016/j.soilbio.2017.06.027

Tolar, B., Herrmann, J., Bargar, J. R., Bedem, H. V. D., Wakatsuki, S., and Francis, C. A. (2017). Integrated structural biology and molecular ecology of N-cycling enzymes from ammonia-oxidizing archaea. *Environ. Microbiol. Rep.* 9, 484–491. doi: 10.1111/1758-2229.12567

Tourna, M., Stieglmeier, M., Spang, A., Könneke, M., Schintlmeister, A., Urich, T., et al. (2011). Nitrososphaera viennensis, an ammonia oxidizing archaeon from soil. *Proc. Natl. Acad. Sci. U.S.A.* 108, 8420–8425. doi: 10.1073/pnas.1013488108

Vinzent, B., Fuss, R., Maidl, F. X., and Hülsbergen, K. J. (2018). N_2O emissions and nitrogen dynamics of winter rapeseed fertilized with different N forms and a nitrification inhibitor. *Agric. Ecosyst. Environ.* 259, 86–97. doi: 10.1016/j.agee.2018.02.028

Wang, J., Zhang, L., Lu, Q., Raza, W., Huang, Q., and Shen, Q. (2014). Ammonia oxidizer abundance in paddy soil profile with different fertilizer regimes. *Appl. Soil Ecol.* 84, 38–44. doi: 10.1016/j.apsoil.2014.06.009

Wang, X., Yan, B., Fan, B., Shi, L., and Liu, G. (2018). Temperature and soil microorganisms interact to affect Dodonaea viscosa growth on mountainsides. *Plant Ecol.* 219, 759–774. doi: 10.1007/s11258-018-0832-4

Wang, Y., Guo, J., Vogt, R. D., Mulder, J., Wang, J., Zhang, X., et al. (2018). Soil pH as the chief modifier for regional nitrous oxide emissions: new evidence and implications for global estimates and mitigation. *Glob. Change Biol.* 24, e617–e626. doi: 10.1111/gcb.13966

Wu, D., Zhao, Z., Han, X., Meng, F., Wu, W., Zhou, M., et al. (2018). Potential dual effect of nitrification inhibitor 3, 4-dimethylpyrazole phosphate on nitrifier denitrification in the mitigation of peak N_2O emission events in North China Plain cropping system. *Soil Biol. Biochem.* 121, 147–153. doi: 10.1016/j.soilbio.2018.03.010

Xia, F., Wang, J., Zhu, T., Zou, B., Rhee, S. K., and Quan, Z. (2018). Ubiquity and Diversity of Complete Ammonia Oxidizers (Comammox). *Appl. Environ. Microbiol.* 84:e01390–18. doi: 10.1128/aem.01390-18

Xia, W., Zhang, C., Zeng, X., Feng, Y., Weng, J., Lin, X., et al. (2011). Autotrophic growth of nitrifying community in an agricultural soil. *ISME J.* 5, 1226–1236. doi: 10.1038/ismej.2011.5

Xu, J., Zhu, T., Xue, W., Ni, D., Sun, Y., Yang, J., et al. (2019). Influences of nitrification inhibitor 3, 4-dimethylpyrazole phosphate (DMPP) and application method on nitrogen dynamics at the centimeter-scale. *Eur. J. Soil Biol.* 90, 44–50. doi: 10.1016/j.ejsobi.2018.12.004

Yang, L., Zhu, G., Ju, X., and Liu, R. (2021). How nitrification-related N_2O is associated with soil ammonia oxidizers in two contrasting soils in China? *Sci. Total Environ.* 770:143212. doi: 10.1016/j.scitotenv.2020.143212

Yin, C., Fan, X., Chen, H., Jiang, Y., Ye, M., Yan, G., et al. (2021). 3, 4-Dimethylpyrazole phosphate is an effective and specific inhibitor of soil ammonia-oxidizing bacteria. *Biol. Fertil. Soils* 57, 753–766. doi: 10.1007/s00374-021-01565-1

Ying, J., Li, X., Wang, N., Lan, Z., He, J., and Bai, Y. (2017). Contrasting effects of nitrogen forms and soil pH on ammonia oxidizing microorganisms and their responses to long–term nitrogen fertilization in a typical steppe ecosystem. *Soil Biol. Biochem.* 107, 10–18. doi: 10.1016/j.soilbio.2016.12.023

You, L., Ros, G. H., Chen, Y., Yang, X., Cui, Z., Liu, X., et al. (2022). Global meta-analysis of terrestrial nitrous oxide emissions and associated functional genes under nitrogen addition. *Soil Biol. Biochem.* 165:108523. doi: 10.1016/j.soilbio.2021.108523

Yu, Q., Ma, J., Zou, P., Lin, H., Sun, W., Yin, J., et al. (2015). Effects of combined application of organic and inorganic fertilizers plus nitrification inhibitor DMPP on nitrogen runoff loss in vegetable soils. *Environ. Sci. Pollut. Res.* 22, 472–481. doi: 10.1007/s11356-014-3366-x

Zerulla, W., Barth, T., Dressel, J., Erhardt, K., von-Locquenghien, K. H., Pasda, G., et al. (2001). 3,4-Dimethylpyrazole phosphate (DMPP)-a new nitrification inhibitor for agriculture and horticulture. *Biol. Fertil. Soils* 34, 79–84. doi: 10.1007/s003740100380

Zhang, A., Liu, Y., Pan, G., Hussain, Q., Li, L., Zheng, J., et al. (2012b). Effect of biochar amendment on maize yield and greenhouse gas emissions from a soil organic carbon poor calcareous loamy soil from Central China Plain. *Plant Soil* 351, 263–275. doi: 10.1007/s11104-011-0957-x

Zhang, L., Hu, H., Shen, J., and He, J. (2012a). Ammonia-oxidizing archaea have more important role than ammonia-oxidizing bacteria in ammonia oxidation of strongly acidic soils. *ISME J.* 6, 1032–1045. doi: 10.1038/ismej.2011.168

Zhang, Z., Gao, Q., Yang, J., Li, L., Li, Y., Liu, J., et al. (2020). Effect of soil organic matter on adsorption of nitrification inhibitor nitrapyrin in black soil. *Commun. Soil Sci. Plant Anal.* 51, 883–895. doi: 10.1080/00103624.2020.1744636

Zhou, X., Wang, S., Ma, S., Zheng, X., Wang, Z., and Lu, C. (2020). Effects of commonly used nitrification inhibitors-dicyandiamide (DCD), 3,4-dimethylpyrazole phosphate (DMPP), and nitrapyrin-on soil nitrogen dynamics and nitrifiers in three typical paddy soils. *Geoderma* 380:114637. doi: 10.1016/j.geoderma.2020.114637

Zhu, G., Song, X., Ju, X., Zhang, J., Müller, C., Sylvester-Bradley, R., et al. (2019). Gross N transformation rates and related N_2O emissions in Chinese and UK agricultural soils. *Sci. Total Environ.* 666, 176–186. doi: 10.1016/j.scitotenv.2019.02.241

frontiers | Frontiers in Microbiology

TYPE Original Research
PUBLISHED 23 September 2022
DOI 10.3389/fmicb.2022.1002009

OPEN ACCESS

EDITED BY
Yong Li,
Zhejiang University,
China

REVIEWED BY
Duntao Shu,
Northwest A&F University, China
Yingyi Fu,
Zhejiang University,
China

*CORRESPONDENCE
Qiang Chai
chaiq@gsau.edu.cn

SPECIALTY SECTION
This article was submitted to Terrestrial Microbiology, a section of the journal Frontiers in Microbiology

RECEIVED 24 July 2022
ACCEPTED 01 September 2022
PUBLISHED 23 September 2022

CITATION
Xu K, Hu F, Fan Z, Yin W, Niu Y, Wang Q and Chai Q (2022) Delayed application of N fertilizer mitigates the carbon emissions of pea/maize intercropping *via* altering soil microbial diversity. *Front. Microbiol.* 13:1002009. doi: 10.3389/fmicb.2022.1002009

Delayed application of N fertilizer mitigates the carbon emissions of pea/maize intercropping *via* altering soil microbial diversity

Ke Xu[1,2], Falong Hu[1,2], Zhilong Fan[1,2], Wen Yin[1,2], Yining Niu[2], Qiming Wang[1,2] and Qiang Chai[1,2]*

[1]College of Agronomy, Gansu Agricultural University, Lanzhou, China, [2]State Key Laboratory of Aridland Crop Science, Lanzhou, China

Strategies to reduce carbon emissions have been a hotspot in sustainable agriculture production. The delayed N fertilizer application had the potential to reduce carbon emissions in pea (*Pisum sativum* L.)/maize (*Zea mays* L.) intercropping, but its microbial mechanism remains unclear. In this study, we investigated the effects of delayed N fertilizer application on CO_2 emissions and soil microbial diversity in pea/maize intercropping. The soil respiration (Rs) rates of intercropped pea and intercropped maize were decreased by 24.7% and 25.0% with delayed application of N fertilizer, respectively. The total carbon emissions (TCE) of the pea/maize intercropping system were also decreased by 21.1% compared with that of the traditional N fertilizer. Proteobacteria, Bacteroidota, and Chloroflexi were dominant bacteria in pea and maize strips. Heatmap analysis showed that the soil catalase activity at the pea flowering stage and the soil $NH_4^+ - N$ at the maize silking stage contributed more to the variations of bacterial relative abundances than other soil properties. Network analysis demonstrated that Rs was positively related to the relative abundance of Proteobacteria and Bacteroidota, while negatively related to the relative abundance of Chloroflexi in the pea/maize intercropping system. Overall, our results suggested that the delayed application of N fertilizer combined with the pea/maize intercropping system altered soil bacterial community diversity, thereby providing novel insights into connections between soil microorganisms and agricultural carbon emissions.

KEYWORDS

N fertilizer postponing application, pea/maize intercropping, soil properties, soil microbial diversity, carbon emission

Introduction

Agricultural production activities are the major source of CO_2, N_2O, and CH_4 emissions, accounting for approximately 14% of the total worldwide (IPCC, 2014). Although agricultural N_2O and CH_4 emissions contribute a higher percentage than CO_2, reducing CO_2 to net-zero by 2050 is imperative due to its long-lasting effect (IPCC, 2018; Lynch et al., 2021).

Additionally, CO_2 is the main source of agricultural GHGs in arid regions of China (Qu et al., 2013). Therefore, exploring ameliorated agronomic practices with low carbon emissions is an urgent technique for the sustainability of modern agriculture.

Agricultural CO_2 emissions can be decreased by optimizing the management practices of cropping systems. Intercropping, cultivating multiple crop species in a field, can boost crop productivity (Li et al., 2001), improve resource use efficiency (Yin et al., 2015; Gou et al., 2017), and most importantly, decrease carbon emissions (Qin et al., 2013; Chai et al., 2014; Wang X. et al., 2021). Among various cropping systems, maize-based intercropping models, such as maize-soybean, maize-wheat, maize-rape, maize-potato, and maize-pea can achieve lower carbon emissions compared to monocropping patterns (Chai et al., 2014; Shen et al., 2018; Sun et al., 2021; Wang X. et al., 2021; Yin et al., 2022). In particular, pea/maize intercropping, widely practiced in northwestern China (Zhao et al., 2016), has been demonstrated to reduce carbon emissions by 31% compared to monoculture maize (Chai et al., 2014). Therefore, further research on mechanisms to mitigate CO_2 emissions in the cereal-legume intercropping system has emerged as a priority point in modern agricultural production.

Intercropping improves microbial diversity and alters soil microbial community composition by indirectly changing soil properties (Song et al., 2007; Gong et al., 2019). Soil microorganisms perform various ecological functions, including N and C cycling, profoundly impacting soil productivity and sustainability (Theuerl and Buscot, 2010; Nimmo et al., 2013). With the development of bioinformatics, the diversity and structure of microorganism have been widely used to indicate their ecological function and changes in soil quality (Chu et al., 2007). Since the microorganisms involved in soil carbon degradation are extremely abundant, the composition of microbial community structures can explain soil degradation (Nannipieri et al., 2017). It is still a research hotspot to explore the role of soil microorganisms of agricultural greenhouse gas (GHG) emissions (Jiang et al., 2021). However, there is little research on how intercropping pattern reduces soil GHG emissions by altering soil microorganisms. Fertilization management, another main factor of causing the GHG on farmland, can greatly influence microbial diversity, soil properties, and enzyme activity (Luo et al., 2018; Huang et al., 2020). The application of the steel slag and biochar has altered the composition of soil bacterial communities, thus mitigating CO_2 emissions in paddies (Chen et al., 2016; Wang et al., 2020). Moreover, biochar and controlled irrigation can be applied to mitigate GHG emissions and mediate the structures of soil microbial communities (Jiang et al., 2021). In addition, organic fertilizer combined with monotypic controlled-release urea can reduce soil CO_2 emissions by satisfying plant and soil microbial C and N demands (Zhang et al., 2020). However, little information is available about the underlying microbial mechanisms for integrating N fertilizer into the intercropping system to reduce CO_2 emissions in agricultural ecosystems.

The association of legume and rhizobia is an effective N_2-fixing system that can reduce chemical fertilizer inputs and the negative impacts of agriculture on the environment. However, in practice, farmers often apply N fertilizer for pea-maize intercropping according to tactics of sole maize, which may restrict the growth of the two crops (Hu et al., 2020). Therefore, N fertilizer management needs to be optimized, which is paramount not only to meet the requirement of the early-maturing crop (pea) but also to attend to the later-maturing crop (maize). It has been demonstrated that in an optimized N management practice, the allocations at the jointing stage and 15-day post-silking stage are 1:3 and 2:2, which can boost system productivity of wheat/maize intercropping (Xu et al., 2021). According to the previous study by our team, the combination of N fertilizer management (jointing top-dress N at 45 kg N ha^{-1} and 15-day post-flowering top-dress N at 135 kg N ha^{-1}) and pea/maize intercropping shows the best effect on CO_2 emission mitigation, mainly regulating the content of inorganic N, soil moisture, and soil temperature. However, little microbial information was available on the effect of optimizing N management on the carbon emission of pea/maize intercropping.

Based on the previous studies related to soil carbon emissions and microbes in other ecosystems, we hypothesized that the delayed application of N-fertilizer could alter the carbon emission, mainly by modifying the compositions of soil bacterial communities. Thus, the objectives of this study were to (1) determine the effects of delayed N-fertilizer application and pea/maize intercropping on soil carbon emissions; (2) compare the responses of bacterial diversity and community composition to delayed N-fertilizer application and intercropping patterns; (3) evaluate the relationships between soil chemical properties, carbon emissions, and soil microbial communities.

Materials and methods

Site description

The experiments were conducted at the Oasis Agricultural Trial Station (37°30′N, 103°5′E, 1,776 m a.s.l.) of Gansu Agricultural University, Gansu Province, China. The long-term (1960–2020) mean annual air temperature is 7.3°C, with a mean annual sunshine duration of 2,945 h, and an accumulated temperature (above 10°C) of 2,985°C. Abundant heat and light resources provide advantages for developing intercropping, and pea/maize intercropping is the most typical intercropping pattern (Chai et al., 2021). The soil at the experimental site is Aridisol 50 and the properties of the topsoil (0–30 cm) are as follows: pH (1:2.5 soil, water) 8.0, soil organic matter 11.3 g kg^{-1}, soil bulk density 1.44 g cm^{-3}, total N 0.94 g kg^{-1}, available phosphorous (P; Olsen-P) 29.2 mg kg^{-1}, and available potassium (K; NH4OAc-extractable-K) 152.6 mg kg^{-1}.

Experimental design

The experiment was a two-factor factorial experimental design in both seasons from 2019 to 2020, including cropping pattern and

delayed N fertilizer application. The cropping pattern was arranged in the main plots, including pea/maize intercropping (three rows of maize alternating with four rows of pea), sole planting of maize, and sole planting of pea. The row spacing between crops in the treatments is shown in Supplementary Figure S1. Based on the treatment, delayed application of N-fertilizer was arranged in the subplots of the experiment, including three application treatments designed according to the main growth stages of maize [i.e., pre-planting, jointing stage (V6), pre-tasseling stage (V12), and 15-day post-silking stage (R2)]. Three kinds of N-fertilizer application for sole maize were applied at the rate of 360 kg ha^{-1}. The allocations at these four stages were 2:1:4:3 for N1, 2:2:4:2 for N2, and 2:3:4:1 for N3. Among them, N3 treatment was the conventional N input of maize production in the region. The application of N fertilizer for pea was at the rate of 90 kg ha^{-1}, in which 80% was base applied at sowing and 20% at flowering stage [i.e., jointing stage of maize (V6)]. The application of N fertilizer for pea/maize intercropping was calculated by the bandwidth ratio. The field experiment included seven treatments with tree replicates (Supplementary Table S1).

Field management

The maize cultivar "Xianyu 335" and the pea cultivar "Longwan 1" were used in the research. The planting densities were 90,000 and 1,800,000 plants ha^{-1} for monoculture maize and pea, respectively. For intercropping maize and pea, they were 52,000 and 760,000 plants ha^{-1}, respectively. In 2019, the pea was sowed on 30 March and maize on 19 April; the pea was harvested on 9 July and maize on 27 September. In 2020, the pea was sowed on 1 April and maize on 20 April; the pea was harvested on 9 July and maize on 27 September. Maize was covered by plastic films (0.01 mm thick and 120 cm wide) that are largely adopted in arid areas to conserve water and promote maize productivity (Gan et al., 2013).

Each experimental plot for intercropping was 34.2 m^2 (6 m × 5.7 m), and the sole cropping plot was 36 m^2 (6 m × 6 m). Each neighboring plot has a ridge 50 cm wide and 30 cm high to eliminate potential water movement. Chemical fertilizers, such as urea (46-0-0, N-P-K) and diammonium phosphate (18-46-0, N-P_2O_5-K_2O), were applied in the research. Phosphorus was applied to the soil before planting maize and pea each year, with application rates of 180 kg P_2O_5 ha^{-1} and 45 kg P_2O_5 ha^{-1}, respectively. Supplemental irrigation was applied to the experimental plot through the drip irrigation method owing to low precipitation (<156 mm annually) in this region. Except for the fertilizer application, other agronomic practices were kept uniform.

Soil sampling

At the full flowering stage of pea (PF) and silking stage of maize (MS), specifically on 5 June and 18 July 2019, five topsoil samples (0–20 cm) in an S-shaped sampling pattern were collected randomly in each field plot using an auger (5 cm in diameter) and then mixed thoroughly as a composite sample. The soil samples in the intercropping system were collected separately according to each crop strip. Then, each soil sample was sieved into two parts through a 2 mm mesh. A portion of topsoil samples was stored at −80°C for molecular analysis, while the other sample was air-dried and stored at room temperature before property analysis.

Soil properties

Soil organic matter (SOM) was determined by oxidizing with potassium dichromate (Zhang et al., 2020). Total N (TN) was measured using an Elementar vario MACRO cube (Elementar, Hanau, Hessen, Germany; Wang et al., 2020). Soil $NO_3^- - N$ and $NH_4^+ - N$ were extracted with 2 M KCl and analyzed using a continuous flow analyzer (Skalar, Breda, Netherlands; Wang J. et al., 2021). Labile organic matter (LOM) was measured by the potassium permanganate oxidation method (Xu et al., 2011). Soil catalase activity (CAT) was estimated according to the method of Nowak et al. (2004).

Soil respiration and total carbon emissions

Soil respiration was measured using an LI-8100A system (LI-COR, 4647 Superior Street Lincoln, Nebraska United States) with a proprietary 20 cm diameter polyvinyl chloride chamber. Specifically, Rs was measured every 2 h from 8:00 a.m. to18:00 p.m. on sunny days based on 15-day intervals before pea harvest and 20-day intervals after pea harvest to monitor seasonal shifts in soil CO_2 fluxes. The average data of measurement time represented CO_2 fluxes for 1 day. Measurements were taken for pea and maize strips, and the average of two strips was used for Rs in the intercropping plot (Supplementary Figure S1).

The TCE was calculated based on Rs by adopting the following formula (Zhai et al., 2011):

$$\mathrm{TCE} = \sum\left[\left(t_{i+1} - t_i\right)\frac{R_{si+1} + R_{si}}{2} \times 0.1584 \times 24\right] \times 0.2727 \times 10 \quad (1)$$

where t is days after the sowing stage, $i+1$ and i are the current and the last monitoring date, respectively; Rs is soil respiration (μmol CO_2 m^{-2} s^{-1}); 0.1584 converts mol CO_2 m^{-2} s^{-1} to g CO_2 m^{-2} h^{-1}; 0.2727 converts g CO_2 m^{-2} h^{-1} to g C m^{-2} h^{-1}; and 10 and 24 converts carbon emissions from g C m^{-2} h^{-1} to kg C ha^{-1}.

Soil DNA extraction, PCR amplification, and illumina sequencing

Microbial community DNA was extracted from 0.5 g samples (fresh soil) using the FastDNA® SPIN Kit for Soil (MP Biomedicals

Co., Ltd., Santa Ana, CA, United States) according to the manufacturer's instructions. The quality of DNA extraction was checked on a 1% agarose gel. The final DNA concentration and purification were determined with a NanoDrop 2000 UV–vis spectrophotometer (Thermo Scientific, Wilmington, United States).

The hypervariable region V3-V4 of the bacterial 16S rRNA gene was amplified with primer pairs 338F (5′-ACTCCTACGGG AGGCAGCAG-3′) and 806R (5′-GGACTACHVGGGTWTCT AAT-3′) by an ABI GeneAmp® 9700 PCR thermocycler (ABI, CA, United States). The PCR amplification of the 16S rRNA gene was performed under the following conditions: initial denaturation at 95°C for 3 min, followed by 27 cycles of denaturing at 95°C for 30 s, annealing at 55°C for 30 s, extension at 72°C for 45 s, single extension at 72°C for 10 min, and end at 4°C. The PCR mixtures contained 4 μl of 5 × *TransStart* FastPfu buffer, 2 μl of 2.5 mM dNTPs, 0.8 μl of forward primer (5 μM), 0.8 μl of reverse primer (5 μM), 0.4 μl of *TransStart* FastPfu DNA Polymerase, 10 ng of template DNA, and 20 μl of ddH_2O. The PCR product, extracted from 2% agarose gels, was purified by the AxyPrep DNA Gel Extraction Kit (Axygen Biosciences, Union City, CA, United States) according to the manufacturer's instructions and quantified using Quantus™ Fluorometer (Promega, United States). The PCR reaction was performed in triplicate.

Each purified PCR was sequenced on the Illumina MiSeq PE 300 platform (San Diego, CA, United States) at Majorbio Bio-Pharm Technology Co., Ltd. (Shanghai, China). The raw reads were deposited into the NCBI Sequence Read Archive (SRA) database (Accession Number: PRJNA842905).

Sequencing data analysis

The raw 16S rRNA sequencing reads were demultiplexed, quality-filtered using fastp version 0.20.0 (Chen et al., 2018), and merged by FLASH version 1.2.7 (Mago and Salzberg, 2011). Sequences were merged when they met the following criteria: (i) high-quality score ($Q \geq 50$); (ii) overlapping sequences longer than 10 bp; (iii) exact barcodes and primers. Operational taxonomic units (OTUs) based on ~97% similarity were clustered using UPARSE version 7.1 (Edgar, 2013). The taxonomy of each OTU representative sequence was identified by the Ribosomal Database Project (RDP) Classifier version 2.2 against the 16S rRNA database (silva138/16s-bacteria) using a confidence threshold of 0.7 (Wang et al., 2007).

Statistical analysis

The variance was analyzed by Duncan's multiple range tests at $p < 0.05$ with SPSS 25.0 software (SPSS Inc., Armonk, NY, United States). The data were analyzed using a one-way analysis of variance (ANOVA) for different treatments ($p < 0.05$), including soil carbon emissions, soil properties, and microbial characteristics.

Taxonomic alpha diversity was measured by the estimated community richness (Chao 1 index) and community diversity (Shannon index) by the Mothur software package (v.1.30.2). Non-metric multi-dimensional scaling (NMDS) based on the Bray-Curtis distance was calculated using the "vegan" package (v.3.3.1) in R and selected to refer to microbial beta diversity. The relative abundance at the phylum level was performed in Circos-0.67-7. In addition, heatmap analysis based on Spearman's correlation was applied using the "pheatmap" package in R v.3.3.1. Network analysis was completed in Cytoscape v3.7.1 (Top 50 dominant bacterial class; Spearman correlation coefficient > 0.5 and $p < 0.05$). Moreover, Origin 2021 and R language were used to draw figures.

Results

Seasonal dynamics of Rs

Pea strip

For both research years, the seasonal variation of Rs in pea strips was typically consistent (Figure 1). The average Rs of pea strips was significantly affected by cropping patterns ($p = 0.042$), N fertilizer applications ($p = 0.002$), and the interactions of the two factors ($p = 0.002$). The influence of pea/maize intercropping on Rs differed from that of sole pea. Compared to the sole pea, the 2-year average Rs of the intercropped pea strip was increased by 22.4% during co-growth periods and was decreased by17.5% after harvesting pea. In the whole growth period, the mean Rs of intercropped pea under N1 treatment was 6.8% lower than that of sole pea, while it was 3.2% and 16.7% higher under N2 and N3, respectively.

The Rs of intercropped pea with different fertilizer N management practices did not differ among years but varied by treatments. Compared to the N3 treatment, the N1 and N2 treatments decreased the average Rs by 25.1% and 14.6% during the pea-maize co-growth period, by 23.9% and 10.2% after harvesting pea, and by 24.7% and 12.9% throughout the growth period, respectively. Compared with the intercropped pea under N1 treatment, the sole pea decreased by 9.8% in the mean Rs during the pea-maize co-growth period but increased by 24.1% after pea harvest. As a result, sole pea increased the average Rs by 6.3% throughout the growth period.

Maize strip

The average Rs of maize strips was significantly affected by cropping patterns, N fertilizer applications ($p < 0.001$), and their interaction ($p = 0.022$). The Rs of maize strips was influenced by the intercropped pea (Figure 2). During the co-growth stage, Rs of the intercropped maize was 14.6%–21.1% lower than that of monocropping while 4.1%–7.4% higher than that of monocropping after harvesting pea. Throughout the period, the Rs of intercropped maize with N1, N2, and N3 treatments was 4.0%, 7.4%, and 6.1% lower than that of monocropping maize, respectively.

A similar trend was found in both cropping patterns, with the N1 treatment featuring the lowest Rs compared to N2 and N3 treatments. During the co-growth stage, N1 and N2 treatments

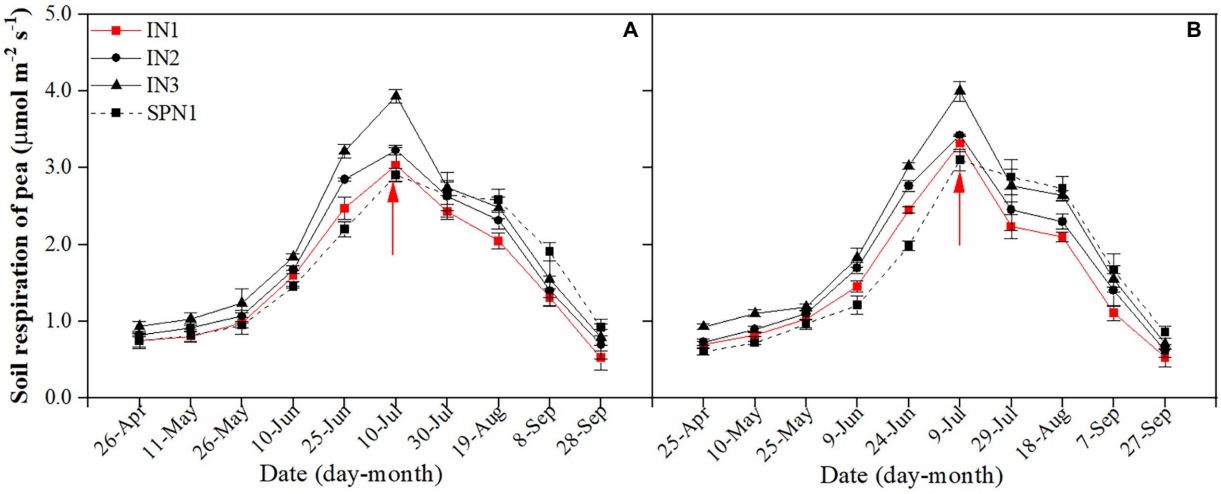

FIGURE 1
Seasonal dynamics of soil respiration of pea strips in 2019 **(A)** and 2020 **(B)**. I, pea/maize intercropping, SP, sole planting of pea. N1, N2, and N3 in the intercropping pattern represent the allocation of four-stage (sowing, jointing stage, pre-tasseling stage, and 15days post-silking stage) was 2:1:4:3, 2:2:4:2, and 2:3:4:1, respectively. N1 in sole pattern represents 80% base fertilizer + 20% topdressing fertilizer at flowering stage. Error bars indicate the standard deviation of three replications. The red arrow shows the harvest time of pea. The description keeps uniform in the following figures.

decreased Rs by 28.3% and 14.9%, 32.4% and 12.2% in intercropping and monocropping patterns compared to N3, respectively, with a similar reduction of 20.0% and 11.6%, 22.2% and 10.2% after pea harvest. Regarding average Rs throughout the growing season, N1 and N2 treatments reduced Rs of intercropping by 25.0% and 12.7% compared to N3, respectively, with a similar reduction of monocropping by 27.6% and 11.3%.

Total carbon emissions

The TCE was significantly influenced by cropping systems, N management practices, and their interactions ($p < 0.001$; Table 1). By comparison the three cropping patterns, the TCE of pea/maize intercropping was 31.1%–58.8% higher than that of monoculture pea but 31.0%–35.0% lower than monoculture maize. The carbon reduction effect was highly significant in N1 and N2, compared to N3 treatment, reducing the TCE of the intercropping system by 21.1% and 10.9% and the monoculture maize by 23.2% and 9.5%, respectively.

In terms of TCE in pea and maize strips of the intercropping pattern, maize strips emitted 63.5% more carbon than pea strips, demonstrating that maize strips contribute more to TCE in the intercropping pattern. Additionally, the TCE of the three cropping patterns showed that the contribution before pea harvest was lower than that after harvest (Supplementary Figure S2). In the intercropping pattern, the TCE before pea harvest accounted for 41.1% and 58.8% after pea harvest. The N1 and N2 treatments decreased the TCE of the intercropping pattern by 27.9% and 14.4% before pea harvest and by 16.7% and 8.6% after harvest, compared to N3 treatment, respectively.

Soil properties of pea and maize strip

Pea strip

The soil $NO_3^- - N$, $NH_4^+ - N$, TN, and CAT at the PF stage were significantly influenced by the cropping system, N management practices, and their interactions, while just CAT was influenced at the MS stage ($p < 0.05$; Table 2). Soil $NO_3^- - N$, $NH_4^+ - N$, TN, and CAT were increased by 31.2%, 19.1%, 5.7%, and 25.0% in the intercropping pattern compared with sole pea at the PF stage but were decreased by 10.4%, 31.8%, 5.2%, and 14.1% at the MS stage. The pea/maize intercropping pattern increased soil SOM and LOM compared with monocropping plots during the period. In the pea/maize intercropping pattern, different levels of N application influenced the soil properties, which was remarkably significant at the high fertilizer level (N3) than at the low fertilizer level (N1).

Maize strip

The cropping patterns significantly influenced $NO_3^- - N$, $NH_4^+ - N$, SOM, and CAT ($p < 0.05$), and N fertilizer application significantly influenced all soil properties at the PF stage ($p < 0.05$; Table 3). At the MS stage, cropping patterns and N fertilizer application significantly influenced LOM and CAT ($p < 0.05$). Their interaction did not influence soil properties during the period ($p > 0.05$). In general, compared to the sole maize, the intercropping pattern decreased the contents of $NO_3^- - N$ and $NH_4^+ - N$ by 11.1% and 15.4% at the PF stage and by 12.4% and 9.4% at the MS stage, respectively. However, the content of TN, SOM, LOM, and CAT in intercropping pattern were 1.7%, 7.5%, 10.6%, and 33.5% lower than that of sole maize at the PF stage but were 3.5%, 2.6%, 3.2%, and 13.5% higher at the MS stage. The influence of different levels of N application on soil properties was

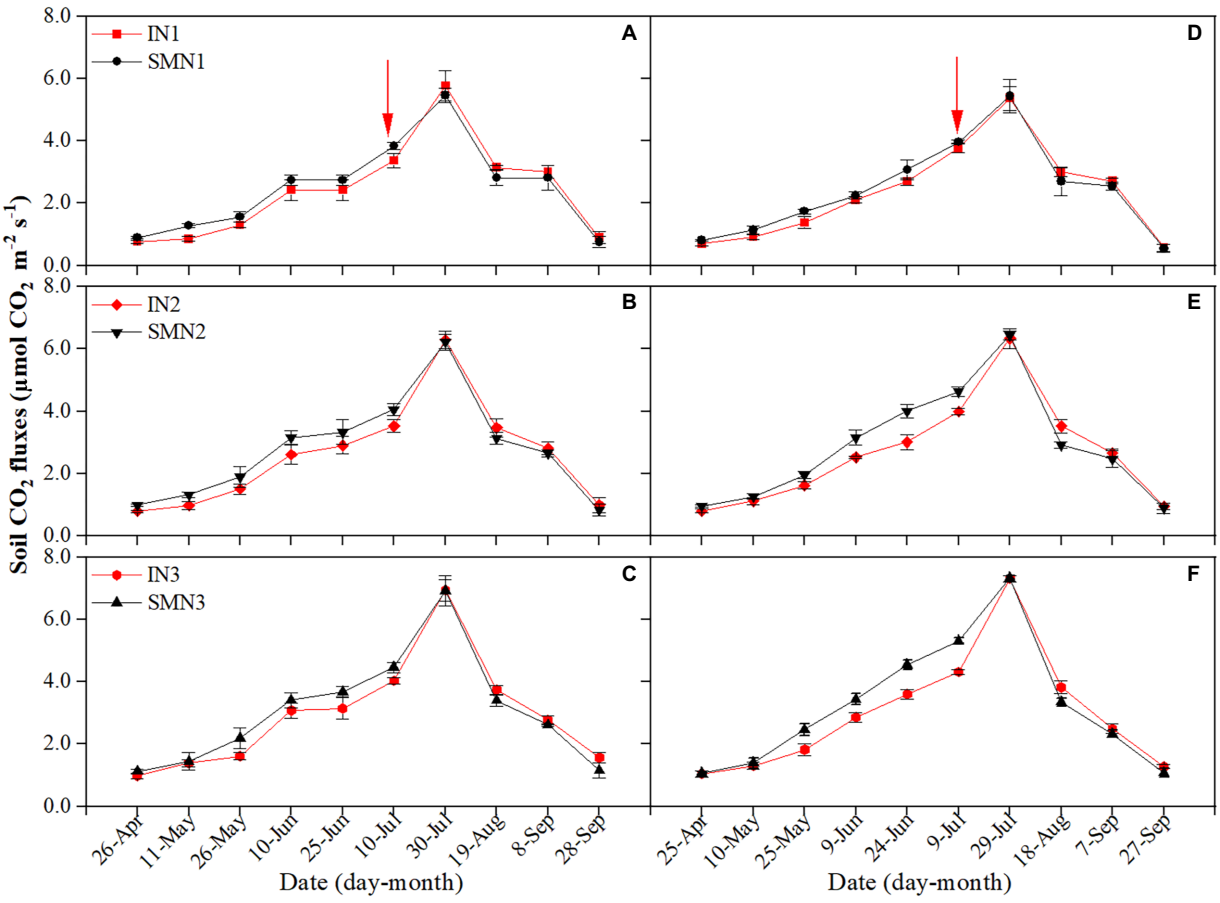

FIGURE 2
Seasonal dynamics of soil respiration of maize strips in 2019 **(A–C)** and 2020 **(D–F)**. I, pea/maize intercropping, SM, sole planting of maize. N1, N2, and N3 represent the allocation of four-stage (sowing, jointing stage, pre-tasseling stage, and 15days post-silking stage) was 2:1:4:3, 2:2:4:2, and 2:3:4:1, respectively. Error bars indicate the standard deviation of three replications. The red arrow shows the harvest time of pea.

consistent, with the N1 level being lower than N2 and N3. On average, N1 treatment decreased the content of $NO_3^- - N$, $NH_4^+ - N$, TN, SOM, LOM, and CAT in pea/maize intercropping by 22.0%, 13.7%, 5.1%, 14.0%, 5.4%, and 27.4% compared to N3, respectively. Similarly, it decreased by 16.6%, 9.4%, 7.5%, 7.7%, 4.6%, and 26.5% in the monoculture maize, respectively.

Bacterial community diversity

Bacterial alpha diversity

After quality sequencing, both bacterial communities (a total of 1,271,742,085 sequences) were obtained using the 338F/806R (bacterial 16S rRNA) primer sets in all soil samples. The number of bacterial sequences ranged from 213 to 535 per sample (mean = 416.9). The datasets were rarefied to 3,049,811 sequences for downstream analysis of bacterial sequences.

The OTU level approach was used to calculate the microbial diversity under different treatments. Variance analysis showed that cropping patterns significantly affected bacterial richness index (Chao 1) and diversity index (Shannon; $p < 0.05$; Table 4). The pea/maize intercropping pattern reduced OTUs but increased the Shannon and Chao 1 indices compared with the sole pea at the PF stage. However, the intercropping pattern increased OTUs and the Chao 1 index at the MS stage. In addition, N1 treatment in the intercropping pattern decreased OTUs, Shannon, and Chao1 indices at the PF stage compared to N3; it increased the Shannon and Chao1 indices at the MS stage.

The cropping system significantly affected the bacteria richness index (OTUs), N management practices significantly affected the diversity index (Shannon; $p < 0.01$), and their interactions did not show an influence ($p > 0.05$; Table 5). Compared with the monocropping maize, the intercropping pattern increased the Shannon and Chao1 indices at the PF stage. However, at the MS stage, OTUs were higher under the intercropping pattern than under the monocropping pattern. Compared with the N3 treatment, N1 treatment in the intercropping pattern increased OTUs by 2.9% at the PF stage and increased OTUs and the Chao1 index by 3.7% and 0.8% at the MS stage. Additionally, OTUs and the Shannon index were 1.1% and 1.7% higher in the sole planting pattern than under N3 treatment at the PF stage, whereas the Shannon and Chao1 were 1.5% and 6.7% higher at the MS stage.

TABLE 1 Total carbon emission (TCE; kgha^{-1}) of pea and maize in intercropping and monoculture patterns affected by N management practice in 2019 and 2020.

Treatments[a]	2019			2020		
	Maize	Pea	Total[c]	Maize	Pea	Total
Intercropping						
IN1	4,329±83e[b]	2,380 ± 48c	3,354 ± 66f	4,097 ± 61d	2,352 ± 33b	3,225 ± 27f
IN2	4,653 ± 116d	2,619 ± 19b	3,636 ± 63e	4,494 ± 91c	2,599 ± 61b	3,547 ± 71e
IN3	5,187 ± 103b	2,938 ± 112a	4,063 ± 94d	4,873 ± 47b	2,943 ± 137a	3,908 ± 87d
Monoculture						
SMN1	4,438 ± 94e	–	4,438 ± 94c	4,178 ± 142d	–	4,178 ± 142c
SMN2	4,897 ± 38c	–	4,897 ± 38b	4,802 ± 91b	–	4,802 ± 91b
SMN3	5,364 ± 76a	–	5,364 ± 76a	5,259 ± 104a	–	5,259 ± 104a
SPN1	–	2,533 ± 104bc	2,533 ± 104g	–	2,487 ± 161b	2,487 ± 161g
Significance (p value)						
Cropping pattern	0.001	0.020	0.000	0.000	0.036	0.000
N management practice (N)	0.000	0.001	0.000	0.000	0.007	0.000
C×N	NS[d]	0.001	0.000	0.042	0.007	0.000

[a]I, pea/maize intercropping, SM, sole planting of maize, SP, sole planting of pea. N1, N2, and N3 for maize represent the allocation of four-stage (sowing, jointing stage, pre-tasseling stage, and 15 days post-silking stage) was 2:1:4:3, 2:2:4:2, and 2:3:4:1, respectively. N1 for pea represents 80% base fertilizer +20% topdressing fertilizer at flowering stage. The description keeps uniform in the following tables.
[b]In the same column, the different lowercase letters indicate significant differences in the same year ($p < 0.05$).
[c]The total carbon emission of pea/maize intercropping was calculated by the average of pea strip and maize strip.
[d]NS indicates not significant at $p < 0.05$.

TABLE 2 Soil chemical properties of pea strips under pea/maize intercropping (I) and sole cropping (S) at different N application treatments.

Period	Treatments[a]	NO_3^- – N (mg/kg)	NH_4^+ – N (mg/kg)	TN (g/kg)	SOM (g/kg)	LOM (g/kg)	CAT (0.01 mol/L $KMnO_4$ ml/g)
PF	IN1	19.5de[b]	6.43bc	0.85cd	9.7ab	2.25bc	1.34c
	IN2	21.7cd	6.97b	0.893ab	10.6ab	2.50ab	1.53b
	IN3	24.3abc	9.04a	0.909a	11.6a	2.66a	1.82a
	SPN1	16.6e	6.28c	0.836cde	9.2b	1.63e	1.25d
Significance (p value)							
Cropping system (C)		0.000	0.000	0.000	0.002	0.000	0.000
N management practice (N)		0.022	0.000	0.000	NS	NS	0.000
C×N		0.022	0.000	0.000	NS	NS	0.000
MS	IN1	23.0bc	3.96f	0.798e	9.6b	1.51ef	0.97f
	IN2	23.7abc	4.14ef	0.824de	10.0ab	1.85de	1.05e
	IN3	26.2ab	4.65e	0.854bcd	10.8ab	2.10cd	1.18d
	SPN1	26.7a	5.58d	0.868bc	9.4b	1.20f	1.21d
Significance (p value)							
Cropping system (C)		0.017	0.000	0.020	NS	0.000	0.000
N management practice (N)		NS[c]	NS	NS	NS	NS	0.000
C×N		NS	NS	NS	NS	NS	0.000

[a]N1, N2, and N3 for intercropping pattern represent the allocation of four-stage (sowing, jointing stage, pre-tasseling stage, and 15 days post-silking stage) was 2:1:4:3, 2:2:4:2, and 2:3:4:1, respectively. N1 for sole pattern represents 80% base fertilizer +20% topdressing fertilizer at flowering stage.
[b]In the same column, the same lowercase letters indicate significant differences ($p < 0.05$).
[c]NS, not significant at the $p < 0.05$ level.

Bacterial beta diversity

The NMDS analysis was conducted to reflect microbial beta diversity (Figure 3). An evident separation of soil bacteria in the pea strip between intercropping and sole planting was observed in the NMDS plot (Figures 3A,B), suggesting the changed community composition by cropping mode. Moreover, the NMDS ordination plot showed that the bacterial community composition varied greatly among treatments at the two growth stages. For

TABLE 3 Soil chemical properties of maize strips under two cropping systems [pea/maize intercropping (I) and sole cropping (S)] and at different N application treatments.

Period	Treatments[a]	$NO_3^- - N$ (mg/kg)	$NH_4^+ - N$ (mg/kg)	TN (g/kg)	SOM (g/kg)	LOM (g/kg)	CAT (0.01 mol/L $KMnO_4$ ml/g)
PF	IN1	17.0e[b]	5.38f	0.827cde	9.2d	1.57f	1.71 g
	IN2	19.0de	5.63ef	0.866abcd	9.4 cd	1.77ef	1.82efg
	IN3	19.8de	6.28de	0.887ab	10.5abcd	2.09 cd	2.08de
	SMN1	19.0de	6.25de	0.839bcde	9.9bcd	1.77ef	2.24 cd
	SMN2	21.0cde	6.69 cd	0.879abc	10.6abcd	1.99de	2.45bc
	SMN3	22.0bcd	7.00bc	0.907a	10.8abcd	2.25bcd	2.81a
Significance (*p* value)							
Cropping system (C)		0.018	0.000	NS	0.014	NS	0.000
N management practice (N)		0.023	0.003	0.006	0.012	0.004	0.000
C × N		NS[c]	NS	NS	NS	NS	NS
MS	IN1	19.5de	6.71 cd	0.797ef	10.8abcd	2.59a	2.00def
	IN2	22.8abcd	7.04bc	0.811e	11.5ab	2.39ab	2.36c
	IN3	24.8abc	7.47ab	0.820de	12.2a	2.30bc	2.66ab
	SMN1	22.9abcd	7.53ab	0.753f	10.8abcd	2.41ab	1.75 fg
	SMN2	25.6ab	7.59ab	0.785ef	11.1abc	2.34abc	2.06de
	SMN3	26.8a	8.09a	0.805ef	11.6ab	2.29bc	2.24 cd
Significance (*p* value)							
Cropping system (C)		NS	0.006	NS	NS	0.028	0.003
N management practice (N)		0.040	NS	NS	NS	0.001	0.001
C × N		NS	NS	NS	NS	NS	NS

[a]N1, N2, and N3 represent the allocation of four-stage (sowing, jointing stage, pre-tasseling stage, and 15 days post-silking stage) was 2:1:4:3, 2:2:4:2, and 2:3:4:1, respectively.
[b]In the same column, the same lowercase letters indicate significant differences ($p < 0.05$).
[c]NS, not significant at the $p < 0.05$ level.

TABLE 4 Alpha-diversity indices of the soil bacteria in pea strips under three N application treatments.

Period	Treatments	OTUs[b]	Shannon	Chao 1
PF	IPN1[a]	38,387±5,965b[c]	6.82 ± 0.05a	4,359 ± 74a
	IPN2	39,240 ± 2,648ab	6.75 ± 0.03b	4,247 ± 173ab
	IPN3	40,608 ± 1,505ab	6.84 ± 0.03a	4,384 ± 123a
	SPN1	56,180 ± 2,073ab	6.7 ± 0.01b	4,044 ± 99c
MS	IPN1	55,785 ± 2,529ab	6.74 ± 0.06b	4,174 ± 68bc
	IPN2	53,753 ± 1,608ab	6.73 ± 0.02b	4,092 ± 58bc
	IPN3	58,644 ± 8,937a	6.70 ± 0.05b	4,074 ± 43bc
	SPN1	52,662 ± 26,350ab	6.74 ± 0.06b	3,800 ± 75d
Significance (*p* value)				
Cropping system (C)		NS[d]	0.021	0.000
N management practice (N)		NS	NS	NS
C × N		NS	NS	NS

[a]I, pea/maize intercropping, SP, sole planting of pea. N1, N2, and N3 for intercropping pattern represent the allocation of four-stage (sowing, jointing stage, pre-tasseling stage, and 15 days post-silking stage) was 2:1:4:3, 2:2:4:2, and 2:3:4:1, respectively. N1 for sole pattern represents 80% base fertilizer +20% topdressing fertilizer at flowering stage.
[b]OTUs: operational taxonomic units (97% similarity).
[c]In the same column, the same lowercase letters indicate significant differences ($p < 0.05$).
[d]NS, not significant at the $p < 0.05$ level.

instance, N1 and N2 were separated from N3 at the PF stage, whereas just N1 was separated from N3 at the MS stage. An evident separation of soil bacteria in maize strips with different N applications was observed in the NMDS plot (Figure 3C; for instance, the separation of N1 and N3 from N2 at the PF stage), suggesting the changed community composition by N managements. However, a similar trend was not found at the MS stage (Figure 3D).

Bacterial community structures

Pea strips

The dominant bacterial phyla at the PF stage were consistent with that at the MS stage (Figure 4). Additionally, the dominant bacterial phyla in the treatments were Proteobacteria, Actinobacteriota, Acidobacteriota, Chloroflexi, Bacteroidota, Gemmatimonadota, Firmicutes, Myxococcota, Methylomirabilota, and Planctomycetota (relative abundance >1%; Figures 4A,B; Supplementary Table S2). It was noticeable that Proteobacteria, Actinobacteriota, and Bacteroidota were more abundant in the monocrop soil than in the intercropped soil at the PF stage. In contrast, Proteobacteria, Actinobacteriota, Chloroflexi, Bacteroidota, and Planctomycetota were more abundant in the

TABLE 5 Alpha-diversity indices of the soil bacteria in maize strips under three N application treatments.

Period	Treatment[a]	OTUs[b]	Shannon	Chao 1
PF	IMN1	38,925±863e[c]	6.69 ± 0.02ab	4,247 ± 97ab
	IMN2	44,883 ± 1,432cde	6.39 ± 0.10c	4,035 ± 262b
	IMN3	40,718 ± 2,772de	6.61 ± 0.07b	4,144 ± 281b
	SMN1	54,107 ± 10,396abc	6.63 ± 0.01ab	4,190 ± 97b
	SMN2	63,139 ± 4,731a	6.40 ± 0.08c	4,033 ± 81b
	SMN3	59,310 ± 5,141ab	6.62 ± 0.06ab	4,095 ± 59b
MS	IMN1	46,932 ± 5,002cde	6.69 ± 0.06ab	4,092 ± 173b
	IMN2	58,590 ± 9,296ab	6.63 ± 0.02ab	4,249 ± 142ab
	IMN3	54,759 ± 4,651abc	6.59 ± 0.08b	4,206 ± 172b
	SMN1	58,247 ± 9,782ab	6.64 ± 0.05ab	4,300 ± 78ab
	SMN2	51,202 ± 1,819bcd	6.61 ± 0.03b	4,124 ± 94b
	SMN3	50,534 ± 2,962bcd	6.73 ± 0.06a	4,494 ± 118a
Significance (*p* value)				
Cropping system (C)		0.003	NS	NS
N management practice (N)		NS[d]	0.001	NS
C × N		NS	NS	NS

[a]I, pea/maize intercropping, SM, sole planting of maize. N1, N2, and N3 represent the allocation of four-stage (sowing, jointing stage, pre-tasseling stage, and 15 days post-silking stage) was 2:1:4:3, 2:2:4:2, and 2:3:4:1, respectively.
[b]OTUs: operational taxonomic units (97% similarity).
[c]In the same column, the same lowercase letters indicate significant differences ($p < 0.05$).
[d]NS, not significant at the $p < 0.05$ level.

intercropped soil than in the monocrop soil at the MS stage. At the class level, the relative abundance of Thermoanaerobaculia, KD4-96, Dehalococcoidia, TK10, Gitt-GS-136, and Gemmatimonadetes at the PF stage was significantly higher in the monocropping system than in the intercropping system, belonging to Acidobacteriota, Chloroflexi, and Gemmatimonadota, respectively. However, the relative abundance of Actinobacteria, Anaerolineae, and Bacteroidia at the MS stage was significantly higher in the intercropped system than in the monocropping system.

In the intercropping pattern, N1 treatment increased the relative abundance of Acidobacteriota, Acidobacteriota, Choroflexi, Gemmatimonadota, Firmicutes, and Planctomycetota at the PF stage compared with N3. Furthermore, at the class level (Supplementary Figure S3; Supplementary Table S2), the relative abundance of Acidimicrobiia, MB-A2-108, Vicinamibacteria, Blastocatellia, Anaerolineae, KD4-96, Dehalococcoidia, Gemmatimonadetes, and Bacilli were increased in N1 treatment. In addition, N1 treatment increased the relative abundance of Chloroflexia, Anaerolineae, KD4-96, Dehalococcoidia, and Bacteroidia, which belong to Choroflexi and Bacteroidota.

Maize strips

According to bacterial community compositions, the dominant bacterial phyla of maize were Proteobacteria, Acitinbacteriota, Acidobacteriota, Choroflexi, Bacteroidota, Gemmatimonadota, Firmicutes, and Myxococcota (relative abundance >1%; Figures 4C,D; Supplementary Table S2). The relative abundance of Proteobacteria, Gemmatimonadota, Firmicutes, and Myxococcota was increased at both sampling stages for pea/maize intercropping than for monoculture maize. Furthermore, at the class level (Supplementary Figure S3; Supplementary Table S3), the intercropping pattern increased the relative abundance of Alphaproteobacteria and Acidimicrobiia but decreased that of Vicinamibacteria, Chloroflexia, and KD4-96 compared to monoculture maize.

The comparison of different N fertilizer managements showed that the relative abundance of Proteobacteria in the intercropping pattern was decreased by the N1 treatment at the PF stage but increased at the MS stage (Supplementary Figure S3; Supplementary Table S2). However, no similar trend was found in the dominant Acidobacteriota and Myxococcota. For the class level, N1 reduced the relative abundance of Alphaproteobacteria and Gammaproteobacteria, the branch of Proteobacteria, in the intercropping system at the PF stage, and increased their abundance at the MS stage compared to N3 treatment.

Correlation relationship among dominant class, soil properties, and Rs

A Spearman correlation heatmap was applied to show the correlations between soil properties and dominant class. The soil properties that correlated with most soil bacteria at the PF stage were CAT (8 classes in total), followed by SOM (2), $NO_3^- - N$, TN, and LOM (1 in each; Figure 5A). Additionally, CAT showed the most negative correlation (6), mainly with Chloroflexia, Methylomirabilia, Thermoanaerobaculia, Unclassified Bacteria, Acidobacteriae, and Nitrospiria and positive correlation (2) with Gammaproteobacteria and Saccharimonadia. Moreover, $NO_3^- - N$ and SOM presented significantly negative correlations with Gemmatimonadetes. Interestingly, LOM showed a significantly positive correlation with Acidobacteriae.

The correlation between soil properties and dominant class at the MS stage differed from that at the PF stage (Figure 5B). The soil properties correlated with most soil bacteria at the MS stage were $NH_4^+ - N$ (17 classes in total), followed by SOM (10), TN (8), LOM and CAT (6 in each), $NO_3^- - N$ (1). In addition, $NH_4^+ - N$ had significantly negative correlations (12), mainly with Blastocatellia, Gemmatimonadetes, Bacilli, Methylomirabilia, Dehalococcoidia, Holophagae, Unclassified Bacteria, MB-A2-108, TK10, Nitrospiria, Uorank NB1-j, and JG30-KF-CM66. Moreover, SOM showed only significantly positive correlations except for Actinobacteria and Verrucomicrobiae; TN and CAT showed only significantly negative correlations except for Actinobacteria, Phycisphaerae, and Bacteroidia, respectively. Interestingly, LOM and $NO_3^- - N$ only presented negative correlations.

To identify the relationships between the main bacterial classes and environmental factors, network analyses were conducted between the top 50 microbial classes, soil properties, and Rs to explore interactions (Figure 6). The complexity of the network increased from the PF stage (number of nodes = 12,

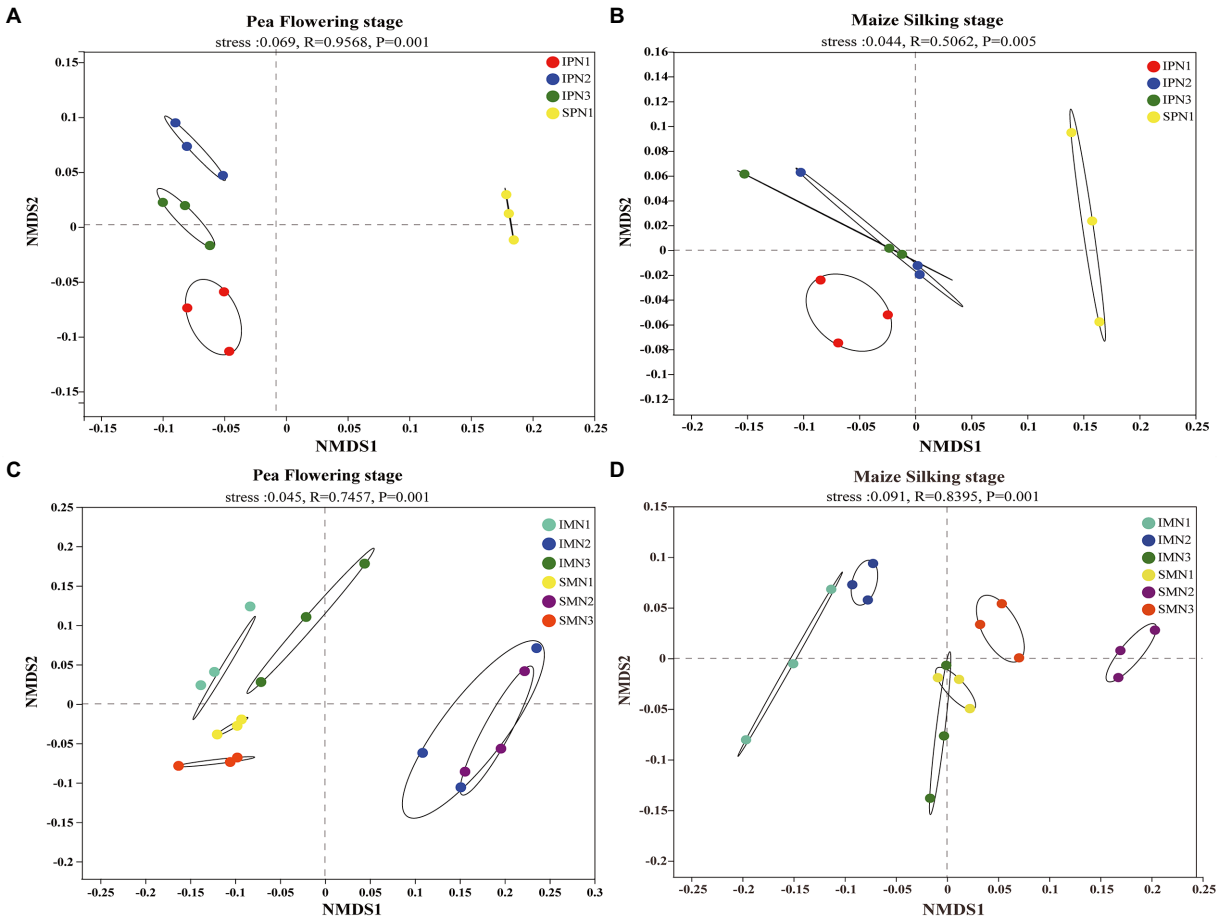

FIGURE 3
Changes in soil bacterial beta diversity (NMDS) of pea strips **(A,B)** and maize strips **(C,D)** under different treatments. I, pea/maize intercropping, SP, sole planting of pea, SM, sole planting of maize. N1, N2, and N3 for maize represent the allocation of four-stage (sowing, jointing stage, pre-tasseling stage, and 15days post-silking stage) was 2:1:4:3, 2:2:4:2, and 2:3:4:1, respectively. N1 in sole pea represents 80% base fertilizer + 20% topdressing fertilizer at flowering stage.

number of edges = 17, average path length = 1.787, and diameter = 3) to the MS stage (number of nodes = 23, number of edges = 37, average path length = 2.300, and diameter = 4). The network at the PF stage showed that Rs had strong positively significant correlations with Gammaproteobacteria belonging to Proteobacteria ($r = 0.752$, $p < 0.01$). Additionally, Rs showed negatively significant correlations with Acidobacteriae, Subgroup_5 (belonged to Acidobacteriota), and S0134_terrestrial_group (belonging to Gemmatimonadota; $|r| > 0.7$, $p < 0.01$). However, the Rs at the MS stage only showed positively significance with Bacteroidia ($r = 0.562$, $p < 0.01$). In contrast, Rs had a significantly negative correlation with Gemmatimonadetes, Methylomirabilia, Unclassified Bacteria, Nitrospiria, JG30-KF-CM66, Norank Latescibacterota, bacteriap25, and Norank RCP2-54 ($|r| > 0.5$, $p < 0.01$). Most importantly, the Rs at PF stage and MS stage were negatively significant correlated with the Chloroflexia ($|r| = 0.646$) and JG30-KF-CM66 ($|r| = 0.519$), which were both belong to Chloroflexi.

Discussion

Impacts of delayed N fertilizer application on the CO_2 emission of pea/maize intercropping systems

Agricultural soil has been considered as the "source" of atmospheric CO_2 since its beginning (Yang et al., 2021). Optimization agronomy measures to decrease soil Rs from farmland acts as a critical strategy in mitigating CO_2 emissions in agricultural production (Gan et al., 2011). Previous studies demonstrated that intercropping patterns could significantly mitigate the Rs rate from the production of field crops (Chai et al., 2014; Yang et al., 2021). Moreover, Rs serves as an effective way to measure carbon emissions from soil (Raich and Tufekciogul, 2000). In the present study, the Rs of intercropping pea was significantly higher than that of monoculture during the co-growth stage, while that of intercropping maize was significantly lower than that of monoculture. This phenomenon could be explained by three driving factors. Firstly,

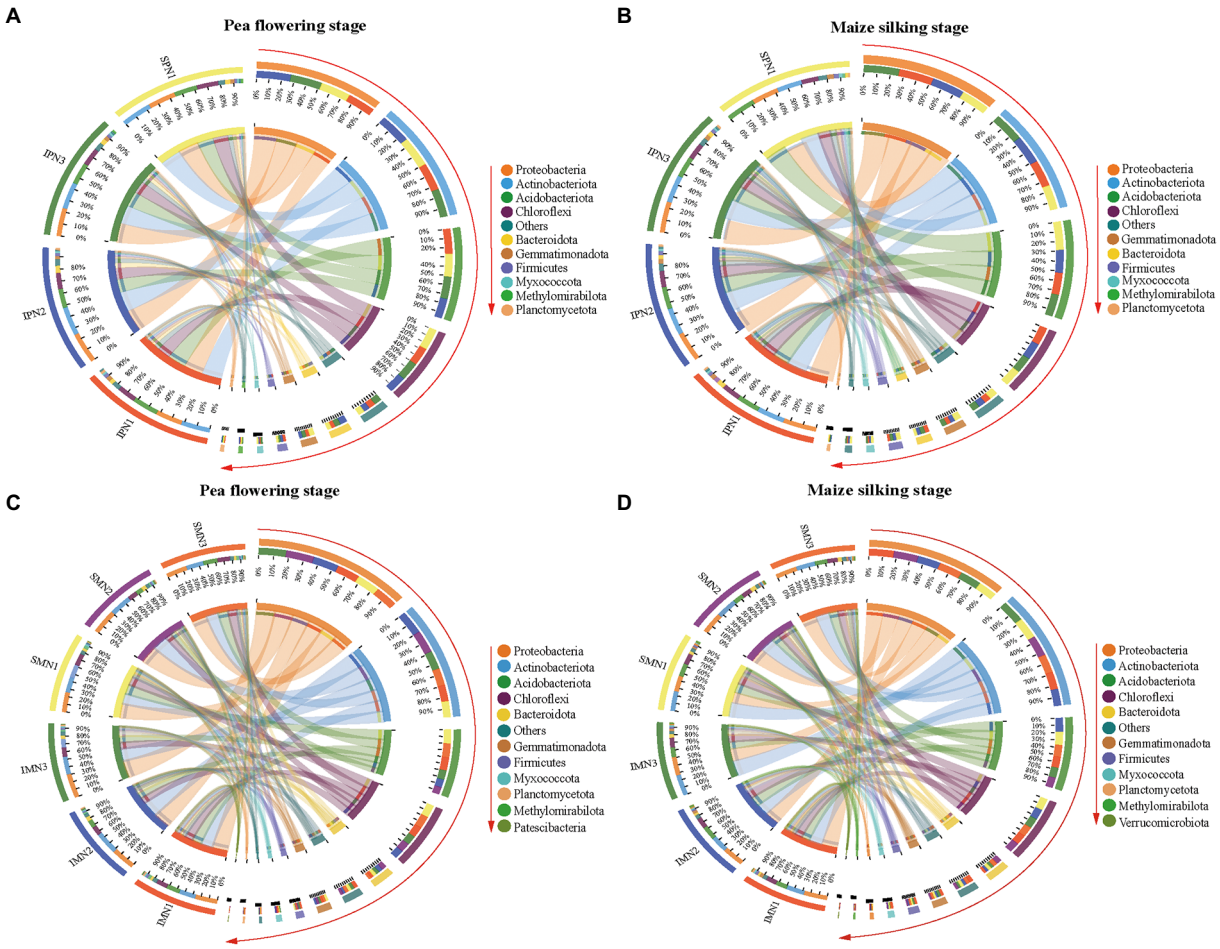

FIGURE 4
Phylum level OTUs abundance profile of bacteria 16S rRNA in pea strips **(A,B)** and maize strips **(C,D)** soils at different growth stages under different nitrogen fertilizer applications (TOP 10 in groups). I, pea/maize intercropping, SP, sole planting of pea, SM, sole planting of maize. N1, N2, and N3 for maize represent the allocation of four-stage (sowing, jointing stage, pre-tasseling stage, and 15days post-silking stage) was 2:1:4:3, 2:2:4:2, and 2:3:4:1, respectively. N1 for sole pea represents 80% base fertilizer + 20% topdressing fertilizer at flowering stage.

pea, an early-maturing, cool-season crop, had a higher competitive edge than maize, a late-maturing, warm-season crop, thereby intercropped pea had a relatively higher competition for resources (Hu et al., 2016). Secondly, applying legumes to the intercropping system could reduce the application of N fertilizer for intercropping systems owing to symbiotic N_2 fixation, thus reducing carbon emission compared to a monoculture (Hauggaard-Nielsen et al., 2016; Hu et al., 2017). Finally, intercropped maize would not be suppressed by the interspecific competition and usually exhibited compensatory growth when pea was harvested, so as to increase carbon emission (Zhao et al., 2019). Therefore, pea/maize intercropping was an effective strategy to achieve carbon emission reduction.

The application of N fertilizers has been commonly adopted to boost crop yield, and excessive application is a crucial influencing factor of GHG in farmland (Yao et al., 2012; Chen et al., 2014; Daly and Hernandez-Ramirez, 2020). The most direct practice to lower GHG is to reduce the amount of N fertilizer applied to farmland. However, when the N fertilizer was not applied to farmland, CO_2 emissions unexpectedly significantly increased (Wang X. et al., 2021), indicating that an excessive reduction of N fertilizer was not a good strategy for mitigating CO_2 emissions in agricultural production. On the premise of the same amount of N application, optimizing N fertilizer management was a possible measure to reduce GHG emissions in farmland. In the present study, delayed application of N fertilizer could decrease the Rs rate of the pea/maize intercropping system, which was consistent with the results in previous study that optimized management practices of N fertilizer could mitigate CO_2 emission (Zhang et al., 2021). One possible reason was that the increasing root respiration and root C inputs as a consequence of N fertilization stimulated soil CO_2 emission (Bicharanloo et al., 2020; Zhang et al., 2020). Another possible reason was that N fertilizer offers C and N substrates as the primary energy sources for microorganism growth, thus stimulating CO_2 emissions (Zang et al., 2016). Furthermore, the delayed application of N fertilizer could match fertilizer N supply with crop N

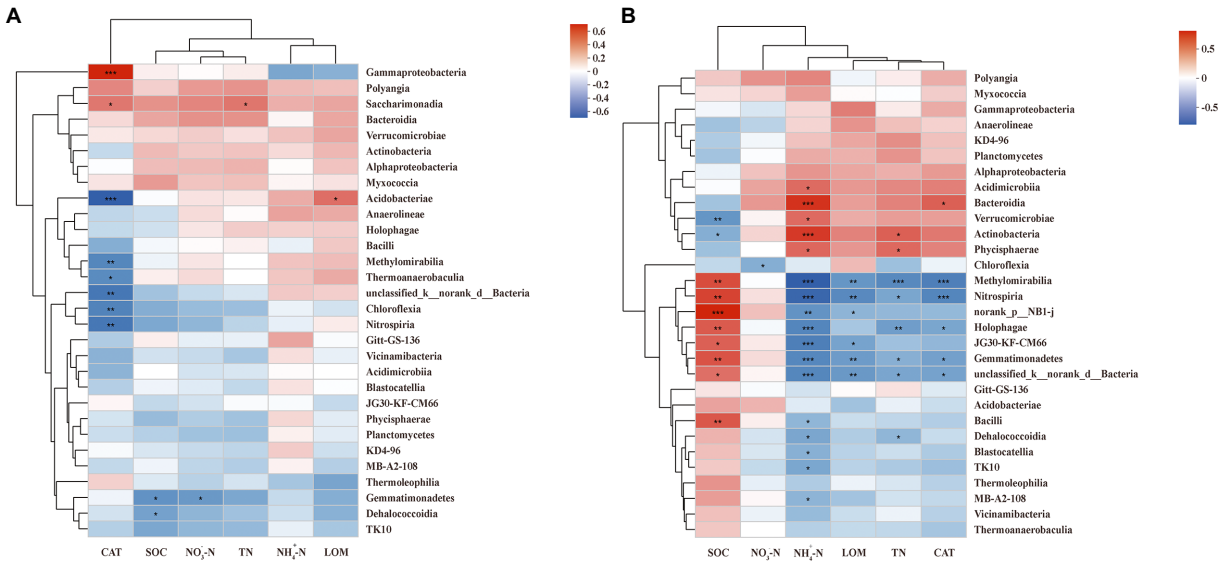

FIGURE 5
Spearman correlation heatmap of dominant class and soil properties at pea flowering stage **(A)** and maize silking stage **(B)**. SOM, soil organic matter; TN, total nitrogen; NO_3^-–N, nitrate; NH_4^+–N, ammonium; CAT, catalase activity; LOM, labile organic matter. ***, **, and * indicate $p<0.001$, $p<0.01$, and $p<0.05$, respectively.

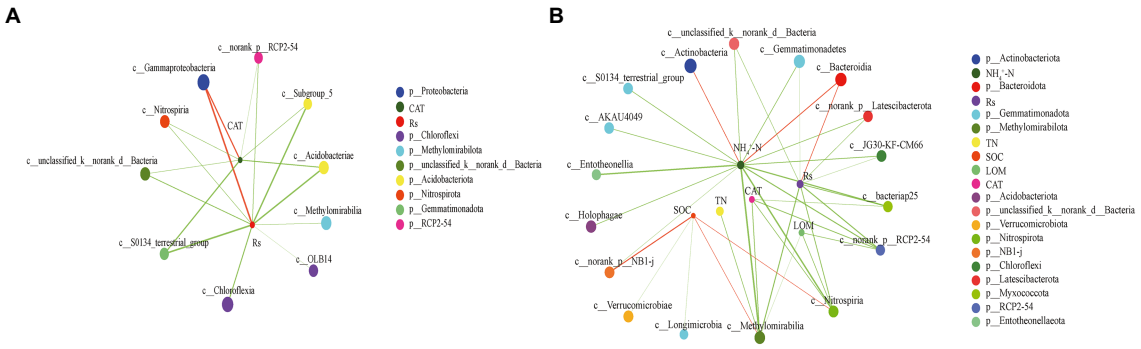

FIGURE 6
Two-factor network constructed around the main class of bacterial 16S rRNA at pea flowering stage **(A)** and maize silking stage **(B)** based on significant Spearman rank correlation coefficients. The circles of different colors indicate different classes, circle size indicates the taxonomic abundance; red and green line indicate positive and negative correlation, respectively; line thickness represents the strength of the correlation, with thicker lines indicating stronger correlations.

requirement, which were crucial to achieve high productivity and mitigate carbon emission (Chai et al., 2014; Hu et al., 2020). Further studies were needed to explore the potential mechanism of mitigating carbon emissions in pea/maize intercropping by delayed application of N fertilizer.

Effects of delayed N fertilizer application on soil bacterial diversity and community structures

Bacteria are the most abundant and dominant of the primary soil microbes in terms of biodiversity and their influence on essential soil processes (Gong et al., 2019). In the present study, the bacterial richness and diversity of intercropped pea and intercropped maize was higher than the corresponding monoculture at the PF stage, while the same trend was not observed at the MS stage. This was probably attributed to the enhancement of crop diversity during the co-growth stage and the strong interspecific relationship, which promoted the growth of soil microorganisms, thus increasing the bacterial diversity and abundance. However, delayed N fertilizer application did not show a positive effect at this stage compared to the conventional N management. Soil nutrient supply capacity was a critical impact factor for soil microbial diversity (Fu et al., 2019). Soil properties

might explain the variations. The delayed N fertilizer application decreased the amount of N fertilizer at the first topdressing compared with the conventional N management. Meanwhile, conventional N management substantially enhanced soil properties which promoted the growth of microorganisms. Previous study had similarly demonstrated that soil properties are improved in N fertilizer application, thereby promoting the growth of microorganisms (Xue et al., 2006). Both cropping patterns and N management influenced the bacterial beta diversity of pea strips, but only the latter affected maize strips. The major reason was that the intercropping pattern changed the soil microenvironment and nutrient content, thus affecting the growth of the soil microorganisms (Cuartero et al., 2022). Moreover, fertilization management regimes could affect microbial beta diversity by altering soil properties, including soil pH, bulk density, electrical conductivity, water content, total nitrogen, organic carbon, $NO_3^- - N$, and available potassium (Ren et al., 2021). Therefore, the soil bacterial diversity was regulated by the cropping patterns and N fertilizer application managements, but the regulation varied with the crops and the growth period.

Changes in bacterial community composition are usually used to reflect nutritional contents and structural features of soils (Mouhamadou et al., 2013). Our analysis revealed that the abundance of Bacteroidota and Chloroflexi in pea strips were regulated by intercropping pattern, but delayed N fertilizer application just increased the abundance of Chloroflexi. The relative abundance of Proteobacteria in intercropped maize was increased at two sampling stages, but increased by the delayed N fertilizer application at MS stage. The universality and importance of these phyla have been demonstrated in previous research (Fu et al., 2019; Guo et al., 2021). These results were consistent with other cereal-legume intercropping system (Gong et al., 2019). The main reason for this phenomenon was the combination of delayed N fertilizer application and the pea/maize intercropping pattern could alter soil properties, thus regulating the structure of bacterial communities. Changes in the chemical properties and nutrient status of soil, mainly the CAT activity at the PF stage and ammonium at the MS stage, are the most important factors causing differences in microbial community structure. Consequently, the composition of bacteria was stimulated by enzyme activities and soil properties with considerable change under cereal-legume intercropping systems (Gong et al., 2019; Yu et al., 2021).

Impacts of applying the delayed N fertilizer application to pea/maize intercropping on CO_2 emissions and the underlying mechanisms

Our results suggested that the delayed application of N fertilizer could decrease the CO_2 under the pea/maize intercropping pattern. A previous study showed that the reduction in CO_2 emissions was mainly due to the changes in bacterial community composition (Wang et al., 2020). Network analysis showed that the Rs rate mainly related to the phylum Proteobacteria and Chloroflexi at the PF stage and the phylum Bacteroidota and Chloroflexi at the MS stage, which were the most abundant bacterial phyla in soil environments (Guo et al., 2021; Cuartero et al., 2022). Furthermore, the relative abundance of Proteobacteria decreased with the reduction in the CAT activity, thereby mitigating the Rs rate at the PF stage. The result was probably because low N input conditions (N1) at co-growth period suppressed the growth of eutrophic bacteria, mainly Proteobacteria, thus reducing the CO_2 emission (Ying et al., 2010). In contrast, the Rs rate at the MS stage decreased by promoting and inhibiting the growth of Chloroflexi and Bacteroidota with the reduction in ammonium content, indicating that the relationship between the Rs rate and the dominant bacterial group might depend on specific soil properties. Based on the data of environmental factors, soil bacterial community, and correlation network analysis, these bacterial groups could be promising biological indicators in soil carbon emissions. Moreover, the results revealed that the combined system could alter soil properties and these bacterial groups, thereby mitigating CO_2 emissions. Further research was needed to regard the overall effect of this N management practice on the bacteria community by increasing sampling time.

Conclusion

This study provided previously unavailable information on the correlation between bacterial communities and CO_2 fluxes in the pea/maize intercropping system. Soil CO_2 emissions were lower in the delayed N fertilizer application than in traditional N fertilizer application. Moreover, a close relationship existed between soil properties (catalase activity and $NH_4^+ - N$) and the dominant group (Proteobacteria, Chloroflexi, and Bacteroidota). Furthermore, the correlation between CO_2 fluxes and the dominant group revealed by the network might imply the mitigation of CO_2 emissions by suppressing the growth of Proteobacteria and Bacteroidota but promoting the growth of Chloroflexi. In conclusion, our results supported the hypothesis that soil CO_2 emissions were influenced by delayed N fertilizer application and cropping patterns, mainly affected the bacterial communities and properties of soils. Further research of these interactions may provide a new horizon for achieving synergy between cropping patterns and N fertilization to mitigate GHG emissions.

Data availability statement

The datasets presented in this study can be found in online repositories. The names of the repository/repositories and accession number(s) can be found at: https://www.ncbi.nlm.nih.gov/, PRJNA842905.

Author contributions

QC designed the experiment. KX carried out the experiment, performed analysis, and wrote the manuscript. FH, ZF, and WY assisted to design the experiments. YN and QW reviewed the manuscript. All authors contributed to the article and approved the submitted version.

Funding

This work was supported by the National Key Research and Development Program of China (2021YFD1700202-02), the 'Double First-Class' Key Scientific Research Project of the Education Department in Gansu Province (GSSYLXM-02), the Natural Science Foundation of China (U21A20218 and 32160765), and the Science and Technology Project of Gansu Province (21JR7RA836 and 20JR5RA037).

Acknowledgments

We appreciate assistance in the field and laboratory by students of the Oasis Agricultural Trial Station of Gansu Agricultural University. We are also grateful to the editor and reviewers for their constructive comments and suggestions on this manuscript.

Conflict of interest

The authors declare that the research was conducted in the absence of any commercial or financial relationships that could be construed as a potential conflict of interest.

Publisher's note

Supplementary material

The Supplementary material for this article can be found online at: https://www.frontiersin.org/articles/10.3389/fmicb.2022.1002009/full#supplementary-material

References

Bicharanloo, B., Shirvan, M. B., Keitel, C., and Dijkstra, F. A. (2020). Rhizodeposition mediates the effect of nitrogen and phosphorous availability on microbial carbon use efficiency and turnover rate. *Soil Biol. Biochem.* 142:107705. doi: 10.1016/j.soilbio.2020.107705

Chai, Q., Nemecek, T., Liang, C., Zhao, C., Yu, A. Z., Coulter, J. A., et al. (2021). Integrated farming with intercropping increases food production while reducing environmental footprint. *Proc. Natl. Acad. Sci. U. S. A.* 118:e2106382118. doi: 10.1073/pnas.2106382118

Chai, Q., Qin, A. Z., Gan, Y. T., and Yu, A. Z. (2014). Higher yield and lower carbon emission by intercropping maize with rape, pea, and wheat in arid irrigation areas. *Agron. Sustain. Dev.* 34, 535–543. doi: 10.1007/s13593-013-0161-x

Chen, X., Cui, Z., Fan, M., Vitousek, P., Zhao, M., Ma, W., et al. (2014). Producing more grain with lower environmental costs. *Nature* 514, 486–489. doi: 10.1038/nature13609

Chen, J., Sun, X., Li, L., Liu, X., Zhang, B., Zheng, J., et al. (2016). Change in active microbial community structure, abundance and carbon cycling in an acid rice paddy soil with the addition of biochar. *Eur. J. Soil Sci.* 67, 857–867. doi: 10.1111/ejss.12388

Chen, S. F., Zhou, Y. Q., Chen, Y. R., and Gu, J. (2018). Fastp: an ultra-fast all-in-one FASTQ preprocessor. *Bioinformatics* 34, i884–i890. doi: 10.1093/bioinformatics/bty560

Chu, H., Lin, X., Fujii, T., Morimoto, S., Yagi, K., Hu, J., et al. (2007). Soil microbial biomass, dehydrogenase activity, bacterial community structure in response to long-term fertilizer management. *Soil Biol. Biochem.* 39, 2971–2976. doi: 10.1016/j.soilbio.2007.05.031

Cuartero, J., Pascual, J. A., Vivo, J. M., Özbolat, O., Sánchez-Navarro, V., Egea-Cortines, M., et al. (2022). A first-year melon/cowpea intercropping system improves soil nutrients and changes the soil microbial community. *Agric. Ecosyst. Environ.* 328:107856. doi: 10.1016/j.agee.2022.107856

Daly, E. J., and Hernandez-Ramirez, G. (2020). Sources and priming of soil N_2O and CO_2 production: nitrogen and simulated exudate additions. *Soil Biol. Biochem.* 149:107942. doi: 10.1016/j.soilbio.2020.107942

Edgar, R. C. (2013). UPARSE: highly accurate OTU sequences from microbial amplicon reads. *Nat. Methods* 10, 996–998. doi: 10.1038/nmeth.2604

Fu, Z. D., Zhou, L., Chen, P., Du, Q., Pang, T., Song, C., et al. (2019). Effects of maize-soybean relay intercropping on crop nutrient uptake and soil bacterial community. *J. Integr. Agric.* 18, 2006–2018. doi: 10.1016/S2095-3119(18)62114-8

Gan, Y. T., Liang, C., Wang, X. Y., and McConkey, B. (2011). Lowering carbon footprint of durum wheat by diversifying cropping systems. *Field Crops Res.* 122, 199–206. doi: 10.1016/j.fcr.2011.03.020

Gan, Y. T., Siddique, K. H. M., Turner, N. C., Li, X. G., Niu, J. Y., Yang, C., et al. (2013). Ridge-furrow mulching systems-an innovative technique for boosting crop productivity in semiarid rain-fed environments. *Adv. Agron.* 118, 429–476. doi: 10.1016/B978-0-12-405942-9.00007-4

Gong, X. W., Liu, C. J., Li, J., Luo, Y., Yang, Q. H., Zhang, W. L., et al. (2019). Responses of rhizosphere soil properties, enzyme activities and microbial diversity to intercropping patterns on the loess plateau of China. *Soil Till. Res.* 195:104355. doi: 10.1016/j.still.2019.104355

Gou, F., van Ittersum, M. K., Simon, E., Leffelaar, P. A., van der Putten, P. E. L., Zhang, L. Z., et al. (2017). Intercropping wheat and maize increases total radiation interception and wheat RUE but lowers maize RUE. *Eur. J. Agron.* 84, 125–139. doi: 10.1016/j.eja.2016.10.014

Guo, J., Wu, Y. Q., Wu, X. H., Ren, Z., and Wang, G. B. (2021). Soil bacterial community composition and diversity response to land conversion is depth-dependent. *Glob. Ecol. Conserv.* 32:e01923. doi: 10.1016/j.gecco.2021.e01923

Hauggaard-Nielsen, H., Lachouani, P., Knudsen, M. T., Ambus, P., Boelt, B., and Gislum, R. (2016). Productivity and carbon footprint of perennial grass-forage legume intercropping strategies with high or low nitrogen fertilizer input. *Sci. Total Environ.* 541, 1339–1347. doi: 10.1016/j.scitotenv.2015.10.013

Hu, F. L., Gan, Y. T., Chai, Q., Feng, F. X., Zhao, C., Yu, A. Z., et al. (2016). Boosting system productivity through the improved coordination of interspecific competition in maize/pea strip intercropping. *Field Crops Res.* 198, 50–60. doi: 10.1016/j.fcr.2016.08.022

Hu, F. L., Tan, Y., Yu, A. Z., Zhao, C., Fan, Z. L., Yin, W., et al. (2020). Optimizing the split of N fertilizer application over time increases grain yield of maize-pea intercropping in arid areas. *Eur. J. Agron.* 119:126117. doi: 10.1016/j.eja.2020.126117

Hu, F. L., Zhao, C., Feng, F. X., Chai, Q., Mu, Y. P., and Zhang, Y. (2017). Improving N management through intercropping alleviates the inhibitory effect of mineral N on nodulation in pea. *Plant Soil* 412, 235–251. doi: 10.1007/s11104-016-3063-2

Huang, R., Wang, Y. Y., Gao, X. S., Liu, J., Wang, Z. F., and Gao, M. (2020). Nitrous oxide emission and the related denitrifier community: a short-term response to organic manure substituting chemical fertilizer. *Ecotoxicol. Environ. Saf.* 192:110291. doi: 10.1016/j.ecoenv.2020.110291

IPCC (2014). "Climate change 2014: Mitigation of climate change," in *Contribution of Working Group III to the Fifth Assessment Report of the Intergovernmental Panel on Climate Change*. (Cambridge, UK and New York, NY: Cambridge University Press).

IPCC (2018). *Global Warming of 1.5°C: An IPCC Special Report on the Impacts of Global Warming of 1.5°C Above Pre-industrial Levels and Related Global Greenhouse Gas Emission Pathways, in the Context of Strengthening the Global Response to the Threat of Climate Change, Sustainable Development, and Efforts to Eradicate Poverty*. World Meteorological Organization, Geneva.

Jiang, Z. W., Yang, S. H., Pang, Q. Q., Xu, Y., Chen, X., Sun, X., et al. (2021). Biochar improved soil health and mitigated greenhouse gas emission from controlled irrigation paddy field: insights into microbial diversity. *J. Clean. Prod.* 318:128595. doi: 10.1016/j.jclepro.2021.128595

Li, L., Sun, J., Zhang, F., Li, X., Yang, S., and Rengel, Z. (2001). Wheat/maize or wheat/soybean strip intercropping: I. yield advantage and interspecific interactions on nutrients. *Field Crops Res.* 71, 123–137. doi: 10.1016/S0378-4290(01)00156-3

Luo, G. W., Rensing, C., Chen, H., Liu, M. Q., Wang, M., Guo, S. W., et al. (2018). Deciphering the associations between soil microbial diversity and ecosystem multifunctionality driven by long-term fertilization management. *Funct. Ecol.* 32, 1103–1116. doi: 10.1111/1365-2435.13039

Lynch, J., Cain, M., Frame, D., and Pierrehumbert, R. (2021). Agriculture's contribution to climate change and role in mitigation is distinct from predominantly fossil CO_2-emitting sectors. *Front. Sustain. Food. Syst.* 4:518039. doi: 10.3389/fsufs.2020.518039

Mago, T., and Salzberg, S. L. (2011). FLASH: fast length adjustment of short reads to improve genome assemblies. *Bioinformatics* 27, 2957–2963. doi: 10.1093/bioinformatics/btr507

Mouhamadou, B., Puissant, J., Personeni, E., Desclos-Theveniau, M., Kastl, E. M., Schloter, M., et al. (2013). Effects of two grass species on the composition of soil fungal communities. *Biol. Fertil. Soils* 49, 1131–1139. doi: 10.1007/s00374-013-0810-x

Nannipieri, P., Ascher-Jenull, J., Ceccherini, M. T., Landi, L., Pietramellara, G., and Renella, G. (2017). Microbial diversity and soil functions. *Eur. J. Soil Sci.* 68, 12–26. doi: 10.1111/ejss.4_12398

Nimmo, J., Lynch, D. H., and Owen, J. (2013). Quantification of nitrogen inputs from biological nitrogen fixation to whole farm nitrogen budgets of two dairy farms in Atlantic Canada. *Nutr. Cycl. Agroecosystems.* 96, 93–105. doi: 10.1007/s10705-013-9579-4

Nowak, J., Kaklewski, K., and Ligocki, M. (2004). Influence of selenium on oxidoreductive enzymes activity in soil and in plants. *Soil Biol. Biochem.* 36, 1553–1558. doi: 10.1016/j.soilbio.2004.07.002

Qin, A. Z., Huang, G. B., Chai, Q., Yu, A. Z., and Huang, P. (2013). Grain yield and soil respiratory response to intercropping systems on arid land. *Field Crops Res.* 144, 1–10. doi: 10.1016/j.fcr.2012.12.005

Qu, J. S., Zeng, J. J., Li, Y., Wang, Q., Maraseni, T., Zhang, L. H., et al. (2013). Household carbon dioxide emissions from peasants and herdsmen in northwestern arid-alpine regions, China. *Energy Policy* 57, 133–140. doi: 10.1016/j.enpol.2012.12.065

Raich, J. W., and Tufekciogul, A. (2000). Vegetation and soil respiration: correlations and controls. *Biogeochemistry* 48, 71–90. doi: 10.1023/A:1006112000616

Ren, J. H., Liu, X. L., Yang, W. P., Yang, X. X., Li, W. G., Xia, Q., et al. (2021). Rhizosphere soil properties, microbial community, and enzyme activities: short-term responses to partial substitution of chemical fertilizer with organic manure. *J. Environ. Manag.* 299:113650. doi: 10.1016/j.jenvman.2021.113650

Shen, Y. W., Sui, P., Huang, J. X., Wang, D., Whalen, J. K., and Chen, Y. Q. (2018). Global warming potential from maize and maize-soybean as affected by nitrogen fertilizer and cropping practices in the North China plain. *Field Crops Res.* 225, 117–127. doi: 10.1016/j.fcr.2018.06.007

Song, Y. N., Zhang, F. S., Marschner, P., Fan, F. L., Gao, H. M., Bao, X. G., et al. (2007). Effect of intercropping on crop yield and chemical and microbiological properties in rhizosphere of wheat (*Triticum aestivum L.*), maize (*Zea mays L.*), and faba bean (*Vicia faba L.*). *Biol. Fertil. Soils* 43, 565–574. doi: 10.1007/s00374-006-0139-9

Sun, T., Zhao, C., Feng, X. M., Yin, W., Gou, Z. W., Lal, R., et al. (2021). Maize-based intercropping systems achieve higher productivity and profitability with lesser environmental footprint in a water-scarce region of Northwest China. *Food Energy Secur.* 10:e260. doi: 10.1002/fes3.260

Theuerl, S., and Buscot, F. (2010). Laccases: toward disentangling their diversity and functions in relation to soil organic matter cycling. *Biol. Fertil. Soils* 46, 215–225. doi: 10.1007/s00374-010-0440-5

Wang, X. L., Chen, Y., Yang, K. P., Duan, F. Y., Liu, P., Wang, Z. G., et al. (2021). Effects of legume intercropping and nitrogen input on net greenhouse gas balances, intensity, carbon footprint and crop productivity in sweet maize cropland in South China. *J. Clean. Prod.* 314:127997. doi: 10.1016/j.jclepro.2021.127997

Wang, Q., Garrity, G. M., Tiedje, J. M., and Cole, J. R. (2007). Naive Bayesian classifier for rapid assignment of rRNA sequences into the new bacterial taxonomy. *Appl. Environ. Microbiol.* 73, 5261–5267. doi: 10.1128/AEM.00062-07

Wang, M. Y., Lan, X. F., Xu, X. P., Fang, Y. Y., Singh, B. P., Sardans, J., et al. (2020). Steel slag and biochar amendments decreased CO_2 emissions by altering soil chemical properties and bacterial community structure over two-year in a subtropical paddy field. *Sci. Total Environ.* 740:140403. doi: 10.1016/j.scitotenv.2020.140403

Wang, J. B., Xie, J. H., Li, L. L., Luo, Z. Z., Zhang, R. Z., Wang, L. L., et al. (2021). The impact of fertilizer amendments on soil autotrophic bacteria and carbon emissions in maize field on the semiarid loess plateau. *Front. Microbiol.* 12:664120. doi: 10.3389/fmicb.2021.664120

Xu, K., Chai, Q., Hu, F. L., Fan, Z. L., and Yin, W. (2021). N-fertilizer postponing application improves dry matter translocation and increases system productivity of wheat/maize intercropping. *Sci. Rep.* 11:22825. doi: 10.1038/s41598-021-02345-5

Xu, M., Lou, Y., Sun, X., Wang, W., Baniyamuddin, M., and Zhao, K. (2011). Soil organic carbon active fractions as early indicators for total carbon change under straw incorporation. *Biol. Fertil. Soils* 47, 745–752. doi: 10.1007/s00374-011-0579-8

Xue, D., Yao, H., and Huang, C. (2006). Microbial biomass, N mineralization and nitrification, enzyme activities, and microbial community diversity in tea orchard soils. *Plant Soil* 288, 319–331. doi: 10.1007/s11104-006-9123-2

Yang, H. W., Hu, F. L., Yin, W., Chai, Q., Zhao, C., Yu, A. Z., et al. (2021). Integration of tillage and planting density improves crop production and carbon mitigation of maize/pea intercropping in the oasis irrigation area of northwestern China. *Field Crops Res.* 272:108281. doi: 10.1016/j.fcr.2021.108281

Yao, Z. S., Zheng, X. H., Dong, H. B., Wang, R., Mei, B. L., and Zhu, J. G. (2012). A 3-year record of N_2O and CH_4 emissions from a sandy loam paddy during rice seasons as affected by different nitrogen application rates. *Agric. Ecosyst. Environ.* 152, 1–9. doi: 10.1016/j.agee.2012.02.004

Yin, W., Chai, Q., Fan, Z. L., Hu, F. L., Fan, H., Guo, Y., et al. (2022). Energy budgeting, carbon budgeting, and carbon footprints of straw and plastic film management for environmentally clean of wheat-maize intercropping system in northwestern China. *Sci. Total Environ.* 826:154220. doi: 10.1016/j.scitotenv.2022.154220

Yin, W., Yu, A. Z., Chai, Q., Hu, F. L., Feng, F., and Gan, Y. T. (2015). Wheat and maize relay-planting with straw covering increases water use efficiency up to 46%. *Agron. Sustain. Dev.* 35, 815–825. doi: 10.1007/s13593-015-0286-1

Ying, J. Y., Zhang, L. M., and He, J. Z. (2010). Putative ammonia-oxidizing bacteria and archaea in an acidic red soil with different land utilization patterns. *Environ. Microbiol. Rep.* 2, 304–312. doi: 10.1111/j.1758-2229.2009.00130.x

Yu, L. L., Luo, S. S., Gou, Y. G., Xu, X., and Wang, J. W. (2021). Structure of rhizospheric microbial community and N cycling functional gene shifts with reduced N input in sugarcane-soybean intercropping in South China. *Agric. Ecosyst. Environ.* 314:107413. doi: 10.1016/j.agee.2021.107413

Zang, H. D., Wang, J. Y., and Kuzyakov, Y. (2016). N fertilization decreases soil organic matter decomposition in the rhizosphere. *Appl. Soil Ecol.* 108, 47–53. doi: 10.1016/j.apsoil.2016.07.021

Zhai, L. M., Liu, H. B., Zhang, J. Z., Huang, J., and Wang, B. R. (2011). Long-term application of organic manure and mineral fertilizer on N_2O and CO_2 emissions in a red soil from cultivated maize-wheat rotation in China. *J. Agric. Sci.* 10, 1748–1757. doi: 10.1016/S1671-2927(11)60174-0

Zhang, K. P., Duan, M. C., Xu, Q. W., Wang, Z. Y., Liu, B. Y., and Wang, L. C. (2020). Soil microbial functional diversity and root growth responses to soil amendments contribute to CO_2 emission in rainfed cropland. *Catena (Amst)* 195:104747. doi: 10.1016/j.catena.2020.104747

Zhang, Z., Yu, Z. W., Zhang, Y. L., and Shi, Y. (2021). Finding the fertilization optimization to balance grain yield and soil greenhouse gas emissions under water-saving irrigation. *Soil Till. Res.* 214:105167. doi: 10.1016/j.still.2021.105167

Zhao, C., Chai, Q., Cao, W. D., Whalen, J. K., Zhao, L. X., and Cai, L. J. (2019). No-tillage reduces competition and enhances compensatory growth of maize (*Zea mays L.*) intercropped with pea (*Pisum sativum L.*). *Field Crops Res.* 243:107611. doi: 10.1016/j.fcr.2019.107611

Zhao, C., Chai, Q., Zhao, Y. H., Mu, Y. P., Zhang, Y., Yu, A. Z., et al. (2016). Interspecific competition and complementation is a function of N management in maize-pea intercropping systems. *Crop Sci.* 56, 3286–3294. doi: 10.2135/cropsci2016.03.0204

frontiers | Frontiers in Microbiology

TYPE Original Research
PUBLISHED 18 October 2022
DOI 10.3389/fmicb.2022.1033210

OPEN ACCESS

EDITED BY
Baoli Zhu,
Institute of Subtropical Agriculture (CAS), China

REVIEWED BY
Yongxin Lin,
Fujian Normal University, China
Hong Pan,
Shandong Agricultural University, China

*CORRESPONDENCE
Huaiying Yao
hyyao@iue.ac.cn

SPECIALTY SECTION
This article was submitted to Terrestrial Microbiology, a section of the journal Frontiers in Microbiology

RECEIVED 31 August 2022
ACCEPTED 03 October 2022
PUBLISHED 18 October 2022

CITATION
Yang Z, She R, Hu L, Yu Y and Yao H (2022) Effects of biochar addition on nitrous oxide emission during soil freeze–thaw cycles. *Front. Microbiol.* 13:1033210. doi: 10.3389/fmicb.2022.1033210

Effects of biochar addition on nitrous oxide emission during soil freeze–thaw cycles

Zhihan Yang[1], Ruihuan She[1], Lanfang Hu[2,3], Yongxiang Yu[1,2,3] and Huaiying Yao[1,2,3]*

[1]Research Center for Environmental Ecology and Engineering, School of Environmental Ecology and Biological Engineering, Wuhan Institute of Technology, Hubei, China, [2]Key Laboratory of Urban Environment and Health, Ningbo Observation and Research Station, Institute of Urban Environment, Chinese Academy of Sciences, Fujian, China, [3]Zhejiang Key Laboratory of Urban Environmental Processes and Pollution Control, CAS Haixi Industrial Technology Innovation Center in Beilun, Zhejiang, China

Biochar applied to soil can reduce nitrous oxide (N_2O) emissions produced by freeze–thaw processes. Nonetheless, how biochar modification affects N_2O emissions during freeze–thaw cycles is not completely clear. In our research, during freeze–thaw cycles, microcosm experiments were conducted to investigate the effects of maize straw biochar (MB) or rice straw biochar (RB) addition on soil N_2O emissions under different water conditions. The N_2O emissions peaked at the initial stage of thawing in all the soils, and the total N_2O emissions were considerably greater in the flooded soils than in the nonflooded soils. Compared with the soils without biochar addition, RB and MB amendments inhibited N_2O emissions by 69 and 67%, respectively. Moreover, after biochar addition, the abundance of AOB *amoA* genes decreased by 9–13%. Biochar addition significantly decreased the content of microbial biomass nitrogen (MBN) in flooded soil during thawing, which was significantly correlated with N_2O emissions and nitrification and denitrification communities. The PLS-PM further revealed that biochar can inhibit the production and emission of soil N_2O by reducing soil MBN during soil thawing. In addition, soil moisture directly significantly affects N_2O emissions and indirectly affects N_2O emissions through its influence on soil physicochemical properties. Our results revealed the important function of biochar in decreasing the emission of N_2O in flooded soil during freeze–thaw cycles.

KEYWORDS

freezing–thawing, soil moisture, biochar, nitrous oxide, paddy soil

Introduction

Freeze–thaw alternation, as a familiar natural phenomenon, affects more than 70% of the land area in cold regions and high latitudes (Mellander et al., 2007). Global climate warming has exacerbated the intensity and frequency of freeze–thaw cycles, leading to an increase in nitrous oxide (N_2O) release in soil. On a 100-year timescale, the global warming potential of N_2O, a significant greenhouse gas, is 298 times higher

than that of carbon dioxide (CO_2; Gao et al., 2015; Pelster et al., 2019). Soil-sourced N_2O emissions account for 60% of total N_2O emissions, and up to 70% of the annual N_2O flux could be emitted in temperate regions during the freeze–thaw period (Yao et al., 2010). In a laboratory experiment, Gao et al. (2015) found that the total N_2O emissions from peatland and meadow soils in the Qinghai-Tibet Plateau sharply increased by 5.8 and 3.9 times after freezing and thawing, respectively. In forest fields, Peng et al. (2019) conducted high-frequency monitoring of N_2O emissions on Changbai Mountain and found that the average daily N_2O emissions rate in the freeze–thaw period was up to 2618.3 $\mu g\, N\, m^{-2} d^{-1}$, and the cumulative emissions in the freeze–thaw period accounted for approximately 58% of the annual emissions. Based on a model, Wagner-Riddle et al. (2017) predicted that farmland soils undergoing seasonal freeze–thaw contributed approximately 1.07 ± 0.59 Tg of N_2O per year, which is considered the largest anthropogenic source of N_2O to date. The enhanced metabolism of substrate microorganisms accumulated during thawing is considered the most likely cause of the high risk of N_2O emission (Kim et al., 2012). Ice films are formed on the surface of soil granules in the process of soil freezing, leading to an anoxic environment and promoting microbial denitrification, hence generating N_2O. Nevertheless, the presence of ice film also inhibited the release of N_2O. While the soil commenced to melt, all captured N_2O was quickly released into the atmosphere (Goldberg et al., 2010).

For the past few years, numerous studies have reported that biochar applied to soils affects the emission of N_2O (Purakayastha et al., 2019; Ahmad et al., 2021; Zhang et al., 2022a). Although biochar contains α-pinene and ethylene, volatile organic compounds called nitrification inhibitors (Spokas et al., 2011; Taghizadeh-Toosi et al., 2011), these influences differ across biochar and soil types and environmental conditions. For example, Bruun et al. (2011) and Clough et al. (2010) discovered that biochar combined with bovine urine or anaerobically digested slurry enhanced soil N_2O emissions. However, it was also asserted that biochar addition did not influence soil N_2O emissions in subtropical grasslands (Scheer et al., 2011). Until now, the impact of biochar on nitrification and denitrification related to N_2O formation remained unclear. For example, Case et al. (2015) found that biochar addition accelerated nitrification and soil N mineralization to produce N_2O, but this practice decreased the total emissions of N_2O by 91% by inhibiting denitrification, which was probably due to the different properties of biochar. Therefore, it is important to investigate the effects of different types of biochar on N_2O emissions during thawing.

As an important environmental factor related to oxygen availability in soil, moisture is closely coupled with biogeochemical cycles (Song et al., 2020). Soil moisture directly affects soil microorganism activity and indirectly regulates nitrification and denitrification processes by affecting soil substrate availability and oxygen diffusion capacity (Chen et al., 2018). Chen et al. (2018) found that soil moisture was positively related to N_2O flux in the nongrowing period and explained approximately 32% of the change in N_2O flux. Initial soil moisture conditions also affect the dynamics of N transformation during freeze–thaw (Stres et al., 2008). Anaerobic or anoxic microenvironments were generally beneficial for denitrifiers to produce N_2O. With the gradual increase in water content, the degree of damage caused by water molecules to soil aggregates becomes more pronounced during freezing. Accordingly, the higher amount of active organic carbon released by the aggregates probably promotes the metabolic activity of heterotrophic microorganisms, including denitrifying microorganisms (Song et al., 2020). In this experiment, maize straw biochar and rice straw biochar were selected to explore the regulatory effect of different biochars on N_2O emissions during the soil freeze–thaw cycles under different water conditions. We hypothesized that biochar addition can reduce N_2O emissions by decreasing the abundance of functional genes related to denitrification.

Materials and methods

Soil analysis

The studied soil was gathered from a typical paddy field that has a long history of rice cultivation in Shuguang Village (123°58′31″ E, 47°23′15” N), Qiqihar City, Heilongjiang Province, China. Influenced by the mid-temperate continental monsoon climate in this area, the average annual temperature was 3.2°C (the monthly average temperature ranged from −20.5°C in January to 22.2°C in July), and the average annual precipitation was 415 mm. The topsoil normally begins to frost around October and thaws in March of the following year due to rising temperatures (Song et al., 2008). We collected surface-layer soil (0–20 cm) after the thawing period in March 2019. Part of the soil samples were air-dried and then sieved through a 2-mm mesh to remove observable stones and roots for physicochemical analysis. The other part of the soil sample was stored at 4°C for subsequent incubation experiments. The soil texture was silty loam. The pH, total nitrogen and total carbon contents of the soil were 6.4, 0.22, and 2.37%, respectively. The basic chemical and physical properties of the soil are listed in Table 1.

TABLE 1 Physicochemical properties of soil samples and biochar.

	C (%)	N (%)	C/N ratio	pH	Soil texture		
					Sand (%)	Silt (%)	Clay (%)
Soil	2.37	0.22	10.4	6.4	38	26	36
MB	75.3	1.35	55.9	8.5	–	–	–
RB	46.5	0.76	60.9	10.4	–	–	–

MB, maize straw biochar; RB, rice straw biochar.

Experimental design

Soil samples of 15.0 g (dry weight) were accurately weighed in a 120-ml brown serum flask, and the soil water content was adjusted to 60% water holding capacity (WHC), 100% WHC, and flooding with a 1-cm water layer thickness. Maize straw biochar (MB) and rice straw biochar (RB) with a mass concentration of 2% were added before incubation. The basic physicochemical properties of the biochar used in this study are listed in Table 1. The surface morphology and structural characteristics of biochar were observed by scanning electron microscopy (SEM; Figure 1). All treatments were precultured at 25°C for 7 days in the dark (the culture vessel was ventilated, and water loss was replenished) to fully recover the microbial activity in the soil. After preculture, the soils were frozen at −20°C for 7 days to simulate winter freezing, and then the temperature was set to 4°C for 12 days to simulate thawing.

Gas sampling and analysis

Nitrous oxide emissions were measured within 12 days after thawing. A gas chromatograph with an electron capture detector (ECD) was used to analyze the concentration of N_2O produced by the soil. Then, the total N_2O emissions of the entire culture period were calculated by the daily emission rate described by Yu et al. (2022).

Soil mineral nitrogen measurement

The cultured fresh soil samples on the first day after thawing were weighed to approximately 3 g, 1 mol/L KCl solution was added at a ratio of 1:10 (w:v), and the sample was fully mixed. The samples were placed on a horizontal oscillator to fully oscillate for 30 min (180 r/min). After shaking, the filtrate was collected by centrifugation at 3,000 r/min. Finally, a flow analyzer determined the contents of nitrate (NO_3^-) and ammonium (NH_4^+; Zhang et al., 2022b).

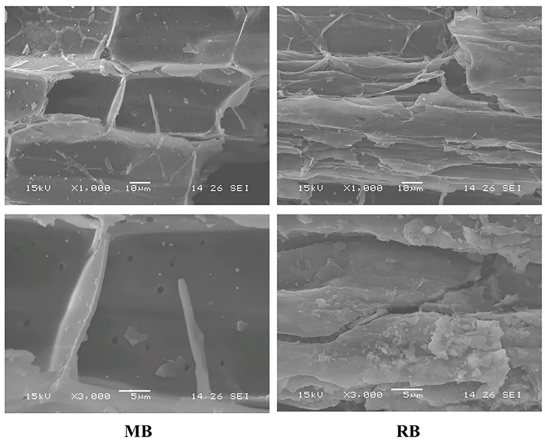

FIGURE 1
Surface morphology and structural characteristics of biochar observed by scanning electron microscopy (SEM; MB: maize straw biochar; RB: rice straw biochar).

Soil dissolved organic carbon and microbial biomass nitrogen measurements

The microbial biomass nitrogen (MBN) contents in the soil were determined by potassium sulfate extraction and chloroform fumigation (Jenkinson et al., 2004). Approximately 3 g of fresh soil on the first day after thawing was weighed and placed in a clean centrifuge tube, and 0.5 ml of ethanol-free chloroform was added and fully mixed. The soils were placed at 25°C for sealed culture in the dark for 24 h, and 10 ml potassium sulfate solution with a concentration of 0.5 mol/l was added. After shaking extraction for 30 min (180 r/min) on the vibrating machine, centrifugal filtration was carried out, and finally, the measurement was carried out on the machine. The control group was extracted without fumigation and determined by potassium sulfate solution. The soil dissolved organic carbon and nitrogen contents were analyzed by a total organic carbon analyzer (MULTI-N/C 2100S, Analytik Jena, Jena, Germany). The organic carbon concentration of the unfumigated sample group is the dissolved organic carbon (DOC) content of the soil sample. The MBN contents were obtained from the difference in total nitrogen (TN) between the fumigated and unfumigated soils multiplied by the corresponding conversion coefficient (kEN = 0.45; Jenkinson et al., 2004).

DNA extraction and quantitative PCR analysis

DNA was extracted from 0.5 g freeze-dried soil using the FastDNA® for Soil Kit (MP Biomedicals, California, United States) strictly according to the manufacturer's instructions. The DNA of the soil samples before freezing and on the first and seventh days of thawing was extracted. Quantitative analysis of functional genes is based on extracted DNA as templates at the gene level. Thus, DNA was used as a template for quantitative analysis of nitrification [ammonia-oxidizing archaea (AOA) *amoA*, ammonia-oxidizing bacteria (AOB) *amoA*] and denitrification (*nirS*, *nirK*, and *nosZ*) functional genes (Zhang et al., 2021). The detailed amplification system, conditions and primers are shown in Table 2.

Quantitative PCR (qPCR) was carried out for analysis using the LightCycler® 480II system (Roche Diagnostics, Basel, Switzerland). The amplification system contained 10 μl Absolute SYBER Fluorescein Mix (Thermo Scientific, New York, United States), 0.5 μl primer, 7 μl nuclease-free water, and 2 μl 10-fold diluted DNA stock as a template (6–26 ng). Negative

TABLE 2 Primers for nitrifier (AOA and AOB *amoA*) and denitrifier (*nirK*, *nirS* and *nosZ*) genes and their thermal cycling conditions for qPCR.

Target genes	Primer	Sequence (5′–3′)	Product length (bp)	Amplification condition	References
AOA *amoA*	*Crenamo*A23f	ATGGTCTGGCTWAGACG	635	95°C 15 s; 53°C 45 s; 72°C	Francis et al. (2005)
	*Crenamo*A616r	GCCATCCATCTGTATGTCCA		45 s; 83°C 15 s; 45 cycles	
AOB *amoA*	*amoA*1F	GGGGTTTCTACTGGTGGTCCC	491	95°C 15 s; 54°C 40 s; 72°C	Francis et al. (2005)
	*amoA*2R	CTCKGSAAAGCCTTCTTC		45 s; 84°C 15 s; 40 cycles	
nirS	*nirS*-cd3aF	GTSAACGTSAAGGARACSGG	425	95°C 15 s; 50°C 45 s; 72°C	Throback et al. (2004)
	nirS-R3cd	GASTTCGGRTGSGTCTTGA		45 s; 88°C 15 s; 50 cycles	
nirK	*F1aCu*	ATCATGGTSCTGCCGCG	514	95°C 10 s; 53°C 45 s; 72°C	Throback et al. (2004)
	R3Cu	GCCTCGATCAGRTTGTGGTT		45 s; 86°C 15 s; 45 cycles	
nosZ	*nosZ*-F	CGYTGTTCMTCGACAGCCAG	453	95°C 15 s; 50°C 30 s; 72°C	Scala and Kerkhof
	nosZ-1662R	CGSACCTTSTTGCCSTYGCG		30 s; 83°C 15 s; 55 cycles	(1998)

controls were replaced with the same amount of nuclease-free water. The functional gene plasmids related to bacterial nitrification and denitrification were extracted by DNA template, and the plasmids were continuously diluted 10 times to form a standard curve for gene quantitative analysis (Yin et al., 2019).

Statistical analysis

The software used for data processing and analysis mainly included Excel 2016, OriginPro 2018, R4.2.1 and SPSS 20.0 (IBM, Chicago, United States). Univariate ANOVA (Tukey's HSD, $p < 0.05$) was used to analyze significant differences in soil chemical and physical properties and abundance of functional genes during thawing. The Mantel test established through the "linkET" program package in R language was used to analyze the interaction influences of different factors. Partial least squares path modeling (PLS-PM) was established through the "plsm" program package in R language to analyze the influence of biochar addition and moisture on N_2O emissions during the thawing process.

Results

Soil N_2O emissions

After different biochar treatments, N_2O gas emissions peaked at the initial stage of soil thawing (within 1 day), declined rapidly, and then tended to be stable (Figure 2). The addition of both biochar types had a remarkable influence on cumulative N_2O emissions during soil thawing in flooded conditions, while there was no remarkable difference in total N_2O emissions between the two nonflooded conditions (Figure 3). The MB and RB treatments inhibited cumulative N_2O emissions by 67 and 69%, respectively. No significant difference was found between the inhibition effects of these two biochars on N_2O emissions during the soil freeze–thaw process.

Soil mineral N and DOC

In our study, contrasted with the control treatment, the NO_3^- content in the nonflooded soil under the MB treatment decreased at 1 day of thawing, while the NO_3^- content in the nonflooded soil increased under the RB treatment. There was no significant difference in NO_3^- content between the different treatments under flooded conditions (Figure 4A). Both biochar amendments increased NH_4^+ content, but there was no significant difference in NH_4^+ content between the two treatments (Figure 4B). Compared with the control treatment, biochar addition increased the content of DOC by 0.32–1.55 times. Moreover, the soil DOC content with RB addition was higher than that with MB addition (Figure 4D). Last, biochar addition reduced the soil MBN content under 100% WHC and flooded soils but did not affect MBN content under 60% WHC soil (Figure 4C).

Microbial functional genes

There was no significant difference in functional gene abundance related to nitrification and denitrification processes on the first day after thawing compared with before freezing, but most of the gene abundance decreased on the seventh day after thawing (Figure 5). The addition of biochar increased the abundance of the nitrifying gene AOA *amoA* (Figure 6A) but reduced AOB *amoA* (Figure 6B). Biochar treatment did not observably influence the abundance of the denitrifying functional gene *nirS* (Figure 6C) but increased the abundance of *nirK* (Figure 6D) and *nosZ* (Figure 6E). In addition, soil moisture had no significant effect on functional gene abundance (Figures 7, 8).

Relationship among different factors and N_2O emissions

The Mantel test showed that biochar, soil moisture, MBN, NO_3^-, AOA *amoA*, and AOB *amoA* had significant influences on

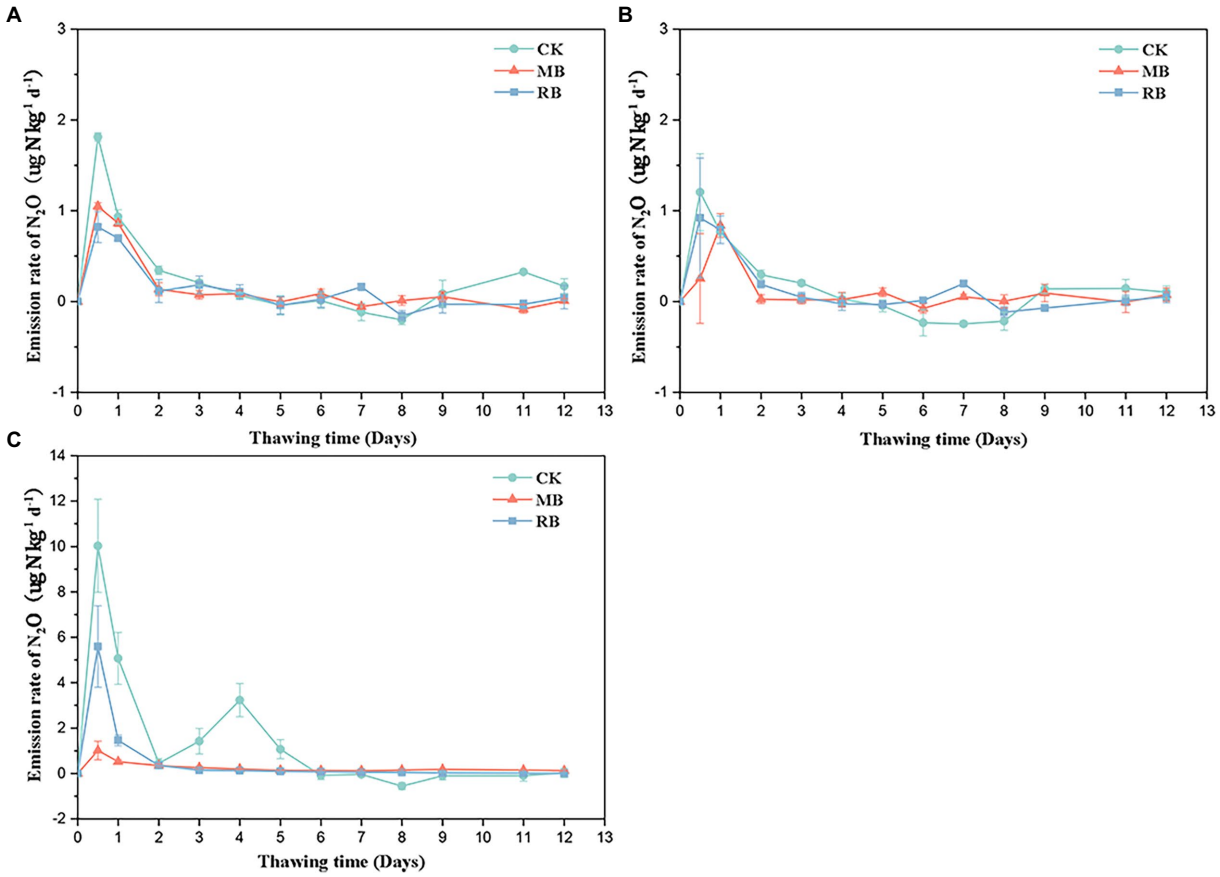

FIGURE 2
Emission rates of soil nitrous oxide (N_2O) with biochar amendments during the thawing period under 60% water holding capacity (WHC; **A**), 100% WHC **(B)**, and flooding **(C)**. (MB: maize straw biochar; RB: rice straw biochar; error bars represent the standard error, n=3).

N_2O emissions. Moreover, soil moisture had negative effects on the content of NO_3^- (Figure 7). PLS-PM showed that the addition of biochar had significant negative effects on nitrifiers and MBN content and indirectly affected N_2O emissions through its effect on soil MBN (Figures 8A,B). Soil moisture directly significantly affects N_2O emissions and indirectly affects N_2O emissions through its influence on soil physicochemical properties (Figures 8A,B).

Discussion

Effect of soil moisture on N_2O emissions during thawing

Previous studies observed peaks of N_2O emission at the start of thawing during the freeze–thaw periods (Prieme and Christensen, 2001; Wu et al., 2020). In the present study, N_2O gas emissions peaked at the initial stage of soil thawing, which mainly contributed to the release of N_2O during the freeze–thaw period. There was no significant difference in N_2O emissions (< 2 μg kg^{-1}) found in this study between soil moisture contents of 60 and 100% WHC during the freeze–thaw process, but the cumulative N_2O emissions significantly increased to 10.9 μg kg^{-1} in the flooded soil. This result was consistent with Bhowmik et al. (2016), who found that N_2O emissions from pasture soil increased from 5.43 to 12.3 μg kg^{-1} during freeze–thaw when the soil moisture content increased from 40 to 80%. This result was probably due to denitrification dominating the N_2O production under saturated water content and then inducing a high risk of N_2O emission during the thawing process (Mathieu et al., 2006; Braker et al., 2010). Overall, our results highlight the importance of water conditions in regulating N_2O emissions during thawing, and it is necessary to develop an efficient approach to inhibit the production of N_2O under flooded conditions.

Soil moisture controls the emission of N_2O mainly by regulating the content of soil oxygen (O_2) and thereby affects the transformation of denitrification and nitrification processes (Li et al., 2021). The flooding conditions with high water content in soil reduced O_2 diffusion and formed anoxic or anaerobic environments, which are conducive to denitrification (Ma and Fan, 2020). However, in this study, there was no significant difference in the abundance of functional genes related to nitrification and denitrification processes. But the soil

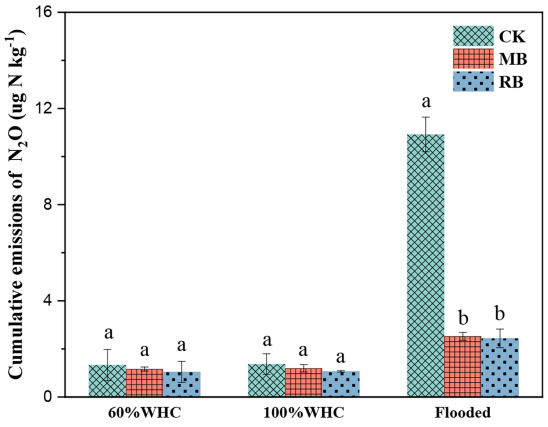

FIGURE 3
Cumulative N_2O emissions with biochar amendments during the thawing period. (CK: control; MB: maize straw biochar; RB: rice straw biochar; and a and b indicate significant differences among the different biochar treatments, $p<0.05$; error bars represent the standard error, $n=3$).

NO_3^- content, as a substrate for denitrifiers, decreased sharply under flooding conditions during thawing. This result showed that soil moisture probably affects N_2O production/reduction by controlling denitrifying microbial activity rather than denitrifying microbial gene abundance.

Effect of biochar addition on N_2O emissions during thawing

Previous studies found that biochar can effectively reduce soil greenhouse gas production (Yin et al., 2021), which might be a possible method to decrease soil N_2O emissions during freeze–thaw. Our results demonstrated that biochar amendment significantly inhibited soil N_2O production by 67–69% during freeze–thaw, which was consistent with the results of Liu et al. (2016), who confirmed that biochar addition inhibited soil N_2O emissions by 20–70% during freeze–thaw. In another experiment, Hou et al. (2020) found that the application of biochar to

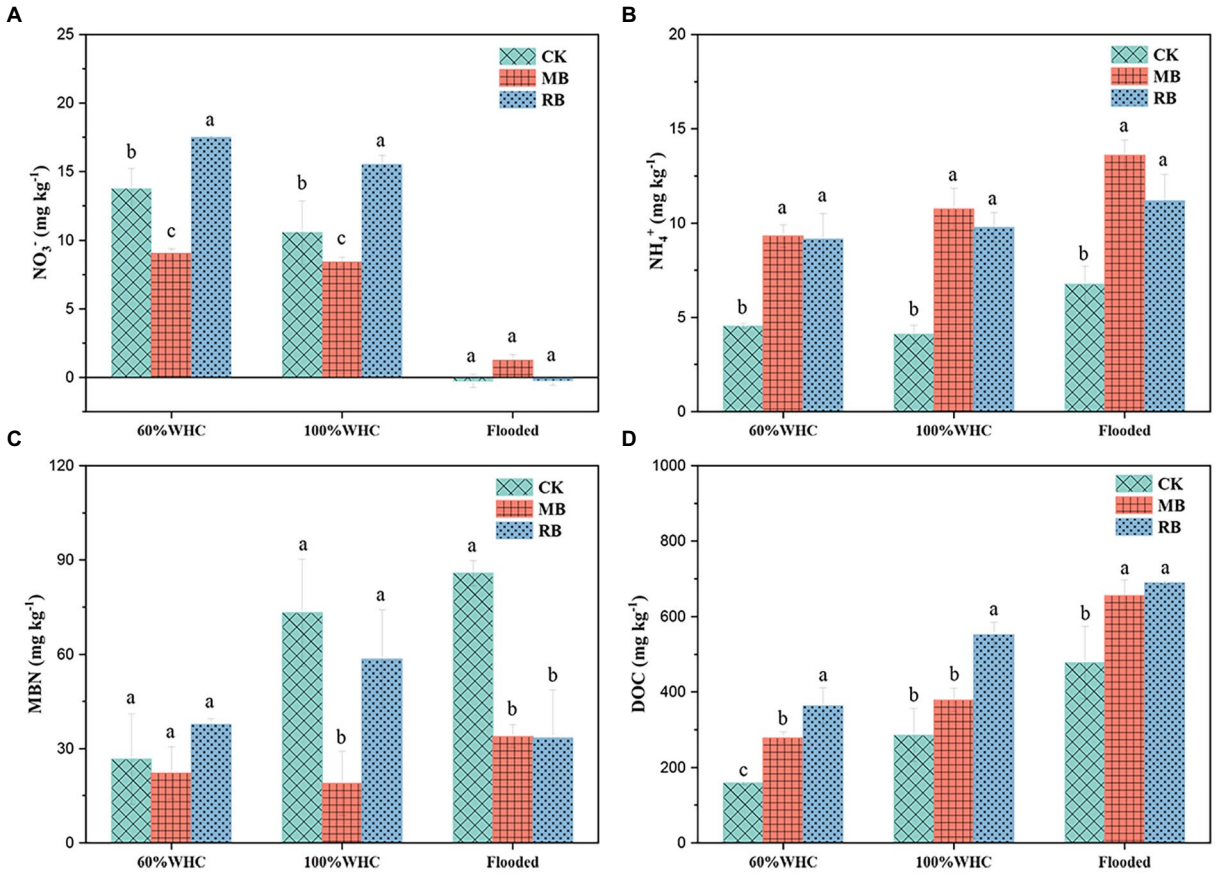

FIGURE 4
Contents of soil NO_3^- **(A)**, NH_4^+ **(B)**, microbial biomass nitrogen (MBN; **C**), and dissolved organic carbon (DOC; **D**) with biochar amendments on the first day after thawing. (CK: control; MB: maize straw biochar; RB: rice straw biochar; a and b indicate significant differences among the different biochar treatments, $p<0.05$; error bars represent the standard error, $n=3$).

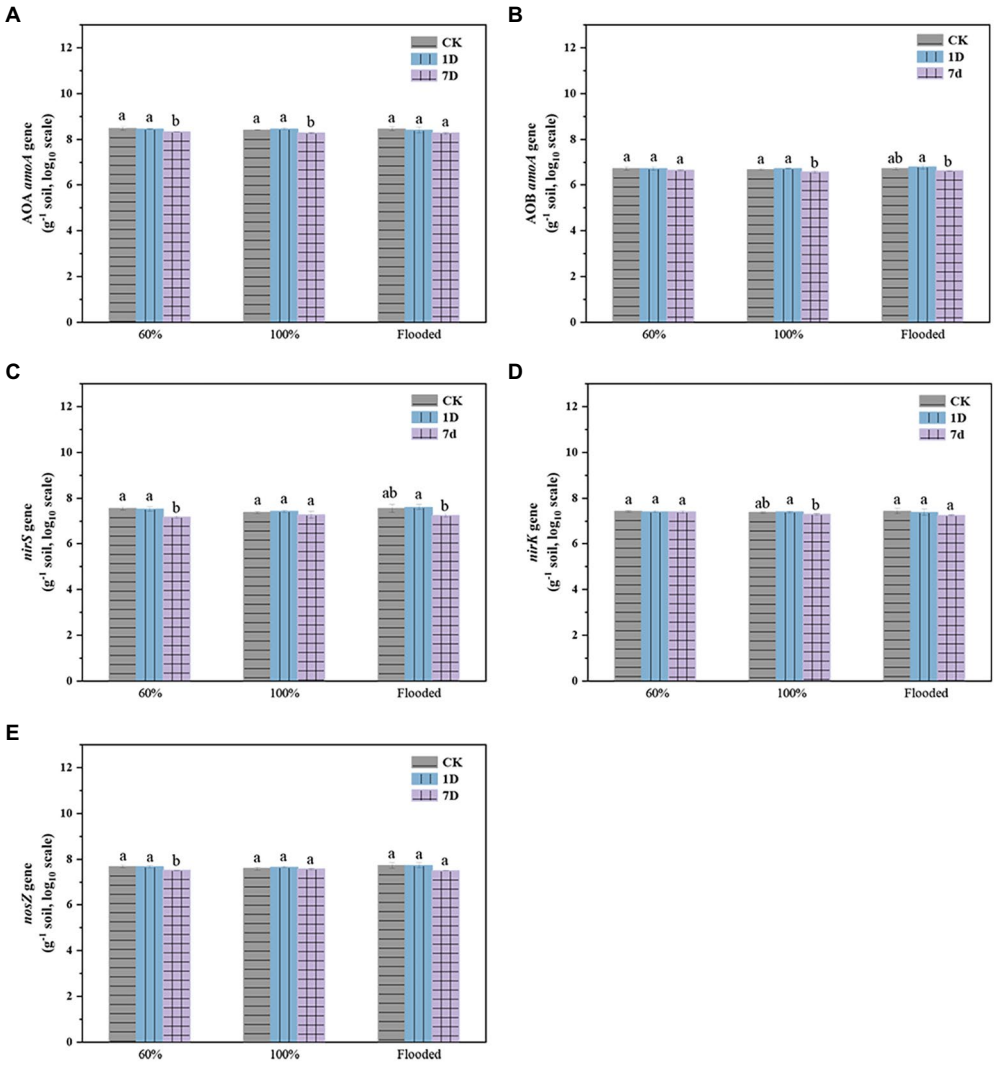

FIGURE 5
Abundance of the AOA *amoA* **(A)**, AOB *amoA* **(B)**, *nirS* **(C)**, *nirK* **(D)**, and *nosZ* **(E)** genes at different times (CK: control; 1D: the first day after thawing; 7D: the seventh day after thawing; a and b indicate significant differences among the different period, $p<0.05$; error bars represent the standard error, $n=3$).

seasonally frozen farmland soil directly reduced cumulative N_2O emissions by 24%. However, Zhou et al. (2017) found that biochar with high porosity interacted with freezing and increased N_2O emissions by microbial lysis. This difference indicated that the effect of biochar amendments on N_2O emissions during the freeze–thaw process varied with their type. Moreover, based on a meta-analysis, Brassard et al. (2016) found that biochar with a lower nitrogen content and higher C/N ratio (>30) was more suitable for mitigating soil N_2O emissions. In this study, compared with MB, although RB contained lower nitrogen content but higher porosity, there was no significant difference in N_2O mitigation potential between the two treatments amended with MB or RB biochar under flooded conditions. This result indicates that the anaerobic environment probably masked the actual impact of biochar properties on N_2O emissions.

It has been reported that biochar can reduce N_2O emissions by affecting soil N availability (Liu et al., 2016). However, under near-saturated conditions, Case et al. (2015) found that biochar inhibited the release of N_2O emissions, but the change in soil inorganic nitrogen (including NH_4^+ and NO_3^-) was not able to explain the reduction in N_2O emissions. In this study, the amendment of rice straw biochar significantly increased NH_4^+ and NO_3^- contents but had a negligible effect on N_2O emissions, indicating that biochar amendment did not affect inorganic N availability for N_2O production (Case et al., 2015; Xie et al., 2020). Moreover, under flooded conditions, the amendment of biochar increased the NH_4^+ content, which supplied an N source for nitrification to produce N_2O. However, the application of biochar significantly reduced N_2O emissions, indicating that the reduction in N_2O was probably due to the inhibitory compounds of biochar

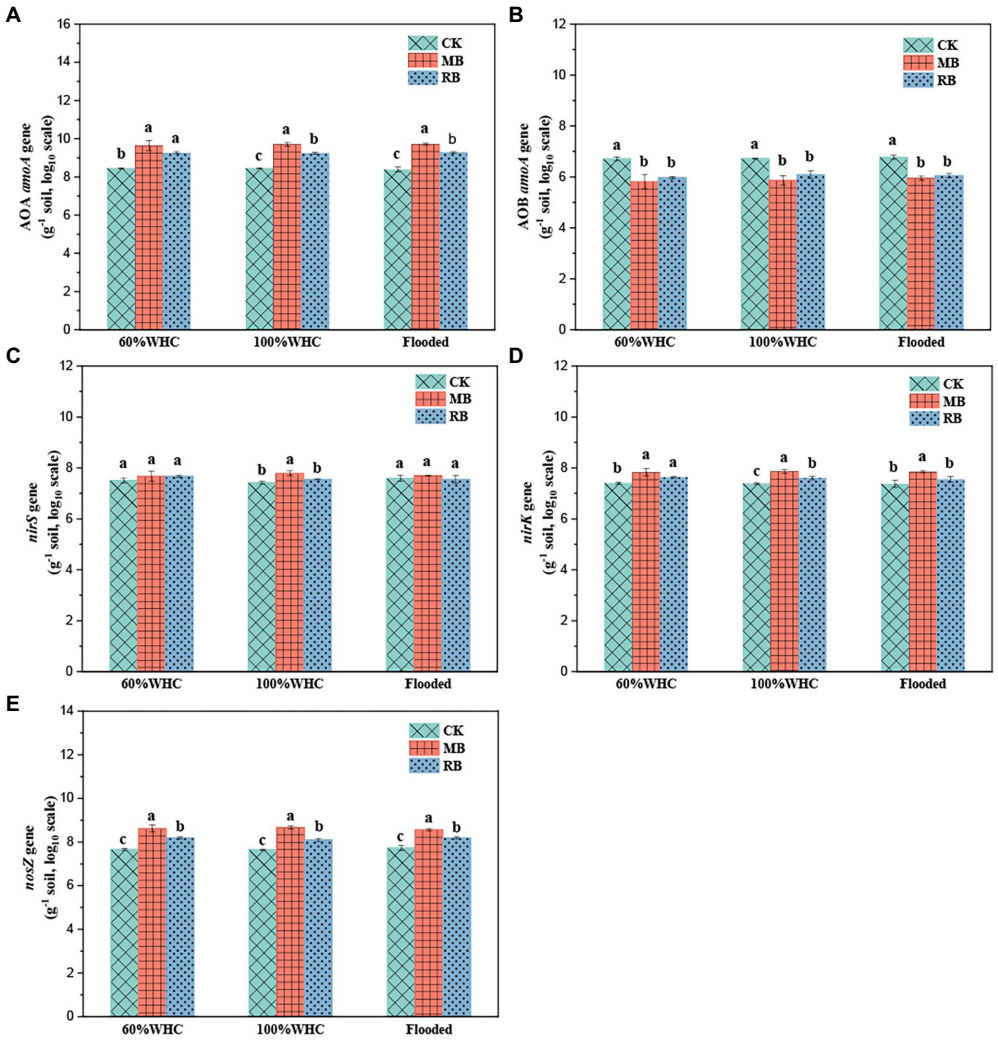

FIGURE 6
Abundance of the AOA *amoA* **(A)**, AOB *amoA* **(B)**, *nirS* **(C)**, *nirK* **(D)**, and *nosZ* **(E)** genes with biochar amendments on the first day after soil thawing (CK: control; MB: maize straw biochar; RB: rice straw biochar; a, b and c indicate significant differences among the different biochar treatments, $p<0.05$; error bars represent the standard error, $n=3$).

on nitrifiers and denitrifiers (Taghizadeh-Toosi et al., 2011; Quilliam et al., 2013; Case et al., 2015) rather than the N substrates.

The inhibitory effect of biochar on N_2O formation was mainly due to its inhibitory compounds on denitrification (Case et al., 2015; Edwards et al., 2018). However, in this study, biochar amendments significantly increased the abundance of the AOA *amoA* gene but reduced AOB *amoA* gene abundance during the freeze–thaw period. In neutral and alkaline soils, Shen et al. (2012) found that AOB dominate nitrification rather than AOA using the DNA stable isotope probing (DNA-SIP) method. Therefore, it is expected that biochar can reduce N_2O production, probably by limiting the nitrification caused by AOB. During the denitrification process, the amendment of biochar significantly increased the abundance of the *nosZ* gene encoding N_2O reductase, indicating that biochar reduced N_2O emission through enhanced N_2O reduction during thawing. In addition, the addition of biochar significantly decreased the content of MBN, indicating that biochar reduced N_2O emissions by inhibiting the substrates for N mineralization. Overall, based on the PLS-PM model, although biochar significantly affects the abundance of nitrifiers and denitrifiers, the change in functional genes related to nitrification and denitrification was not able to explain the reduction in N_2O emissions. Further study should focus on the impact of biochar on the activity of nitrifiers and denitrifiers.

Conclusion

In the absence of biochar, there was no significant difference in N_2O emissions between soil water holding capacities of 60 and 100% during the freezing–thawing period. However, microbial-mediated denitrification and nitrification processes in flooded soil led to a large increase in N_2O produced by freeze–thaw processes. During

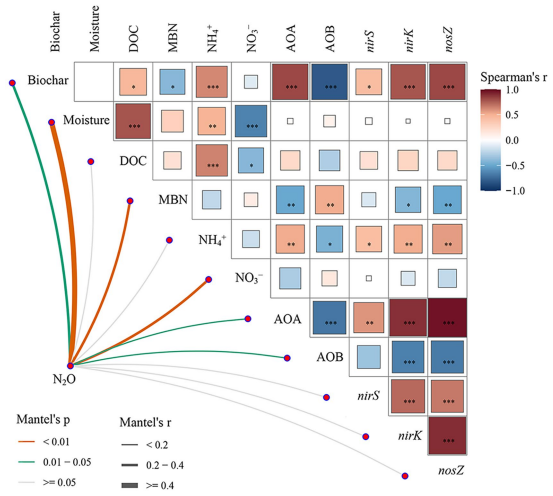

FIGURE 7
Pairwise comparisons of different factors are shown, with a color gradient denoting Spearman's correlation coefficients. N_2O emissions were related to each factor by Mantel tests. Edge width corresponds to Mantel's r statistic for the corresponding distance correlations, and edge color denotes the statistical significance based on 9,999 permutations. *, **, and *** indicate $p < 0.05$, $p < 0.01$, and $p < 0.001$, respectively.

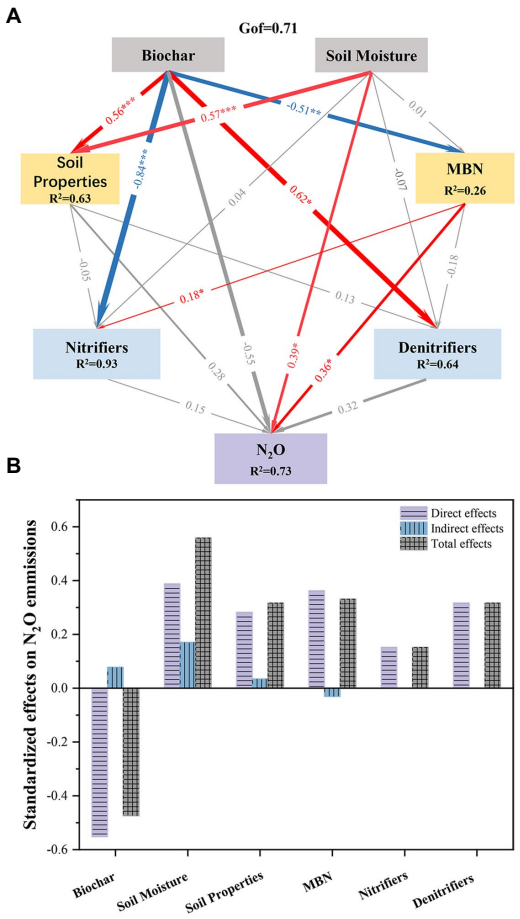

FIGURE 8
PLS-PM showing the direct and indirect effects of different factors on N_2O emissions with biochar amendment. (**A**: PLS-PM showing the relationships among biochar, soil moisture, soil properties, microbial biomass nitrogen, nitrifiers, and denitrifiers with respect to N_2O emissions. Blue and red arrows indicate positive and negative effects, respectively; the width of arrows indicates the path coefficients; *, **, and *** indicate $p<0.05$, $p<0.01$, and $p<0.001$, respectively; Gof indicates the goodness of fit; **B**: Standardized direct and indirect mean effects).

the thawing period, the application of biochar to soil had a negligible effect on N_2O emissions under nonflooded conditions but significantly reduced cumulative N_2O emissions by 67–69% under flooded condition. The reduction in N_2O emissions in the flooded environment was mainly due to biochar reducing N_2O production by decreasing the AOB *amoA* gene abundance and enhancing N_2O reduction by increasing the *nosZ* gene, which encodes N_2O reductase. However, across the different water conditions, the change in functional genes related to nitrification and denitrification processes was not able to explain the reduction in N_2O emissions. Further study should focus on the impact of biochar on the activity of nitrifiers and denitrifiers. Overall, our study showed that field water management was important for the release of N_2O in the freezing–thawing stage of paddy soil, and biochar addition could alleviate the N_2O produced in the freezing–thawing stage of flooding soil.

Data availability statement

The raw data supporting the conclusions of this article will be made available by the authors, without undue reservation.

Author contributions

HY and YY: conceptualization, supervision, and funding acquisition. HY, YY, RS, and ZY: methodology. ZY, RS, and YY: software, formal analysis, and data curation. RS, YY, LH, and ZY: validation. RS and LH: investigation. YY and HY: resources and visualization. ZY, RS, and LH: writing–original draft preparation. LH and YY: writing–review and editing. YY and RS: project administration. All authors contributed to the article and approved the submitted version.

Funding

This work was funded by the National Natural Science Foundation of China (42277109, 42077036, and 42021005) and the Ningbo Key Research and Development Program (2022Z159).

Conflict of interest

The authors declare that the research was conducted in the absence of any commercial or financial relationships that could be construed as a potential conflict of interest.

Publisher's note

References

Ahmad, Z., Mosa, A., Zhan, L., and Gao, B. (2021). Biochar modulates mineral nitrogen dynamics in soil and terrestrial ecosystems: a critical review. *Chemosphere* 278:130378. doi: 10.1016/j.chemosphere.2021.130378

Bhowmik, A., Fortuna, A. M., Cihacek, L. J., Bary, A. I., and Cogger, C. G. (2016). Use of biological indicators of soil health to estimate reactive nitrogen dynamics in long-term organic vegetable and pasture systems. *Soil Biol. Biochem.* 103, 308–319. doi: 10.1016/j.soilbio.2016.09.004

Braker, G., Schwarz, J., and Conrad, R. (2010). Influence of temperature on the composition and activity of denitrifying soil communities. *FEMS Microbiol. Ecol.* 73, 134–148. doi: 10.1111/j.1574-6941.2010.00884.x

Brassard, P., Godbout, S., and Raghavan, V. (2016). Soil biochar amendment as a climate change mitigation tool: key parameters and mechanisms involved. *J. Environ. Manag.* 181, 484–497. doi: 10.1016/j.jenvman.2016.06.063

Bruun, E. W., Muller-Stover, D., Ambus, P., and Hauggaard-Nielsen, H. (2011). Application of biochar to soil and N_2O emissions: potential effects of blending fast-pyrolysis biochar with anaerobically digested slurry. *Eur. J. Soil Sci.* 62, 581–589. doi: 10.1111/j.1365-2389.2011.01377.x

Case, S. D. C., McNamara, N. P., Reay, D. S., Stott, A. W., Grant, H. K., and Whitaker, J. (2015). Biochar suppresses N_2O emissions while maintaining N availability in a sandy loam soil. *Soil Biol. Biochem.* 81, 178–185. doi: 10.1016/j.soilbio.2014.11.012

Chen, Z., Yang, S. Q., Zhang, A. P., Jing, X., Song, W. M., Mi, Z. R., et al. (2018). Nitrous oxide emissions following seasonal freeze-thaw events from arable soils in Northeast China. *J. Integr. Agric.* 17, 231–246. doi: 10.1016/s2095-3119(17)61738-6

Clough, T. J., Bertram, J. E., Ray, J. L., Condron, L. M., O'Callaghan, M., Sherlock, R. R., et al. (2010). Unweathered wood biochar impact on nitrous oxide emissions from a bovine-urine-amended pasture soil. *Soil Sci. Soc. Am. J.* 74, 852–860. doi: 10.2136/sssaj2009.0185

Edwards, J. D., Pittelkow, C. M., Kent, A. D., and Yang, W. H. (2018). Dynamic biochar effects on soil nitrous oxide emissions and underlying microbial processes during the maize growing season. *Soil Biol. Biochem.* 122, 81–90. doi: 10.1016/j.soilbio.2018.04.008

Francis, C. A., Roberts, K. J., Beman, J. M., Santoro, A. E., and Oakley, B. B. (2005). Ubiquity and diversity of ammonia-oxidizing archaea in water columns and sediments of the ocean. *Proc. Natl. Acad. Sci. U. S. A.* 102, 14683–14688. doi: 10.1073/pnas.0506625102

Gao, Y. H., Zeng, X. Y., Xie, Q. Y., and Ma, X. X. (2015). Release of carbon and nitrogen from alpine soils during thawing periods in the eastern Qinghai-Tibet plateau. *Water Air Soil Pollut.* 226:209. doi: 10.1007/s11270-015-2479-2

Goldberg, S. D., Borken, W., and Gebauer, G. (2010). N_2O emission in a Norway spruce forest due to soil frost: concentration and isotope profiles shed a new light on an old story. *Biogeochemistry* 97, 21–30. doi: 10.1007/s10533-009-9294-z

Hou, R. J., Li, T. X., Fu, Q., Liu, D., Li, M., Zhou, Z. Q., et al. (2020). Effects of biochar and straw on greenhouse gas emission and its response mechanism in seasonally frozen farmland ecosystems. *Catena* 194:104735. doi: 10.1016/j.catena.2020.104735

Jenkinson, D. S., Brookes, P. C., and Powlson, D. S. (2004). Measuring soil microbial biomass. *Soil Biol. Biochem.* 36, 5–7. doi: 10.1016/j.soilbio.2003.10.002

Kim, D. G., Vargas, R., Bond-Lamberty, B., and Turetsky, M. R. (2012). Effects of soil rewetting and thawing on soil gas fluxes: a review of current literature and suggestions for future research. *Biogeosciences* 9, 2459–2483. doi: 10.5194/bg-9-2459-2012

Li, J. B., Zhao, Y., Zhang, A. F., Song, B., and Hill, R. L. (2021). Effect of grazing exclusion on nitrous oxide emissions during freeze-thaw cycles in a typical steppe of Inner Mongolia. *Agric. Ecosyst. Environ.* 307:107217. doi: 10.1016/j.agee.2020.107217

Liu, X., Wang, Q., Qi, Z. M., Han, J. G., and Li, L. H. (2016). Response of N_2O emissions to biochar amendment in a cultivated sandy loam soil during freeze-thaw cycles. *Sci. Rep.* 6:35411. doi: 10.1038/srep35411

Ma, Y. H., and Fan, X. J. (2020). Detection and analysis of soil water content based on experimental reflectance spectrum data. *Asia Pac. J. Chem. Eng.* 15:e2507. doi: 10.1002/apj.2507

Mathieu, O., Henault, C., Leveque, J., Baujard, E., Milloux, M. J., and Andreux, F. (2006). Quantifying the contribution of nitrification and denitrification to the nitrous oxide flux using N-15 tracers. *Environ. Pollut.* 144, 933–940. doi: 10.1016/j.envpol.2006.02.005

Mellander, P. E., Lofvenius, M. O., and Laudon, H. (2007). Climate change impact on snow and soil temperature in boreal scots pine stands. *Clim. Chang.* 85, 179–193. doi: 10.1007/s10584-007-9254-3

Pelster, D. E., Chantigny, M. H., Rochette, P., Bertrand, N., Angers, D., Zebarth, B. J., et al. (2019). Rates and intensity of freeze-thaw cycles affect nitrous oxide and carbon dioxide emissions from agricultural soils. *Can. J. Soil Sci.* 99, 472–484. doi: 10.1139/cjss-2019-0058

Peng, B., Sun, J. F., Liu, J., Dai, W. W., Sun, L. F., Pei, G. T., et al. (2019). N_2O emission from a temperate forest soil during the freeze-thaw period: a mesocosm study. *Sci. Total Environ.* 648, 350–357. doi: 10.1016/j.scitotenv.2018.08.155

Prieme, A., and Christensen, S. (2001). Natural perturbations, drying-wetting and freezing-thawing cycles, and the emission of nitrous oxide, carbon dioxide and methane from farmed organic soils. *Soil Biol. Biochem.* 33, 2083–2091. doi: 10.1016/s0038-0717(01)00140-7

Purakayastha, T. J., Bera, T., Bhaduri, D., Sarkar, B., Mandal, S., Wade, P., et al. (2019). A review on biochar modulated soil condition improvements and nutrient dynamics concerning crop yields: pathways to climate change mitigation and global food security. *Chemosphere* 227, 345–365. doi: 10.1016/j.chemosphere.2019.03.170

Quilliam, R. S., Rangecroft, S., Emmett, B. A., Deluca, T. H., and Jones, D. L. (2013). Is biochar a source or sink for polycyclic aromatic hydrocarbon (PAH) compounds in agricultural soils? *Glob. Change Biol. Bioenergy* 5, 96–103. doi: 10.1111/gcbb.12007

Scala, D. J., and Kerkhof, L. J. (1998). Nitrous oxide reductase (nos Z) gene-specific PCR primers for detection of denitrifiers and three *nos Z* genes from marine sediments. *FEMS Microbiol. Lett.* 162, 61–68. doi: 10.1016/s0378-1097(98)00103-7

Scheer, C., Grace, P. R., Rowlings, D. W., Kimber, S., and Van Zwieten, L. (2011). Effect of biochar amendment on the soil-atmosphere exchange of greenhouse gases from an intensive subtropical pasture in northern New South Wales. *Plant Soil* 345, 47–58. doi: 10.1007/s11104-011-0759-1

Shen, J. P., Zhang, L. M., Di, H. J., and He, J. Z. (2012). A review of ammonia-oxidizing bacteria and archaea in Chinese soils. *Front. Microbiol.* 3:296. doi: 10.3389/fmicb.2012.00296

Song, X. Y., Wang, G. X., Ran, F., Huang, K. W., Sun, J. Y., and Song, C. L. (2020). Soil moisture as a key factor in carbon release from thawing permafrost in a boreal forest. *Geoderma* 357:113975. doi: 10.1016/j.geoderma.2019.113975

Song, C. C., Zhang, J. B., Wang, Y. Y., Wang, Y. S., and Zhao, Z. C. (2008). Emission of CO_2, CH_4 and N_2O from freshwater marsh in northeast of China. *J. Environ. Manag.* 88, 428–436. doi: 10.1016/j.jenvman.2007.03.030

Spokas, K. A., Novak, J. M., Stewart, C. E., Cantrell, K. B., Uchimiya, M., DuSaire, M. G., et al. (2011). Qualitative analysis of volatile organic compounds on biochar. *Chemosphere* 85, 869–882. doi: 10.1016/j.chemosphere.2011.06.108

Stres, B., Danevcic, T., Pal, L., Fuka, M. M., Resman, L., Leskovec, S., et al. (2008). Influence of temperature and soil water content on bacterial, archaeal and denitrifying microbial communities in drained fen grassland soil microcosms. *FEMS Microbiol. Ecol.* 66, 110–122. doi: 10.1111/j.1574-6941.2008.00555.x

Taghizadeh-Toosi, A., Clough, T. J., Condron, L. M., Sherlock, R. R., Anderson, C. R., and Craigie, R. A. (2011). Biochar incorporation into pasture soil suppresses in situ nitrous oxide emissions from ruminant urine patches. *J. Environ. Qual.* 40, 468–476. doi: 10.2134/jeq2010.0419

Throback, I. N., Enwall, K., Jarvis, A., and Hallin, S. (2004). Reassessing PCR primers targeting nirS, nirK and *nosZ* genes for community surveys of denitrifying bacteria with DGGE. *FEMS Microbiol. Ecol.* 49, 401–417. doi: 10.1016/j.femsec.2004.04.011

Wagner-Riddle, C., Congreves, K. A., Abalos, D., Berg, A. A., Brown, S. E., Ambadan, J. T., et al. (2017). Globally important nitrous oxide emissions from croplands induced by freeze-thaw cycles. *Nat. Geosci.* 10:279. doi: 10.1038/ngeo2907

Wu, X., Li, T., Wang, D. B., Wang, F. F., Fu, B. J., Liu, G. H., et al. (2020). Soil properties mediate the freeze-thaw-related soil N_2O and CO_2 emissions from temperate grasslands. *Catena* 195:104797. doi: 10.1016/j.catena.2020.104797

Xie, Y., Yang, C., Ma, E. D., Tan, H., Zhu, T. B., and Muller, C. (2020). Biochar stimulates NH_4^+ turnover while decreasing NO_3^- production and N_2O emissions in

soils under long-term vegetable cultivation. *Sci. Total Environ.* 737:140266. doi: 10.1016/j.scitotenv.2020.140266

Yao, Z. S., Wu, X., Wolf, B., Dannenmann, M., Butterbach-Bahl, K., Brueggemann, N., et al. (2010). Soil-atmosphere exchange potential of NO and N_2O in different land use types of Inner Mongolia as affected by soil temperature, soil moisture, freeze-thaw, and drying-wetting events. *J. Geophys. Res.-Atmos.* 115:D17116. doi: 10.1029/2009jd013528

Yin, M., Gao, X., Tenuta, M., Gui, D., and Zeng, F. (2019). Presence of spring-thaw N_2O emissions are not linked to functional gene abundance in a drip-fertigated cropped soil in arid northwestern China. *Sci. Total Environ.* 695:133670. doi: 10.1016/j.scitotenv.2019.133670

Yin, Y. A., Yang, C., Li, M. T., Zheng, Y. C., Ge, C. J., Gu, J., et al. (2021). Research progress and prospects for using biochar to mitigate greenhouse gas emissions during composting: a review. *Sci. Total Environ.* 798:149294. doi: 10.1016/j.scitotenv.2021.149294

Yu, Y. X., Li, X., Feng, Z. Y., Xiao, M. L., Ge, T. D., Li, Y. Y., et al. (2022). Polyethylene microplastics alter the microbial functional gene abundances and increase nitrous oxide emissions from paddy soils. *J. Hazard. Mater.* 432:128721. doi: 10.1016/j.jhazmat.2022.128721

Zhang, Y. X., Li, X., Xiao, M., Feng, Z. Y., Yu, Y. X., and Yao, H. Y. (2022b). Effects of microplastics on soil carbon dioxide emissions and the microbial functional genes involved in organic carbon decomposition in agricultural soil. *Sci. Total Environ.* 806:150714. doi: 10.1016/j.scitotenv.2021.150714

Zhang, L. Y., Zhang, M. X., Li, Y. T., Li, J. L., Jing, Y. M., Xiang, Y. Z., et al. (2022a). Linkage of crop productivity to soil nitrogen dynamics under biochar addition: a meta-analysis across field studies. *Agronomy* 12:247. doi: 10.3390/agronomy12020247

Zhang, B., Zhou, M., Zhu, B., Xiao, Q., Wang, T., Tang, J., et al. (2021). Soil type affects not only magnitude but also thermal sensitivity of N_2O emissions in subtropical mountain area. *Sci. Total Environ.* 797:149127. doi: 10.1016/j.scitotenv.2021.149127

Zhou, Y. X., Berruti, F., Greenhalf, C., Tian, X. H., and Henry, H. A. L. (2017). Increased retention of soil nitrogen over winter by biochar application: implications of biochar pyrolysis temperature for plant nitrogen availability. *Agric. Ecosyst. Environ.* 236, 61–68. doi: 10.1016/j.agee.2016.11.011

frontiers | Frontiers in Microbiology

TYPE Original Research
PUBLISHED 04 January 2023
DOI 10.3389/fmicb.2022.1080847

OPEN ACCESS

EDITED BY
Zengming Chen,
Institute of Soil Science (CAS), China

REVIEWED BY
Wei Lin,
Chinese Academy of Agricultural Sciences, China
Koki Maeda,
Japan International Research Center for Agricultural Sciences (JIRCAS), Japan

*CORRESPONDENCE
Stefan Karlowsky
✉ karlowsky@igzev.de

SPECIALTY SECTION
This article was submitted to Terrestrial Microbiology, a section of the journal Frontiers in Microbiology

RECEIVED 26 October 2022
ACCEPTED 06 December 2022
PUBLISHED 04 January 2023

CITATION
Karlowsky S, Buchen-Tschiskale C, Odasso L, Schwarz D and Well R (2023) Sources of nitrous oxide emissions from hydroponic tomato cultivation: Evidence from stable isotope analyses. *Front. Microbiol.* 13:1080847. doi: 10.3389/fmicb.2022.1080847

Sources of nitrous oxide emissions from hydroponic tomato cultivation: Evidence from stable isotope analyses

Stefan Karlowsky[1]*, Caroline Buchen-Tschiskale[2], Luca Odasso[1], Dietmar Schwarz[1,3] and Reinhard Well[2]

[1]Leibniz Institute of Vegetable and Ornamental Crops (IGZ) e.V., Großbeeren, Germany, [2]Thünen Institute of Climate-Smart Agriculture, Federal Research Institute for Rural Areas, Forestry and Fisheries, Braunschweig, Germany, [3]Operation Mercy, Amman, Jordan

Introduction: Hydroponic vegetable cultivation is characterized by high intensity and frequent nitrogen fertilizer application, which is related to greenhouse gas emissions, especially in the form of nitrous oxide (N_2O). So far, there is little knowledge about the sources of N_2O emissions from hydroponic systems, with the few studies indicating that denitrification could play a major role.

Methods: Here, we use evidence from an experiment with tomato plants (*Solanum lycopersicum*) grown in a hydroponic greenhouse setup to further shed light into the process of N_2O production based on the N_2O isotopocule method and the ^{15}N tracing approach. Gas samples from the headspace of rock wool substrate were collected prior to and after ^{15}N labeling at two occasions using the closed chamber method and analyzed by gas chromatography and stable isotope ratio mass spectrometry.

Results: The isotopocule analyses revealed that either heterotrophic bacterial denitrification (bD) or nitrifier denitrification (nD) was the major source of N_2O emissions, when a typical nutrient solution with a low ammonium concentration (1–6 mgL^{-1}) was applied. Furthermore, the isotopic shift in ^{15}N site preference and in $\delta^{18}O$ values indicated that approximately 80–90% of the N_2O produced were already reduced to N_2 by denitrifiers inside the rock wool substrate. Despite higher concentrations of ammonium present during the ^{15}N labeling (30–60 mgL^{-1}), results from the ^{15}N tracing approach showed that N_2O mainly originated from bD. Both, ^{15}N label supplied in the form of ammonium and ^{15}N label supplied in the form of nitrate, increased the ^{15}N enrichment of N_2O. This pointed to the contribution of other processes than bD. Nitrification activity was indicated by the conversion of small amounts of ^{15}N-labeled ammonium into nitrate.

Discussion/Conclusion: Comparing the results from N_2O isotopocule analyses and the ^{15}N tracing approach, likely a combination of bD, nD, and coupled nitrification and denitrification (cND) was responsible for the vast part of N_2O emissions observed in this study. Overall, our findings help to better understand the processes underlying N_2O and N_2 emissions from hydroponic tomato cultivation, and thereby facilitate the development of targeted N_2O mitigation measures.

KEYWORDS

glasshouse vegetable production, horticulture, greenhouse gas emission, N_2O isotopocules, ^{15}N labeling, denitrification

1. Introduction

Based on a variety of technical innovations in greenhouse vegetable production, the use of soilless culture systems (commonly referred to as "hydroponics") has grown in importance during the last 30–40 years (Gruda, 2009; Savvas et al., 2013; Savvas and Gruda, 2018). Controlled environment systems are considered by some as key part of future food production (Lakhiar et al., 2018; Cowan et al., 2022). This is largely due to the possibility of operating hydroponic systems in greenhouses in regions with unfavorable climatic conditions and in urban areas (Sharma et al., 2018; Small et al., 2019). Closed hydroponic systems also allow the re-utilization of drained nutrient solution from the root zone by recirculating the collected drain after mixing with stock solution. The high water and nutrient efficiency of closed hydroponic systems as well as the reduction of soil-borne diseases are considered as major advantages compared to soil-based cultivation (Gruda, 2009; Savvas and Gruda, 2018). Besides, the high water and nutrient efficiency makes hydroponic systems also interesting for the production of supplemental fresh food during space missions (Wheeler, 2017). Nonetheless, there are still losses occurring in the form of gaseous nitrogen (N) emissions, which may sum up to more than 10% of the N applied in the nutrient solution (Daum and Schenk, 1996a). Due to the high N application rate and dosage frequency in hydroponics, there is also a high potential for gaseous N emissions, in particular nitrous oxide (N_2O) from microbial processes such as nitrification (Ni) and heterotrophic bacterial denitrification (bD; Daum and Schenk, 1996b; Lin et al., 2022). If bD is complete, N losses in the form of molecular nitrogen (N_2) due to N_2O reduction might also occur. So far, only a few studies investigated volatile N losses from hydroponic systems. Some of these studies found N_2O emission factors higher than the IPCC estimate of 1% N_2O-N for applied N fertilizer in soil cultivation (Daum and Schenk, 1996a; Hashida et al., 2014; Yoshihara et al., 2016), while others found lower N_2O emission factors (Llorach-Massana et al., 2017; Halbert-Howard et al., 2021; Karlowsky et al., 2021).

The specialty of hydroponic systems is that inert substrates such as sand, perlite, or rock wool can be used, which limits the availability of organic carbon for heterotrophic denitrifiers. In this case, the hydroponic growing medium consists only of the substrate matrix and the supplied nutrient solution, which is mostly composed of mineral fertilizers dissolved in water. Nevertheless, bD has been considered as the main source of gaseous N emissions from hydroponic systems with inert substrates (Daum and Schenk, 1996a, 1996b, 1998). Whereas a more recent study by Lin et al. (2022) with tomato plants cultivated on peat and coir substrates found also significant shares of N_2O produced by Ni, which depended on the substrate used. In hydroponic systems with inert growing media, various factors may favor bD over Ni activity, i.e., (i) frequent irrigation pulses, (ii) slightly acidic pH values (pH 5–6.5) in the nutrient solution, (iii) often high nitrate (NO_3^-) to ammonium (NH_4^+) ratios, and (iv) the presence of root exudates and debris. Yet, there is little knowledge on the processes underlying gaseous N emissions from hydroponic systems. In particular, it is unclear to which extend other processes such as fungal denitrification (fD), nitrifier denitrification (nD), or coupled nitrification and denitrification (cND) play a role in hydroponic systems. A study of functional microbial genes by Hashida et al. (2014) found 3–5 times higher gene copy numbers for denitrifiers than for nitrifiers, but the abundance of functional Ni and bD genes had no clear relationship with measured N_2O emissions. N_2 emissions from bD, which are more difficult to analyze due to the high atmospheric concentration of N_2, have only been researched by Daum and Schenk (1996a, 1996b, 1997, 1998) in hydroponic systems, using the acetylene inhibition method. However, today, it is known that this method is not suitable to quantify N_2 production, mainly due to catalytic decomposition of NO in presence of O_2 (Felber et al., 2012; Nadeem et al., 2013), which cannot be excluded in the setup used in the Daum and Schenk studies (*ibid.*).

Alternative methods for detecting N_2 emissions include (i) the use of closed chambers filled with other inert gases such as helium and the analysis of N_2 in gas samples on a gas chromatograph (helium incubation method) (Scholefield et al., 1997), (ii) the labeling with ^{15}N supplied by the fertilizer and the measurement of ^{15}N contents in N_2O and N_2 (^{15}N tracing approach) (e.g., Stevens and Laughlin, 1998; Buchen et al., 2016), and (iii) the analysis of the isotopic composition ($\delta^{18}O$, $\delta^{15}N$bulk value and the intramolecular distribution of ^{15}N in N_2O) of the four most abundant N_2O isotopocules, which are indicative for N_2O production pathways, but also altered during the N_2O reduction process (N_2O isotopocule method) (e.g., Decock and Six, 2013; Lewicka-Szczebak et al., 2017). Unfortunately, the helium incubation method to directly measure N_2 emissions requires a high technical effort and is very prone to leakage and is therefore mainly used for the analysis of soil cores in the laboratory (Groffman et al., 2006). Both, the N_2O isotopocule method and the ^{15}N tracing approach, require little technical effort in the field or greenhouse, can be combined with the usual chamber-based gas flux measurements for detecting N_2O emission rates, and are suitable to assess the microbial processes that drive the N_2O emission (Lewicka-Szczebak et al., 2020). The N_2 isotopocule method works well with natural abundance stable isotope ratios and only requires the capacity for stable isotope analyses. However, due to the multitude of possible N_2O processes (Butterbach-Bahl et al., 2013) and the variability found in isotope contents and fractionation factors, uncertainties of its results have to be taken into account (Wu et al., 2019). The ^{15}N tracing approach allows to quantify the conversion of ^{15}N-enriched substrates such as NO_3^- or NH_4^+ to different products, including N_2O and N_2 (^{15}N mass balance). Though to obtain sufficient ^{15}N enrichment of N_2 for detection of N_2 production, high amounts of expensive ^{15}N tracer have to be applied, limiting the use of the ^{15}N tracing approach for detecting N_2 fluxes by the experimental budget. Moreover, under ambient atmosphere, its sensitivity is quite low (Zaman et al., 2021).

In this study, we used a combination of the N_2O isotopocule method and the ^{15}N tracing approach to further shed light into the processes underlying gaseous N emissions from hydroponic systems. Analyzing the N_2O isotopocules and using the dual isotope plot ("isotopocule mapping approach") is the most common interpretation strategy to estimate the fractions of N_2O produced by bD and/or nD, fD, and Ni (e.g., Lewicka-Szczebak et al., 2017). The results from N_2O isotopocule analysis were also recently found to be in good accordance with the analysis of functional nitrifier and denitrifier genes (Lin et al., 2022). In contrast to the isotopocule method, the ^{15}N tracing approach allows to estimate the fraction of N_2O derived from bD, without overlapping nD (e.g., Deppe et al., 2017). Hence, by combining the N_2O isotopocule method and the ^{15}N tracing approach, it is possible to assess potential contributions of not well-studied microbial processes such as nD or cND in N_2O formation. Furthermore, we used two types of ^{15}N label, i.e., $^{15}NH_4^+$ and $^{15}NO_3^-$, to determine the contribution of each N form in the emitted N_2O and to gain additional insights into N transformation processes. In our study, we focused on rock wool hydroponics and used tomato plants as a model, as the use of rock wool substrate is widespread in modern production greenhouses (Dannehl et al., 2015; Savvas and Gruda, 2018) and tomato is the most important vegetable crop worldwide (Schwarz et al., 2014). We conducted two sampling campaigns: (i) at the beginning of flowering and (ii) during fruit ripening, at which we expected different N_2O emission rates. In previous studies with rock wool substrate, higher N_2O emissions were found during tomato fruit ripening compared to earlier plant stages (Hashida et al., 2014; Karlowsky et al., 2021), and were attributed to shifts in plant physiology.

Overall, our aim was to better understand which microbial processes contribute to N_2O emission from hydroponic systems to enable tailored mitigation measures. We hypothesized that bD is the main source of N_2O emissions from hydroponic tomato cultivation on rock wool, and that NO_3^- is contributing to a higher share to N_2O emissions than NH_4^+. Furthermore, we assumed that most of the applied ^{15}N tracer can be recovered in the labeled nutrient solution, plant biomass, and gaseous N emissions in a hydroponic system with inert rock wool substrate.

2. Materials and methods

2.1. Experimental setup and hydroponic tomato cultivation

The experiment took place in an experimental glasshouse consisting of multiple heated cabins, each with a size of 64 m^2 and a roof top height of 4 m. Two of these cabins were used for this study, cabin no. 7 for pre-cultivating tomato plants (*Solanum lycopersicum* cv. 'Cheramy F1') and cabin no. 5 for conducting the experiment. Temperature in the cabins was set to 20/18°C (day/night), and roof top ventilation was opened at temperatures above 23/20°C (day/night). Shading was done automatically at photosynthetically active radiation (PAR) values above 900 µmol m^{-2} s^{-1} and artificial lighting was applied between 5:00 and 12:00 CET, if PAR values were below 180 µmol m^{-2} s^{-1}. Air temperature and humidity in the cabins as well as roof top PAR were continuously monitored by a climate computer (Supplementary Figure S1). Tomato plants were sown on 26th July 2021 and after germination in moistened sand, 64 seedlings were transplanted into pre-weighed rock wool cubes (10 × 10 × 6.5 cm; Grodan B.V., Roermond, Netherlands) for further cultivation. On 2nd September each two planted rock wool cubes were put on one rock wool slab (100 × 20 × 7.5 cm; Grodan Vital, Grodan B.V., Roermond, Netherlands) at a distance of 50 cm. One-half of the planted rock wool slabs were installed in eight hydroponic units with elevated gutters in cabin no. 5, which included separate fertigation systems and were later used for the ^{15}N labeling. The other half was further cultivated in cabin no. 7 in four gutters on the ground, which shared one fertigation system. In both cases, the collected drain solution (i.e., leachate) was re-used and mixed with fresh nutrient solution in storage tanks as needed (closed hydroponic system with re-circulating nutrient solution). The nutrient solution from the storage tanks was supplied to plants *via* pumps, PE tubes, and drippers inserted into the rock wool cubes. The tomato plants were supplied with a custom-made nutrient solution modified after the recipe of de Kreij et al. (2003), which had a high NO_3^- to NH_4^+ ratio (~20:1) that was found optimal for tomato cultivation. Macro and micro nutrients were dissolved in de-ionized water targeting a pH of 5.6 and an electrical conductivity (EC) of 2 mS cm^{-1}. The pH and EC values in the storage tanks were regularly monitored (Supplementary Figure S2). Tomato seedlings were supplied with an N concentration of 361 mg L^{-1} at the beginning (starter solution; 338 mg L^{-1} NO_3^--N and 23 mg L^{-1} NH_4^+-N). After the development of the 5th truss and the first green fruits on, from 4th October, the N concentration in the nutrient solution was reduced to 165 mg L^{-1} (refill solution; 151 mg L^{-1} NO_3^--N and 14 mg L^{-1} NH_4^+-N). The composition of the different nutrient solutions used in this study can be found in Supplementary Table S1. Each hydroponic unit in cabin no. 5 consisted of a 4 m gutter in which three rock wool slabs, two with plants and one unplanted, were placed and a nutrient solution storage tank filled up to approximately 40 L (Supplementary Figure S3). Two sampling periods were selected according to expected differences in plant N uptake and associated assimilate distribution in the root-shoot system, representing high growth and N uptake rates during early development and a more balanced assimilate distribution during fruit ripening. The first sampling and ^{15}N labeling campaign were performed on 22nd and 23rd September, when the tomato plants developed the 3rd truss and first flowers. Subsequently, the 16 planted rock wool slabs (32 plants) in cabin no. 5 were completely removed (destructive sampling, described below) and replaced by the other 16 planted rock wool slabs pre-cultivated in cabin no. 7 on 24th September. The eight unplanted rock wool slabs were also exchanged with fresh rock wool slabs. To avoid carryover of ^{15}N label, the hydroponic gutters were covered with plastic film below the rock

wool slabs until 23rd September to reduce contact with the ^{15}N-enriched nutrient solution. Both, the gutters and pumps for nutrient solution, were thoroughly cleaned with a detergent/disinfectant (MENNO Florades®, MENNO CHEMIE-VERTRIEB GMBH, Langer Kamp, Germany) before installing the unlabeled plants and rock wool slabs. Furthermore, the storage tanks and the tubing as well as the drippers for nutrient solution were completely replaced with new material. To ensure the supply of further growing plants with water and nutrients, larger storage tanks were used (Supplementary Figure S4) and filled up to approximately 200 l. The experiment ended with the second sampling and ^{15}N labeling campaign on 3rd and 4th November, when the tomato plants developed the 8th truss and the first fruits were ripe.

2.2. Gas flux measurements

For measuring the gas fluxes, the closed chamber method as described by Karlowsky et al. (2021) was used. Acrylic glass chambers with two small openings for plant stems were fitted around the rock wool slabs (planted and unplanted) and sealed with foam rubber to obtain a closed headspace with a volume of approximately 16 l (Supplementary Figure S5). Over a period of 1 hour after closing, four gas samples (each 30 ml) were taken in 20 min intervals with a 30 ml syringe through a sampling port on top of the chamber. The gas samples were transferred to 20 ml glass vials with silicone/PTFE septa (type N17, MACHEREY-NAGEL GmbH & Co. KG, Düren, Germany) for transport and were analyzed on the same day by a gas chromatograph (GC 2010 Plus, Shimadzu Corporation, Kyoto, Japan) equipped with an electron capture detector (ECD) for N_2O. The measured concentrations in µmol mol^{-1} were converted to µmol m^{-3} by applying the ideal gas law, including a correction for the temperature at the time of sampling. Afterward, gas fluxes were calculated using the R package "gasfluxes" [version 0.4–4; (Fuss et al., 2020)] by robust linear regression (except one case with only 3 time points, for which standard linear regression had to be used). Input variables used were gas concentration (µmol m^{-3}), chamber volume (m^3), time after closing the chamber (h), and area covered (m^2). The latter was set to 1 m^2 assuming a typical density of greenhouse-cultivated tomato plants of 2 plants m^{-2}. The resulting gas fluxes in µmol m^{-2} h^{-1} were further converted to g ha^{-1} d^{-1} based on molar masses.

2.3. Sampling and ^{15}N labeling

Natural abundance samples were taken on 22nd September and 3rd November shortly before the ^{15}N labeling from each hydroponic unit in cabin no. 5 (from here on called "experimental unit"). These included plant samples, nutrient solution samples, and gas samples from planted rock wool slabs. For the latter, 140 ml of air was collected from the headspace of rock wool substrate with a syringe at the end of gas flux measurements after 1 h of N_2O enrichment in the closed chambers. The gas samples were transferred into 120 ml crimp-cap glass vials closed with gray butyl septa (type ND20, IVA Analysentechnik GmbH & Co. KG, Meerbusch, Germany) for later stable isotope analysis. To determine natural abundance δ^{15}N values of plants, the tips (first three leaflets) of 2–3 fully developed leaves from one plant in each experimental unit were sampled and dried at 80°C for at least 48 h. Approximately 15 ml of nutrient solution (mixture with leachates) was sampled from the storage tank of each experimental unit and then stored at −20°C for later δ^{15}N analyses. In addition, three samples of de-ionized water were taken to determine the natural abundance δ^{18}O values of the nutrient solution water.

On both dates, the ^{15}N labeling took place directly after the natural abundance sampling at approximately 12:00 pm CET. The remaining nutrient solution in the experimental units was removed as far as possible and 15 l of ^{15}N-labeled nutrient solution was added in the storage tanks of each unit. In a randomized way, four units received a nutrient solution with ^{15}N-enriched NH_4^+ ($^{15}NH_4^+$) and four units received a nutrient solution with ^{15}N-enriched NO_3^- ($^{15}NO_3^-$). This was done by adding ammonium nitrate (NH_4NO_3; SIGMA-ALDRICH, Saint Louis, MO, United States) with 10.5/11 atom-% ^{15}N ($^{15}NH_4^+/^{15}NO_3^-$) as only N source. The composition of the nutrient solution used for the ^{15}N labeling can also be found in Supplementary Table S1. In total, 115 mg of ^{15}N was applied to each $^{15}NH_4^+$ unit and 120 mg of ^{15}N to each $^{15}NO_3^-$ unit (3.1 g NH_4NO_3 per unit), yielding an N concentration of 146 mg L^{-1} (comparable to the standard refill solution). To distribute the ^{15}N label in the hydroponic system, drip fertigation was run continuously for 30 min after adding the ^{15}N labeled nutrient solution to the experimental units. After 4 h, a first sampling to determine the ^{15}N enrichment in plant, nutrient solution and gas samples took place. The sampling was done analogously to the natural abundance sampling, including the determination of gas flux rates and the collection of gas samples for isotopic analyses as well as leaf and nutrient solution samples. Following the same scheme, the last sampling took place 24 h after the labeling. This time, also samples from the tomato stems, roots and fruits were taken. From the middle of the tomato plant *ca.*, 10 cm of the stem was cut. Around 0.5 g of fresh roots was sampled from the interface of rock wool cubes and rock wool slabs, where a dense root net allowed to obtain root material without rock wool fibers. Root samples were washed in de-ionized water and dried with lint-free cellulose wipes to remove the ^{15}N label from adhering nutrient solution. During the second sampling campaign, each three green fruits from different positions (top, mid, and bottom) of one plant per experimental unit were sampled. All plant samples were dried for a minimum of 48 h at 80°C before later processing for analysis. Different plants were used for obtaining plant material before labeling, 4 h after labeling, and 24 h after labeling in order to minimize sampling effects on ^{15}N uptake. Gas samplings for stable isotope analysis always took place on the rock wool slab in the middle of each experimental unit, from which plant samples were taken only after the last gas sampling (24 h after labeling). On the unplanted rock wool slabs,

additional gas flux measurements took place shortly before the 24 h sampling to determine the N_2O emission potential from re-circulated nutrient solution with leachate and therein contained organic carbon.

2.4. Analyses on nutrient solution, plant, and gas samples

The concentrations of NO_3^- and NH_4^+ [mg N L^{-1}] were determined using flow injection analysis with photometric detection (FIAmodula; MLE GmbH, Dresden, Germany). Measurements of $\delta^{18}O$ values in water samples were done by TC/EA coupled to a Delta V plus IRMS (Thermo Finnigan, Bremen, Germany) *via* a ConFlo IV interface. The $\delta^{15}N$ values of NH_4^+ and NO_3^- were determined according to Dyckmans et al. (2021) using a sample preparation unit for inorganic nitrogen (SPIN) coupled to a membrane inlet isotope ratio mass spectrometer (MIRMS; Delta plus; Thermo Finnigan) *via* a ConFlo III interface. Additional nutrient solution samples taken one day after the labeling were analyzed for their dissolved organic carbon content (DOC) using a liquiTOC analyzer (Elementar Analysensysteme GmbH, Langenselbold, Germany). Dried plant samples were transferred into 20 ml HDPE vials (Zinsser Analytic GmbH, Eschborn, Germany) and ground to a fine powder using a steel ball mill (MM400; RETSCH GmbH, Haan, Germany). Plant samples were analyzed for total N content (N_t) and their $\delta^{15}N$ values using an Elemental Analyzer (EA) Flash 2000 (Thermo Fisher Scientific, Bremen, Germany), coupled with a Delta V isotope ratio mass spectrometer *via* a ConFlo IV interface (Thermo Fisher Scientific, Bremen, Germany). Data were normalized to the international scale for atmospheric nitrogen, by analysis of the international standards USGS40 and USGS41 (L-glutamic acid). Gas samples were analyzed for N_2O isotopocules ($\delta^{15}N_{N2O}$, $\delta^{18}O_{N2O}$) using a Delta V Isotope ratio mass spectrometer (Thermo Scientific, Bremen, Germany), coupled to an automatic preparation system with Precon plus Trace GC Isolink (Thermo Scientific, Bremen, Germany). In this setup, N_2O was pre-concentrated, separated, and purified, and afterward m/z 44, 45, and 46 of the intact N_2O^+ ions as well as m/z 30 and 31 of NO^+ fragment ions were determined (Lewicka-Szczebak et al., 2014). All measured delta values (δ) were expressed in permil (‰) deviation from the $^{15}N/^{14}N$ and $^{18}O/^{16}O$ ratios of the international reference standards (i.e., atmospheric N_2 and Vienna Standard Mean Ocean Water (VSMOW), respectively).

2.5. Data processing and calculations

Data from the analysis of natural abundance gas samples were evaluated for $\delta^{15}N\alpha$ ($\delta^{15}N$ of the central N position of the N_2O molecule), $\delta^{15}N\beta$ ($\delta^{15}N$ of the peripheral N position of the N_2O), and $\delta^{18}O$ according to Toyoda and Yoshida (1999) and Röckmann et al. (2003). The ^{15}N site preference ($\delta^{15}N^{SP}$) was defined as the difference of $\delta^{15}N\alpha$ and $\delta^{15}N\beta$. The $\delta^{18}O$ values of N_2O depend on $\delta^{18}O$ values of precursors, i.e., for denitrification to >80% on H_2O-O of the nutrient solution (Lewicka-Szczebak et al., 2016). Therefore, $\delta^{18}O$ values of the emitted N_2O ($\delta^{18}O_{N2O}$) were corrected for the $\delta^{18}O$ values measured in the de-ionized water ($\delta^{18}O_{H2O}$) and expressed as $\delta^{18}O_{N2O/H2O}$ values:

$$\delta^{18}O_{N2O/H2O} = \delta^{18}O_{N2O} - \delta^{18}O_{H2O} \quad (1)$$

In the case of nitrification, the $\delta^{18}O_{N2O}$ values depend on atmospheric oxygen (O_2) as a precursor (Kool et al., 2007). In contrast to bulk $\delta^{15}N_{N2O}$, $\delta^{15}N^{SP}$ is known to be independent from source processes. During chamber air sampling, the collected N_2O was a mixture of atmospheric and substrate-emitted N_2O. Thus, δ values of substrate-emitted N_2O were corrected using a basic isotope mixing model according to Well et al. (2006). To calculate the contribution of N_2O production pathways and N_2O reduction to N_2, the isotopocule mapping approach based on $\delta^{15}N^{SP}{}_{N2O}$ and $\delta^{18}O_{N2O}$ values was applied (Lewicka-Szczebak et al., 2017; Buchen et al., 2018). For the mapping approach, literature values for $\delta^{18}O$ and $\delta^{15}N^{SP}{}_{N2O}$ of bD, fD, nD, and Ni were used as proposed by Yu et al. (2020) and Lewicka-Szczebak et al. (2020). To account for differences in oxygen precursors between denitrification and Ni, the literature values for $\delta^{18}O_{N2O}$ of bD, fD, and nD were adjusted by the addition of $\delta^{18}O_{H2O}$ (Lewicka-Szczebak et al., 2020). Based on the sample position in the map, the contribution of bD and/or nD, Ni, and fD was calculated based on mixing equations, while the contribution of N_2O reduction to N_2 was calculated from the Rayleigh equation. All calculations were done as described in detail by Buchen et al. (2018) and Zaman et al. (2021) (Chapter 7: "Isotopic Techniques to Measure N_2O, N_2 and Their Sources). Two possible cases of N_2O mixing and reduction were assumed: (i) N_2O, which is produced by bD is first partially reduced to N_2, followed by mixing of the residual N_2O with N_2O from other pathways or (ii) N_2O produced by various pathways is first mixed and then reduced to N_2. A detailed description is given in the supplement of Wu et al. (2019). Five samples from sampling 1 and four samples from sampling 2 with a low fraction of substrate-derived N_2O were excluded from the data analyses because the uncertainty in substrate-derived δ values increases exponentially as sample and atmospheric N_2O concentrations converge. Similar to Buchen et al. (2018), a threshold was used for the minimum difference between sample and atmospheric N_2O concentrations, which was determined based on measured N_2O concentrations in ambient air during the sampling. For sampling 1, the threshold was 337 ppb and for sampling 2, it was 359 ppb (65 ppb above the ambient air N_2O concentration). This was supported by a Gaussian error propagation, with the threshold limiting the propagated errors of $\delta^{15}N^{SP}{}_{N2O}$ and $\delta^{18}O_{N2O}$ to <6‰ and < 5‰, respectively.

Data from the analysis of ^{15}N-enriched gas samples were only evaluated for bulk $\delta^{15}N_{N2O}$. For further calculations, $\delta^{15}N$ values were converted to atom-$\%_{15N}$ to express the ^{15}N enrichment:

$$atom\text{-}\%^{15}N = \frac{100\%}{\frac{1}{\left(\frac{\delta^{15}N}{1000‰}+1\right)\times R_{STD}}+1} \quad (2)$$

with R_{STD} being the isotopic ratio ($^{15}N/^{14}N = 0.0036765$) of atmospheric nitrogen. Calculations of the contributions of N_2O originating from the labeled and non-labeled pools were based on the non-equilibrium distribution of N_2O isotopocules, as described by Spott et al. (2006) and Bergsma et al. (2001). For labeling with $^{15}NO_3^-$, this approach directly determines the ^{15}N enrichment of the labeled N pool producing N_2O (ap_{N2O}) and the fraction of N_2O derived from that pool. Considering, the fraction of atmospheric N_2O in the samples, the fraction of NO_3^--derived N_2O in the emitted N_2O (f_{PN2O}) can be calculated. A detailed procedure is given in Deppe et al. (2017). However, due to the experimental setup, labeled N_2O could originate from two pools (NO_3^-, NH_4^+, or a mixture of both pools). Thus, for labeling with $^{15}NH_4^+$, f_{PN2O} was estimated based on the ^{15}N atom fraction of emitted N_2O ($^{15}a_{N2O}$) using a mixing equation:

$$f_{PN2O} = \frac{^{15}a_{N2O} - {}^{15}aNH_4^+}{^{15}aNO_3^- - {}^{15}aNH_4^+} \quad (3)$$

with $^{15}aNO_3^-$ being the ^{15}N enrichment of the NO_3^- pool and $^{15}aNH_4^+$ being the ^{15}N enrichment of the NH_4^+ pool (*cf.* Eq. 2). The N_2O flux from the NO_3^- pool (NO_3^--derived N_2O) was calculated from f_{PN2O} by ordinary linear regression using the measured N_2O concentrations at t0 and after 1 h of chamber closure to determine the total N_2O flux (total N_2O), assuming that the increase in the N_2O emitted from the ^{15}N-labeled pool was also linear as shown for the emission of total N_2O (Buchen et al., 2016). The N_2O flux from the NH_4^+ pool (NH_4^+-derived N_2O) was calculated analogously based on the fraction of NH_4^+-derived N_2O in the emitted N_2O (f_{NH4}), which was deduced from f_{PN2O} ($f_{NH4} = 1 - f_{PN2O}$). Thus, the NH_4^+-derived N_2O was calculated as the difference between total N_2O and NO_3^--derived N_2O.

2.6. Calculation of excess ^{15}N and ^{15}N mass balance

To determine the amount of ^{15}N tracer, which was recovered in the different pools 4 and 24 h after the labeling (excess ^{15}N), atom-$\%_{15N}$ values were used to calculate atom-% ^{15}N excess (APE):

$$APE = atom\text{-}\%^{15}N,labeled - atom\text{-}\%^{15}N,natural\ abundance \quad (4)$$

with $atom\text{-}\%_{15N,labeled}$ being the atom-$\%_{15N}$ values of labeled samples and $atom\text{-}\%_{15N,natural\ abundance}$ being the atom-$\%_{15N}$ values of natural abundance samples. Afterward, excess ^{15}N [mg ^{15}N unit^{-1}] for each pool was calculated:

$$excess\ ^{15}N = \frac{APE}{100\%} \times N_{pool} \quad (5)$$

with N_{pool} being the N amount in each pool [mg N unit^{-1}] at the time of sampling (4/24 h after labeling). The N_{pool} values for plant biomass were calculated by multiplying the measured dry weight [g] of shoots (leaves + stems), roots and fruits per unit with their N_t content [g N $g_{dry\ weight}^{-1}$]. The N_{pool} values for NO_3^--N and NH_4^+-N from the nutrient solution were calculated by multiplying the measured N concentrations [mg N L^{-1}] with the total volume of nutrient solution per unit [L]. The latter was a mixture of nutrient solution added for the labeling and remaining (unlabeled) nutrient solution in the rock wool substrate. The total volume of the nutrient solution was estimated based on the dilution of NH_4^+-N concentrations from the labeled nutrient solution (73 mg N L^{-1} in 15 l) at the 4 h sampling point, assuming that NH_4^+-N concentrations in the unlabeled nutrient solutions were negligible (measured concentrations in natural abundance samples <2.5 mg N L^{-1} at first sampling campaign and <7 mg N L^{-1} at second sampling campaign) and that the N_t content as well as composition in the mixed nutrient solution did not substantially change during the 4 h. For the calculation of excess ^{15}N, two neighboring units were excluded from the second sampling campaign, because of a spillover of labeled nutrient solution between these units. The N_{pool} values for N_2O were calculated from the measured gas flux rates [mg N h^{-1}] of planted and unplanted rock wool slabs. For the planted rock wool slabs, cumulative N_2O emissions [mg N] were calculated by linear integration between the natural abundance (0 h), 4 h, and 24 h samplings, and summation of hourly gas fluxes. For unplanted rock wool slabs, constant N_2O emission rates were assumed and used to calculate cumulative N_2O emissions, as they were not affected by plant activity. For calculating the N_{pool} value per unit, cumulative N_2O emissions from planted rock wool slabs were multiplied by 2 (two planted slabs per unit) and the cumulative N_2O emissions from unplanted slabs (one per unit) were added. Finally, the excess ^{15}N values from the different pools were summed up to obtain the total amount of ^{15}N recovered from the labeling ($^{15}N_{total}$) and the ^{15}N recovery rate [%] was calculated:

$$^{15}N\ recovery\ rate = \frac{^{15}N_{total}}{^{15}N_{label}} \times 100\% \quad (6)$$

with $^{15}N_{label}$ being the amount of ^{15}N tracer [mg ^{15}N unit^{-1}] added during the labeling.

2.7. Statistical analyses

All statistical analyses were done using the R software (version 4.2.0). Linear mixed-effects models were done using the R package

'lme4' (version 1.1–29), including the effects of individual hydroponic units as random intercept. *Post-hoc* tests on linear mixed-effects models were done using the R package "emmeans" (version 1.7.4–1), applying the Holm-Bonferroni correction method for multiple comparisons. If necessary, data were log- or square root-transformed prior to analysis to fulfill the requirements of normality and variance homogeneity.

3. Results

3.1. N_2O flux, isotopocule, and ^{15}N tracer analyses

The N_2O flux measurements from this study are summarized in Table 1. In general, all fluxes were in the same range, except for the measurement 24 h after labeling during the first sampling, which was significantly ($p < 0.05$) higher than the other measurements. There was no significant difference between planted and unplanted rock wool slabs from the same sampling campaign. The trend to higher N_2O emissions from unplanted substrate during sampling 2 was reflected by higher DOC contents in the nutrient solution compared to sampling 1 (Table 1).

Results from isotopic analyses of N_2O are shown in Figure 1 as a $\delta^{15}N^{SP}_{N2O}/\delta^{18}O_{N2O}$ map. The δ values from both samplings clearly scatter around the reduction line of N_2O derived from bD, indicating that either bD or nD or a mixture of both was the main source of N_2O. Moreover, the increased $\delta^{15}N^{SP}_{N2O}$ and $\delta^{18}O_{N2O}$ values compared to the literature value for bD indicate that a high share of N_2O was reduced before emitted to the atmosphere. Altogether, the differences in isotopic results between the first and the second sampling campaign were negligible (Table 2). Depending on which scenario (mixing of bD and fD or bD and Ni) and case (first reduction than mixing or first mixing than reduction) was assumed, the fraction of bD varied between 0.85 and 0.90, while the $N_2O/(N_2O + N_2)$ ratio of bD (r_{N2O}) varied between 0.08 and 0.14. In consequence, the calculated N_2 fluxes were between six to ten times higher than the measured N_2O fluxes.

Although the same amounts of NO_3^--N and NH_4^+-N were added in the form of NH_4NO_3 during each ^{15}N labeling, NO_3-concentrations were clearly higher than NH_4+ concentrations in the nutrient solution after labeling (Table 3). This indicated that a significant amount of unlabeled nutrient solution with a high NO_3^- to NH_4^+ ratio was still present in the rock wool substrate during ^{15}N labeling. Regardless of the higher dilution of $^{15}NO_3^-$ label (Table 3; Supplementary Figure S6), the ^{15}N tracer could be detected in the emitted N_2O independent of the applied form ($^{15}NH_4^+$ or $^{15}NO_3^-$). The $^{15}a_{N2O}$ values mirrored the ^{15}N enrichments of the labeled NO_3^- and NH_4^+ pools, with higher values in of $^{15}NH_4^+$-labeled units compared to $^{15}NO_3^-$-labeled units (Supplementary Figure S6). The label dilution was considered for calculating NO_3^--derived N_2O and NH_4^+-derived N_2O. The NO_3^--derived N_2O (Figures 2A,B) reflected the N_2O emission rates measured by GC (Table 1), with highest values found 24 h after the first labeling. There was no clear difference in NO_3^--derived N_2O between the $^{15}NH_4^+$ and $^{15}NO_3^-$ labels. In general, the NH_4^+-derived N_2O values (Figures 2C,D) were lower than the NO_3^--derived N_2O values, but also followed the dynamics of N_2O emission rates measured by GC. Notably, NH_4^+-derived N_2O was higher for $^{15}NO_3^-$-labeled units compared to $^{15}NH_4^+$-labeled units during sampling 2. Consequently, the calculated average f_{PN2O} values varied from 0.4 to 0.9 between the applied label forms, sampling times, and sampling campaigns (Figures 2C,D). During both sampling campaigns, an increase of f_{PN2O} from 4 h to 24 h after labeling was present for the $^{15}NO_3^-$-labeled units, while there was no effect of sampling time for the $^{15}NH_4^+$-labeled units. The latter showed higher f_{PN2O} values during the second sampling campaign, which was also significantly higher than for the $^{15}NO_3^-$-labeled units at 4 h after labeling.

TABLE 1 N_2O fluxes (determined by gas chromatography) and dissolved organic carbon (DOC) concentrations at the two sampling campaigns (sampling 1, S1; sampling 2, S2).

Date	Sampling, sample	N_2O flux ($g\text{-}Nha^{-1}\ d^{-1}$)	DOC (mgL^{-1})
2021-09-22	S1, T0	0.21 ± 0.22^{a}	–
	S1, T4	0.44 ± 0.27^{ab}	–
2021-09-23	S1, unplanted	0.52 ± 0.55^{ab}	8.9 ± 0.6^{a}
	S1, T24	2.59 ± 1.32^{c}	–
2021-11-03	S2, T0	0.38 ± 0.30^{ab}	–
	S2, T4	0.29 ± 0.13^{ab}	–
2021-11-04	S2, unplanted	0.91 ± 0.76^{b}	16.8 ± 0.9^{b}
	S2, T24	0.27 ± 0.16^{ab}	–

[a–c]Small letters indicate significant differences ($p < 0.05$) between individual gas flux/DOC measurements. N_2O fluxes from planted rock wool slabs were measured before ^{15}N labeling (T0), 4 h after ^{15}N labeling (T4), and 24 h (T24) after ^{15}N labeling. N_2O fluxes from unplanted rock wool slabs (unplanted) and DOC concentrations were measured once during each sampling campaign. Shown are average values ±SD of $n = 8$ replicates (including low N_2O fluxes removed for stable isotope analysis of natural abundance samples).

3.2. Recovery of ^{15}N tracer in different pools

The natural abundance $\delta^{15}N$ values from both samplings were equal (leaves) or slightly lower (NH_4^+, NO_3^- and N_2O) at the second sampling, indicating that no carryover of ^{15}N label occurred from the first sampling. The amount of ^{15}N tracer from the ^{15}N-enriched NH_4NO_3 added during the labelings that was recovered in different pools (dissolved NH_4^+ and NO_3^-, N_2O, plant biomass) was calculated as excess ^{15}N ($^{15}N_{exc}$). At both samplings, most of the ^{15}N label remained in its original form after 24 h, i.e., as dissolved NH_4^+ and NO_3^- (Table 4). There was a notable increase of $^{15}N_{exc}$ of dissolved NO_3^- in the $^{15}NH_4^+$-labeled units, indicating the conversion of NH_4^+ to NO_3^- by Ni (up to 2% of added label during sampling 1). On the other side, the $^{15}N_{exc}$ of

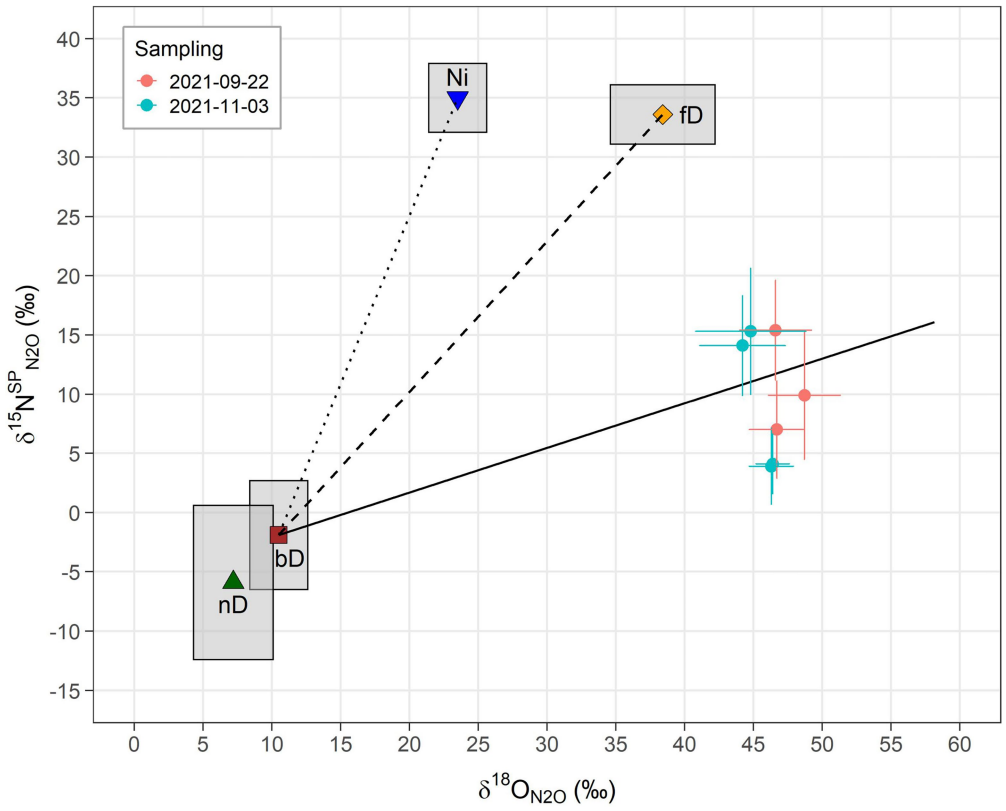

FIGURE 1
Results from N_2O isotopocule analysis of natural abundance ^{15}N gas samples illustrated as $\delta^{15}N^{SP}_{N2O}/\delta^{18}O_{N2O}$ map. The vertical axis shows the ^{15}N site preference of N_2O ($\delta^{15}N^{SP}_{N2O}$) and the horizontal axis the abundance of the ^{18}O isotope in the N_2O molecules ($\delta^{18}O_{N2O}$). Sample $\delta^{18}O_{N2O}$ values were corrected for the ^{18}O composition of water from the nutrient solution ($\delta^{18}O_{N2O/H2O}$) as described in Eq. 1. Closed circles represent the measurement-derived values and the corresponding error bars the estimated uncertainty. Other symbols indicate literature values as compiled in Lewicka-Szczebak et al. (2020) for N_2O produced from different microbial processes and the surrounding boxes reflect their variation (based on SD): Ni, nitrification (Yoshida, 1988; Sutka et al., 2006; Mandernack et al., 2009; Frame and Casciotti, 2010); fD, fungal denitrification (Sutka et al., 2008; Rohe et al., 2014; Maeda et al., 2015; Rohe et al., 2017); nD, nitrifier denitrification (Sutka et al., 2006; Frame and Casciotti, 2010); and bD, bacterial denitrification (Barford et al., 1999; Toyoda et al., 2005; Sutka et al., 2006; Lewicka-Szczebak et al., 2014, 2016; Rohe et al., 2017). According to Lewicka-Szczebak et al. (2020), the literature values of bD, fD and nD were adjusted by addition of the $\delta^{18}O$ of water (−8.5‰) measured in this study to display expected endmember ranges. The solid line indicates the isotopic shift of N_2O due to fractionation from the partial reduction of N_2O to N_2 by bD (Menyailo and Hungate, 2006; Ostrom et al., 2007; Jinuntuya-Nortman et al., 2008; Well and Flessa, 2009; Lewicka-Szczebak et al., 2014, 2015) and is shown for theoretical r_{N2O} values of 1 to 0.05. The dotted and the dashed lines represent expected values for different mixing ratios of N_2O from bD and fD (bD-fD line) and N_2O from bD and Ni (bD-Ni line), respectively.

dissolved NH_4^+ in the $^{15}NO_3^-$-labeled units was comparably low (at maximum 0.3% of added label during sampling 1). The $^{15}N_{exc}$ of N_2O strongly differed between the two samplings, with up to 20 times higher values at sampling 1, reflecting the APE values of N_2O (Supplementary Figure S7). Despite the higher dilution of ^{15}N tracer in the NO_3^- pool (Table 3) and the resulting lower ^{15}N enrichments in the $^{15}NO_3^-$-labeled units compared to $^{15}NH_4^+$-labeled units (Supplementary Figure S6), there were no significant differences between the label types regarding the amount of ^{15}N tracer found in N_2O, as shown by the $^{15}N_{exc}$ values (Table 4). In all cases, the $^{15}N_{exc}$ of total plant biomass was higher than the $^{15}N_{exc}$ of N_2O. The highest plant ^{15}N uptake was observed during the second sampling in $^{15}NH_4^+$-labeled units. Irrespective of the generally higher ^{15}N-enrichment of roots (Supplementary Table S2), most ^{15}N tracer was found in shoots (i.e., the sum of stem leaf biomass; Table 4), as a consequence of the biomass difference (root to shoot ratio of 0.23). Only marginal amounts of ^{15}N tracer were found in tomato fruits during sampling 2. Overall, the majority of ^{15}N added during labelings was recovered in the studied pools, with the calculated ^{15}N recovery rates varying around 100%.

4. Discussion

In this study, we applied the N_2O isotopocule and ^{15}N tracing approaches to better understand the sources of N_2O emission from hydroponic vegetable production systems, using tomato cultivation on rock wool substrate as a model. Furthermore, in our study, we determined r_{N2O} using the isotopocule mapping method (Lewicka-Szczebak et al., 2017), which had been shown to be in good agreement with the ^{15}N gas flux method (Buchen et al., 2018; Lewicka-Szczebak et al., 2020). Therefore, for

TABLE 2 Measured N_2O flux, estimated fraction of N_2O from bacterial denitrification (f_{bD}), estimated $N_2O/(N_2O+N_2)$ ratio of denitrification (r_{N2O}), and estimated N_2 flux for different mixing scenarios (bacterial denitrification and fungal denitrification, bD-fD; bacterial denitrification and nitrification, bD-Ni) and cases (reduction of N_2O from denitrification followed by mixing with N_2O from other sources, red-mix; mixing of N_2O from denitrification and other source followed by N_2O reduction, mix-red).

Variable	Scenario	Case	Value sampling 1	Value sampling 2	Unit
f_{bD}	bD-fD	All	0.85 ± 0.05	0.87 ± 0.13	-
	bD-Ni	All	0.88 ± 0.04	0.90 ± 0.10	
r_{N2O}	bD-fD	Red-mix	0.09 ± 0.01	0.10 ± <0.01	
		Mix-red	0.13 ± 0.02	0.14 ± 0.04	
	bD-Ni	Red-mix	0.08 ± 0.01	0.09 ± 0.01	
		Mix-red	0.11 ± 0.01	0.12 ± 0.02	
N_2O flux	All	All	1.7 ± 0.2	2.5 ± 1.0	$\mu g\,N\,m^{-2}\,h^{-1}$
N_2 flux	bD-fD	Red-mix	14.5 ± 0.2	19.9 ± 10.2	
		Mix-red	11.4 ± 1.0	17.8 ± 11.7	
	bD-Ni	Red-mix	17.0 ± 1.0	21.9 ± 8.8	
		Mix-red	13.8 ± 0.2	19.6±10.4	

Shown are average values ± SD ($n = 3$ for Sampling 1; $n = 4$ for Sampling 2).

TABLE 3 Concentrations and ^{15}N-enrichment of dissolved ammonium and nitrate in the nutrient solution during the two sampling campaigns, including samples taken before ^{15}N labeling (T0) and 4/24h afterward (T4/T24).

Label	Sampling	Time	Dissolved NH_4^+		Dissolved NO_3^-	
			N content (mgL^{-1})	^{15}N-enrichment (atom-% ^{15}N excess)	N content (mgL^{-1})	^{15}N-enrichment (atom-% ^{15}N excess)
$^{15}NH_4^+$	S1	T0	1.6 ± 0.7	–	166 ± 12	–
		T4	36 ± 9	10.04 ± 0.04	111 ± 11	0.012 ± 0.008
		T24	33 ± 6	9.96 ± 0.06	122 ± 16	0.061 ± 0.024
	S2	T0	5.9 ± 0.7	–	258 ± 11	–
		T4	61 ± 9	6.59 ± 0.04	232 ± 14	0.0004 ± 0.0018
		T24	53 ± 12	6.53 ± 0.07	250 ± 15	0.009 ± 0.007
$^{15}NO_3^-$	S1	T0	1.0 ± 0.6	–	161 ± 8	–
		T4	36 ± 8	0.025 ± 0.005	124 ± 17	3.3 ± 1.2
		T24	32 ± 9	0.033 ± 0.004	131 ± 19	2.8 ± 1.0
	S2	T0	5.8 ± 0.8	–	248 ± 8	–
		T4	59 ± 11	0.007 ± 0.001	221 ± 16	2.0 ± 0.4
		T24	50 ± 10	0.007 ± 0.001	246 ± 18	1.7 ± 0.3

Shown are mean values ± SD of $n = 4$ replicates ($n = 3$ for T4 and T24 at S2 due to spillover of labeled nutrient solution between two rows).

hydroponic systems, we determined this ratio for the first using an appropriate method.

As we hypothesized, the results from both N_2O isotope analyses (non-labeled and ^{15}N-labeled) point to bD as main source of N_2O emissions from the hydroponic units. The scattering of the values around the reduction line of bD in the mapping approach of the N_2O isotopocules (Figure 1) suggests that most of the N_2O was produced by bD. Unfortunately, nD cannot be clearly separated from bD by the N_2O isotopocule mapping approach (Lewicka-Szczebak et al., 2017), due to the overlap of endmember values (i.e., theoretical values determined from literature values of pure cultures and the isotopic composition of water and N substrates). Thus, the calculated f_{bD} could actually be a mixture of bD and nD. The same is true for the fraction of Ni in N_2O emission (f_{Ni}), which cannot be clearly separated from the fraction of fD (f_{fD}) in the mapping approach. However, a mixed fraction ($f_{Ni/fD} = 1 - f_{bD}$) can be calculated, as previously done by Buchen et al. (2018). Depending on the mapping scenario and sampling campaign, the $f_{Ni/fD}$ values vary between 0.10 and 0.15 in our study. In consequence, the contribution of fD and/or Ni seems small under typical tomato growing conditions in rock wool hydroponics with low NH_4^+ supply. For better distinction of bD, we used the ^{15}N tracing approach to determine the fraction of

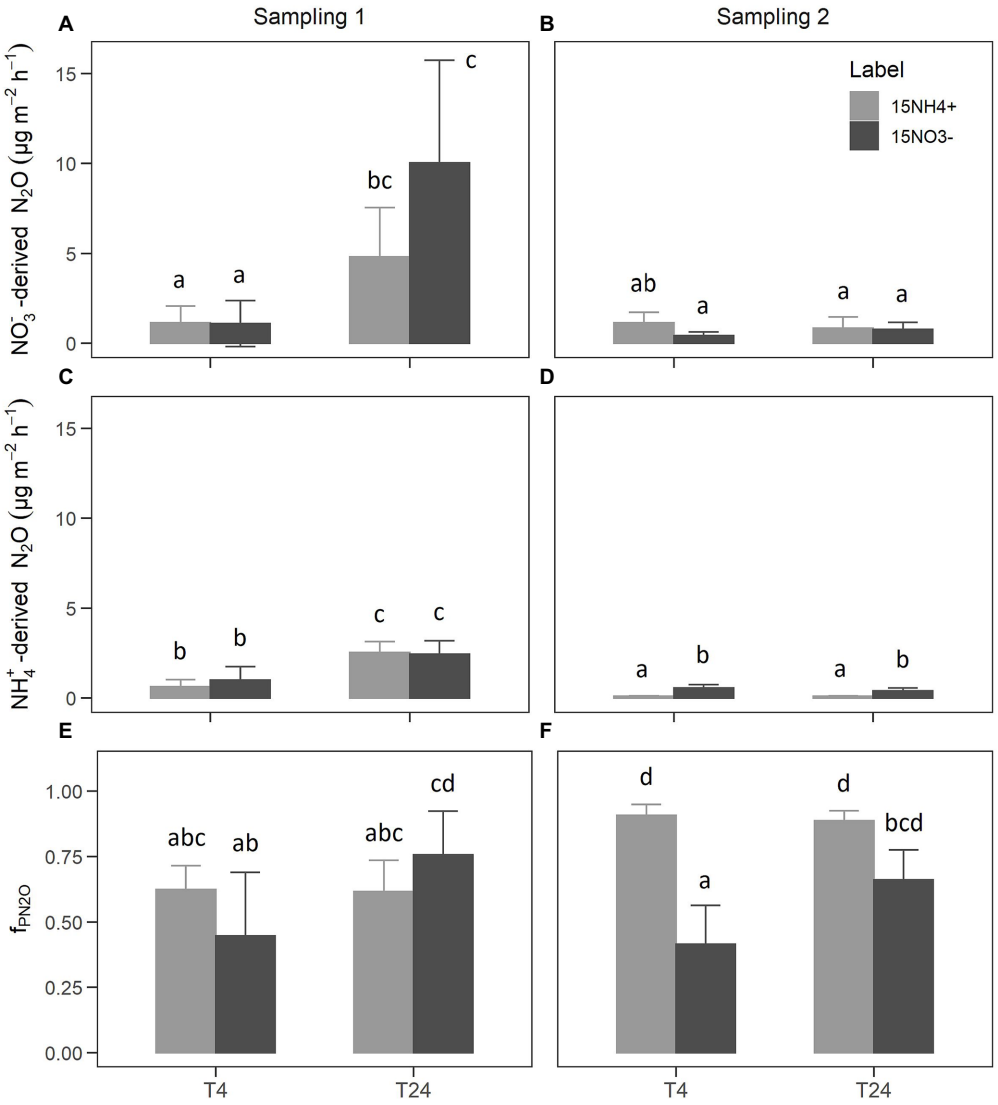

FIGURE 2
NO_3^--derived N_2O fluxes **(A,B)**, NH_4^+-derived N_2O fluxes **(C,D)**, and the estimated share of NO_3^--derived N_2O fluxes [f_{PN2O}; **(E,F)**]. Bars show the mean of n=4 replicates and error bars the corresponding SD. Small letters indicate levels of significance for differences between label and sampling with p<0.05 from linear mixed-effects models and Tukey *post-hoc* tests.

NO_3^--derived N_2O fluxes, i.e., f_{PN2O}. While f_{PN2O} can principally also include contributions from fD, we assume its impact was minor as shown by the isotopocule map (Figure 2). Therefore we assume f_{PN2O} is equivalent to f_{bD} from the isotopocule mapping approach but does not include N_2O fluxes from nD. Although the f_{PN2O} values are relatively variable (Figures 2E,F), they generally show that bD was the main source of N_2O emissions, even under increased NH_4^+ supply. Hence the results from N_2O isotope analysis and ^{15}N tracing were in good accordance with each other. On the other hand, the results from the ^{15}N-labeling also show that a large part of N_2O can be formed from NH_4^+ (Figures 2C,D), suggesting processes other than denitrification of added NO_3^- (Firestone and Davidson, 1989). Possibly, the increase of the NH_4^+ concentration in the nutrient solution used for ^{15}N-labeling compared to the non-labeled nutrient solution could have increased Ni and the associated N_2O formation from NH_4^+. This is supported by the slight ^{15}N-enrichment of NO_3^- found in units labeled with $^{15}NH_4^+$ (Table 4), indicating the presence of Ni. Notably, the average f_{bD} values of ~0.87 from N_2O isotopocule analysis (Table 2) were higher than the average f_{PN2O} values of ~0.68 from ^{15}N tracing (Figure 2). Assuming that microbial activities did no significantly change after adding the NH_4^+-rich ^{15}N label, we hypothesize that the observed difference in f_{bD} and f_{PN2O} values is due to microbial processes other than Ni that are associated with the release of N_2O from NH_4^+.

TABLE 4 Excess ^{15}N ($^{15}N_{exc}$) found in different pools 24h after labeling with $^{15}NH_4^+$ and $^{15}NO_3^-$, total recovered ^{15}N and recovery rate of ^{15}N tracer from the labeling.

Parameter	Sampling 1		Sampling 2		Unit
	$^{15}NH_4^+$ label	$^{15}NO_3^-$ label	$^{15}NH_4^+$ label	$^{15}NO_3^-$ label	
^{15}N in NH_4^+	96 ± 2	0.33 ± 0.03	94 ± 13*	0.09 ± 0.01*	mg ^{15}N unit^{-1}
^{15}N in NO_3^-	2.1 ± 0.6	112 ± 5.42	0.54 ± 0.34*	107 ± 5*	
^{15}N in N_2O	5.0 ± 0.8^b	4.4 ± 2.0^b	0.22 ± 0.17^a	0.33 ± 0.17^a	
^{15}N in shoots	5.6 ± 4.4^a	6.4 ± 1.9^{ab}	18 ± 13^b	3.6 ± 0.9^a	
^{15}N in roots	3.9 ± 1.7^b	1.3 ± 0.4^a	8.1 ± 2.1^c	1.9 ± 0.7^{ab}	
^{15}N in fruits	–	–	0.79 ± 0.45	BDL	
Total plant ^{15}N	9.5 ± 5.4^a	7.6 ± 2.0^a	26 ± 15^b	5.5 ± 0.9^a	
Total recovered ^{15}N	112 ± 5	124 ± 4	120 ± 16	111 ± 6	
^{15}N recovery rate	98 ± 4	103 ± 3	105 ± 14	93 ± 5	

*Only $n = 3$ replicates due to spillover of nutrient solution between two hydroponic units. $^{a-c}$Small letters indicate significant differences ($p < 0.05$) between labeling and added ^{15}N tracer for all parameters except dissolved NH_4^+ and NO_3^- (^{15}N source from labeling). BDL, below detection limit. Presented are mean values ± SD of $n = 4$ replicates.

Besides the conversion of hydroxyl amine (NH_2OH) to N_2O during Ni, there are several known pathways that explain the production of N_2O derived from NH_4^+, in particular nD and cND (Baggs, 2011). Wrage-Mönnig et al. (2018) argue in their review that nD can be the predominant source of N_2O emissions under certain conditions. For example, this includes "environments with fluctuating aerobic-anaerobic conditions", which are likely to occur in hydroponic systems with regular irrigation intervals (Schröder and Lieth, 2002). In contrast, Bakken and Frostegard (2017) fundamentally disagree with the concept of nD, based on the preferential electron flow in nitrifiers, and rather suggest that it is cND that accounts for the observations after all. In this sense, the O_2 consumption by Ni could lead to anoxic conditions facilitating bD (Zhu et al., 2015). Additionally, a process that also needs to be taken into account is co-denitrification (coD), i.e., the formation of hybrid N_2O and N_2 molecules with each one N atom derived from the classical denitrification pathway (N species: nitrite, NO_2^-; nitric oxide, NO) and one N atom from another N species such as NH_2OH or amino compounds (Spott et al., 2011). In our study, coD may have been stimulated by the increased NH_4^+ availability after adding the nutrient solutions for ^{15}N labeling. This is supported by the lower ap_{N2O} values compared to the $^{15}aNO_3^-$ values found in $^{15}NO_3^-$-labeled units (Supplementary Figures S6A,B,E,F; Spott and Stange, 2007), suggesting that part of the emitted N_2O was derived from non-labeled NH_4^+. Albeit the use of NH_4^+ in coD was found quite rarely and organic N sources are thus perceived as the main source for forming hybrid N_2O/N_2 molecules with NO_2^--N or NO-N (Spott et al., 2011). Therefore, the combined fraction of nD and cND ($f_{nD/cND}$) can be estimated from f_{PN2O} and f_{bD} as described by Deppe et al. (2017), i.e., by calculating the difference of f_{bD} and f_{PN2O} ($f_{nD/cND} = f_{bD} - f_{PN2O}$). Depending on the scenario for f_{bD}, the values of $f_{nD/cND}$ vary between 0.40–0.48 at T4 and 0.09–0.24 at T24 for the $^{15}NO_3^-$-labeled units during both sampling campaigns. For the $^{15}NH_4^+$-labeled units, this comparison seems not appropriate because the estimated f_{PN2O} values were partially higher than f_{bD} values. This is probably due to the assumption used in Eq. 3, i.e., that the labeled pool ($^{15}NO_3^-$ and $^{15}NH_4^+$) is the same as the active pool. In contrast, the f_{PN2O} values of $^{15}NO_3^-$-labeled units were determined *via* the non-random distribution of N_2O isotopologues and delivered the fraction of the active labeled pool used for N_2O production, which is not necessarily identical to the bulk NO_3^- pool (Deppe et al., 2017; Zaman et al., 2021).

Notably, measured N_2O emissions from the experimental units we used were low compared to previous studies of hydroponic systems (Daum and Schenk, 1996a; Hashida et al., 2014; Karlowsky et al., 2021), which reported emission rates that were one to two orders of magnitude higher. The low N_2O emission rates could have been a result of unfavorable conditions for denitrifier activity, such as low organic carbon contents and/or high oxygen availability in the substrate (Morley and Baggs, 2010). The accumulation of organic carbon due to root exudation and root decay might be key to N_2O emissions from inert substrates like rock wool, as we found in a previous study a steep increase of N_2O emission rates after 5 months of tomato cultivation following a phase of low N_2O emission rates (Karlowsky et al., 2021). In this study, we found an increase of DOC in the re-circulating nutrient solution from sampling 1 to sampling 2, but this was not related to higher N_2O emissions. Here, the slightly acidic conditions (pH values <4.6; Supplementary Figure S2) during sampling 2 may have limited denitrification, considering that N emissions from denitrification typically decrease at low pH values (Daum and Schenk, 1998; Farquharson and Baldock, 2007), which is also associated with a higher r_{N2O} value (e.g., Liu et al., 2010), but this was only visible in trend (Table 2). In general, N_2O fluxes were highly variable (Table 1), with a trend to higher emissions from planted rock wool slabs compared to unplanted rock wool slabs, especially during

sampling 1. Thus, our findings indicate that considerable N_2O emissions may also occur from re-circulated nutrient solution, e.g., in collection and storage tanks or bio-filtration/disinfection units. Although it is unclear to which extent the rock wool matrix with its high pore space volumes (Dannehl et al., 2015) and a large surface area for microbial biofilms (Brand and Wohanka, 2001) might have promoted N_2O emissions from the re-circulated nutrient solution.

In addition to the above-discussed findings, we performed a ^{15}N mass balance to check the plausibility of r_{N2O} and the calculated N_2O and N_2 emissions from the mapping approach, and to gain more insights into N dynamics in the hydroponic units. Unfortunately, the proportion of applied ^{15}N label recovered as N_2O strongly varied between the two samplings, which can be attributed to temporal fluctuations resulting in a peak of N_2O emission rates at 24 h after labeling during sampling 1. This peak probably led to an overestimation of cumulative N_2O fluxes, especially considering that N_2O emission rates are typically lower during nighttime when no fertigation is done (Daum and Schenk, 1998; Yoshihara et al., 2016; Karlowsky et al., 2021). Due to highly variable and generally very moderate N_2O emissions as well as the high variability of ^{15}N excess in plant material, the ^{15}N mass balance in our case proved to be too uncertain to validate the calculated gas fluxes from the isotopocule mapping approach. In general, the results of the ^{15}N mass balance reflect the findings from the ^{15}N tracing approach and show in addition that the majority of ^{15}N tracer applied to the hydroponic units was recovered in the nutrient solution, plant biomass, and N_2O emissions after 24 h. However, since only short-term N dynamics are included in the ^{15}N mass balance, N use efficiency cannot be calculated with these data.

5. Conclusion

The findings of our study clearly show that bD was the major source of N_2O emissions from hydroponic tomato cultivation on rock wool substrate, and that up to 90% of initially produced N_2O was reduced to N_2 before gas emission. The combined results of N_2O isotopocule analysis and ^{15}N tracing suggest that other microbial processes related to N_2O formation from NH_4^+ (i.e., Ni, nD, and cND) play only a moderate role. However, with the methods used, it was not possible to determine the individual contribution of each of these processes to the observed N_2O emissions. Furthermore, the involvement of fD and coD remains unclear, but seems less likely since organic matter is supplied only by plant roots in the rock wool substrate. Therefore, future studies are needed to better distinguish N_2O sources other than bD, possibly combing isotopic approaches with molecular genetic methods such as functional gene analysis. As we also found N_2O emissions from root-less rock wool substrate, potential N_2O emissions from drained nutrient solution should be further researched. Ultimately, on the basis of our study, measures to reduce denitrifier activity appear to be the most promising option to mitigate N_2O emissions and N losses from hydroponic cultivation.

Data availability statement

The raw data supporting the conclusions of this article will be made available by the authors, without undue reservation.

Author contributions

SK: conceptualization, investigation, formal analysis, and writing—original draft. CB-T: investigation, formal analysis, and writing—original draft. LO: investigation and formal analysis. DS: conceptualization and methodology. RW: methodology and writing—review and editing. All authors contributed to the article and approved the submitted and revised version.

Funding

This project is supported by the Federal Ministry of Food and Agriculture (BMEL) based on the decision of the Parliament of the Federal Republic of Germany *via* the Federal Office for Agriculture and Food (BLE) under the innovation support program (funding code 281B204116 for project "HydroN2O").

Acknowledgments

We thank Gundula Aust and the gardener team at IGZ for setting up and maintaining the experiment in the greenhouse. Martina Heuer, Jennifer Gier und Ute Rieß at Thünen Institute for help during isotopic analyses. Jens Dyckmanns and his team at Göttingen University for SPIN-MIRMS analysis.

Conflict of interest

The authors declare that the research was conducted in the absence of any commercial or financial relationships that could be construed as a potential conflict of interest.

Publisher's note

Supplementary material

The Supplementary material for this article can be found online at: https://www.frontiersin.org/articles/10.3389/fmicb.2022.1080847/full#supplementary-material

References

Baggs, E. M. (2011). Soil microbial sources of nitrous oxide: recent advances in knowledge, emerging challenges and future direction. *Curr. Opin. Environ. Sustain.* 3, 321–327. doi: 10.1016/j.cosust.2011.08.011

Bakken, L. R., and Frostegard, A. (2017). Sources and sinks for N2O, can microbiologist help to mitigate N2O emissions? *Environ. Microbiol.* 19, 4801–4805. doi: 10.1111/1462-2920.13978

Barford, C. C., Montoya, J. P., Altabet, M. A., and Mitchell, R. (1999). Steady-state nitrogen isotope effects of N2 and N2O production in *Paracoccus denitrificans*. *Appl. Environ. Microbiol.* 65, 989–994. doi: 10.1128/AEM.65.3.989-994.1999

Bergsma, T., Ostrom, N., Emmons, M., and Robertson, G. (2001). Measuring simultaneous fluxes from soil of N_2O and N_2 in the field using the ^{15}N-gas "nonequilibrium" technique. *Environ. Sci. Technol.* 35, 4307–4312. doi: 10.1021/es010885u

Brand, T., and Wohanka, W. (2001). Importance and characterization of the biological component in slow filters. *Acta Hortic.* 554, 313–322. doi: 10.17660/ActaHortic.2001.554.34

Buchen, C., Lewicka-Szczebak, D., Flessa, H., and Well, R. (2018). Estimating N_2O processes during grassland renewal and grassland conversion to maize cropping using N_2O isotopocules. *Rapid Commun. Mass Spectrom.* 32, 1053–1067. doi: 10.1002/rcm.8132

Buchen, C., Lewicka-Szczebak, D., Fuß, R., Helfrich, M., Flessa, H., and Well, R. (2016). Fluxes of N_2 and N_2O and contributing processes in summer after grassland renewal and grassland conversion to maize cropping on a plaggic anthrosol and a histic gleysol. *Soil Biol. Biochem.* 101, 6–19. doi: 10.1016/j.soilbio.2016.06.028

Butterbach-Bahl, K., Baggs, E. M., Dannenmann, M., Kiese, R., and Zechmeister-Boltenstern, S. (2013). Nitrous oxide emissions from soils: how well do we understand the processes and their controls? *Philos. Trans. R. Soc. B* 368, 20130122–20130113. doi: 10.1098/rstb.2013.0122

Cowan, N., Ferrier, L., Spears, B., Drewer, J., Reay, D., and Skiba, U. (2022). CEA systems: the means to achieve future food security and environmental sustainability? *Front. Sustain. Food Syst.* 6:891256. doi: 10.3389/fsufs.2022.891256

Dannehl, D., Suhl, J., Ulrichs, C., and Schmidt, U. (2015). Evaluation of substitutes for rock wool as growing substrate for hydroponic tomato production. *J. Appl. Bot. Food Qual.* 88, 68–77. doi: 10.5073/JABFQ.2015.088.010

Daum, D., and Schenk, M. K. (1996a). Gaseous nitrogen losses from a soilless culture system in the greenhouse. *Plant Soil* 183, 69–78. doi: 10.1007/bf02185566

Daum, D., and Schenk, M. K. (1996b). Influence of nitrogen concentration and form in the nutrient solution on N_2O and N_2 emissions from a soilless culture system. *Plant Soil* 203, 279–288. doi: 10.1023/a:1004350628266

Daum, D., and Schenk, M. K. (1997). Evaluation of the acetylene inhibition method for measuring denitrification in soilless plant culture systems. *Biol. Fertil. Soils* 24, 111–117. doi: 10.1007/bf01420230

Daum, D., and Schenk, M. K. (1998). Influence of nutrient solution pH on N2O and N-2 emissions from a soilless culture system. *Plant Soil* 203, 279–287. doi: 10.1023/A:1004350628266

de Kreij, C., Voogt, W., and Baas, R. (2003). "*Nutrient Solutions and Water Quality for Soilless Cultures*". (Naaldwijk, The Netherlands: Applied Plant Research, Division Glasshouse).

Decock, C., and Six, J. (2013). How reliable is the intramolecular distribution of 15N in N2O to source partition N2O emitted from soil? *Soil Biol. Biochem.* 65, 114–127. doi: 10.1016/j.soilbio.2013.05.012

Deppe, M., Well, R., Giesemann, A., Spott, O., and Flessa, H. (2017). Soil N_2O fluxes and related processes in laboratory incubations simulating ammonium fertilizer depots. *Soil Biol. Biochem.* 104, 68–80. doi: 10.1016/j.soilbio.2016.10.005

Dyckmans, J., Eschenbach, W., Langel, R., Szwec, L., and Well, R. (2021). Nitrogen isotope analysis of aqueous ammonium and nitrate by membrane inlet isotope ratio mass spectrometry (MIRMS) at natural abundance levels. *Rapid Commun. Mass Spectrom.* 35:e9077. doi: 10.1002/rcm.9077

Farquharson, R., and Baldock, J. (2007). Concepts in modelling N2O emissions from land use. *Plant Soil* 309, 147–167. doi: 10.1007/s11104-007-9485-0

Felber, R., Conen, F., Flechard, C. R., and Neftel, A. (2012). Theoretical and practical limitations of the acetylene inhibition technique to determine total denitrification losses. *Biogeosciences* 9, 4125–4138. doi: 10.5194/bg-9-4125-2012

Firestone, M. K., and Davidson, E. A. (1989). "Microbiological basis of NO and N2O production and consumption in soil" in *Exchange of Trace Gases Between Terrestrial Ecosystems and the Atmosphere: Report of the Dahlem Workshop on Exchange of Trace Gases Between Terrestrial Ecosystems and the Atmosphere*. eds. M. O. Andreae and D. S. Schimel (New York, NY, USA: Wiley), 7–21.

Frame, C. H., and Casciotti, K. L. (2010). Biogeochemical controls and isotopic signatures of nitrous oxide production by a marine ammonia-oxidizing bacterium. *Biogeosciences* 7, 2695–2709. doi: 10.5194/bg-7-2695-2010

Fuss, R., Hueppi, R., and Pedersen, A.R. (2020). gasfluxes: Greenhouse Gas Flux Calculation from Chamber Measurements: Functions for greenhouse gas flux calculation from chamber measurements; Version: 0.4-4, Depends: R (>= 3.5.0) [Software]. https://CRAN.R-project.org/package=gasfluxes

Groffman, P. M., Altabet, M. A., Böhlke, J. K., Butterbach-Bahl, K., David, M. B., Firestone, M. K., et al. (2006). Methods for measuring denitrification: diverse approaches to a difficult problem. *Ecol. Appl.* 16, 2091–2122. doi: 10.1890/1051-0761(2006)016[2091:Mfmdda]2.0.Co;2

Gruda, N. (2009). Do soilless culture systems have an influence on product quality of vegetables? *J. Appl. Bot. Food Qual.* 82, 141–147. doi: 10.18452/9433

Halbert-Howard, A., Hafner, F., Karlowsky, S., Schwarz, D., and Krause, A. (2021). Evaluating recycling fertilizers for tomato cultivation in hydroponics, and their impact on greenhouse gas emissions. *Environ. Sci. Pollut. Res.* 28, 59284–59303. doi: 10.1007/s11356-020-10461-4

Hashida, S.-N., Johkan, M., Kitazaki, K., Shoji, K., Goto, F., and Yoshihara, T. (2014). Management of nitrogen fertilizer application, rather than functional gene abundance, governs nitrous oxide fluxes in hydroponics with rockwool. *Plant Soil* 374, 715–725. doi: 10.1007/s11104-013-1917-4

Jinuntuya-Nortman, M., Sutka, R. L., Ostrom, P. H., Gandhi, H., and Ostrom, N. E. (2008). Isotopologue fractionation during microbial reduction of N2O within soil mesocosms as a function of water-filled pore space. *Soil Biol. Biochem.* 40, 2273–2280. doi: 10.1016/j.soilbio.2008.05.016

Karlowsky, S., Gläser, M., Henschel, K., and Schwarz, D. (2021). Seasonal nitrous oxide emissions from hydroponic tomato and cucumber cultivation in a commercial greenhouse company. *Front. Sustain. Food Syst.* 5:626053. doi: 10.3389/fsufs.2021.626053

Kool, D. M., Wrage, N., Oenema, O., Dolfing, J., and Van Groenigen, J. W. (2007). Oxygen exchange between (de)nitrification intermediates and H2O and its implications for source determination of NO3- and N2O: a review. *Rapid Commun. Mass Spectrom.* 21, 3569–3578. doi: 10.1002/rcm.3249

Lakhiar, I. A., Gao, J., Syed, T. N., Chandio, F. A., and Buttar, N. A. (2018). Modern plant cultivation technologies in agriculture under controlled environment: a review on aeroponics. *J. Plant Interact.* 13, 338–352. doi: 10.1080/17429145.2018.1472308

Lewicka-Szczebak, D., Augustin, J., Giesemann, A., and Well, R. (2017). Quantifying N_2O reduction to N_2 based on N_2O isotopocules – validation with independent methods (helium incubation and ^{15}N gas flux method). *Biogeosciences* 14, 711–732. doi: 10.5194/bg-14-711-2017

Lewicka-Szczebak, D., Dyckmans, J., Kaiser, J., Marca, A., Augustin, J., and Well, R. (2016). Oxygen isotope fractionation during N2O production by soil denitrification. *Biogeosciences* 13, 1129–1144. doi: 10.5194/bg-13-1129-2016

Lewicka-Szczebak, D., Lewicki, M. P., and Well, R. (2020). N2O isotope approaches for source partitioning of N2O production and estimation of N2O reduction – validation with the 15N gas-flux method in laboratory and field studies. *Biogeosciences* 17, 5513–5537. doi: 10.5194/bg-17-5513-2020

Lewicka-Szczebak, D., Well, R., Bol, R., Gregory, A. S., Matthews, G. P., Misselbrook, T., et al. (2015). Isotope fractionation factors controlling isotopocule signatures of soil-emitted N(2)O produced by denitrification processes of various rates. *Rapid Commun. Mass Spectrom.* 29, 269–282. doi: 10.1002/rcm.7102

Lewicka-Szczebak, D., Well, R., Köster, J., Fuß, R., Senbayram, M., Dittert, K., et al. (2014). Experimental determinations of isotopic fractionation factors associated with N_2O production and reduction during denitrification in soils. *Geochim. Cosmochim. Acta* 134, 55–73. doi: 10.1016/j.gca.2014.03.010

Lin, W., Li, Q., Zhou, W., Yang, R., Zhang, D., Wang, H., et al. (2022). Insights into production and consumption processes of nitrous oxide emitted from soilless culture systems by dual isotopocule plot and functional genes. *Sci. Total Environ.* 856:159046. doi: 10.1016/j.scitotenv.2022.159046

Liu, B., Morkved, P. T., Frostegard, A., and Bakken, L. R. (2010). Denitrification gene pools, transcription and kinetics of NO, N2O and N2 production as affected by soil pH. *FEMS Microbiol. Ecol.* 72, 407–417. doi: 10.1111/j.1574-6941.2010.00856.x

Llorach-Massana, P., Muñoz, P., Riera, M. R., Gabarrell, X., Rieradevall, J., Montero, J. I., et al. (2017). N2O emissions from protected soilless crops for more precise food and urban agriculture life cycle assessments. *J. Clean. Prod.* 149, 1118–1126. doi: 10.1016/j.jclepro.2017.02.191

Maeda, K., Spor, A., Edel-Hermann, V., Heraud, C., Breuil, M. C., Bizouard, F., et al. (2015). N2O production, a widespread trait in fungi. *Sci. Rep.* 5:9697. doi: 10.1038/srep09697

Mandernack, K. W., Mills, C. T., Johnson, C. A., Rahn, T., and Kinney, C. (2009). The δ15N and δ18O values of N2O produced during the co-oxidation of ammonia by methanotrophic bacteria. *Chem. Geol.* 267, 96–107. doi: 10.1016/j.chemgeo.2009.06.008

Menyailo, O. V., and Hungate, B. A. (2006). Stable isotope discrimination during soil denitrification: production and consumption of nitrous oxide. *Glob. Biogeochem. Cycles* 20:GB3025. doi: 10.1029/2005gb002527

Morley, N., and Baggs, E. M. (2010). Carbon and oxygen controls on N2O and N2 production during nitrate reduction. *Soil Biol. Biochem.* 42, 1864–1871. doi: 10.1016/j.soilbio.2010.07.008

Nadeem, S., Dörsch, P., and Bakken, L. R. (2013). Autoxidation and acetylene-accelerated oxidation of NO in a 2-phase system: implications for the expression of denitrification in ex situ experiments. *Soil Biol. Biochem.* 57, 606–614. doi: 10.1016/j.soilbio.2012.10.007

Ostrom, N. E., Pitt, A., Sutka, R., Ostrom, P. H., Grandy, A. S., Huizinga, K. M., et al. (2007). Isotopologue effects during N2O reduction in soils and in pure cultures of denitrifiers. *J. Geophys. Res.* 112:287. doi: 10.1029/2006jg000287

Röckmann, T., Kaiser, J., Brenninkmeijer, C., and Brand, W. (2003). Gas chromatography/isotope-ratio mass spectrometry method for high-precision position-dependent ^{15}N and ^{18}O measurements of atmospheric nitrous oxide. *Rapid Commun. Mass Spectrom.* 17, 1897–1908. doi: 10.1002/rcm.1132

Rohe, L., Anderson, T. H., Braker, G., Flessa, H., Giesemann, A., Lewicka-Szczebak, D., et al. (2014). Dual isotope and isotopomer signatures of nitrous oxide from fungal denitrification - a pure culture study. *Rapid Commun. Mass Spectrom.* 28, 1893–1903. doi: 10.1002/rcm.6975

Rohe, L., Well, R., and Lewicka-Szczebak, D. (2017). Use of oxygen isotopes to differentiate between nitrous oxide produced by fungi or bacteria during denitrification. *Rapid Commun. Mass Spectrom.* 31, 1297–1312. doi: 10.1002/rcm.7909

Savvas, D., Gianquinto, G., Tuzel, Y., and Gruda, N. (2013). "Good agricultural practices for greenhouse vegetable crops - principles for Mediterranean climate areas, 12: soilless culture" in *FAO Plant Production and Protection Paper* eds. W. Baudoin, R. Nono-Womdim, N. Lutaladio, A. Hodder, N. Castilla, C. Leonardi, S.D. Pascale, M. Qaryouti R. Duffy et al. (Rome, Italy: Food and Agriculture Organization of the United Nations).

Savvas, D., and Gruda, N. (2018). Application of soilless culture technologies in the modern greenhouse industry – a review. *Eur. J. Hortic. Sci.* 83, 280–293. doi: 10.17660/eJHS.2018/83.5.2

Scholefield, D., Hawkins, J. M. B., and Jackson, S. M. (1997). Development of a helium atmosphere soil incubation technique for direct measurement of nitrous oxide and dinitrogen fluxes during denitrification. *Soil Biol. Biochem.* 29, 1345–1352. doi: 10.1016/s0038-0717(97)00021-7

Schröder, F.-G., and Lieth, J. H. (2002). "Chapter 7 irrigation control in hydroponics" in *Hydroponic Production of Vegetables and Ornamentals*. eds. D. Savvas and H. Passam (Egaleo, Greece: Embryo Publications).

Schwarz, D., Thompson, A. J., and Klaring, H. P. (2014). Guidelines to use tomato in experiments with a controlled environment. *Front. Plant Sci.* 5:625. doi: 10.3389/fpls.2014.00625

Sharma, N., Acharya, S., Kumar, K., Singh, N., and Chaurasia, O. P. (2018). Hydroponics as an advanced technique for vegetable production: an overview. *J. Soil Water Conserv.* 17:364. doi: 10.5958/2455-7145.2018.00056.5

Small, G. E., McDougall, R., and Metson, G. S. (2019). Would a sustainable city be self-sufficient in food production? *Int. J. Des. Nat. Ecodyn.* 14, 178–194. doi: 10.2495/dne-v14-n3-178-194

Spott, O., Russow, R., Apelt, B., and Stange, C. (2006). A ^{15}N-aided artificial atmosphere gas flow technique for online determination of soil N_2 release using the zeolite Köstrolith SX6®. *Rapid Commun. Mass Spectrom.* 20, 3267–3274. doi: 10.1002/rcm.2722

Spott, O., Russow, R., and Stange, C. F. (2011). Formation of hybrid N2O and hybrid N2 due to codenitrification: first review of a barely considered process of microbially mediated N-nitrosation. *Soil Biol. Biochem.* 43, 1995–2011. doi: 10.1016/j.soilbio.2011.06.014

Spott, O., and Stange, C. F. (2007). A new mathematical approach for calculating the contribution of anammox, denitrification and atmosphere to an N2 mixture based on a 15N tracer technique. *Rapid Commun. Mass Spectrom.* 21, 2398–2406. doi: 10.1002/rcm.3098

Stevens, R. J., and Laughlin, R. J. (1998). Measurement of nitrous oxide and di-nitrogen emissions from agricultural soils. *Nutr. Cycl. Agroecosyst.* 52, 131–139. doi: 10.1023/a:1009715807023

Sutka, R. L., Adams, G. C., Ostrom, N. E., and Ostrom, P. H. (2008). Isotopologue fractionation during N(2)O production by fungal denitrification. *Rapid Commun. Mass Spectrom.* 22, 3989–3996. doi: 10.1002/rcm.3820

Sutka, R. L., Ostrom, N. E., Ostrom, P. H., Breznak, J. A., Gandhi, H., Pitt, A. J., et al. (2006). Distinguishing nitrous oxide production from nitrification and denitrification on the basis of isotopomer abundances. *Appl. Environ. Microbiol.* 72, 638–644. doi: 10.1128/AEM.72.1.638-644.2006

Toyoda, S., Mutobe, H., Yamagishi, H., Yoshida, N., and Tanji, Y. (2005). Fractionation of N2O isotopomers during production by denitrifier. *Soil Biol. Biochem.* 37, 1535–1545. doi: 10.1016/j.soilbio.2005.01.009

Toyoda, S., and Yoshida, N. (1999). Determination of nitrogen isotopomers of nitrous oxide on a modified isotope ratio mass spectrometer. *Anal. Chem.* 71, 4711–4718. doi: 10.1021/ac9904563

Well, R., and Flessa, H. (2009). Isotopologue enrichment factors of N(2)O reduction in soils. *Rapid Commun. Mass Spectrom.* 23, 2996–3002. doi: 10.1002/rcm.4216

Well, R., Kurganova, I., de Gerenyu, V., and Flessa, H. (2006). Isotopomer signatures of soil-emitted N_2O under different moisture conditions - a microcosm study with arable loess soil. *Soil Biol. Biochem.* 38, 2923–2933. doi: 10.1016/j.soilbio.2006.05.003

Wheeler, R. M. (2017). Agriculture for space: people and places paving the way. *Open Agric.* 2, 14–32. doi: 10.1515/opag-2017-0002

Wrage-Mönnig, N., Horn, M. A., Well, R., Müller, C., Velthof, G., and Oenema, O. (2018). The role of nitrifier denitrification in the production of nitrous oxide revisited. *Soil Biol. Biochem.* 123, A3–A16. doi: 10.1016/j.soilbio.2018.03.020

Wu, D., Well, R., Cárdenas, L., Fuß, R., Lewicka-Szczebak, D., Köster, J., et al. (2019). Quantifying N_2O reduction to N_2 during denitrification in soils via isotopic mapping approach: model evaluation and uncertainty analysis. *Environ. Res.* 179:108806. doi: 10.1016/j.envres.2019.108806

Yoshida, N. (1988). 15N-depleted N2O as a product of nitrification. *Nature* 335, 528–529. doi: 10.1038/335528a0

Yoshihara, T., Tokura, A., Hashida, S. N., Kitazaki, K., Asobe, M., Enbutsu, K., et al. (2016). N2O emission from a tomato rockwool culture is highly responsive to photoirradiation conditions. *Sci. Hortic.* 201, 318–328. doi: 10.1016/j.scienta.2016.02.014

Yu, L., Harris, E., Lewicka-Szczebak, D., Barthel, M., Blomberg, M. R. A., Harris, S. J., et al. (2020). What can we learn from N_2O isotope data? - analytics, processes and modelling. *Rapid Commun. Mass Spectrom.* 34:e8858. doi: 10.1002/rcm.8858

Zaman, M., Kleineidam, K., Bakken, L., Berendt, J., Bracken, C., Butterbach-Bahl, K., et al. (2021). "Isotopic techniques to measure N_2O, N_2 and their sources" in *Measuring emission of agricultural greenhouse gases and developing mitigation options using nuclear and related techniques: Applications of nuclear techniques for GHGs*. eds. M. Zaman, L. Heng and C. Müller (Cham: Springer International Publishing), 213–301. doi: 10.1007/978-3-030-55396-8_7

Zhu, K., Bruun, S., Larsen, M., Glud, R. N., and Jensen, L. S. (2015). Heterogeneity of O_2 dynamics in soil amended with animal manure and implications for greenhouse gas emissions. *Soil Biol. Biochem.* 84, 96–106. doi: 10.1016/j.soilbio.2015.02.012

frontiers | Frontiers in Microbiology

TYPE Original Research
PUBLISHED 12 January 2023
DOI 10.3389/fmicb.2022.1110151

OPEN ACCESS

EDITED BY
Yong Li,
Zhejiang University,
China

REVIEWED BY
Pengpeng Duan,
Institute of Subtropical Agriculture (CAS),
China
Xiuzhen Shi,
Fujian Normal University,
China

*CORRESPONDENCE
Zhifeng Yan
✉ yanzf17@tju.edu.cn

SPECIALTY SECTION
This article was submitted to Terrestrial Microbiology, a section of the journal Frontiers in Microbiology

RECEIVED 28 November 2022
ACCEPTED 28 December 2022
PUBLISHED 12 January 2023

CITATION
Wang H, Yan Z, Ju X, Song X, Zhang J, Li S and Zhu-Barker X (2023) Quantifying nitrous oxide production rates from nitrification and denitrification under various moisture conditions in agricultural soils: Laboratory study and literature synthesis.
Front. Microbiol. 13:1110151.
doi: 10.3389/fmicb.2022.1110151

Quantifying nitrous oxide production rates from nitrification and denitrification under various moisture conditions in agricultural soils: Laboratory study and literature synthesis

Hui Wang[1], Zhifeng Yan[1,2]*, Xiaotang Ju[3], Xiaotong Song[4], Jinbo Zhang[5], Siliang Li[1,2] and Xia Zhu-Barker[6]

[1]School of Earth System Science, Institute of Surface-Earth System Science, Tianjin University, Tianjin, China, [2]Critical Zone Observatory of Bohai Coastal Region, Tianjin Key Laboratory of Earth Critical Zone Science and Sustainable Development in Bohai Rim, Tianjin University, Tianjin, China, [3]College of Tropical Crops, Hainan University, Haikou, China, [4]State Key Laboratory of Urban and Regional Ecology, Research Center for Eco-Environmental Sciences, Chinese Academy of Sciences, Beijing, China, [5]School of Geography Sciences, Nanjing Normal University, Nanjing, China, [6]Department of Soil Science, University of Wisconsin-Madison, Madison, WI, United States

Biogenic nitrous oxide (N_2O) from nitrification and denitrification in agricultural soils is a major source of N_2O in the atmosphere, and its flux changes significantly with soil moisture condition. However, the quantitative relationship between N_2O production from different pathways (i.e., nitrification vs. denitrification) and soil moisture content remains elusive, limiting our ability of predicting future agricultural N_2O emissions under changing environment. This study quantified N_2O production rates from nitrification and denitrification under various soil moisture conditions using laboratory incubation combined with literature synthesis. ^{15}N labeling approach was used to differentiate the N_2O production from nitrification and denitrification under eight different soil moisture contents ranging from 40 to 120% water-filled pore space (WFPS) in the laboratory study, while 80 groups of data from 17 studies across global agricultural soils were collected in the literature synthesis. Results showed that as soil moisture increased, N_2O production rates of nitrification and denitrification first increased and then decreased, with the peak rates occurring between 80 and 95% WFPS. By contrast, the dominant N_2O production pathway switched from nitrification to denitrification between 60 and 70% WFPS. Furthermore, the synthetic data elucidated that moisture content was the major driver controlling the relative contributions of nitrification and denitrification to N_2O production, while NH_4^+ and NO_3^- concentrations mainly determined the N_2O production rates from each pathway. The moisture treatments with broad contents and narrow gradient were required to capture the comprehensive response of soil N_2O production rate to moisture change, and the response is essential for accurately predicting N_2O emission from agricultural soils under climate change scenarios.

KEYWORDS

nitrous oxide, soil moisture, nitrification, denitrification, ^{15}N-labeled technique

1. Introduction

Nitrous oxide (N_2O) is a potent long-lived greenhouse gas, with global warming potential 296 times higher than carbon dioxide (CO_2; Tian et al., 2020). Agricultural soil has been identified as a major source of atmospheric N_2O, accounting for approximately 60% of the global anthropogenic N_2O emissions (Reay et al., 2012; Cui et al., 2021). Soil moisture content is a primary regulator to control N_2O emissions from agricultural systems (Congreves et al., 2019). Particularly, the N_2O emissions from the soils under high moisture conditions (e.g., after rainfall or irrigation events) can constitute more than 30% of the annual emission (Trost et al., 2013; Ju and Zhang, 2017); this proportion will likely increase with the intensive use of irrigation under droughts and the increase in the frequency of heavy rainfalls, both of which were projected as a consequence of climate change (Reichstein et al., 2013; Siebert et al., 2015). However, the quantitative relationships between soil N_2O emissions from various biological processes, including nitrification, dentification, dissimilatory nitrate reduction to ammonium (DNRA) and anaerobic ammonia oxidation, and soil moisture content remain understudied (Castellano et al., 2010; Hall et al., 2018; Li et al., 2022), impeding our ability to predict the future N_2O emission from agricultural systems.

Nitrification and denitrification are two of the most important biological processes to produce N_2O (Butterbach-Bahl et al., 2013), and soil moisture content substantially controls the relative contributions of these two pathways and their production rates of N_2O (Ciarlo et al., 2007; Congreves et al., 2019). Therefore, how to accurately describe the relationships between N_2O production rates of nitrification and denitrification and moisture content in mathematical models is crucial for estimating and predicting the N_2O emission from soils (Yue et al., 2019). Current models, such as DNDC (Li et al., 2000) and DayCent (Parton et al., 1996), have used various types of relationships, including linear, parabolic, and exponential ones, to depict the response of N_2O production rate to moisture change (Wang et al., 2021), regardless of the fact that the N_2O production rates from nitrification and denitrification were theoretically expected to first increase and then decrease as moisture content increases (Davidson et al., 2000). These divergent relationships inevitably result in large uncertainty in simulating soil N_2O emission (Gaillard et al., 2018), and accurately quantifying the relationships between N_2O production rate and moisture content is urgently required.

Although many studies have measured the response of total N_2O production rate to changes in moisture content (Dobbie and Smith, 2001; Schaufler et al., 2010; Cheng et al., 2014; Hall et al., 2018; Kuang et al., 2019), only a few quantified the N_2O production rates of nitrification and denitrification under different moisture conditions (Pihlatie et al., 2004; Bateman and Baggs, 2005). In these studies, unidirectional increases in the N_2O production rates of denitrification and nitrification were often reported as moisture increased, which contrasted with the classic hole-in-pipe model (Davidson et al., 2000). This inconsistency can be attributed to many factors such as soil physicochemical properties and measurement approaches (Liu et al., 2018; Qin et al., 2021). Among these factors, moisture treatments used in different studies should be the primary driver, since the majority of these studies adopted insufficient gradients and inadequate levels of soil moisture (Bateman and Baggs, 2005; Chen et al., 2014), which failed to capture the comprehensive change in N_2O production rates in response to varied moisture conditions (Smith, 2017). Therefore, sufficient moisture treatments with broad range and narrow gradient are required to fill the gap between measurements and expectations.

This study hypothesizes that the production rates of N_2O from both nitrification and denitrification first increase and then decrease as moisture content increases. We tested this hypothesis by using both laboratory incubation and literature synthesis. In the laboratory study, a ^{15}N-labeled technique was applied to distinguish the nitrification and denitrification under eight moisture levels in the agricultural soils from the North China Plain. For the literature synthesis, data derived from different differentiation approaches under various moisture conditions across global agricultural soils were analyzed. The results refined the quantitative relationships between N_2O production rate and moisture content from both nitrification and denitrification, and laid a foundation to improve the modeling of N_2O emissions from agricultural soils.

2. Materials and methods

2.1. Site description and soil sampling

Soil samples (0–15 cm) were collected from agricultural fields in two locations: Shang Zhuang (SZ), Beijing (39°48′N, 116°28′E) and Luan Cheng (LC), Hebei (37°53′ N, 114°41′E), North China Plain, in October 2020.The annual average temperature is 12.5°C, and the annual precipitation is 500–700 mm with high variation among different years. The cropping system in this region is winter wheat-summer maize rotation. The fertilizer application rates were 280 and 600 kg N ha^{-1} year^{-1} in SZ and LC soils, respectively. Collected soils were air-dried and sieved to 2 mm. Visible roots and leaves were removed with tweezers and the soil was immediately stored at 4°C until the beginning of laboratory experiment. The soils

are both classified as silt loam, with 36.1% sand, 56.4% silt, and 7.5% clay for the SZ soil and 29.2% sand, 64.1% silt, and 6.7% clay for the LC soil. For the SZ soil, pH was 7.89, bulk density was 1.02 g cm^{-3}, soil organic carbon was 10.93 g kg^{-1}, total N was 1.13 g kg^{-1}, NH_4^+-N was 3.07 mg kg^{-1}, and NO_3^--N was 22.5 mg kg^{-1}. For the LC soil, pH was 7.92, bulk density was 1.00 g cm^{-3}, soil organic carbon was 19.82 g kg^{-1}, total N was 2.11 g kg^{-1}, NH_4^+-N was 2.08 mg kg^{-1}, and NO_3^--N was 30.49 mg kg^{-1}.

2.2. ^{15}N tracing incubation experiment

Soils (20 g oven-dry equivalent) were placed into 120 ml incubation flasks and distilled water was added to the soils to below the target moisture contents [i.e., 40, 60, 70, 80, 90, 95, 100, and 120% water-filled pore space (WFPS)]. The microcosms were then pre-incubated at 25°C for 7 days to initiate microbial activity. For each moisture content treatment, $^{15}NH_4Cl$ (10.08 atom%) + KNO_3 or $K^{15}NO_3$ (10.16 atom%) + NH_4Cl were applied at a rate of 50 mg NH_4^+-N kg^{-1} and 50 mg NO_3^--N kg^{-1} after pre-incubation. To assure uniform distribution, 2 ml of ^{15}N solution was applied in water solution and sprayed onto the soils to obtain the target moisture content. The experimental design and treatment application were set up as completely randomized blocks and incubated in dark for 48 h at 25°C after ^{15}N application.

Each treatment was replicated three times for gas analyses, with gas samples collected at 12, 24, and 48 h. Before sampling, the flasks were flushed with ambient air using a multiport vacuum manifold, and the N_2O concentration in the headspace was then measured. Thereafter, the flasks were immediately sealed for 12 h and N_2O concentration was measured again. The difference between the two N_2O concentrations was used to calculate the N_2O production rate. The concentrations of N_2O and CO_2 were determined using gas chromatography (Agilent 7,890, Santa Clara, CA, United States) and the ^{15}N signature of N_2O was determined using a Thermo Finnigan MAT-253 spectrometer (Thermo Fisher Scientific, Waltham, MA, United States). Another group of flasks, also replicated three times, were used for soil sampling at 0.5, 12, 24, and 48 h after N application. Soils were extracted with 1 M KCl (20 g soil to 100 ml KCl solution), shaken for 1 h, and filtered. The concentrations of NH_4^+-N and NO_3^--N in the extracts were measured using a continuous-flow analyzer (Skalar Analytical, Breda, Netherlands). Isotope analysis of NH_4^+-N and NO_3^--N were performed on aliquots of the extracts using a diffusion technique (Brooks et al., 1989) and the ^{15}N isotopic signature was measured by isotope ratio mass spectrometry (IRMS 20–22, Sercon, Crewe, United Kingdom).

2.3. Calculation

Nitrous oxide and CO_2 fluxes (F, μg N kg^{-1} h^{-1} or mg C kg^{-1} h^{-1}) were determined from the concentrations at each sampling time, using the background N_2O and CO_2 concentrations in the ambient air as the initial time point, which were calculated as follows:

$$F = \frac{\rho \times \Delta c \times V \times 273}{W \times \Delta t \times (273 + T)} \quad (1)$$

where ρ is the density of gas under standard conditions (kg m^{-3}), ΔC is the variation in gas concentration during the flask-covering period (the units of N_2O and CO_2 are ppbv and ppmv, respectively), and V is the effective volume of a given flask (m^3), T is the incubation temperature (°C), Δt is the incubation time (h), and W is the weight of soil (oven-dried basis, kg).

The contributions of denitrification, C_d, and nitrification, C_n to the production of N_2O were calculated using the following equation (Stevens et al., 1997):

$$C_d = \frac{(a_{N_2O} - a_{NH_4})}{(a_{NO_3} - a_{NH_4})} \text{ with } a_{NO_3} \neq a_{NH_4} \quad (2)$$

$$C_n = 1 - C_d \quad (3)$$

where a_{N_2O} is the ^{15}N atom% enrichment of the N_2O produced by both processes, and a_{NO_3} and a_{NH_4} are the ^{15}N atom% enrichment of soil NO_3^- and NH_4^+ at the time of gas sampling.

Rates of N_2O production from nitrification (N_2O_n) and denitrification (N_2O_d) were calculated as follows:

$$N_2O_n = C_n \times N_2O_T \quad (4)$$

$$N_2O_d = C_d \times N_2O_T \quad (5)$$

where N_2O_T is the total N_2O production rate from the soils, $N_2O_T = N_2O_n + N_2O_d$.

Since the concentrations and abundances of NH_4^+ at 48 h could not be reliably determined in most treatments, the average C_d, C_n, N_2O_n and N_2O_d over the first 24 h incubation were used to analyze the rates of N_2O production from nitrification and denitrification.

2.4. Literature synthesis

Data on the N_2O production rates of nitrification and denitrification were collected from published peer-reviewed journal articles. The following criteria were used for data collection: (1) incubation experiments used agricultural soils solely; (2) soil moisture metric was expressed as WFPS. Meanwhile, soil characteristics and incubation conditions, including pH, BD, clay content, SOC content, concentrations of

TN, NH_4^+, and NO_3^-, incubation temperature and WFPS, were collected. GetData Graph Digitizer 2.26 was used when data were only graphically shown. The autotrophic nitrification and heterotrophic nitrification were summed and treated as nitrification during the data analysis if they were reported as individual pathways in the literature. In total, 80 groups of data from 17 studies were obtained (Supplementary Table S1).

2.5. Statistical analysis

All statistical analyses were evaluated by one-way analysis of variance (ANOVA) for comparisons among multiple factors and t-test for contrasts between two factors, followed by the least significant difference test at $P<0.05$. The relationships between the contributions of nitrification and denitrification to N_2O production or their rates and the controlling factors were examined by correlation and regression analysis. All statistical analyses were carried out in SPSS v25.0 software for Windows (SPSS Inc., Chicago, United States).

3. Results

3.1. Changes in concentrations of NH_4^+ and NO_3^- and production rate of nitrous oxide

The concentration of soil NH_4^+ decreased over the incubation course in all moisture treatments (Figures 1A,B). For both SZ and LC soils, the declining rates of NH_4^+ over the first 24 h were nearly twice larger in the treatments of WFPS ≤80% than in the treatments of WFPS ≥90%. After the first 24 h, the declining rate slowed down clearly when WFPS ≤80%, especially for the LC soil (Figure 1B), while it nearly kept constant under WFPS ≥90%. Among all the WFPS treatments, the largest consumption rate of NH_4^+ occurred at 60% WFPS for both SZ and LC soils.

The concentration of soil NO_3^- increased as NH_4^+ was nitrified (Figures 1C,D). In correspondence to the changes in NH_4^+ concentration, NO_3^- concentration increased faster when WFPS ≤80% than when WFPS ≥90%, especially for the LC soil during the first 24 h. The initial NO_3^- concentration exhibited large variances for different moisture contents, since nitrification increased NO_3^- concentration under low moisture content while denitrification reduced NO_3^- concentration under high moisture during the pre-incubation period. As the initial NO_3^- concentration markedly reduced as WFPS increased, the NO_3^- concentration varied largely at the end of incubation especially for the LC soil, changing from 170.3 to 75.0 mg N kg^{-1} as WFPS increased from 60 to 120%.

The N_2O production rate changed substantially with moisture content and time (Figure 2). At the beginning of incubation, high N_2O production rates (> 5 μg N kg^{-1} h^{-1}) occurred under 80% ≤ WFPS ≤100% in the SZ soil and under 70% ≤ WFPS ≤100% in the LC soil, whereas the rates remained low under the lower or higher moisture conditions. As the incubation proceeded, the N_2O production rate first increased and then decreased under the intermediate moisture conditions (e.g., WFPS = 70, 90, and 95%) in the SZ soil, but consistently reduced under all moisture conditions in the LC soil. Finally, the N_2O production rates declined to below 5 μg N kg^{-1} h^{-1} under all moisture contents for both soils at the end of incubation. By contrast, CO_2 production rates were higher at WFPS ≥90% than at WFPS <90% for both soils, except for 95% WFPS in the LC soil ($P<0.05$; Supplementary Figure S1).

3.2. Nitrous oxide production from nitrification and denitrification

The ^{15}N enrichment of N_2O remained between the ^{15}N enrichments of NH_4^+ and NO_3^- during the first 24 h, illustrating that N_2O was derived from both nitrification and denitrification (Supplementary Figure S2). The average contribution of denitrification to N_2O production, C_d, increased with moisture content in the SZ and LC soils up to 100 and 95% WFPS, respectively, after which C_d declined significantly (Figure 3). In both soils, nitrification was the main pathway producing N_2O under low moisture conditions while denitrification dominated N_2O production under high moisture conditions, with the threshold occurred at 70 and 60% WFPS for the SZ and LC soils, respectively. Denitrification contributed more than 65% of the total N_2O production when WFPS ≥70%, and this percentage promoted as the incubation proceeded (Supplementary Table S2).

Nitrous oxide production rates derived from nitrification (N_2O_n), denitrification (N_2O_d) and the combined processes (N_2O_T) responded to moisture change in a pattern similar to Gaussian function in both SZ and LC soils (Figure 4). As moisture increased, the N_2O_n increased slowly, reaching peaks around 2.5 μg N kg^{-1} h^{-1} in both SZ and LC soils, while the N_2O_d increased steeply, reaching peaks of 10.1 and 12.5 μg N kg^{-1} h^{-1} in the SZ and LC soils, respectively. Correspondingly, the optimal WFPS with respect to the peak rates were the same for the nitrification and denitrification processes (90% WFPS) in the SZ soil, but diverged for the two pathways (80 and 95% WFPS, respectively) in the LC soil. The N_2O production rates remained below 3 μg N kg^{-1} h^{-1} under either low or flooded moisture condition.

3.3. Literature synthesis: Nitrous oxide production from nitrification and denitrification across agricultural soils

By synthesizing literature data across global agricultural soils, moisture (WFPS) and incubation temperature (T) were found to be the most significant factors controlling the contributions of nitrification and denitrification to N_2O production (Table 1), with WFPS exerting a stronger correlation (R = 0.45) than T (R = 0.37; Figure 5; Supplementary Figure S3). Compared with the literature data (R = 0.36), the measured data in this study exhibited a

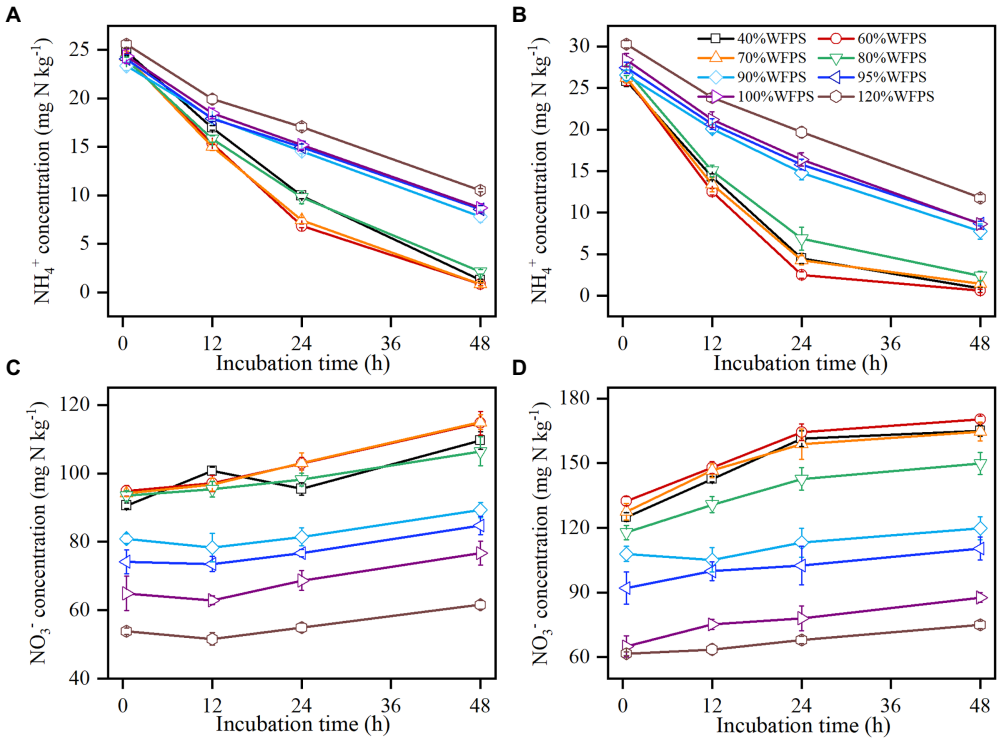

FIGURE 1
Changes in concentrations of ammonium (NH_4^+) and nitrate (NO_3^-) over 48h of incubations in SZ **(A,C)** and LC **(B,D)** soils. Vertical bars are standard deviations of the means (n=6).

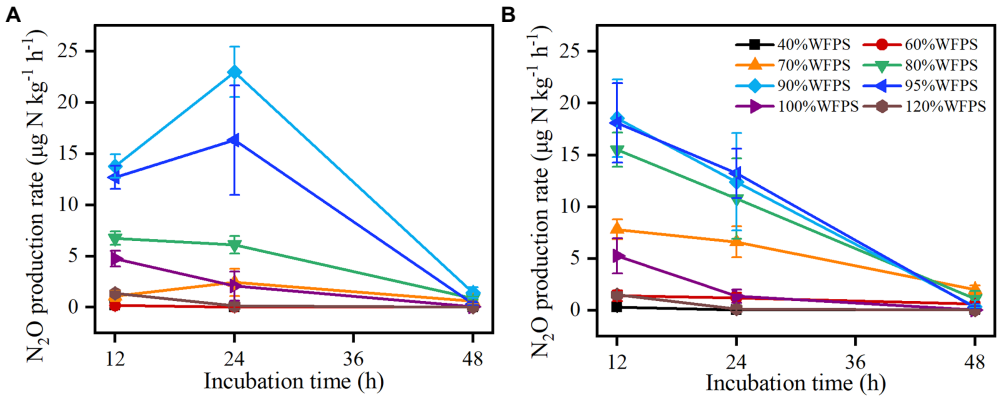

FIGURE 2
Changes in N_2O production rate over 48h of incubations from SZ **(A)** and LC **(B)** soils. Vertical bars are the standard deviations of the means (n=6).

stronger positive correlation between C_d and WFPS (R = 0.73; Figure 5). Furthermore, a stronger correlation between C_d and WFPS occurred in alkaline soils than in acidic soils (Supplementary Figure S4A). Similarly, compared with carbon-rich soils with SOC ≥ 4%, mineral soils with SOC < 4% showed a stronger correlation (Supplementary Figure S4B).

Based on the literature synthesis, the N_2O_n and N_2O_d generally first increased and then decreased as WFPS increased (Figure 6). The relationships between the N_2O production rates of nitrification and denitrification and WFPS were fitted by Gaussian function. Compared with nitrification (Figure 6A), denitrification (Figure 6B) showed a smaller standard deviation, 5% vs. 14%, and a higher maximum rate, 106 vs. 12 μg N kg^{-1} h^{-1}, though both of their peak rates occurred at around 85% WFPS. The correlations between N_2O production rates and various soil properties were also analyzed (Supplementary Table S3). The results indicated that NH_4^+ and NO_3^- concentrations were the most powerful drivers to explain the changes in N_2O_n and N_2O_d. Both N_2O_n and N_2O_d

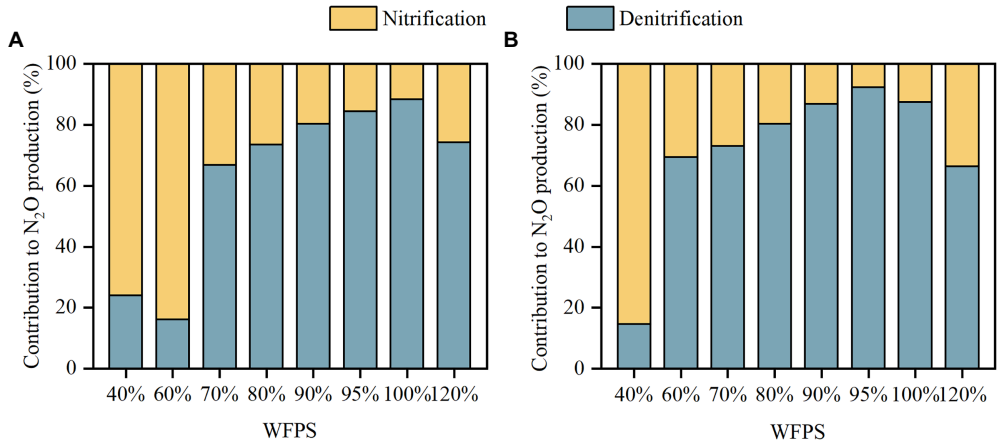

FIGURE 3
The contributions of nitrification and denitrification to N_2O production in SZ **(A)** and LC **(B)** soils.

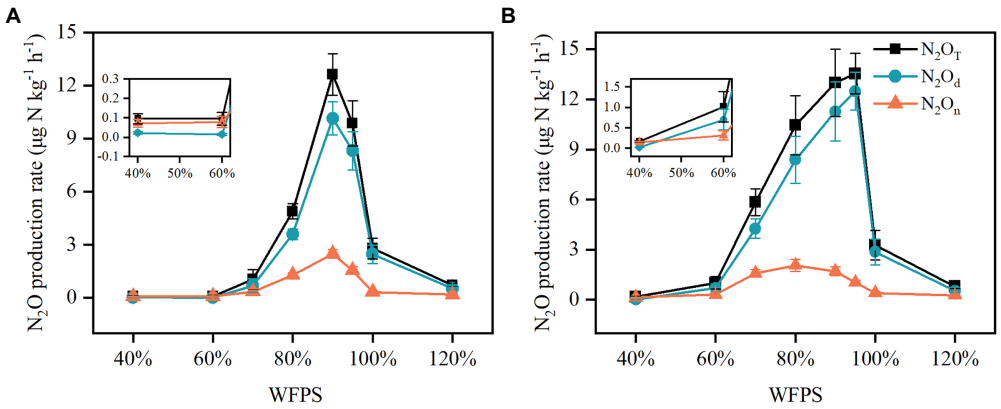

FIGURE 4
The N_2O production rates derived from nitrification (N_2O_n), denitrification (N_2O_d) and the combined processes (N_2O_T) in the SZ **(A)** and LC **(B)** soils under different WFPS.

increased positively with the increases in NH_4^+ ($P<0.05$; Supplementary Figures S5A,C) and NO_3^- concentrations ($P<0.01$; Supplementary Figures S5B,D), though the variances of rates were large as the concentrations were high.

4. Discussion

4.1. Contributions of nitrification and denitrification to nitrous oxide production

Both laboratory incubation and literature synthesis showed that nitrification and denitrification dominated N_2O production under low and high moisture conditions, respectively. Under high moisture conditions as soil oxygen availability was constrained, denitrification outcompeted nitrification as the main source of N_2O production (Smith, 2017; Song et al., 2019; Chang et al., 2022), which was aligned with other experiments (Pihlatie et al., 2004; Friedl et al., 2021). The dominant pathway of N_2O production switched between 60 and 70% WFPS (Figure 5), depending on soil properties and climatic conditions. For instance, the thresholds for SZ and LC soil were 70 and 60% WFPS (Figure 3), respectively. This is because the SOC content was higher in the LC soil (19.82 g kg^{-1}) than in the SZ soil (10.93 g kg^{-1}), stimulating N_2O production by promoting denitrification process (Ruser et al., 2006; Chantigny et al., 2013). Besides, the N_2O production rate in the LC soil (1.02 μg N kg^{-1} h^{-1}) was almost 10 times that in SZ soil (0.1 μg N kg^{-1} h^{-1}) under 60% WFPS, further indicating the dominating effects of denitrification in the N_2O production in the LC soil. The literature synthesis also confirmed that large SOC content increased the contribution of denitrification to N_2O production under relatively low soil moisture content (Supplementary Figure S4B). Besides SOC, other factors such as BD, NH_4^+ and NO_3^- concentrations, and especially incubation temperature, also modulated the contributions of

TABLE 1 Correlations between the contribution of denitrification (C_d) and soil properties as well as environmental conditions, which include soil pH, bulk density (BD), clay content, soil organic carbon (SOC), total nitrogen (TN) concentrations, NH_4^+ and NO_3^- concentrations, incubation temperature (T) and water-filled pore space (WFPS), across agricultural soils.

		pH	BD	Clay	SOC	TN	NH_4^+	NO_3^-	T	WFPS
C_d	R	0.076	−0.147	−0.022	0.112	0.088	0.198	−0.249	0.369	0.446
	P	0.462	0.335	0.858	0.340	0.414	0.187	0.096	<0.01	<0.01
	n	96	45	70	75	89	46	46	94	96

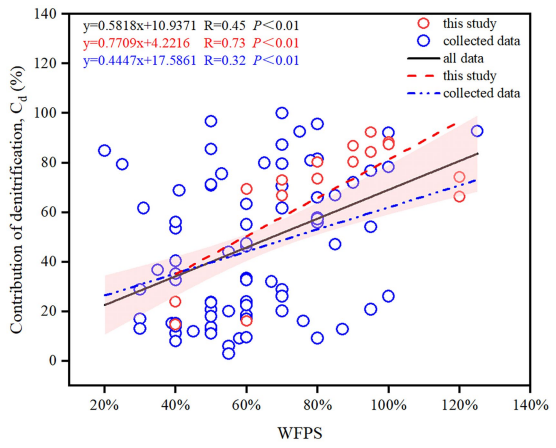

FIGURE 5
Changes in the contribution of denitrification to N_2O production (C_d) with WFPS across global agricultural soils. The shaded region represents the 95% confidence interval for all data.

nitrification and denitrification to N_2O production (Table 1), which might explain why the contribution proportions between nitrification and denitrification varied significantly among different soils even though the soil moisture status were similar (Figure 5).

Accurately determining the contributions of nitrification and denitrification to N_2O production is crucial to evaluate N_2O emissions from agricultural soils (Zhu et al., 2013). Currently, different approaches were used to quantify these contributions, including ^{15}N site preference (Thilakarathna and Hernandez-Ramirez, 2021), acetylene inhibition (Pihlatie et al., 2004), and ^{15}N tracing techniques (Friedl et al., 2021). The applications of these approaches often caused large discrepancies in quantifying C_d and C_n under different moisture conditions (Butterbach-Bahl et al., 2013), and likely resulted in different contribution proportions even though the experimental setup and the operating conditions were the same (Zhu et al., 2013). Therefore, a careful comparison among different approaches and developing a guideline or protocol for using these approaches merit further investigations. Although certain factors such as pH value and N concentrations exerted insignificant impacts on the contribution of different pathways to N_2O production (Table 1), their integrative impacts remain unclear (Hu et al., 2015). In addition, factors such as moisture and temperature, often changed synchronously in fields (Song et al., 2018), and studying their integrative impacts will significantly improve our understanding of N_2O emission dynamics and facilitate N_2O abatement (Mathieu et al., 2006).

4.2. Nitrous oxide production rates of nitrification and denitrification

Both laboratory study and literature synthesis validated the hypothesis that the rates of N_2O production from both nitrification and denitrification first increased and then decreased as soil moisture increased (Figures 4, 6). The relationships between N_2O production rate and moisture content followed the classic hole-in-pipe model (Davidson et al., 2000), though the rates changed with soil properties (Figure 4). For instance, the LC soil produced generally larger N_2O_d than the SZ soil, since it contained more NO_3^- and SOC, which stimulated N_2O production from denitrification under high moisture content (Smith, 2017). By comparison, the two soils exhibited approximate N_2O_n due to the similar NH_4^+ concentrations. The literature synthesis further confirmed that NO_3^- and NH_4^+ were the two most important factors to determine N_2O production rates (Supplementary Table S3). Interestingly, NO_3^- concentration was the most powerful driver to explain the changes in N_2O derived from nitrification, although its explaining power was close to that of NH_4^+ concentration. This result might be caused by the large N_2O production rates from nitrification under high NO_3^- concentrations and large soil moisture contents (Supplementary Figure S5) and warrant further investigations. However, the rates of N_2O_d and N_2O_n depended on not only the above factors but also moisture content, and their interactions control N_2O emission from soils (Zhu et al., 2013). Therefore, higher substrate concentration unnecessarily resulted in larger N_2O emissions, as being observed in many laboratory and field experiments (Senbayram et al., 2012; Liu et al., 2018).

In contrast to the first increased and then decreased N_2O production rates in response to increase in soil moisture content from the laboratory incubation in this study, the studies in the collected literatures presented divergent consequences among different experiments (Supplementary Table S1). Among the 17 collected studies, as moisture increased, only five reported a decline in N_2O production rate for nitrification and no study found a decline for denitrification. The underrepresented decline in the rates can be mainly attributed to the insufficient gradients and

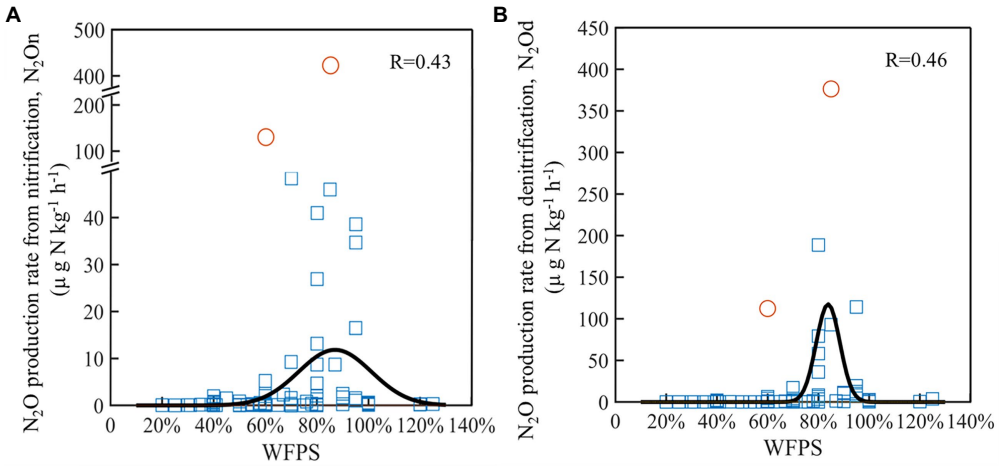

FIGURE 6
Changes in N_2O production rates from nitrification **(A)** and denitrification **(B)** under different WFPS across agricultural soils. The black lines were the fitted curves using Gaussian function after excluding the abnormal values (the circles).

inadequate levels of moisture content applied in these studies, which commonly used soil moisture containing less than four levels and below 90% WFPS (Supplementary Table S1). Such sparse moisture levels likely did not capture the inflection point of N_2O production rate (Barton et al., 2015), while the low moisture condition might not be adequate to capture the turning point (Bateman and Baggs, 2005; Liu et al., 2016). Therefore, N_2O emission under relatively high moisture conditions with sufficient moisture treatments deserves further investigations. The interactions of soil moisture with other factors such as SOC content (Qin et al., 2017), nutrient availability (Senbayram et al., 2012), and pH value (Zhang et al., 2015) together determine the relationship between N_2O emission rates and moisture contents (Zhu et al., 2020).

4.3. Implications and looking forward

Both laboratory study and literature synthesis illustrated that N_2O emissions declined as moisture content exceeded certain threshold. Current models using linear or exponential relationships between N_2O production rate and moisture content could significantly overestimate N_2O emissions from agricultural systems (Yue et al., 2019; Wang et al., 2021), especially as the intensive irrigation and extreme rainfall are projected to increase under climate change scenarios (Smith et al., 2017). Therefore, comprehensive relationships that can capture the first increased and then decreased N_2O production rates in response to elevated soil moisture content are required. However, the large variances in N_2O production rates of both nitrification and denitrification among different studies induce great challenges to develop such a relationship. One potential breakthrough can be to quantify this relationship for different types of soils by incorporating intense moisture treatments similar to this study. Meanwhile, additional experiments are required to quantify the impacts of other key factors, such as temperature, NO_3^- and NH_4^+ concentrations and their interactions, on the relationship. Once sufficient data measured using the same experimental protocol are collected, it will be possible to derive quantitative relationships between N_2O production rate and moisture content across different soils by using a general function, such as Gaussian function, with parameters depending on key edaphic and climatic drivers (Yan et al., 2018).

5. Conclusion

This study quantified the response of soil N_2O production rates from nitrification and denitrification to changes in a broad range of moisture contents using both laboratory study and literature synthesis. The results showed that the N_2O production rates of nitrification and denitrification first increased and then decreased as moisture increased for both particular and global agricultural soils, following the classic hole-in-pipe model. The inflection points of moisture content, under which the N_2O production rate maximized, for the two pathways occurred between 80 and 95% WFPS, which value depended on incubation temperature and soil properties. By contrast, the switching point of soil moisture from nitrification-dominating to denitrification-dominating occurred between 60 and 70% WFPS. The unidirectional increase in N_2O production rates reported in most literatures should be attributed to the insufficient gradients and inadequate levels of moisture content applied in the incubation experiments, and moisture treatments containing broad

moisture contents with narrow gradient are required to obtain the comprehensive relationship between soil N_2O production rate and moisture content, which is crucial to accurately predict future N_2O emission from global agricultural soils in response to climate change.

Data availability statement

The raw data supporting the conclusions of this article will be made available by the authors, without undue reservation.

Author contributions

HW conducted the experiments and wrote the first draft. ZY guided the experiments and completed the final draft. XZ-B, XJ, XS, JZ, and SL helped to improve the manuscript. All authors contributed to the article and approved the submitted version.

Funding

This work was financially supported by the National Key Research and development Program of China (No. 2022YFF1301002), National Natural Science Foundation of China (No. 42077009), and Haihe Laboratory of Sustainable Chemical Transformations.

Acknowledgments

We would like to thank Zengming Chen from Institute of Soil Science, Chinese Academy of Sciences and Yi Cheng from Nanjing Normal University for their selfless support.

Conflict of interest

The authors declare that the research was conducted in the absence of any commercial or financial relationships that could be construed as a potential conflict of interest.

Publisher's note

All claims expressed in this article are solely those of the authors and do not necessarily represent those of their affiliated organizations, or those of the publisher, the editors and the reviewers. Any product that may be evaluated in this article, or claim that may be made by its manufacturer, is not guaranteed or endorsed by the publisher.

Supplementary material

The Supplementary material for this article can be found online at: https://www.frontiersin.org/articles/10.3389/fmicb.2022.1110151/full#supplementary-material

References

Barton, L., Wolf, B., Rowlings, D., Scheer, C., Kiese, R., Grace, P., et al. (2015). Sampling frequency affects estimates of annual nitrous oxide fluxes. *Sci. Rep.* 5, 1–9. doi: 10.1038/srep15912

Bateman, E. J., and Baggs, E. M. (2005). Contributions of nitrification and denitrification to N_2O emissions from soils at different water-filled pore space. *Biol. Fert. Soils* 41, 379–388. doi: 10.1007/s00374-005-0858-3

Brooks, P., Stark, J. M., McInteer, B., and Preston, T. (1989). Diffusion method to prepare soil extracts for automated nitrogen-15 analysis. *Soil Sci. Soc. Am. J.* 53, 1707–1711. doi: 10.2136/sssaj1989.03615995005300060016x

Butterbach-Bahl, K., Baggs, E. M., Dannenmann, M., Kiese, R., and Zechmeister-Boltenstern, S. (2013). Nitrous oxide emissions from soils: how well do we understand the processes and their controls? *Philos. Soc. B.* 368, 20130122–20130197. doi: 10.1098/rstb.2013.0122

Castellano, M. J., Schmidt, J. P., Kaye, J. P., Walker, C., Graham, C. B., Lin, H., et al. (2010). Hydrological and biogeochemical controls on the timing and magnitude of nitrous oxide flux across an agricultural landscape. *Glob. Chang. Biol.* 16, 2711–2720. doi: 10.1111/j.1365-2486.2009.02116.x

Chang, B., Yan, Z., Ju, X., Song, X., Li, Y., Li, S., et al. (2022). Quantifying biological processes producing nitrous oxide in soil using a mechanistic model. *Biogeochemistry* 159, 1–14. doi: 10.1007/s10533-022-00912-0

Chantigny, M. H., Pelster, D. E., Perron, M. H., Rochette, P., Angers, D. A., Parent, L. É., et al. (2013). Nitrous oxide emissions from clayey soils amended with paper sludges and biosolids of separated pig slurry. *J. Environ. Qual.* 42, 30–39. doi: 10.2134/jeq2012.0196

Chen, Z., Ding, W., Luo, Y., Yu, H., Xu, Y., Müller, C., et al. (2014). Nitrous oxide emissions from cultivated black soil: a case study in Northeast China and global estimates using empirical model. *Glob. Biogeochem. Cycle* 28, 1311–1326. doi: 10.1002/2014GB004871

Cheng, Y., Wang, J., Wang, S., Zhang, J., and Cai, Z. (2014). Effects of soil moisture on gross N transformations and N_2O emission in acid subtropical forest soils. *Biol. Fert. Soils* 50, 1099–1108. doi: 10.1007/s00374-014-0930-y

Ciarlo, E., Conti, M., Bartoloni, N., and Rubio, G. (2007). The effect of moisture on nitrous oxide emissions from soil and the $N_2O/(N_2O+N_2)$ ratio under laboratory conditions. *Biol. Fert. Soils* 43, 675–681. doi: 10.1007/s00374-006-0147-9

Congreves, K. A., Phan, T., and Farrell, R. E. (2019). A new look at an old concept: using $^{15}N_2O$ isotopomers to understand the relationship between soil moisture and N_2O production pathways. *Soil* 5, 265–274. doi: 10.5194/soil-5-265-2019

Cui, X., Zhou, F., Ciais, P., Davidson, E. A., Tubiello, F. N., Niu, X., et al. (2021). Global mapping of crop-specific emission factors highlights hotspots of nitrous oxide mitigation. *Nat. Food.* 2, 886–893. doi: 10.1038/s43016-021-00384-9

Davidson, E. A., Keller, M., Erickson, H. E., Verchot, L. V., and Veldkamp, E. (2000). Testing a conceptual model of soil emissions of nitrous and nitric oxides. *Bio Sci.* 50, 667–680. doi: 10.1641/0006-3568(2000)050[0667:TACMOS]2.0.CO;2

Dobbie, K. E., and Smith, K. A. (2001). The effects of temperature, water-filled pore space and land use on N_2O emissions from an imperfectly drained gleysol. *Eur. J. Soil Sci.* 52, 667–673. doi: 10.1046/j.1365-2389.2001.00395.x

Friedl, J., Scheer, C., De Rosa, D., Müller, C., Grace, P. R., and Rowlings, D. W. (2021). Sources of nitrous oxide from intensively managed pasture soils: the hole in the pipe. *Environ. Res. Lett.* 16:065004. doi: 10.1088/1748-9326/abfde7

Gaillard, R. K., Jones, C. D., Ingraham, P., Collier, S., Izaurralde, R. C., Jokela, W., et al. (2018). Underestimation of N_2O emissions in a comparison of the DayCent, DNDC, and EPIC models. *Ecol. Appl.* 28, 694–708. doi: 10.1002/eap.1674

Hall, S., Reyes, L., Huang, W., and Homyak, P. (2018). Wet spots as hotspots: moisture responses of nitric and nitrous oxide emissions from poorly drained agricultural soils. *J. Geophys. Res. Biogeo.* 123, 3589–3602. doi: 10.1029/2018JG004629

Hu, H., Chen, D., and He, J. (2015). Microbial regulation of terrestrial nitrous oxide formation: understanding the biological pathways for prediction of emission rates. *FEMS Microbiol. Rev.* 39, 729–749. doi: 10.1093/femsre/fuv021

Ju, X., and Zhang, C. (2017). Nitrogen cycling and environmental impacts in upland agricultural soils in North China: a review. *J. Integr. Agric.* 16, 2848–2862. doi: 10.1016/S2095-3119(17)61743-X

Kuang, W., Gao, X., Tenuta, M., Gui, D., and Zeng, F. (2019). Relationship between soil profile accumulation and surface emission of N_2O: effects of soil moisture and fertilizer nitrogen. *Biol. Fert. Soils* 55, 97–107. doi: 10.1007/s00374-018-01337-4

Li, C., Aber, J., Stange, F., Butterbach-Bahl, K., and Papen, H. (2000). A process-oriented model of N_2O and NO emissions from forest soils: 1 Model development. *J. Geophys. Res. Atmos.* 105, 4369–4384. doi: 10.1029/1999JD900949

Li, S., Liu, X., Yue, F., Yan, Z., Wang, T., Li, S., et al. (2022). Nitrogen dynamics in the critical zones of China. *Prog. Phys. Geogr.* 46, 869–888. doi: 10.1177/03091333221114732

Liu, H., Ding, Y., Zhang, Q., Liu, X., Xu, J., Li, Y., et al. (2018). Heterotrophic nitrification and denitrification are the main sources of nitrous oxide in two paddy soils. *Plant Soil* 445, 39–53. doi: 10.1007/s11104-018-3860-x

Liu, R., Hayden, H. L., Suter, H., Hu, H., Lam, S. K., He, J., et al. (2016). The effect of temperature and moisture on the source of N_2O and contributions from ammonia oxidizers in an agricultural soil. *Biol. Fert. Soils* 53, 141–152. doi: 10.1007/s00374-016-1167-8

Mathieu, O., Hénault, C., Lévêque, J., Baujard, E., Milloux, M. J., and Andreux, F. (2006). Quantifying the contribution of nitrification and denitrification to the nitrous oxide flux using ^{15}N tracers. *Environ. Pollut.* 144, 933–940. doi: 10.1016/j.envpol.2006.02.005

Parton, W. J., Mosier, A. R., Ojima, D. S., Valentine, D. W., Schimel, D. S., Weier, K., et al. (1996). Generalized model for N_2 and N_2O production from nitrification and denitrification. *Glob. Biogeochem. Cycle* 10, 401–412. doi: 10.1029/96gb01455

Pihlatie, M., Syvasalo, E., Simojoki, A., Esala, M., and Regina, K. (2004). Contribution of nitrification and denitrification to N_2O production in peat, clay and loamy sand soils under different soil moisture conditions. *Nutr. Cycl. Agroecosystems* 70, 135–141. doi: 10.1023/B:FRES.0000048475.81211.3c

Qin, S., Hu, C., Clough, T. J., Luo, J., Oenema, O., and Zhou, S. (2017). Irrigation of DOC-rich liquid promotes potential denitrification rate and decreases N_2O/(N_2O+N_2) product ratio in a 0–2 m soil profile. *Soil Biol. Biochem.* 106, 1–8. doi: 10.1016/j.soilbio.2016.12.001

Qin, H., Wang, D., Xing, X., Tang, Y., Wei, X., Chen, X., et al. (2021). A few key nirK-and nosZ-denitrifier taxa play a dominant role in moisture-enhanced N2O emissions in acidic paddy soil. *Geoderma* 385:114917. doi: 10.1016/j.geoderma.2020.114917

Reay, D. S., Davidson, E. A., Smith, K. A., Smith, P., Melillo, J. M., Dentener, F., et al. (2012). Global agriculture and nitrous oxide emissions. *Nat. Clim. Chang.* 2, 410–416. doi: 10.1038/nclimate1458

Reichstein, M., Bahn, M., Ciais, P., Frank, D., Mahecha, M. D., Seneviratne, S. I., et al. (2013). Climate extremes and the carbon cycle. *Nature* 500, 287–295. doi: 10.1038/nature12350

Ruser, R., Flessa, H., Russow, R., Schmidt, G., Buegger, F., and Munch, J. C. (2006). Emission of N_2O, N_2 and CO_2 from soil fertilized with nitrate: effect of compaction, soil moisture and rewetting. *Soil Biol. Biochem.* 38, 263–274. doi: 10.1016/j.soilbio.2005.05.005

Schaufler, G., Kitzler, B., Schindlbacher, A., Skiba, U., Sutton, M., and Zechmeister-Boltenstern, S. (2010). Greenhouse gas emissions from European soils under different land use: effects of soil moisture and temperature. *Eur. J. Soil Sci.* 61, 683–696. doi: 10.1111/j.1365-2389.2010.01277.x

Senbayram, M., Chen, R., Budai, A., Bakken, L., and Dittert, K. (2012). N_2O emission and the N_2O/(N_2O + N_2) product ratio of denitrification as controlled by available carbon substrates and nitrate concentrations. *Agric. Ecosyst. Environ.* 147, 4–12. doi: 10.1016/j.agee.2011.06.022

Siebert, S., Kummu, M., Porkka, M., Döll, P., Ramankutty, N., and Scanlon, B. R. (2015). A global data set of the extent of irrigated land from 1900 to 2005. *Hydrol. Earth Syst. Sci.* 19, 1521–1545. doi: 10.5194/hess-19-1521-2015

Smith, K. A. (2017). Changing views of nitrous oxide emissions from agricultural soil: key controlling processes and assessment at different spatial scales. *Eur. J. Soil Sci.* 68, 137–155. doi: 10.1111/ejss.12409

Smith, A. P., Bond-Lamberty, B., Benscoter, B. W., Tfaily, M. M., Hinkle, C. R., Liu, C., et al. (2017). Shifts in pore connectivity from precipitation versus groundwater rewetting increases soil carbon loss after drought. *Nat. Commun.* 8:1335. doi: 10.1038/s41467-017-01320-x

Song, X., Ju, X., Topp, C. F. E., and Rees, R. M. (2019). Oxygen regulates nitrous oxide production directly in agricultural soils. *Environ. Sci. Technol.* 53, 12539–12547. doi: 10.1021/acs.est.9b03089

Song, X., Liu, M., Ju, X., Gao, B., Su, F., Chen, X., et al. (2018). Nitrous oxide emissions increase exponentially when optimum nitrogen fertilizer rates are exceeded in the North China plain. *Environ. Sci. Technol.* 52, 12504–12513. doi: 10.1021/acs.est.8b03931

Stevens, R., Laughlin, R., Burns, L., Arah, J., and Hood, R. (1997). Measuring the contributions of nitrification and denitrification to the flux of nitrous oxide from soil. *Soil Biol. Biochem.* 29, 139–151. doi: 10.1016/S0038-0717(96)00303-3

Thilakarathna, S. K., and Hernandez-Ramirez, G. (2021). Primings of soil organic matter and denitrification mediate the effects of moisture on nitrous oxide production. *Soil Biol. Biochem.* 155:108166. doi: 10.1016/j.soilbio.2021.108166

Tian, H., Xu, R., Canadell, J. G., Thompson, R. L., Winiwarter, W., Suntharalingam, P., et al. (2020). A comprehensive quantification of global nitrous oxide sources and sinks. *Nature* 586, 248–256. doi: 10.1038/s41586-020-2780-0

Trost, B., Prochnow, A., Drastig, K., Meyer-Aurich, A., Ellmer, F., and Baumecker, M. (2013). Irrigation, soil organic carbon and N_2O emissions: A review. *Agron. Sustain. Dev.* 33, 733–749. doi: 10.1007/s13593-013-0134-0

Wang, C., Amon, B., Schulz, K., and Mehdi, B. (2021). Factors that influence nitrous oxide emissions from agricultural soils as well as their representation in simulation models: a review. *Agronomy* 11:770. doi: 10.3390/agronomy11040770

Yan, Z., Bond-Lamberty, B., Todd-Brown, K. E., Bailey, V. L., Li, S., Liu, C., et al. (2018). A moisture function of soil heterotrophic respiration that incorporates microscale processes. *Nat. Commun.* 9:2562. doi: 10.1038/s41467-018-04971-6

Yue, Q., Cheng, K., Ogle, S., Hillier, J., Smith, P., Abdalla, M., et al. (2019). Evaluation of four modelling approaches to estimate nitrous oxide emissions in China's cropland. *Sci. Total Environ.* 652, 1279–1289. doi: 10.1016/j.scitotenv.2018.10.336

Zhang, J., Müller, C., and Cai, Z. (2015). Heterotrophic nitrification of organic N and its contribution to nitrous oxide emissions in soils. *Soil Biol. Biochem.* 84, 199–209. doi: 10.1016/j.soilbio.2015.02.028

Zhu, X., Burger, M., Doane, T. A., and Horwath, W. R. (2013). Ammonia oxidation pathways and nitrifier denitrification are significant sources of N_2O and NO under low oxygen availability. *Proc. Natl. Acad. Sci. U. S. A.* 110, 6328–6333. doi: 10.1073/pnas.1219993110

Zhu, Y., Merbold, L., Leitner, S., Xia, L., Pelster, D. E., Diaz-Pines, E., et al. (2020). Influence of soil properties on N_2O and CO_2 emissions from excreta deposited on tropical pastures in Kenya. *Soil Biol. Biochem.* 140:107636. doi: 10.1016/j.soilbio.2019.107636

frontiers | Frontiers in Microbiology

TYPE Original Research
PUBLISHED 08 February 2023
DOI 10.3389/fmicb.2023.1120466

OPEN ACCESS

EDITED BY
Baoli Zhu,
Institute of Subtropical Agriculture (CAS), China

REVIEWED BY
Chao Wang,
Institute of Applied Ecology (CAS), China
Simon Guerrero-Cruz,
Asian Institute of Technology, Thailand
Zhe Wang,
Technical University of Munich, Germany

*CORRESPONDENCE
Shuping Qin
✉ qinshuping@sjziam.ac.cn

SPECIALTY SECTION
This article was submitted to Terrestrial Microbiology, a section of the journal Frontiers in Microbiology

RECEIVED 10 December 2022
ACCEPTED 23 January 2023
PUBLISHED 08 February 2023

CITATION
Song W, Hu C, Luo Y, Clough TJ, Wrage-Mönnig N, Ge T, Luo J, Zhou S and Qin S (2023) Nitrate as an alternative electron acceptor destabilizes the mineral associated organic carbon in moisturized deep soil depths.
Front. Microbiol. 14:1120466.
doi: 10.3389/fmicb.2023.1120466

Nitrate as an alternative electron acceptor destabilizes the mineral associated organic carbon in moisturized deep soil depths

Wei Song[1], Chunsheng Hu[2], Yu Luo[3], Tim J. Clough[4], Nicole Wrage-Mönnig[5], Tida Ge[6], Jiafa Luo[7], Shungui Zhou[1] and Shuping Qin[2]*

[1]Fujian Provincial Key Laboratory of Soil Environmental Health and Regulation, College of Resources and Environment, Fujian Agriculture and Forestry University, Fuzhou, Fujian, China, [2]Hebei Provincial Key Laboratory of Soil Ecology, Center for Agricultural Resources Research, Institute of Genetic and Developmental Biology, Chinese Academy of Sciences, Shijiazhuang, Hebei, China, [3]Zhejiang Provincial Key Laboratory of Agricultural Resources and Environment, Institute of Soil and Water Resources and Environmental Science, Zhejiang University, Hangzhou, China, [4]Faculty of Agriculture and Life Sciences, Lincoln University, Lincoln, New Zealand, [5]Faculty of Agricultural and Environmental Sciences, Grassland and Fodder Sciences, University of Rostock, Rostock, Germany, [6]State Key Laboratory for Managing Biotic and Chemical Threats to the Quality and Safety of Agro-Products, Key Laboratory of Biotechnology in Plant Protection of Ministry of Agriculture and Zhejiang Province, Institute of Plant Virology, Ningbo University, Ningbo, China, [7]AgResearch Ltd., Hamilton, New Zealand

Numerous studies have investigated the effects of nitrogen (N) addition on soil organic carbon (SOC) decomposition. However, most studies have focused on the shallow top soils <0.2 m (surface soil), with a few studies also examining the deeper soil depths of 0.5–1.0 m (subsoil). Studies investigating the effects of N addition on SOC decomposition in soil >1.0 m deep (deep soil) are rare. Here, we investigated the effects and the underlying mechanisms of nitrate addition on SOC stability in soil depths deeper than 1.0 m. The results showed that nitrate addition promoted deep soil respiration if the stoichiometric mole ratio of nitrate to O_2 exceeded the threshold of 6:1, at which nitrate can be used as an alternative acceptor to O_2 for microbial respiration. In addition, the mole ratio of the produced CO_2 to N_2O was 2.57:1, which is close to the theoretical ratio of 2:1 expected when nitrate is used as an electron acceptor for microbial respiration. These results demonstrated that nitrate, as an alternative acceptor to O_2, promoted microbial carbon decomposition in deep soil. Furthermore, our results showed that nitrate addition increased the abundance of SOC decomposers and the expressions of their functional genes, and concurrently decreased MAOC, and the ratio of MAOC/SOC decreased from 20% before incubation to 4% at the end of incubation. Thus, nitrate can destabilize the MAOC in deep soils by stimulating microbial utilization of MAOC. Our results imply a new mechanism on how above-ground anthropogenic N inputs affect MAOC stability in deep soil. Mitigation of nitrate leaching is expected to benefit the conservation of MAOC in deep soil depths.

KEYWORDS

nitrate leaching, global warming, greenhouse gas emission, MAOC, deep soil

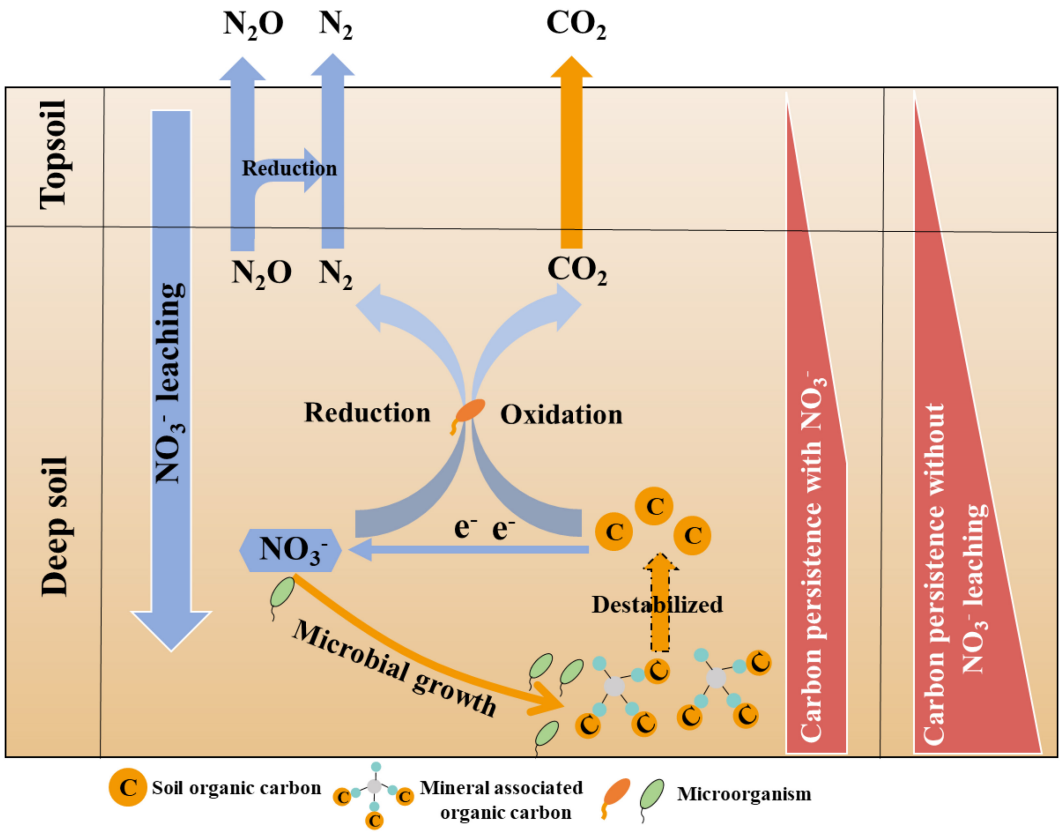

GRAPHICAL ABSTRACT
Mechanisms of nitrate on deep soil MAOC.

1. Introduction

Globally, the stock of soil organic carbon (SOC) is estimated to be as high as 2300 Pg in the 3 m depth, which is about 3-fold the size of the atmospheric carbon dioxide (CO_2) pool (770 Pg) (Lal, 2004). The annual CO_2 emissions due to soil respiration are reported to range from 60 to 100 Pg C yr^{-1}, which is an order of magnitude greater than current fossil fuel CO_2 emissions (Bond-Lamberty and Thomson, 2010; Oertel et al., 2016; Xu and Shang, 2016) and account for 5∼25% of total annual CO_2 emissions globally (Raich and Potter, 1995; Wang et al., 2018). CO_2 is the dominant greenhouse gas and the atmospheric concentration of CO_2 has increased from 277 $\mu l l^{-1}$ in 1750 to 411 $\mu l l^{-1}$ in 2019 (Friedlingstein et al., 2020; Walker et al., 2021). Thus, any enhanced loss of CO_2 *via* SOC decomposition has significant implications for global warming (Zhang et al., 2020).

Anthropogenic nitrogen (N) inputs are reported to significantly affect SOC content (Mazzoncini et al., 2011; Riggs and Hobbie, 2016; Chen et al., 2021). Globally, anthropogenic N inputs have increased from 156 Tg N yr^{-1} in 1995 to 193 Tg N yr^{-1} in 2010 (Galloway et al., 2008; Fowler et al., 2015), and it is estimated that by 2050 the global rate of N inputs will double the rate in 1995 (Penuelas et al., 2020). A considerable portion of the anthropogenically derived N is transformed into nitrate, which can leach to depth (>1 m) within the soil profile (Van Meter et al., 2016; Xin et al., 2019; Yang et al., 2020; Gao et al., 2021). As the soil profile deepens, persistent hypoxia or even anoxia can establish, potentially resulting in nitrate being reduced *via* the denitrification or dissimilatory nitrate reduction to ammonium (DNRA) pathways, which require SOC as an electron donor (Laursen and Seitzinger, 2002; Giblin et al., 2013). Consequently, anthropogenic N inputs potentially affect SOC decomposition not only at the soil surface but also in the deeper soil profile.

The SOC in deep soil is expected to respond to N addition differently from that of surface soil due to carbon sources being distinctively different between the surface soil and deep soil (Salomé et al., 2010). In surface soil, plant residues and root exudates are important sources of SOC. In line with this, increased CO_2 emission following N addition were found to be derived from plant residues and root exudates (Schulte-Uebbing and de Vries, 2018; Xu et al., 2021). This mechanism would be expected to be less significant in deep soil since the contribution of plant residue and roots to SOC sharply decreased with the increasing soil depth (Poirier et al., 2018). Furthermore, oxygen (O_2), an electron acceptor for SOC oxidation, is more available to SOC decomposers in surface soil than in deep soil. The soil O_2 concentration generally declines sharply from the surface to a depth of approximately 1.0 m, then continues to decline slowly with the increase of soil depth (Sierra and Renault, 1998; Orem et al., 2011; Kautz, 2015). Thus, nitrate in deep soil has a larger opportunity to replace O_2 as an alternative electron acceptor for SOC oxidation. Compared with the SOC in surface soil, the SOC in deep soil is generally absorbed or co-precipitated with minerals as mineral associated organic carbon (MAOC), which potentially decreases its accessibility for soil microbial decomposition (Stuckey et al., 2018; Jilling et al., 2021). The observed increase in decomposers, induced by N addition in deep soil, is expected to enhance the potential for decomposers to destabilize MAOC (Feng et al., 2022).

Thus, the response of the carbon following N addition differs since the distinct SOC in surface and deep soils. Most previous studies have only investigated the response of SOC following N addition in the surface soil (<1.0 m depth). Many of these studies reported that N addition increased SOC content (Riggs et al., 2015; Philben et al., 2019), while other studies reported that N addition decreased (Mo et al., 2008; Treseder, 2008; Bulseco et al., 2019) or did not affect SOC content (Högberg, 2007; Lu et al., 2011), this may be attributed to the form of N, the level of application and soil type. While, few studies have investigated the effects of N addition on carbon decomposition in deep soil (Li et al., 2014; Xu et al., 2021). Such information is relevant for understanding MAOC stability in the deep soil and carbon sequestration.

In this study, we investigated the responses and relevant mechanisms of MAOC stability following nitrate addition to deep soil. Nitrate was selected as the N source because it is the main form of anthropogenic N that leaches into deep soil.

2. Materials and methods

2.1. Experimental site and sample collection

Soil samples were collected from the campus of the Fujian Agriculture and Forestry University, Fuzhou, China (26°06′ N, 119°13′ E). Three depths of soil (1.5–1.7, 2.0–2.2, and 2.5–2.7 m) were collected. Deep soil in this study is defined as soil depths >1.0 m. The soil samples were passed through a 2 mm sieve to remove as much live and dead root material, then basic soil physicochemical properties were determined, which are shown in **Table 1**. Soils were placed in sealed ziplock bags, with excess air removed using vacuum package machine to minimize exposure to O_2, and stored at −20°C about 3 days, then we started the experiments. Soils were thawed at 4°C and preincubated at 20°C (Fontaine et al., 2007; Condron et al., 2014) for 5 days under anaerobic condition to recover microbial activity prior to commencing experiments.

The SOC content was determined using an elemental analyzer (Vario Macro Cube, Elementar, Germany). Soil moisture content was determined by drying fresh soil samples to constant weight at 105°C oven. Soil samples were extracted with 1 M KCl solution (soil: liquid ratio was 1:5) and then filtered (0.45 μm, Jinteng, China). The soil extracts were then analyzed for dissolved organic carbon (DOC) concentration using a total organic carbon analyzer (TOC-LCPH, Shimadzu, Japan), for nitrate, nitrite and ammonium concentrations using a UV-1800 spectrophotometer (Shimadzu, Japan) and the colorimetric method (Norman and Stucki, 1981; Dorich and Nelson, 1983; Norman et al., 1985), and for pH using a pH meter (LeiCi PHSJ-3F, China). After extracting soil samples with distilled water (soil: water ratio was 1:5) and filtering, the electrical conductivity (EC) was determined with a conductivity meter (LeiCi DDSJ-308F, China). Soil texture was determined using a laser particle analyzer (Malvern Mastersizer 3000, UK) according to the protocol (Pieri et al., 2006).

TABLE 1 The basic physicochemical properties of the soil.

	Soil depth		
	1.5–1.7 m	2.0–2.2 m	2.5–2.7 m
SOC (g C kg^{-1} dry soil)	4.25 ± 0.09a	4.14 ± 0.01a	3.50 ± 0.04b
DOC (mg C kg^{-1} dry soil)	73.81 ± 11.78a	68.33 ± 5.75a	59.69 ± 6.19a
NO_3^- (mg N kg^{-1} dry soil)	3.09 ± 0.19b	11.20 ± 0.26a	2.22 ± 0.21c
NO_2^- (mg N kg^{-1} dry soil)	1.14 ± 0.06b	2.20 ± 0.48a	1.34 ± 0.08b
NH_4^+ (mg N kg^{-1} dry soil)	15.26 ± 0.73a	16.91 ± 3.63a	14.85 ± 0.90a
Moisture content	19.98%	26.96%	23.87%
EC (mS cm^{-1})	79.1	94.5	50.9
pH	5.17	5.05	5.15
Sand (%)	69.13	59.62	46.16
Silt (%)	29.27	37.46	48.47
Clay (%)	1.6	2.92	5.36

Different letters indicate significant differences ($P < 0.05$) among the soil depths.

2.2. Experimental design

2.2.1. Experiment 1: Effects of nitrate addition on deep soil respiration, microbial community structure and key functional genes responsible for C degradation

In order to determine the effect of nitrate addition on CO_2 emission from deep soil, two treatments were conducted: (1) nitrate addition treatment: 15 g of fresh soil was placed in to 120 ml flasks and a KNO_3 solution was added to the flasks to reach 100 mg NO_3^--N kg^{-1} dry soil; (2) control treatment: 15 g fresh soil received an equal amount of distilled water. Moisture is reported to be the most important factor affecting SOC mineralization (Huang and Hall, 2017). Thus, three gravimetric water contents were applied: 35% (2 ml 50 mM KNO_3), 70% (5 ml 20 mM KNO_3), and 200% (20 ml 5 mM KNO_3). There was a total of 54 flasks (2 treatments × 3 soil depths × 3 soil moisture contents × 3 replicates). All flasks were sealed with air-tight butyl rubber septa and aluminum caps. The headspace gas was alternatively evacuated (0.1 kPa) and flushed with pure helium (99.999%, 120 kPa) five times to remove O_2 (Yuan et al., 2019), the initial O_2 concentrations was 35.5 μmol L^{-1} at this time. All flasks were incubated at 20°C (Fontaine et al., 2007; Condron et al., 2014) in the dark for 55 days.

During the incubation, the headspace CO_2 concentrations were periodically determined using a robotized sampling and analysis system (Molstad et al., 2007). Briefly, the robotized system consisted of an incubation system linked with a gas collection and analysis system. It enabled sampling of the headspace gas by puncturing the butyl rubber septa of the anaerobic flasks and then pumping of 2 ml sample gas through the loop of the GC with a peristaltic pump. An electron capture detector (ECD) was used for determination of N_2O and a thermal conductivity detector (TCD) was used to measure CO_2, O_2 and N_2.

At the end of the 70% water content incubation, soil samples from the nitrate addition and control treatments, for each soil depth, were collected to determine the soil microbial community structure, and the key functional genes responsible for C degradation. Soil microbial DNA was extracted from these samples using the PowerSoil DNA isolation kit (MoBio, Carlsbad, CA) according to the manufacturer's instructions. V3-V4 variable region of the 16S rRNA gene were amplified with primers 338F (ACTCCTACGGGAGGCAGCAG)/806R (GGACTACHVGGGTWTCTAAT). The sequencing operation was

completed by Beijing Allwegene technology Co., Ltd. (Beijing, China). Sample sequences were clustered with a threshold of 97% similarity to obtain representative operational taxonomic units (OTUs). Paired-end sequencing was performed using an Illumina Miseq PE300 platform (Wu et al., 2019).

The total RNA was extracted from 1 g soil samples using the RNA Extraction Kit (Tiangen Biochemical Science Technologies Co., Ltd., Beijing, China) according to the manufacturer's protocols. The RNA concentration and purity were determined using an ND-2000 spectrophotometer (Thermo Scientific), then RNA integrity was assessed using a Tanon 1600 imaging system (Tanon Science and Technology Co., Ltd., Shanghai, China). The primers were synthesized by Invitrogen (Shanghai, China), subsequently, RNA was converted to cDNA using the Prime Script^{TM} RT reagent Kit with gDNA Eraser (TaKaRa). Then quantitative Real-Time PCR (qRT-PCR) was performed using an ABI7500 quantitative PCR system (Applied Biosystems, USA) with each sample conducted in triplicate. The relative abundances of genes responsible for the degradation of starch, hemicellulose, cellulose, chitin, aromatics, lignin and lignin from labile to recalcitrant (*amyA*, *arA*, *cbhI*, *chi*, *AceB*, *lip*, and laccase-like multi-copper oxidase (*Lmco*), respectively) were determined using the $2^{-\Delta\Delta Ct}$ method (Wang et al., 2019), with the 16S rRNA gene used as an internal reference gene, the denitrification genes for qRT-PCR were *narG*, *nirK*, and *nosZ* genes. The primer sequences of qRT-PCR are presented in **Supplementary Tables 1, 2**.

2.2.2. Experiment 2: Effects of supplemental amount of nitrate on deep soil CO_2 emissions

We further tested whether the increase in soil CO_2 emissions was linearly correlated with the supplemental rate of nitrate addition, using the soil sample from 2.0 to 2.2 m depth with a 70% water content, including the subsequent experiments. The reason for continuing using 2.0–2.2 m depth was the higher level of nitrate concentration in this layer than other layers and the reason for continuing using 70% moisture content was more reasonable and a real condition to explore the mechanism. Five nitrate levels were applied: 0, 10, 20, 50, and 100 mg NO_3^--N kg^{-1} dry soil. Each level was replicated three times and flasks were incubated in the dark at 20°C for 98 days. The CO_2 concentration was determined every 7 days and analysis methods were identical to that used in Experiment 1.

2.2.3. Experiment 3: Effects of ammonium addition on deep soil CO_2 emissions

We further tested if other inorganic N types beside nitrate, e.g., ammonium, could promote deep soil CO_2 emissions. Three treatments were applied, (1) nitrate addition treatment: 15 g fresh soil of the 2.0–2.2 m depth was cultured in 120 ml flasks with 5 ml of 20 mM KNO_3 (the final nitrate content was 100 mg NO_3^--N kg^{-1} dry soil); (2) ammonium addition treatment: 15 g fresh soil of the 2.0–2.2 m depth was cultured in 120 ml flasks with

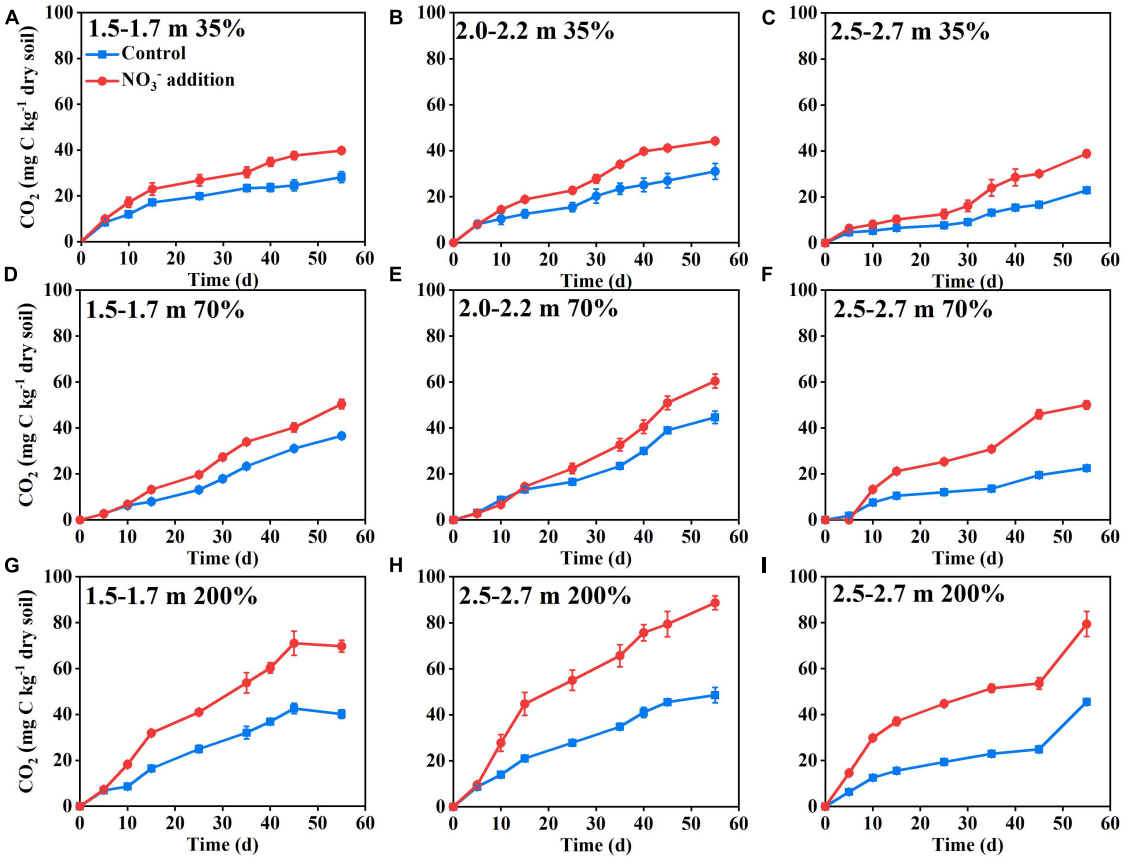

FIGURE 1
Nitrate addition effects on the cumulative CO_2 emissions from deep soil depths: 1.5–1.7 m **(A,D,G)**, 2.0–2.2 m **(B,E,H)**, and 2.5–2.7 m **(C,F,I)** with soil gravimetric water contents of 35% **(A–C)**, 70% **(D–F)**, and 200% **(G–I)** in Experiment 1. The blue lines and red lines represent control and nitrate addition treatments, respectively. Data are shown as the mean ± standard deviation (n = 3).

5 ml of 20 mM NH_4Cl (the final ammonium content was 100 mg NH_4^+-N kg^{-1} dry soil); (3) control treatment: 15 g fresh soil of the 2.0–2.2 m depth received 5 ml of distilled water. The flasks were incubated in the dark at 20°C for 98 days and headspace gas sampling occurred every 7 days.

2.2.4. Experiment 4: Effects of O_2 level on the stimulation of nitrate on deep soil CO_2 emissions

We further determined if nitrate acted as an alternative electron acceptor to O_2 in stimulating deep soil CO_2 emission. The initial O_2 concentration in the flasks was set at 1% by volume. During the incubation, the O_2 concentration was expected to gradually decrease. Two treatments were set up: (1) 1% O_2 treatment: 15 g fresh soil from the 2.0 to 2.2 m depth was incubated with 5 ml of distilled water in 120 ml flasks; (2) 1% O_2 + NO_3^- treatment: 15 g fresh soil from the 2.0 to 2.2 m depth was incubated with 5 ml of 20 mM KNO_3 solution in 120 ml flasks. The headspace of the flasks was alternatively evacuated (0.1 kPa) and re-flushed with high-purity helium/O_2 mixture gas (1% O_2 and 99% helium, 120 kPa) five times, the initial O_2 concentrations was 565 μmol L^{-1} at this time, and supplemented with 1% O_2 again when O_2 concentrations declined below 100 μmol L^{-1}. A total of 96 flasks were prepared (48 flasks for each treatment)

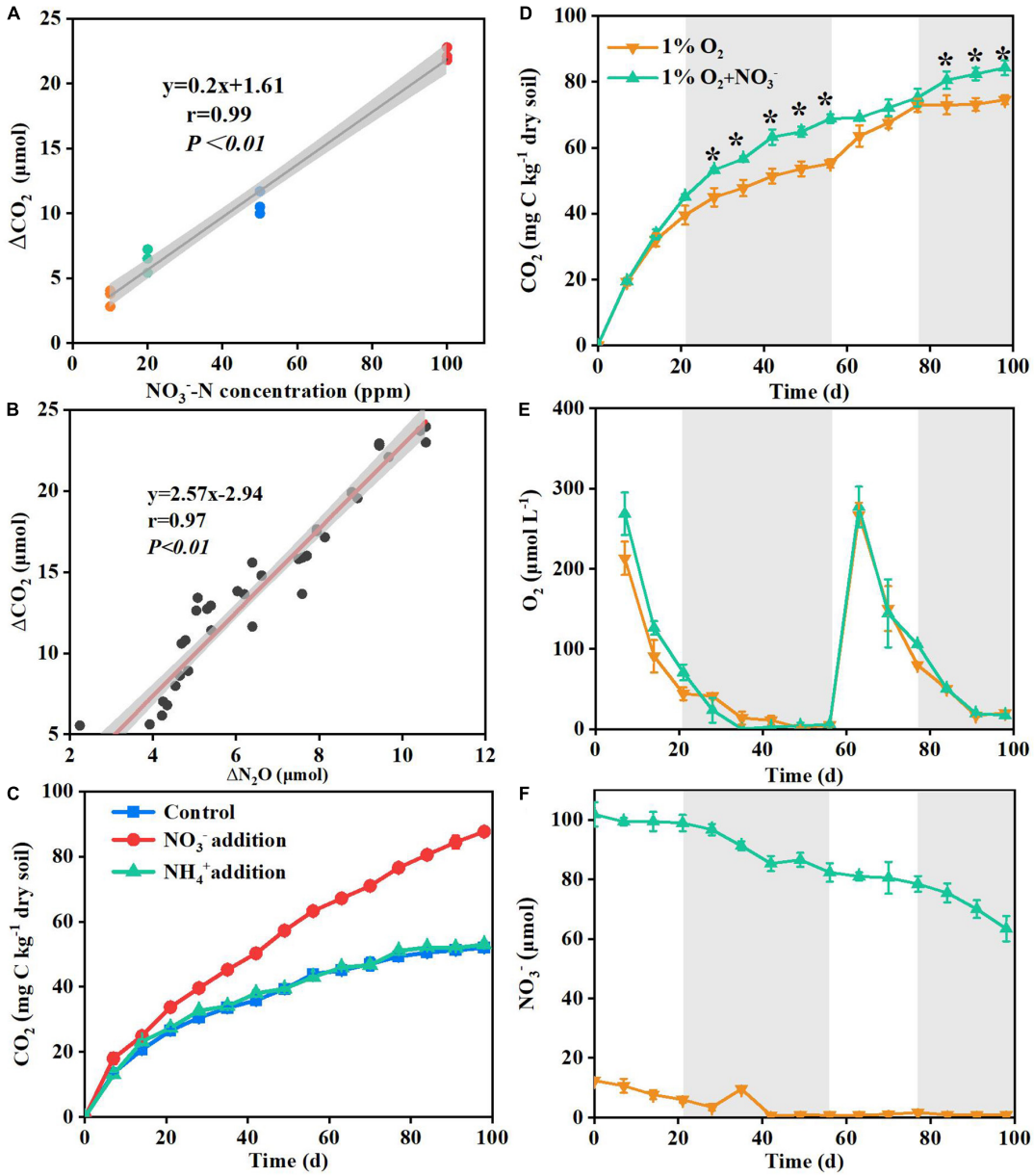

FIGURE 2
Correlation between the rate of the supplemented nitrate and the increasing concentration of ΔCO_2 under the nitrate addition treatment in Experiment 2 **(A)**; correlation between the increasing amounts of the produced ΔCO_2 and ΔN_2O at 100 ppm NO_3^--N treatment in Experiment 2 **(B)**; ammonium versus nitrate addition effects on the cumulative CO_2 emissions from deep soil in Experiment 3 **(C)**; dynamics of CO_2 **(D)**, O_2 **(E)** and NO_3^- **(F)** concentrations in flasks under 1% O_2 and 1% O_2 + NO_3^- treatments in Experiment 4. Delta indicates the value of nitrate addition treatment minus non-nitrate control within each sampling day. The gray areas in panels **(A,B)** indicate 95% confidence intervals. The gray areas in panels **(D–F)** indicate anaerobic conditions with O_2 concentrations below 100 μmol L^{-1}. Asterisk denotes significant difference ($P < 0.05$) between the two treatments. Data are shown as the mean ± standard deviation ($n = 3$).

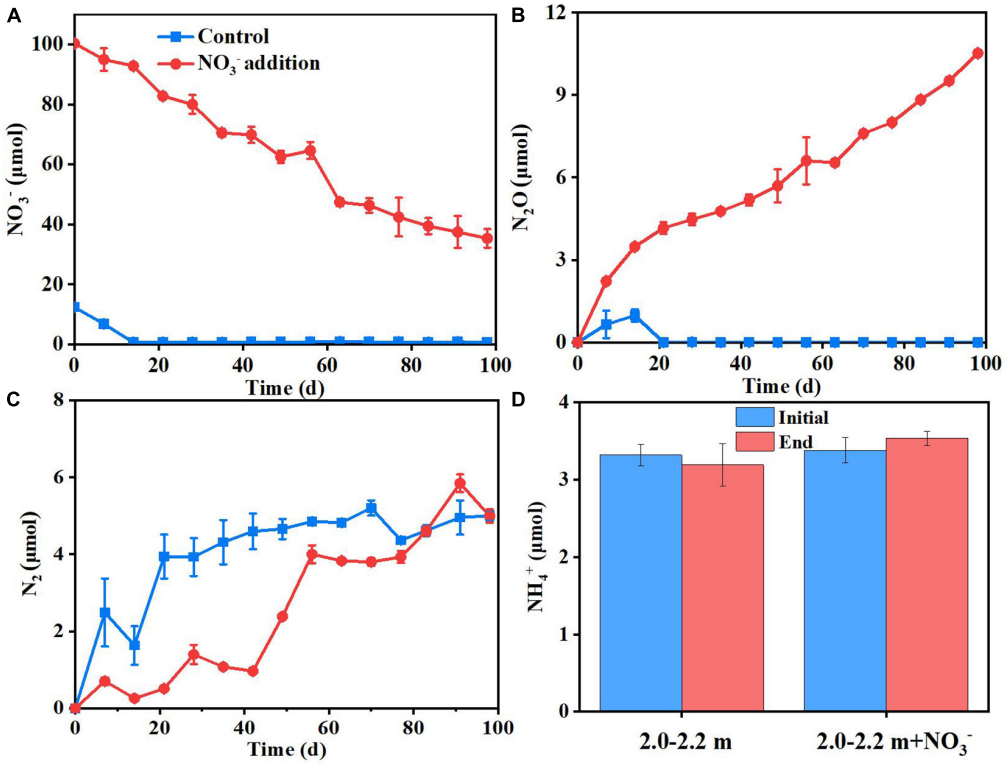

FIGURE 3
Dynamics of NO_3^- **(A)**, N_2O **(B)**, and N_2 **(C)** concentrations in flasks under control and nitrate addition treatments. NH_4^+ concentrations at initial and end of the incubation under two treatments **(D)**.

and incubated under dark conditions at 20°C for 98 days. At the beginning of the incubation, three flasks from each treatment were randomly selected for periodically determining the headspace O_2 and CO_2 concentrations at a frequency of four measurements per month, using the robotized sampling and analyzing system as noted above in Experiment 1. To calculate the stoichiometric mole ratio of nitrate and oxygen when nitrate was used as an electron acceptor, during the incubation, three flasks of each treatment were randomly selected each week to destructively sample the soil for determining the nitrate concentrations.

2.2.5. Experiment 5: Effects of nitrate addition on microbial biomass N and C contents, MAOC, and redox potential in deep soil

We further tested whether the promotion of microbial respiration by nitrate would stimulate microbial proliferation and consequently increase the microbial utilization of on MAOC in deep soil. Two treatments were conducted: (1) 15 g soil samples from the 2.0 to 2.2 m depth were incubated with 5 ml of 20 mM KNO_3; (2) 15 g soil samples from the 2.0 to 2.2 m depth were incubated with 5 ml of distilled water. A total of 54 flasks (27 flasks for each treatment) were prepared and their headspaces were exchanged with high-purity helium as described in Experiment 1. The flasks were incubated in the dark at 20°C for 98 days. Three flasks for each treatment were randomly selected every 14-day for destructive sampling to determine the MAOC content using the citrate-bicarbonate-dithionite (CBD) method (Lalonde et al., 2012). At the end of the incubation, three flasks from each treatment were used to measure the microbial biomass carbon (MBC) and nitrogen (MBN) using the fumigation-extraction method (Vance et al., 1987) and perform 16S DNA gene copy numbers together to estimate microbial proliferation. The last three flasks for each treatment were used to measure soil redox potential (Eh) using an Eh meter (Model HLY-216, China) and pH by using the probe inserted into the soil.

2.3. Statistical analysis

The statistical package SPSS 24.0 (SPSS Inc., Chicago, IL, USA) was used to perform all statistical analysis. Analysis of variance (ANOVA) was used to determine the difference ($P < 0.05$) among treatments after the Shapiro–Wilk and Levene tests were used to confirm the normality and homogeneity of the data.

3. Results and discussion

3.1. Nitrate addition promote microbial respiration in deep soil by acting as an alternative electron acceptor to O_2

The results of Experiment 1 showed that there was little difference in the cumulative CO_2 emissions from deep soil between the nitrate addition treatment and the control treatment during the initial 10 days of incubation (**Figure 1**). With increasing incubation time, the cumulative CO_2 emissions differed significantly between the two

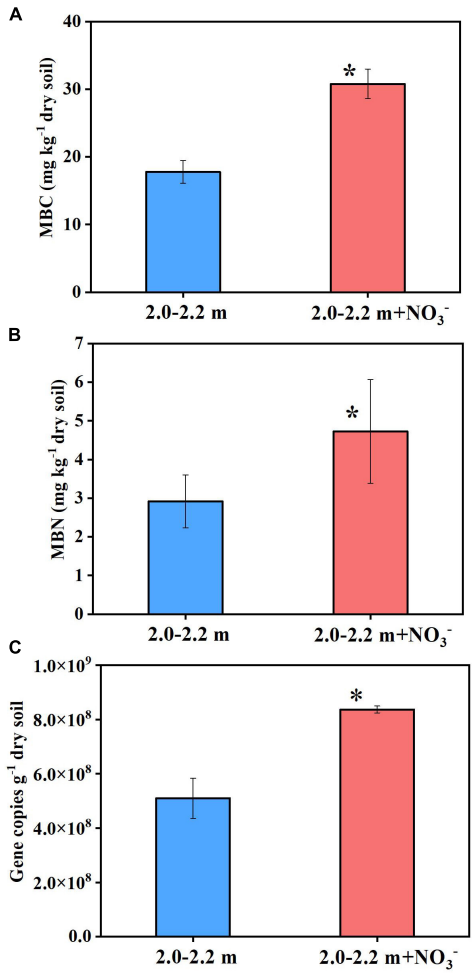

FIGURE 4
Nitrate addition effects on the MBC **(A)**, MBN **(B)**, and 16S DNA gene copies **(C)** in deep soil after 98 days at the end of Experiment 5. Data are shown as the mean ± standard deviation (n = 3). Asterisk denotes significant difference ($P < 0.05$) between the two treatments.

treatments (**Figure 1**). At the end of Experiment 1 (55 days of incubation), the cumulative CO_2 emissions under the nitrate addition treatment had increased 40–140% relative to the control treatment, with the increase dependent on soil water moisture content and soil depth (**Supplementary Figure 1**). The 200% water content significantly contributed to ΔCO_2 at three depths compared to the 35 and 70% water contents, soil moisture affects the various life activities of soil microorganisms, under low soil moisture conditions microbial activity may be limited, while increased moisture could significantly enhance microbial activity, leading to an improvement in soil respiration. Compared to depths 1.5–1.7, 2.0–2.2, and 2.5–2.7 m depth had higher ΔCO_2 at 35, 70, and 200% water content, reaching 60, 120, and 150%, respectively, indicating a higher sensitivity for the deeper soils. These results demonstrate that nitrate addition stimulated the microbial respiration in the deep soil depths under anaerobic conditions. Results of Experiment 2, where the increase in CO_2 emission was significantly correlated ($P < 0.01$) with the nitrate addition rate (**Figure 2**), also support this.

There was a lag in the CO_2 emission response to nitrate addition during the incubation (**Figure 1**). This lag was probably caused by the residual O_2 in the soil pores which removed the need for nitrate to be used as an alternative electron acceptor (Parkin and Tiedje, 1984; Song et al., 2019). This was tested by monitoring the responses of soil respiration to varying O_2 concentration. The results showed that the promoting effects of nitrate addition on soil respiration appeared when the headspace O_2 concentration was below 100 μmol L^{-1}, then disappeared after the injection of additional O_2, and finally re-appeared after the O_2 concentration was again below 100 μmol L^{-1} (**Figure 2**). By calculation, we found that the role of nitrate was activated when the stoichiometric mole ratio of nitrate to O_2 exceeded 6:1 (77.4 μmol/12.7 μmol). Further evidence supporting the effect of nitrate in promoting soil respiration was the mole ratio of the CO_2 to N_2O produced under the nitrate addition treatment, which was 2.57:1 and close to the theoretical mole ratio 2:1 (Mørkved et al., 2006) when nitrate is used as an electron acceptor for microbial respiration (**Figure 2**).

Apart from acting as an alternative electron acceptor for microbial respiration, nitrate is a key N source for soil microbes (Geisseler et al., 2010; Wang et al., 2015). Previous studies have shown that N addition can promote surface soil respiration by serving as a nutrient (Soong et al., 2018). In order to test whether the positive effects of nitrate on soil respiration were caused as the result of enhanced N supply, equal amounts of nitrate-N or ammonium-N were added into the 2.0–2.2 m depth soil in Experiment 3. The results showed that, contrary to the nitrate-N treatment, the ammonium-N treatment did not significantly increase soil respiration (**Figure 2**). These results indicated that deep soil respiration could not be facilitated by merely changing the soil N status without acting as an electron acceptor. Briefly, above results suggested that the positive effects of nitrate on deep soil respiration were the result of it acting as an electron acceptor.

3.2. The enhancement of microbial respiration by nitrate promotes microbial growth and consequently destabilize MAOC in deep soil

The increase in microbial access to an electron acceptor for respiration following nitrate addition tends to promote microbial assimilation and reproduction (Dyckmans et al., 2006). As **Figure 3** shows, the soil ammonium concentration did not change significantly ($P > 0.05$) between the beginning and end of the incubations, which indicated that dissimilatory nitrate reduction to ammonium (DNRA) was negligible. In addition, study showed that DNRA may be a minimal pathway at high nitrate concentrations (Handler et al., 2022), it is generally believed that low nitrogen and high carbon will tilt the balance to DNRA (Van Den Berg et al., 2016; Pandey et al., 2020; Wei et al., 2022), the opposite is the high nitrogen and lower carbon contents in this study. Denitrification was the main nitrate reduction pathway, the amount of nitrate consumed (65 μmol N) was significantly larger than the cumulative amount of the N_2O plus N_2 (31 μmol N) produced by day 98 (Experiment 2). This indicates that about ~50% of the added nitrate could have been assimilated by microbes for cell proliferation. In deep soils, microorganisms are expected to be in short supply of both C and N, because the microbial available C and N species, such as glucose, nitrate and ammonia, generally decrease sharply from the surface soil to deep soil. Consequently, the nitrate addition is expected to relief the microbial N starvation

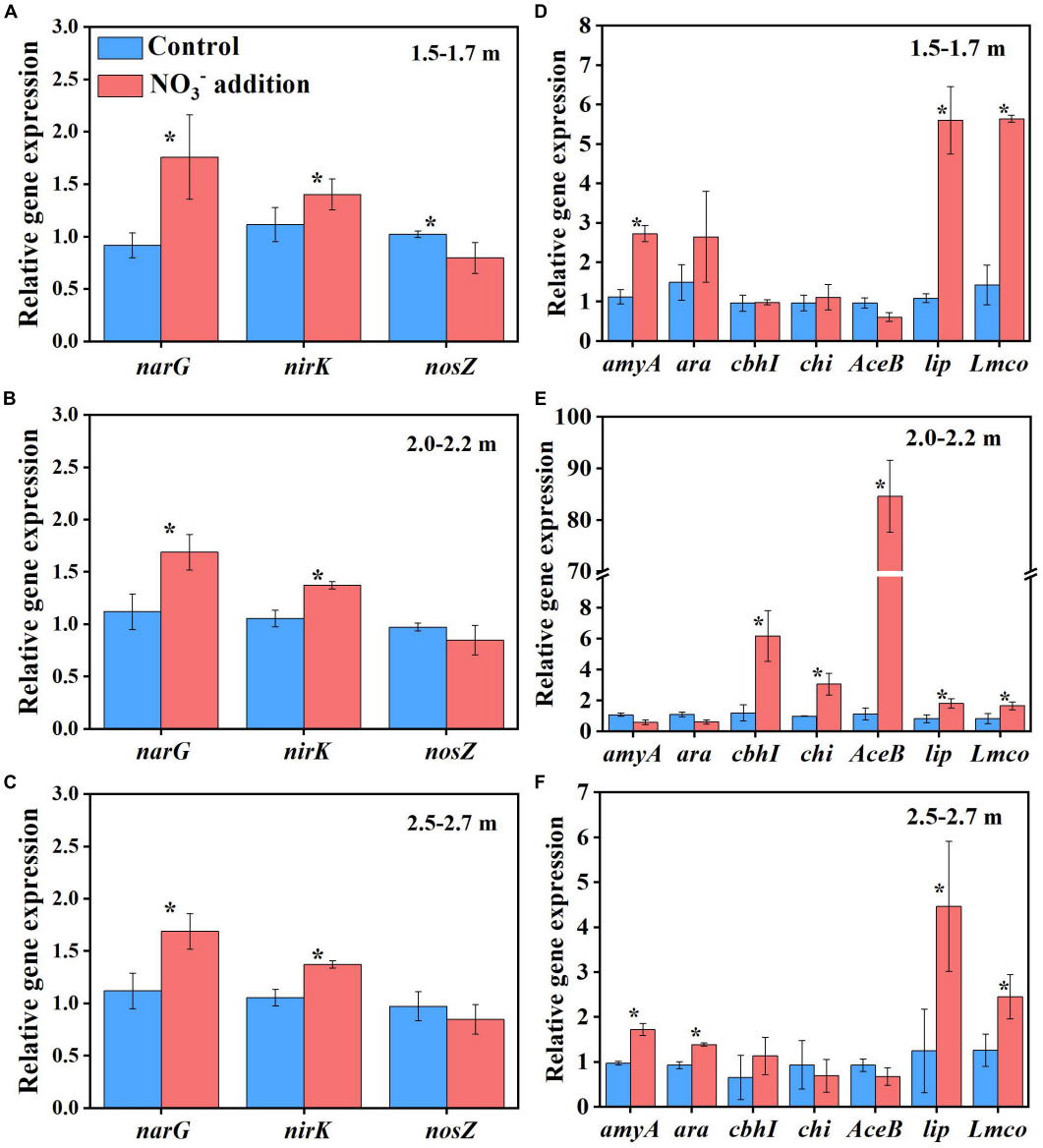

FIGURE 5
Nitrate addition effects on the relative gene abundances of denitrification genes (*narG*, *nirK*, and *nosZ*) and key and recognized C degradation genes (*amyA*, *arA*, *cbhI*, *chi*, *AceB*, *lip*, and *Lmco*) in deep soil depths of 1.5–1.7 m **(A,D)**, 2.0–2.2 m **(B,E)**, and 2.5–2.7 m **(C,F)** after 55 days at the end of Experiment 1. Data are shown as the mean ± standard deviations (n = 3). Asterisk denotes significant difference ($P < 0.05$) between the two treatments.

in deep soil and in turn promote the microbial growth there. In support of this were the measured increases ($P < 0.05$) in microbial DNA concentration (**Supplementary Figure 2**), MBC and MBN, and 16S DNA gene copy numbers (**Figure 4**) under nitrate addition relative to the control treatment at the end of Experiment 1 and 5. Thus, nitrate addition promoted microbial growth.

Apart from increasing microbial biomass, the nitrate addition treatment in Experiment 1 also significantly changed the soil microbial community composition (**Supplementary Figure 2**). Compared with the control treatment, nitrate addition significantly increased the relative abundances of *Bacillus*, *Aquabacterium*, *Sediminibacterium*, and *Acidibacter* at the genus level across all depths, and *Caproiciproducens* at 1.5–1.7 and 2.0–2.2 m (**Supplementary Figure 3**). It has been suggested that *Bacillus* and *Aquabacterium* contribute to denitrification in terrestrial and possibly other ecosystems (Verbaendert et al., 2011; Zhang et al., 2016). In addition, *Bacillus* and *Aquabacterium* were previously reported to play a key role in accelerating SOC decomposition (Lin et al., 2019; Yin et al., 2019). *Caproiciproducens* genus could accelerate the use of carbon sources for conversion to CO_2 (Kim et al., 2015). In this study, the amounts of CO_2 and N_2O emitted were correlated with the relative abundances of *Bacillus*, *Aquabacterium* and *Sediminibacterium* (**Supplementary Figure 4**), indicating that these microbes could have contributed to the positive effects of nitrate addition on deep soil respiration. In addition, the expressions of functional genes of *narG* and *nirK* under the nitrate addition treatment was significantly ($P < 0.05$) higher than control treatment, while the *nosZ* gene was not significantly different between the two treatments ($P > 0.05$) at 2.0–2.2 and 2.5–2.7 m depths except for a decrease for the nitrate addition treatment at 1.5 m depth (**Figure 5**).

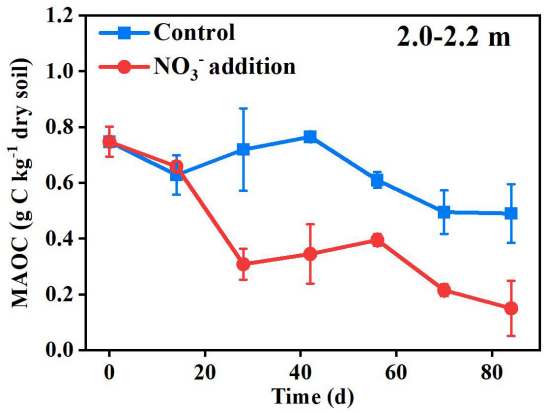

FIGURE 6
Nitrate addition effects on the content of MAOC in the 2.0–2.2 m depth over time in Experiment 5. Data are shown as the mean ± standard deviations (n = 3).

The SOC in deep soils is generally bound to soil minerals, which protect SOC from microbial attack (Han et al., 2016; Gartzia-Bengoetxea et al., 2020). Previously, it was reported that the fluctuation of pH and Eh may also cause solubilization of MAOC, with the solubilization rapidly activated when the Eh decreased below 150 mV (Grybos et al., 2009). In this study, the pH and Eh were not significantly different ($P > 0.05$) between the control treatment (5.09 ± 0.07 and 156.67 ± 4.04 mV) and the nitrate addition treatment (5.15 ± 0.06 and 153.00 ± 4.36 mV) at the end of incubation (**Supplementary Figure 5**), indicating that the pH and Eh were not responsible for the difference in MAOC between the two treatments. On the contrary, the expressions of functional genes typically responsible for carbon decomposition, such as *amyA* at 1.5–1.7 and 2.5–2.7 m, *AceB* at 2.0–2.2 m and *lip* and *Lmco* at all three depths were significantly greater ($P < 0.05$) under the nitrate addition treatment than under the control treatment at the end of Experiment 1 (**Figure 5**). The increases in carbon decomposer abundance, as noted above, and their functional gene expression were previously reported to increase the microbial utilization of MAOC (Li H. et al., 2021). Our results show that the content of the MAOC under the nitrate addition treatment was significantly lower than that under the control treatment from as early as day 28 of the incubation, and the ratio of MAOC/SOC decreased from 20% before incubation to 4% at the end of incubation (**Figure 6**), which is in accordance with previous studies reporting that N addition not only modified the composition and abundance of bacteria, but also decreased the MAOC complexes (Qin et al., 2020; Li J. et al., 2021). These results indicate that the increase in microbial utilization of MAOC, under the nitrate addition treatment, destabilizes the MAOC.

4. Conclusion

This study demonstrated that nitrate acted as an alternative electron acceptor to O_2 for microbial respiration and consequently promoted the growth of SOC decomposers in deep soil (depths > 1 m). The increases in SOC decomposer abundances and functional genes known to align with SOC decomposition in turn increased the microbial utilization of the MAOC, resulting in the acceleration of SOC decomposition in deep soil. Our results have implications for understanding the contribution of deep SOC to atmospheric CO_2 in response to anthropogenic reactive N enrichment of the environment. According to the results of this study, increased nitrate leaching under anaerobic conditions will enhance the decomposition of MAOC in deep soil. Since the promoting effects of nitrate on soil respiration is derived from its role as alternative respiration acceptor to O_2, the potential of nitrate to destabilize MAOC is expected to be favored in deep soils with clay texture and higher water content. Consequently, reducing nitrate leaching will assist in preserving MAOC in deep soil.

Data availability statement

The data presented in this study are deposited in the NCBI repository, accession number: PRJNA911917.

Author contributions

WS: methodology, visualization, formal analysis, and writing – original draft. CH, YL, TC, NW-M, TG, and JL: review and editing. SZ: supervision and review and editing. SQ: funding acquisition, conceptualization, and writing – review and editing. All authors read and approved the final manuscript.

Funding

This work was supported by the National Key R&D Program of China (2021YFD1500400), the National Natural Science Foundation of Hebei Province (D2022503014), and the National Natural Science Foundation of China (No. 41771331).

Conflict of interest

JL was employed by AgResearch Ltd.

The remaining authors declare that the research was conducted in the absence of any commercial or financial relationships that could be construed as a potential conflict of interest.

Publisher's note

Supplementary material

The Supplementary Material for this article can be found online at: https://www.frontiersin.org/articles/10.3389/fmicb.2023.1120466/full#supplementary-material

References

Bond-Lamberty, B., and Thomson, A. (2010). A global database of soil respiration data. *Biogeosciences* 7, 1915–1926. doi: 10.5194/bg-7-1915-2010

Bulseco, A. N., Giblin, A. E., Tucker, J., Murphy, A. E., Sanderman, J., Hiller-Bittrolff, K., et al. (2019). Nitrate addition stimulates microbial decomposition of organic matter in salt marsh sediments. *Glob. Chang. Biol.* 25, 3224–3241. doi: 10.1111/gcb.14726

Chen, Y., Liu, X., Hou, Y., Zhou, S., and Zhu, B. (2021). Particulate organic carbon is more vulnerable to nitrogen addition than mineral-associated organic carbon in soil of an alpine meadow. *Plant Soil* 458, 93–103. doi: 10.1007/s11104-019-04279-4

Condron, L. M., Hopkins, D. W., Gregorich, E. G., Black, A., and Wakelin, S. A. (2014). Long-term irrigation effects on soil organic matter under temperate grazed pasture. *Eur. J. Soil Sci.* 65, 741–750. doi: 10.1111/ejss.12164

Dorich, R., and Nelson, D. (1983). Direct colorimetric measurement of ammonium in potassium chloride extracts of soils. *Soil Sci. Soc. Am. J.* 47, 833–836. doi: 10.2136/sssaj1983.03615995004700040042x

Dyckmans, J., Flessa, H., Lipski, A., Potthoff, M., and Beese, F. (2006). Microbial biomass and activity under oxic and anoxic conditions as affected by nitrate additions. *J. Plant Nutr. Soil Sci.* 169, 108–115. doi: 10.1002/jpln.200521735

Feng, X., Qin, S., Zhang, D., Chen, P., Hu, J., Wang, G., et al. (2022). Nitrogen input enhances microbial carbon use efficiency by altering plant-microbe-mineral interactions. *Glob. Chang. Biol.* 28, 4845–4860. doi: 10.1111/gcb.16229

Fontaine, S., Barot, S., Barre, P., Bdioui, N., Mary, B., and Rumpel, C. (2007). Stability of organic carbon in deep soil layers controlled by fresh carbon supply. *Nature* 450, 277–280. doi: 10.1038/nature06275

Fowler, D., Steadman, C. E., Stevenson, D., Coyle, M., Rees, R. M., Skiba, U. M., et al. (2015). Effects of global change during the 21st century on the nitrogen cycle. *Atmos. Chem. Phys.* 15, 13849–13893. doi: 10.5194/acp-15-13849-2015

Friedlingstein, P., O'sullivan, M., Jones, M. W., Andrew, R. M., Hauck, J., Olsen, A., et al. (2020). Global carbon budget 2020. *Earth Syst. Sci. Data* 12, 3269–3340. doi: 10.5194/essd-12-3269-2020

Galloway, J. N., Townsend, A. R., Erisman, J. W., Bekunda, M., Cai, Z., Freney, J. R., et al. (2008). Transformation of the nitrogen cycle: Recent trends, questions, and potential solutions. *Science* 320, 889–892. doi: 10.1126/science.1136674

Gao, J., Wang, S., Li, Z., Wang, L., Chen, Z., and Zhou, J. (2021). High nitrate accumulation in the vadose zone after land-use change from croplands to orchards. *Environ. Sci. Technol.* 55, 5782–5790. doi: 10.1021/acs.est.0c06730

Gartzia-Bengoetxea, N., Virto, I., Arias-Gonzalez, A., Enrique, A., Fernandez-Ugalde, O., and Barre, P. (2020). Mineral control of organic carbon storage in acid temperate forest soils in the Basque Country. *Geoderma* 358:113998. doi: 10.1016/j.geoderma.2019.113998

Geisseler, D., Horwath, W. R., Joergensen, R. G., and Ludwig, B. (2010). Pathways of nitrogen utilization by soil microorganisms–a review. *Soil Biol. Biochem.* 42, 2058–2067. doi: 10.1016/j.soilbio.2010.08.021

Giblin, A. E., Tobias, C. R., Song, B., Weston, N., Banta, G. T., and Rivera-Monroy, V. H. (2013). The importance of dissimilatory nitrate reduction to ammonium (DNRA) in the nitrogen cycle of coastal ecosystems. *Oceanography* 26, 124–131. doi: 10.5670/oceanog.2013.54

Grybos, M., Davranche, M., Gruau, G., Petitjean, P., and Pedrot, M. (2009). Increasing pH drives organic matter solubilization from wetland soils under reducing conditions. *Geoderma* 154, 13–19. doi: 10.1016/j.geoderma.2009.09.001

Han, L., Sun, K., Jin, J., and Xing, B. (2016). Some concepts of soil organic carbon characteristics and mineral interaction from a review of literature. *Soil Biol. Biochem.* 94, 107–121. doi: 10.1016/j.soilbio.2015.11.023

Handler, A. M., Suchy, A. K., and Grimm, N. B. (2022). Denitrification and DNRA in urban accidental wetlands in phoenix, Arizona. *J. Geophys. Res. Biogeosci.* 127:e2021JG006552. doi: 10.1029/2021JG006552

Högberg, P. (2007). Nitrogen impacts on forest carbon. *Nature* 447, 781–782. doi: 10.1038/447781a

Huang, W., and Hall, S. J. (2017). Elevated moisture stimulates carbon loss from mineral soils by releasing protected organic matter. *Nat. Commun.* 8:1774. doi: 10.1038/s41467-017-01998-z

Jilling, A., Keiluweit, M., Gutknecht, J. L. M., and Grandy, A. S. (2021). Priming mechanisms providing plants and microbes access to mineral-associated organic matter. *Soil Biol. Biochem.* 158:108265. doi: 10.1016/j.soilbio.2021.108265

Kautz, T. (2015). Research on subsoil biopores and their functions in organically managed soils: A review. *Renew. Agr. Food Syst.* 30, 318–327.

Kim, B. C., Jeon, B. S., Kim, S., Kim, H., Um, Y., and Sang, B. I. (2015). *Caproiciproducens galactitolivorans* gen. nov., sp. nov., a bacterium capable of producing caproic acid from galactitol, isolated from a wastewater treatment plant. *Int. J. Syst. Evol. Microbiol.* 65, 4902–4908. doi: 10.1099/ijsem.0.000665

Lal, R. (2004). Soil carbon sequestration impacts on global climate change and food security. *Science* 304, 1623–1627. doi: 10.1126/science.1097396

Lalonde, K., Mucci, A., Ouellet, A., and Gelinas, Y. (2012). Preservation of organic matter in sediments promoted by iron. *Nature* 483, 198–200. doi: 10.1038/nature10855

Laursen, A. E., and Seitzinger, S. P. (2002). The role of denitrification in nitrogen removal and carbon mineralization in Mid-Atlantic Bight sediments. *Cont. Shelf Res.* 22, 1397–1416.

Li, H., BöLscher, T., Winnick, M., Tfaily, M. M., Cardon, Z. G., and Keiluweit, M. (2021). Simple plant and microbial exudates destabilize mineral-associated organic matter via multiple pathways. *Environ. Sci. Technol.* 55, 3389–3398. doi: 10.1021/acs.est.0c04592

Li, J., Cheng, B., Zhang, R., Li, W., Shi, X., Han, Y., et al. (2021). Nitrogen and phosphorus additions accelerate decomposition of slow carbon pool and lower total soil organic carbon pool in alpine meadows. *Land Degrad. Dev.* 32, 1761–1772. doi: 10.1002/ldr.3824

Li, Y., Song, C., Hou, C., and Wang, X. (2014). Effects of nitrogen addition on carbon mineralization in boreal peatlands soil in northeast China: A laboratory study. *Fresenius Environ. Bull.* 23, 970–975.

Lin, Y., Ye, G., Kuzyakov, Y., Liu, D., Fan, J., and Ding, W. (2019). Long-term manure application increases soil organic matter and aggregation, and alters microbial community structure and keystone taxa. *Soil Biol. Biochem.* 134, 187–196. doi: 10.1016/j.soilbio.2019.03.030

Lu, M., Zhou, X., Luo, Y., Yang, Y., Fang, C., Chen, J., et al. (2011). Minor stimulation of soil carbon storage by nitrogen addition: A meta-analysis. *Agric. Ecosyst. Environ.* 140, 234–244. doi: 10.1016/j.agee.2010.12.010

Mazzoncini, M., Sapkota, T. B., Barberi, P., Antichi, D., and Risaliti, R. (2011). Long-term effect of tillage, nitrogen fertilization and cover crops on soil organic carbon and total nitrogen content. *Soil Till. Res.* 114, 165–174. doi: 10.1016/j.still.2011.05.001

Mo, J., Zhang, W., Zhu, W., Gundersen, P., Fang, Y., Li, D., et al. (2008). Nitrogen addition reduces soil respiration in a mature tropical forest in southern China. *Glob. Chang. Biol.* 14, 403–412. doi: 10.1111/j.1365-2486.2007.01503.x

Molstad, L., Dörsch, P., and Bakken, L. R. (2007). Robotized incubation system for monitoring gases (O_2, NO, N_2O N_2) in denitrifying cultures. *J. Microbiol. Meth.* 71, 202–211. doi: 10.1016/j.mimet.2007.08.011

Mørkved, P. T., Dörsch, P., Henriksen, T. M., and Bakken, L. R. (2006). N_2O emissions and product ratios of nitrification and denitrification as affected by freezing and thawing. *Soil Biol. Biochem.* 38, 3411–3420. doi: 10.1016/j.soilbio.2006.05.015

Norman, R. J., and Stucki, J. W. (1981). The determination of nitrate and nitrite in soil extracts by ultraviolet spectrophotometry. *Soil Sci. Soc. Am. J.* 45, 347–353. doi: 10.2136/sssaj1981.03615995004500020024x

Norman, R. J., Edberg, J. C., and Stucki, J. W. (1985). Determination of nitrate in soil extracts by dual-wavelength ultraviolet spectrophotometry. *Soil Sci. Soc. Am. J.* 49, 1182–1185. doi: 10.2136/sssaj1985.03615995004900050022x

Oertel, C., Matschullat, J., Zurba, K., Zimmermann, F., and Erasmi, S. (2016). Greenhouse gas emissions from soils—A review. *Geochemistry* 76, 327–352. doi: 10.1016/j.chemer.2016.04.002

Orem, W., Gilmour, C., Axelrad, D., Krabbenhoft, D., Scheidt, D., Kalla, P., et al. (2011). Sulfur in the South Florida ecosystem: Distribution, sources, biogeochemistry, impacts, and management for restoration. *Crit. Rev. Environ. Sci. Technol.* 41, 249–288. doi: 10.1080/10643389.2010.531201

Pandey, C., Kumar, U., Kaviraj, M., Minick, K., Mishra, A., and Singh, J. (2020). DNRA: A short-circuit in biological N-cycling to conserve nitrogen in terrestrial ecosystems. *Sci. Total Environ.* 738:139710. doi: 10.1016/j.scitotenv.2020.139710

Parkin, T. B., and Tiedje, J. M. (1984). Application of a soil core method to investigate the effect of oxygen concentration on denitrification. *Soil Biol. Biochem.* 16, 331–334. doi: 10.1016/0038-0717(84)90027-0

Penuelas, J., Janssens, I. A., Ciais, P., Obersteiner, M., and Sardans, J. (2020). Anthropogenic global shifts in biospheric N and P concentrations and ratios and their impacts on biodiversity, ecosystem productivity, food security, and human health. *Glob. Chang. Biol.* 26, 1962–1985. doi: 10.1111/gcb.14981

Philben, M., Zheng, J., Bill, M., Heikoop, J., Perkins, G., Yang, Z., et al. (2019). Stimulation of anaerobic organic matter decomposition by subsurface organic N addition in tundra soils. *Soil Biol. Biochem.* 130, 195–204. doi: 10.1016/j.soilbio.2018.12.009

Pieri, L., Bittelli, M., and Pisa, P. R. (2006). Laser diffraction, transmission electron microscopy and image analysis to evaluate a bimodal Gaussian model for particle size distribution in soils. *Geoderma* 135, 118–132. doi: 10.1016/j.geoderma.2005.11.009

Poirier, V., Roumet, C., and Munson, A. D. (2018). The root of the matter: Linking root traits and soil organic matter stabilization processes. *Soil Biol. Biochem.* 120, 246–259. doi: 10.1016/j.soilbio.2018.02.016

Qin, L., Tian, W., Yang, L., Freeman, C., and Jiang, M. (2020). Nitrogen availability influences microbial reduction of ferrihydrite-organic carbon with substantial implications for exports of iron and carbon from peatlands. *Appl. Soil Ecol.* 153:103637. doi: 10.1016/j.apsoil.2020.103637

Raich, J. W., and Potter, C. S. (1995). Global patterns of carbon-dioxide emissions from soils. *Glob. Biogeochem. Cyc.* 9, 23–36. doi: 10.1029/94gb02723

Riggs, C. E., and Hobbie, S. E. (2016). Mechanisms driving the soil organic matter decomposition response to nitrogen enrichment in grassland soils. *Soil Biol. Biochem.* 99, 54–65. doi: 10.1016/j.soilbio.2016.04.023

Riggs, C. E., Hobbie, S. E., Bach, E. M., Hofmockel, K. S., and Kazanski, C. E. (2015). Nitrogen addition changes grassland soil organic matter decomposition. *Biogeochemistry* 125, 203–219. doi: 10.1007/s10533-015-0123-2

Salomé, C., Nunan, N., Pouteau, V., Lerch, T. Z., and Chenu, C. (2010). Carbon dynamics in topsoil and in subsoil may be controlled by different regulatory mechanisms. *Glob. Chang. Biol.* 16, 416–426. doi: 10.1111/j.1365-2486.2009.01884.x

Schulte-Uebbing, L., and de Vries, W. (2018). Global-scale impacts of nitrogen deposition on tree carbon sequestration in tropical, temperate, and boreal forests: A meta-analysis. *Glob. Chang. Biol.* 24, 416–431. doi: 10.1111/gcb.13862

Sierra, J., and Renault, P. (1998). Temporal pattern of oxygen concentration in a hydromorphic soil. *Soil Sci. Soc. Am. J.* 62, 1398–1405. doi: 10.2136/sssaj1998.03615995006200050036x

Song, X., Ju, X., Topp, C. F. E., and Rees, R. M. (2019). Oxygen regulates nitrous oxide production directly in agricultural soils. *Environ. Sci. Technol.* 53, 12539–12547. doi: 10.1021/acs.est.9b03089

Soong, J. L., Maranon-Jimenez, S., Cotrufo, M. F., Boeckx, P., Bode, S., Guenet, B., et al. (2018). Soil microbial CNP and respiration responses to organic matter and nutrient additions: Evidence from a tropical soil incubation. *Soil Biol. Biochem.* 122, 141–149. doi: 10.1016/j.soilbio.2018.04.011

Stuckey, J. W., Goodwin, C., Wang, J., Kaplan, L. A., Vidal-Esquivel, P., Beebe, T. P. Jr., et al. (2018). Impacts of hydrous manganese oxide on the retention and lability of dissolved organic matter. *Geochem. Trans.* 19:6. doi: 10.1186/s12932-018-0051-x

Treseder, K. K. (2008). Nitrogen additions and microbial biomass: A meta-analysis of ecosystem studies. *Ecol. Lett.* 11, 1111–1120. doi: 10.1111/j.1461-0248.2008.01230.x

Van Den Berg, E. M., Boleij, M., Kuenen, J. G., Kleerebezem, R., and Van Loosdrecht, M. C. (2016). DNRA and denitrification coexist over a broad range of acetate/N-NO_3^- ratios, in a chemostat enrichment culture. *Front. Microbiol.* 7:1842. doi: 10.3389/fmicb.2016.01842

Van Meter, K. J., Basu, N. B., Veenstra, J. J., and Burras, C. L. (2016). The nitrogen legacy: Emerging evidence of nitrogen accumulation in anthropogenic landscapes. *Environ. Res. Lett.* 11:035014. doi: 10.1088/1748-9326/11/3/035014

Vance, E. D., Brookes, P. C., and Jenkinson, D. S. (1987). An extraction method for measuring soil microbial biomass-C. *Soil Biol. Biochem.* 19, 703–707. doi: 10.1016/0038-0717(87)90052-6

Verbaendert, I., Boon, N., De Vos, P., and Heylen, K. (2011). Denitrification is a common feature among members of the genus *Bacillus*. *Syst. Appl. Microbiol.* 34, 385–391. doi: 10.1016/j.syapm.2011.02.003

Walker, A. P., De Kauwe, M. G., Bastos, A., Belmecheri, S., Georgiou, K., Keeling, R. F., et al. (2021). Integrating the evidence for a terrestrial carbon sink caused by increasing atmospheric CO_2. *New Phytol.* 229, 2413–2445. doi: 10.1111/nph.16866

Wang, B., Li, H., Li, Z., Jian, L., Gao, Y., Qu, Y., et al. (2019). Maternal folic acid supplementation modulates the growth performance, muscle development and immunity of Hu sheep offspring of different litter size. *J. Nutr. Biochem.* 70, 194–201. doi: 10.1016/j.jnutbio.2019.05.011

Wang, M., Li, X., Wang, S., Wang, G., and Zhang, J. (2018). Patterns and controls of temperature sensitivity of soil respiration in a meadow steppe of the Songnen Plain, Northeast China. *PLoS One* 13:0204053. doi: 10.1371/journal.pone.0204053

Wang, Y., Cheng, S., Fang, H., Yu, G., Xu, X., Xu, M., et al. (2015). Contrasting effects of ammonium and nitrate inputs on soil CO_2 emission in a subtropical coniferous plantation of southern China. *Biol. Fert. Soils* 51, 815–825. doi: 10.1007/s00374-015-1028-x

Wei, Z., Senbayram, M., Zhao, X., Li, C., Jin, K., Wu, M., et al. (2022). Biochar amendment alters the partitioning of nitrate reduction by significantly enhancing DNRA in a paddy field. *Biochar* 4, 1–18. doi: 10.1007/s42773-022-00166-x

Wu, D., Su, Y., Xi, H., Chen, X., and Xie, B. (2019). Urban and agriculturally influenced water contribute differently to the spread of antibiotic resistance genes in a mega-city river network. *Water Res.* 158, 11–21. doi: 10.1016/j.watres.2019.03.010

Xin, J., Liu, Y., Chen, F., Duan, Y., Wei, G., Zheng, X., et al. (2019). The missing nitrogen pieces: A critical review on the distribution, transformation, and budget of nitrogen in the vadose zone-groundwater system. *Water Res.* 165:114977. doi: 10.1016/j.watres.2019.114977

Xu, C., Xu, X., Ju, C., Chen, H., Wilsey, B. J., Luo, Y., et al. (2021). Long-term, amplified responses of soil organic carbon to nitrogen addition worldwide. *Glob. Chang. Biol.* 27, 1170–1180. doi: 10.1111/gcb.15489

Xu, M., and Shang, H. (2016). Contribution of soil respiration to the global carbon equation. *J. Plant Physiol.* 203, 16–28. doi: 10.1016/j.jplph.2016.08.007

Yang, S., Wu, H., Dong, Y., Zhao, X., Song, X., Yang, J., et al. (2020). Deep nitrate accumulation in a highly weathered subtropical critical zone depends on the regolith structure and planting year. *Environ. Sci. Technol.* 54, 13739–13747. doi: 10.1021/acs.est.0c04204

Yin, Y., Gu, J., Wang, X., Zhang, Y., Zheng, W., Chen, R., et al. (2019). Effects of rhamnolipid and Tween-80 on cellulase activities and metabolic functions of the bacterial community during chicken manure composting. *Bioresour. Technol.* 288:121507. doi: 10.1016/j.biortech.2019.121507

Yuan, H., Zhang, Z., Li, M., Clough, T., Wrage-Monnig, N., Qin, S., et al. (2019). Biochar's role as an electron shuttle for mediating soil N_2O emissions. *Soil Biol. Biochem.* 133, 94–96. doi: 10.1016/j.soilbio.2019.03.002

Zhang, X., Li, A., Szewzyk, U., and Ma, F. (2016). Improvement of biological nitrogen removal with nitrate-dependent Fe(II) oxidation bacterium *Aquabacterium parvum* B6 in an up-flow bioreactor for wastewater treatment. *Bioresour. Technol.* 219, 624–631. doi: 10.1016/j.biortech.2016.08.041

Zhang, Y., Xie, Y., Ma, H., Jing, L., Matthew, C., and Li, J. (2020). Rebuilding soil organic C stocks in degraded grassland by grazing exclusion: A linked decline in soil inorganic C. *PeerJ* 8:e8986. doi: 10.7717/peerj.8986

frontiers | Frontiers in Microbiology

TYPE Original Research
PUBLISHED 16 February 2023
DOI 10.3389/fmicb.2023.1105723

OPEN ACCESS

EDITED BY
Zengming Chen,
Institute of Soil Science (CAS), China

REVIEWED BY
Yangquanwei Zhong,
Northwestern Polytechnical University, China
Kerou Zhang,
Chinese Academy of Forestry, China
Zihan Jiang,
Chinese Academy of Sciences, China

*CORRESPONDENCE
Kefeng Wang
✉ wangkf@nwu.edu.cn

SPECIALTY SECTION
This article was submitted to Terrestrial Microbiology, a section of the journal Frontiers in Microbiology

RECEIVED 23 November 2022
ACCEPTED 30 January 2023
PUBLISHED 16 February 2023

CITATION
Qu R, Liu G, Yue M, Wang G, Peng C, Wang K and Gao X (2023) Soil temperature, microbial biomass and enzyme activity are the critical factors affecting soil respiration in different soil layers in Ziwuling Mountains, China.
Front. Microbiol. 14:1105723.
doi: 10.3389/fmicb.2023.1105723

Soil temperature, microbial biomass and enzyme activity are the critical factors affecting soil respiration in different soil layers in Ziwuling Mountains, China

Ruosong Qu[1,2], Guanzhen Liu[1,2], Ming Yue[1,2], Gangsheng Wang[3], Changhui Peng[4], Kefeng Wang[1,2]* and Xiaoping Gao[5]

[1]Key Laboratory of Resource Biology and Biotechnology in Western China, Ministry of Education, Northwest University, Xi'an, China, [2]College of Life Science, Northwest University, Xi'an, China, [3]State Key Laboratory of Water Resources and Hydropower Engineering Sciences, Institute for Water-Carbon Cycles and Carbon Neutrality, Wuhan University, Wuhan, China, [4]Department of Biology Sciences, Institute of Environment Sciences, University of Quebec at Montreal, Montreal, QC, Canada, [5]Shuanglong State-Owned Ecological Experimental Forest Farm of Qiaoshan State-Owned Forestry Administration of Yan'an City, Yan'an, Shaanxi, China

Soil microorganisms are critical biological indicators for evaluating soil health and play a vital role in carbon (C)-climate feedback. In recent years, the accuracy of models in terms of predicting soil C pools has been improved by considering the involvement of microbes in the decomposition process in ecosystem models, but the parameter values of these models have been assumed by researchers without combining observed data with the models and without calibrating the microbial decomposition models. Here, we conducted an observational experiment from April 2021 to July 2022 in the Ziwuling Mountains, Loess Plateau, China, to explore the main influencing factors of soil respiration (R_S) and determine which parameters can be incorporated into microbial decomposition models. The results showed that the R_S rate is significantly correlated with soil temperature (T_S) and moisture (M_S), indicating that T_S increases soil C loss. We attributed the non-significant correlation between R_S and soil microbial biomass carbon (MBC) to variations in microbial use efficiency, which mitigated ecosystem C loss by reducing the ability of microorganisms to decompose organic resources at high temperatures. The structural equation modeling (SEM) results demonstrated that T_S, microbial biomass, and enzyme activity are crucial factors affecting soil microbial activity. Our study revealed the relations between T_S, microbial biomass, enzyme activity, and R_S, which had important scientific implications for constructing microbial decomposition models that predict soil microbial activity under climate change in the future. To better understand the relationship between soil dynamics and C emissions, it will be necessary to incorporate climate data as well as R_S and microbial parameters into microbial decomposition models, which will be important for soil conservation and reducing soil C loss in the Loess Plateau.

KEYWORDS

climate change, carbon cycle, soil microbial activity, microbial decomposition model, soil respiration (CO_2)

1. Introduction

The Intergovernmental Panel on Climate Change (IPCC) assessment reports that global average temperatures will rise by 2.1–3.5°C, and the frequency and intensity of extreme heatwaves and precipitation events are also likely to increase (Tollefson, 2021). This climate change is expected to put general stress on ecosystems. The soil ecosystem is an important part of the terrestrial ecosystem and the hub of material and energy flow in the biosphere (Piao et al., 2010b). Carbon (C) is the basic element of life forms, without which life cannot exist, so the C cycle is one of the most important biogeochemical cycles (Bot and Bernites, 2005), and terrestrial soil C cycle research is an important component of global change research. Soil microbes are largely involved in the soil C cycle and play a crucial role in climate feedback (Jansson and Hofmockel, 2020), including CO_2, N_2O, and other greenhouse gas emissions. As the most active component of soil, microorganisms are significant biological indicators for evaluating soil health (Fierer et al., 2021). In recent years, it has been proposed that soil microbial characteristics can be used as biological indicators of soil health to guide soil ecosystem management (Schloter et al., 2003; Cardoso et al., 2013). Sicardi et al. (2004) believe that soil microbial characteristics, such as soil respiration (R_S), microbial biomass, and enzyme activity, vary significantly from season to season, suggesting that they are sensitive and reliable indicators of changes in soil physicochemical properties.

R_S refers to the process by which soil releases CO_2 into the atmosphere and the most important component of R_S is the heterotrophic respiration of soil microorganisms (Wang et al., 2019). C is stored in the soil as organic matter, its storage is approximately twice that of the atmospheric C pool and it plays a significant role in the C cycle of the terrestrial ecosystem (Mahajan et al., 2021). Therefore, R_S can significantly affect the global C cycle in terrestrial ecosystems (Zhou et al., 2009). The world is now experiencing a period of rapid warming due to the effects of human activities and CO_2 emissions, and R_S, which releases more than 10 times more CO_2 into the atmosphere than the combustion of fossil fuel (Marland, 1983), is the second-largest source of continental C fluxes (Hu et al., 2019). Due to the enormous storage capacity of soil organic carbon (SOC), even a small change in soil C storage and R_S will significantly affect the CO_2 concentration in the atmosphere, thereby affecting the feedback effect of terrestrial ecosystems on climate change (Davidson et al., 2006).

In ecosystems, microorganisms play a crucial role in soil metabolism as decomposers that drive nutrient turnover in soil ecosystems by mineralizing organic matter (Wieder et al., 2015). Soil microbial biomass is the active component of soil organic matter (SOM) and the most active soil factor (Jenkinson and Ladd, 1981). Since soil microbial biomass is very sensitive to environmental factors, slight changes in soil can change it (Chander et al., 1998), so various environmental disturbances can be predicted earlier.

All soil biochemical processes proceed because soil enzymes act as the driving force. An essential soil microbial function is to decompose key nutrients in litter and accumulate organic matter through soil enzymes (Caldwell, 2005). For example, cellobiohydrolase (CBH) and β-1,4-glucosidase (βG) are required to decompose cellulose in a litter (Sinsabaugh et al., 1992), and peroxidase (PER) and polyphenol oxidase (PPO) also play important roles in lignin decomposition (Lucas et al., 2007). Green et al. demonstrated that oxidase is an important factor affecting soil microbial respiration (Green and Oleksyszyn, 2002). In addition, Sinsabaugh et al. (2008) also demonstrated that soil microbial biomass determines the organic matter decomposition process of soil enzymes. Therefore, soil enzyme activity and other soil microbial indicators can be used to identify early warnings of soil ecosystems under stress conditions and anthropogenic disturbances (Boerner R. et al., 2005).

The results of most ecosystem models show that climate change will stimulate the microbial decomposition of SOM and generate feedback on global climate change (Friedlingstein et al., 2006). The positive feedback system model for climate change over time has a poor effect in simulating the global SOC pool and has great uncertainty (Voigt et al., 2016). Therefore, the global ecosystem model needs to consider microbial effects to accurately predict the feedback relationship between climate warming and SOM decomposition (Ji et al., 2018). In recent researches, the accuracy of the models in predicting soil C pools has been improved by considering microbial involvement in the decomposition process in ecosystem models (Abs et al., 2020; Guo et al., 2020), but the parameter values of these models are assumed by researchers without integrating the observed data with the models and calibrating the microbial decomposition models. Therefore, to improve the accuracy of microbial ecosystem models, it is also necessary to calibrate microbial parameters, and R_S, microbial biomass, and enzyme activity are the most reliable observations for model calibration and validation (Hanson et al., 2000; Wang et al., 2015). In addition, dynamic data (e.g., soil temperature and moisture) can represent real-world climatic and environmental conditions, which can be beneficial for the model and understanding soil C cycling more realistically (Wang et al., 2020).

Forest soil microorganisms, which are vital part of forest ecosystems, play an important role in the decomposition of litter and soil nutrient cycling (Barberan et al., 2015). Forest R_S occupies an important proportion of terrestrial ecosystems, and its dynamic changes will have an important impact on the global C balance (Laganière et al., 2012). Forest R_S is also one of the important research objects of the long-term monitoring CO_2 flux network currently being established, which is of great significance to scientific ecology and earth system research (Schlesinger and Andrews, 2000).

The Loess Plateau is a mixture of arid, semiarid and semihumid areas but is generally considered a semiarid area (Yu et al., 2020) and has always been known for severe land degradation, low land productivity, and soil erosion (Fu et al., 2016). The Ziwuling Mountains are located in the hinterland of the Loess Plateau, which is a well-preserved natural secondary forest area that plays a critical role in improving the surrounding ecological environment and climate regulation (Kang et al., 2014). From April 2021 to July 2022, we carried out an observational experiment in the Ziwuling Mountains, Loess Plateau, China, to record the monthly diurnal changes in R_S and the monthly dynamic changes in soil microbial biomass and enzyme activity. Since soil physicochemical properties can vary significantly at different soil depths (Rahman et al., 2022), we collected topsoil (0–30 cm) and subsoil (30–100 cm) respectively in the process of collecting soil samples. We hypothesized that the topsoil and subsoil physicochemical and microbial properties would be significantly different, and soil microbial properties would also change significantly in different months or seasons. The main goals of this study were to I) explore the main influencing factors of R_S and II) determine which parameters can be incorporated into a microbial decomposition model.

2. Materials and methods

2.1. Study site

Field sampling and observation experiments were conducted from April 2021 to July 2022. The study site (Figure 1) was located in the Shuanglong Forest Farm (35°39′ ~ 35°43'N, 108°56′ ~ 108°58′E), a natural secondary forest in the Ziwuling Mountains of North China (Zhang et al., 2022). Our study site was 100 × 100 m. The climate of this site was a warm temperate semihumid climate, with a mean annual temperature of approximately 7.4°C and a mean annual precipitation of 587.6 mm (Chai et al., 2016). The main soil type was loessial soil, which was turbid brown or orange. The soil texture was loose and soft with few roots and pores, which indicated silt loam. The typical arbor species include *Betula platyphylla, Swida macrophylla, Carpinus turczaninowii Hance, Quercus aliena Bl, Quercus liaotungensis, Rhus potaninii Maxim, and cer davidii Franch*. The typical shrub species include *Acer tataricum subsp.ginnala, Viburnum dilatatum Thunb, Cotoneaster multiflorus Bge, Rhamnus leptophylla Schneid, Lonicera hispida Pall. ex Roem. et Schult*.

2.2. R_S observation experiment

Three sites with flat terrain were selected as sampling points for the measurement of the R_S rate (μ mol m^{-2} s^{-1}). We installed ACE automatic R_S monitoring systems on iron rings with the inner diameter of 20 cm and the height of 10 cm (ACE-200, Ecotech Ecological Technology Ltd) and inserted 4–5 cm into the soil at each sampling point. R_S measurement sites were chosen to be more than 50 cm away from the surrounding vegetation, with each site being more than three meters away. To reduce soil disturbance, we inserted the iron rings at least 24 h before the measurement, and the broken roots and litter on the soil surface were removed. From April 2021 to July 2022, we used automatic R_S monitoring systems to monitor the R_S rate every 30 min for all sample points every month for 24 h. The R_S monitoring systems could simultaneously measure and record the soil temperature (T_S, °C) and soil moisture (M_S, %vol) within 0–10 cm below the surface soil of the sampling site. A meteorological monitoring station (CR200Series) was established at the research site to collect air temperature and moisture data from April 2021 to July 2022.

2.3. Soil sample collection

During the study period, from April 2021 to July 2022, soil sampling was performed every 2 months. Five sampling points were set at the research site using the five-point sampling method. To avoid edge effects, the sampling points were neither close to the edge of the plot nor far from the edge of the sample plot. Each sampling site was 5 × 0.5 m plot. The sampling sites were surrounded by abundant vegetation and the soil surface had obvious humus layers. We divided each sampling point into 12 areas, assigned a random block to all the

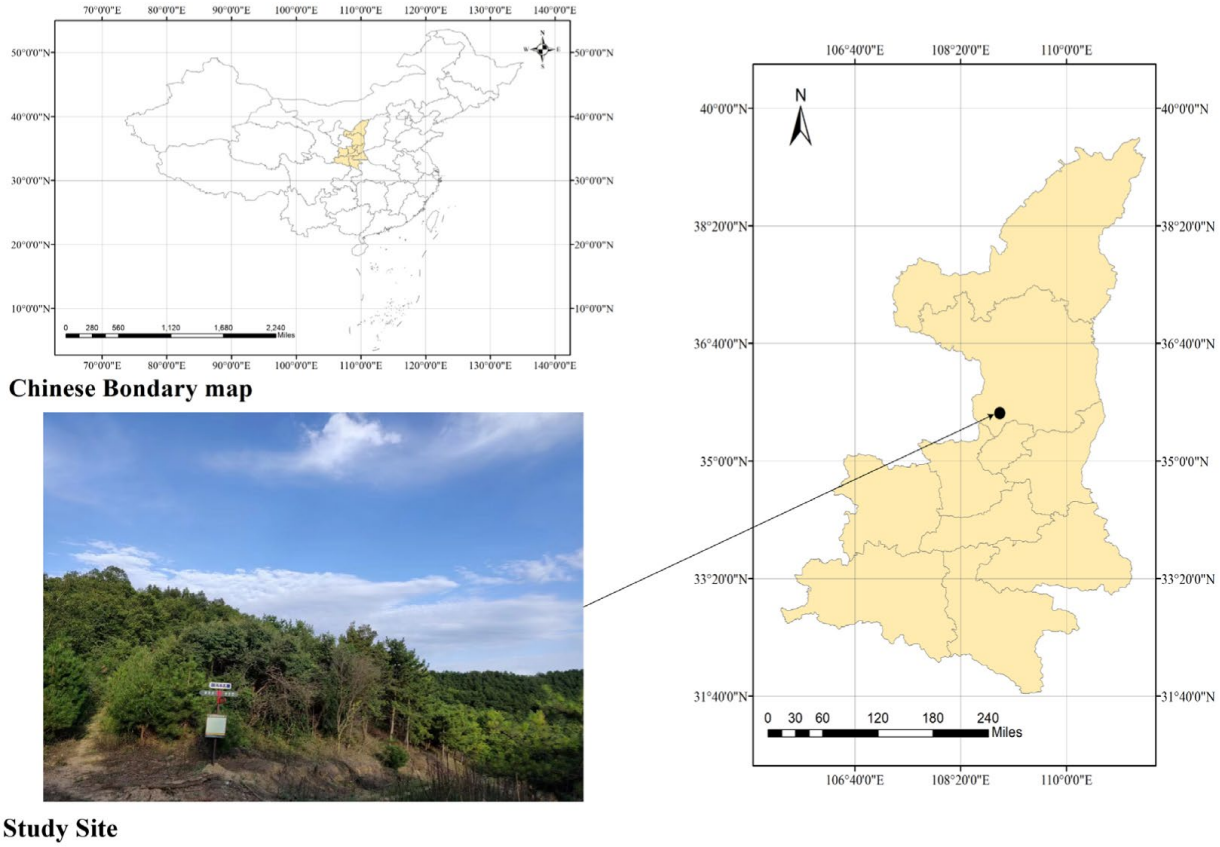

FIGURE 1
Map of study site. The Shuanglong Forest Farm is located in Shuanglong Town, Huangling County, Yan'an City, Shaanxi Province, China. It is located in the Ziwuling Mountains and is a natural secondary forest.

sampling points, and conducted sampling according to the random block order (Supplementary Figure S1). The sampling depth was divided into two types. The soil at a depth of 0–30 cm below the surface soil was used as topsoil, and the soil at a depth of 30–100 cm was used as subsoil. A total of five replicates were collected separately for topsoil and subsoil. The soil from each depth at each sampling point was mixed evenly after collection, and the broken roots and litter in the soil were removed to reduce errors in the analysis process. Sterile gloves were worn during soil collection to prevent soil contamination. The soil samples were transported in sterile sampling bags, stored in a freezer, and taken to a laboratory by car for further analysis.

2.4. Soil sample analysis

We used the Kjeldahl method (Bradstreet, 1965) to determine the total soil nitrogen (TN), and the soil was hydrolyzed under alkaline conditions in a diffusion dish (Wang, 2010) to calculate the content of alkaline hydrolyzed nitrogen (HN). We used the alkali fusion-Mo-Sb antispectrophotometric method (Chen et al., 2018) to determine the total phosphorus (TP) and sodium bicarbonate solution (Cade-Menun and Lavkulich, 1997) to determine the available phosphorus (AP). The soil-available potassium (AK) was determined by ammonium acetate flame photometry (Zanati et al., 1973).The potassium dichromate oxidation-external heating method was used to determine soil organic matter (SOM), and then the SOM was determined by titration with a standard ferrous iron solution (Zhu et al., 2020). The soil pH was measured by using a pH meter. Microbial biomass carbon (MBC), microbial biomass nitrogen (MBN), and microbial biomass phosphorus (MBP) were determined by using the chloroform fumigation extraction method (Vance and Brookes, 1987). The soil samples were leached with KCL solution and then analyzed using a continuous flow analyzer to determine NH_4^+--N and NO_3^---N (Liu et al., 2014).

We used a fluorometric method (Eivazi and Tabatabai, 1988) to measure the β-1,4-glucosidase (βG) activity in the soil and a nitrophenol colorimetric method (Wood and Bhat, 1988) to measure the cellobiohydrolase (CBH) activity. Polyphenol oxidase (PPO) was determined spectrophotometrically by using pyrogallol (1,2,3-trihydroxy benzene) as a substrate (Bach et al., 2013). Peroxidase (PER) was measured by calculating the rate of substrate oxidation after the addition of H_2O_2 (Burns et al., 2013).

2.5. Statistical analysis

The R_S mean value and error were calculated from three replicate measurements. The mean values and errors of soil physicochemical and microbial properties were calculated from five replicate measurements. Pearson correlation analysis was used to examine the correlation of R_S with T_S and M_S. Origin 2017 software was used to obtain the regression equations between R_S rate, T_S, and soil M_S, and then these regression relationships were plotted. Monthly and seasonal differences in R_S and soil physicochemical and microbial properties were tested by ANOVA. The datasets were checked for normality and homogeneity assumptions before performing ANOVA. The magnitude of this feedback largely depends on the temperature sensitivity of SOM decomposition (Q_{10}).

Q_{10} was measured by the exponential relationship between R_S and T_S and was calculated as follows:

$$R_S = \mathrm{aeb}T_S \quad (1)$$

$$Q_{10} = e^{10b} \quad (2)$$

where T_S is the soil temperature, a is the R_S rate when the soil temperature is 0°C, and b is the temperature coefficient reflecting the temperature sensitivity of R_S.

To examine how soil microbial characteristics influenced R_S, structural equation modeling (SEM) was performed with Amos software (IBM SPSS Amos 26.0.0) for different soil layers. In stepwise multiple regression (Supplementary Tables S1, S2), in order to optimize the model, we removed the non-significant variables and paths. We evaluated the goodness of fit of the model according to the low chi-square (χ^2; the model is a great fit when $0 \leq \chi^2/df \leq 2$) (Tabachnick and Fidell, 2007), the high whole-model p value (if $p > 0.05$, there is no path loss and the model was a great fit), the comparative fit index (CFI; the model is a great fit when $0.97 \leq CFI \leq 1$) (Hu and Bentler, 1999), and a root mean square error of approximation (RMSEA; the model is a great fit when $0 \leq RMSEA \leq 0.05$) (Vile et al., 2006).

3. Results

3.1. Atmospheric temperature and humidity observation values and soil physicochemical and microbial properties

The monthly variations in air temperature and air moisture are shown in Figure 2. During the observation period from April 2021 to July 2022, the average air temperature was 16.1°C, the highest temperature was 22.2°C, and the lowest temperature was 4.9°C. The average air moisture was 61.7%, the maximum moisture was 75.68%, and the minimum moisture was 46.70% (Figure 2A).

During the observation period, the T_S showed a pattern consistent with the seasonal variations in air temperature and air moisture. That is, the T_S gradually increased from April to July 2021, reaching a maximum value of 19.4°C in July 2021, and then the T_S decreased for the rest of the year. The M_S had obvious monthly variations during the observation period, reaching a maximum value in October 2021 and minimum value in June 2021 (Figure 2B). The maximum and minimum values were 92.44 and 42.20%, respectively.

The soil at the study site was alkaline, and there was no significant difference in pH between the topsoil (0–30 cm) and the subsoil (30–100 cm) (Table 1). The TP content in the subsoil was significantly higher than that in the topsoil, while the other soil physicochemical properties in the subsoil were lower than those in the topsoil, and AK and SOM were significantly reduced in the subsoil ($p < 0.01$).

3.2. Diurnal, monthly and seasonal variations in R_S

The diurnal variation in the R_S rate in different months is shown in Supplementary Figure S2. The R_S rate showed a multi-peak distribution trend, and the R_S rate reached its peak at noon every day except in April and May within the 24 h observation period of each month. Except in June and August 2021, the R_S rate showed a minimum value in the morning (approximately 5:00 to 8:00 AM), and then the R_S rate gradually increased.

10.3389/fmicb.2023.1105723

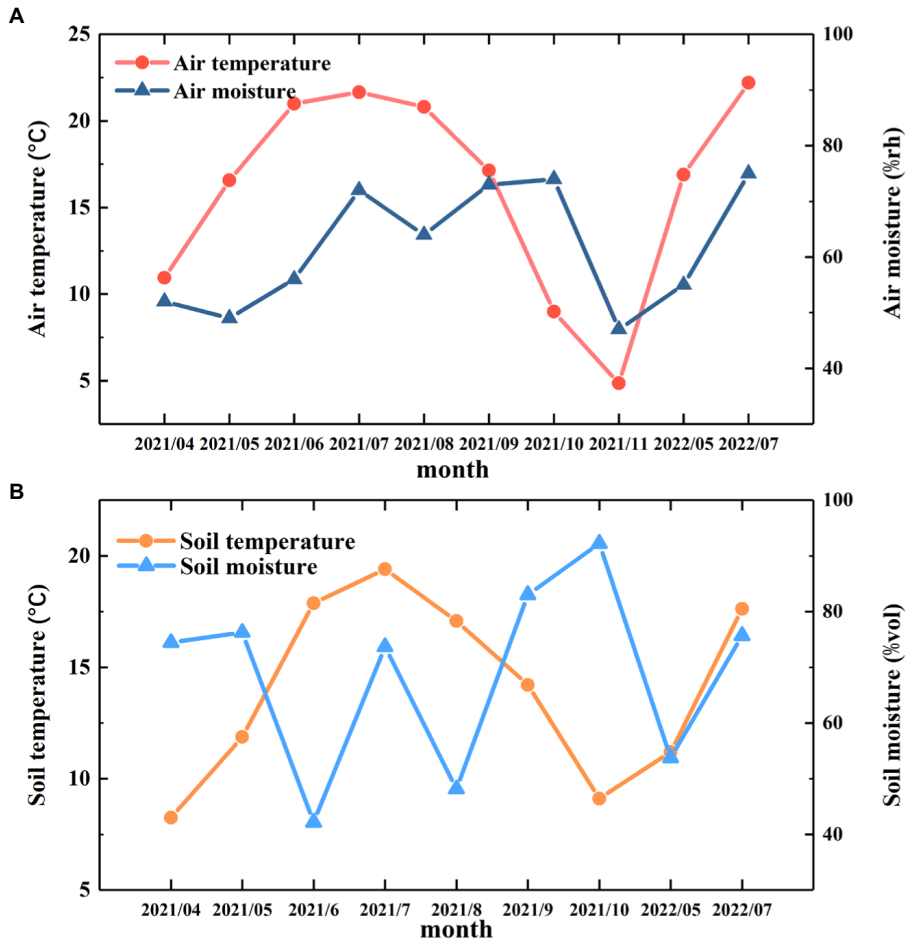

FIGURE 2
Monthly variations in temperature and moisture. **(A)** The monthly changes in air temperature and moisture from April 2021 to July 2022. **(B)** The monthly variations in soil temperature and moisture from April 2021 to July 2022.

TABLE 1 Soil physicochemical properties in the topsoil (0–30cm) and subsoil (30–100cm).

Variables	Soil layer	
	Topsoil	Subsoil
TN (g/kg)	1.91 ± 0.23	0.66 ± 0.03
TP (mg/kg)	385.06 ± 25.43**	474.61 ± 48.02**
HN (mg/kg)	194.91 ± 21.32	49.04 ± 2.73
AP (mg/kg)	6.27 ± 1.02	2.20 ± 0.49
AK (mg/kg)	208.84 ± 32.78**	107.67 ± 8.87**
SOM (g/kg)	27.77 ± 5.61**	16.99 ± 5.11**
pH	8.42 ± 0.02	8.69 ± 0.02

* denotes significant differences among different layers at $p < 0.05$. ** denotes significant differences among different layers at $p < 0.01$. TN, total nitrogen; TP, total phosphorus; HN, hydrolysable nitrogen; AP, available phosphorus; AK, available potassium; SOM, soil organic matter. The data are expressed as the mean values ± SEs.

The monthly variation in the R_S rate showed a trend of increasing and then decreasing. The R_S rate gradually increased after April, reached a maximum in July 2021, and then gradually decreased (Supplementary Figure S3).

The seasonal changes in the R_S rate are shown in Figure 3. On the seasonal scale, there were significant differences between the R_S rates in different seasons. In 2021, the average R_S rate in summer was 0.75 μmol m^{-2} s^{-1}, which was significantly higher than that in spring (0.52 μmol m^{-2} s^{-1}) and autumn (0.37 μmol m^{-2} s^{-1}) ($p < 0.05$). In 2022, the average R_S rate in summer was 0.97 μmol m^{-2} s^{-1} (Figure 3).

3.3. Relationship between T_S, M_S, and R_S

The correlation analysis results showed that there were significant correlations between T_S, M_S, and R_S ($p < 0.01$). The relationship between T_S and the linear equation fitting the diurnal-scale variation in R_S is shown in Figure 4, and the relationship between M_S and the linear equation fitting the diurnal-scale variation in R_S is shown in Supplementary Figure S4. The R_S rate increased with T_S and decreased with M_S. According to Eq. (1), Q_{10} is 2.61, which is within the normal range (Zhou et al., 2009).

3.4. Soil inorganic nitrogen, microbial biomass, and enzyme activity

In the topsoil, the NO_3^---N from August 2021 to July 2022 was significantly higher than that from April to June 2021, and the MBC from October 2021 to July 2022 was significantly higher than that from

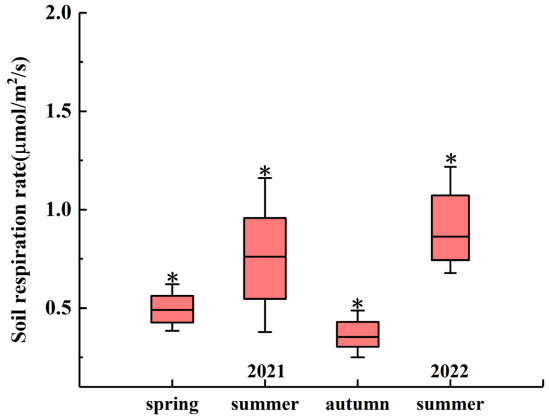

FIGURE 3
Seasonal R_S rates from April 2021 to July 2022. The asterisk (*) indicates significant differences in R_S rates between different seasons at a significance level of 0.05.

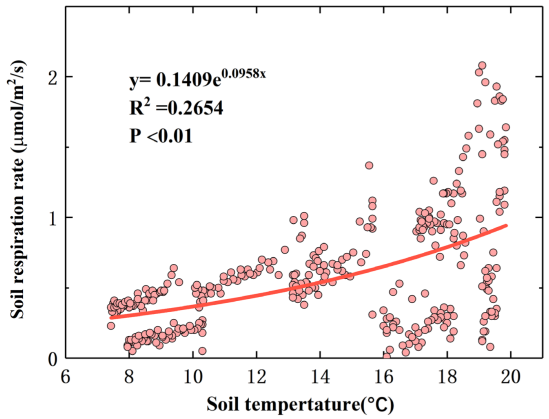

FIGURE 4
Relationship between R_S and soil temperature.

April to August 2021. NH_4^+--N reached a maximum (12.59 mg/kg) in August 2021, and there were no significant differences in NH_4^+--N between other months except in August 2021. The MBP in the topsoil in August 2021 was significantly higher than that in the other months. The MBN reached the maximum (34.95 mg/kg) in May 2022 (Figure 5A). In the subsoil, the NO_3^---N from April 2021 to June 2021 was significantly higher than that in other months, and there was no significant difference in NH_4^+--N among the 6 months. The MBC reached a maximum (113.88 mg/kg) in October 2021. The MBN from May to July 2022 was significantly higher than that from April 2021 to August 2021. There were no significant changes in MBP from April 2021 to July 2022 (Figure 5B).

The soil enzyme activity in the topsoil and subsoil varied significantly among different months ($p < 0.05$). The PER activity in the topsoil in May 2022 and July 2022 was significantly lower than that in the other months, and in the subsoil there were significant differences in the PER activity between April 2021 and July 2022. The PPO activity in both the topsoil and subsoil varied significantly among different months. Similar to that in the topsoil, in the subsoil, the βG activity in May 2022 was significantly higher than that in other months. The βG activity in the topsoil in April, June, and August 2021 was significantly different from the βG activity in the subsoil. The CBH activity in the topsoil in August 2021 was significantly lower than that in other months, and in the subsoil, the CBH activity in May 2022 was significantly higher than that from April to August 2021 but not significantly different from that in other months. In addition, from April 2021 to August 2021, the CBH and βG activities were significantly different in the topsoil and subsoil, so we believe that the CBH and βG activities in the topsoil were generally greater than those in the subsoil (Table 2).

3.5. Relationship between soil microbial biomass, enzyme activity and R_S

Based on the stepwise multiple regression results (Supplementary Tables S1, S2), we determined the variables that mostly explained the variation in R_S. Model optimization was performed continually until the model fits well. SEM demonstrated the influence of R_S in different soil layers (Figure 6). The model for topsoil showed values of $\chi^2 = 2.809$, $p = 0.422$, df = 3, RMSEA = 0, and CFI = 1 (Figure 6A); the model for whole soil showed values of $\chi^2 = 4.339$, $p = 0.362$, df = 4, RMSEA = 0, and CFI = 1 (Figure 6B).

In the topsoil, T_S, βG, MBP, and PPO all directly affected R_S, except for MBP, T_S, βG and PPO, which were significantly and positively correlated with R_S, and T_S, βG were the variables that had the strongest effects on R_S. In the whole soil, T_S, βG, MBP, MBN, and PPO all directly affected R_S, except for MBP, T_S, βG, PPO, MBN, which were significantly and positively correlated with R_S, and T_S, βG, PPO were the variables that had the strongest effects on R_S.

4. Discussion

4.1. Effects of T_S and M_S on R_S

Global warming not only increases the temperature of the atmosphere but also leads to changes in precipitation, which in turn causes greater variation in T_S and M_S (Zhang et al., 2016). In this study, the air temperature reached its highest value in summer and then gradually decreased, and the atmospheric moisture showed a multipeak trend, which experienced a decrease followed by an increase in the summer (Figure 1A). This may be related to the specific climate of the Loess Plateau. Since the Loess Plateau is an area sensitive to climate change, changes in atmospheric temperature and precipitation caused by global warming often lead to frequent droughts in many areas (Piao et al., 2010a). The climate of the Loess Plateau showed a trend of aridity in spring and summer (Hou et al., 2021) and then experienced violent precipitation in autumn, causing the air temperature to decrease after August, while air moisture began to increase significantly after August, reaching a maximum in October, and then gradually decreased again. T_S and M_S also show similar trends to air temperature and moisture (Figure 1B).

It has been demonstrated in previous studies that R_S is closely related to T_S (Wang et al., 2006). During the observation period, the monthly diurnal variation in R_S showed a multi-peak trend, and the R_S rate reached its peak value at noon and decreased to a minimum value in the morning (Supplementary Figure S2). This is consistent with the results of Wang et al. (2018). A possible explanation for this phenomenon is that the reaction process of R_S is mainly catalyzed by soil enzymes, and temperature is the main limiting factor affecting soil enzyme activity

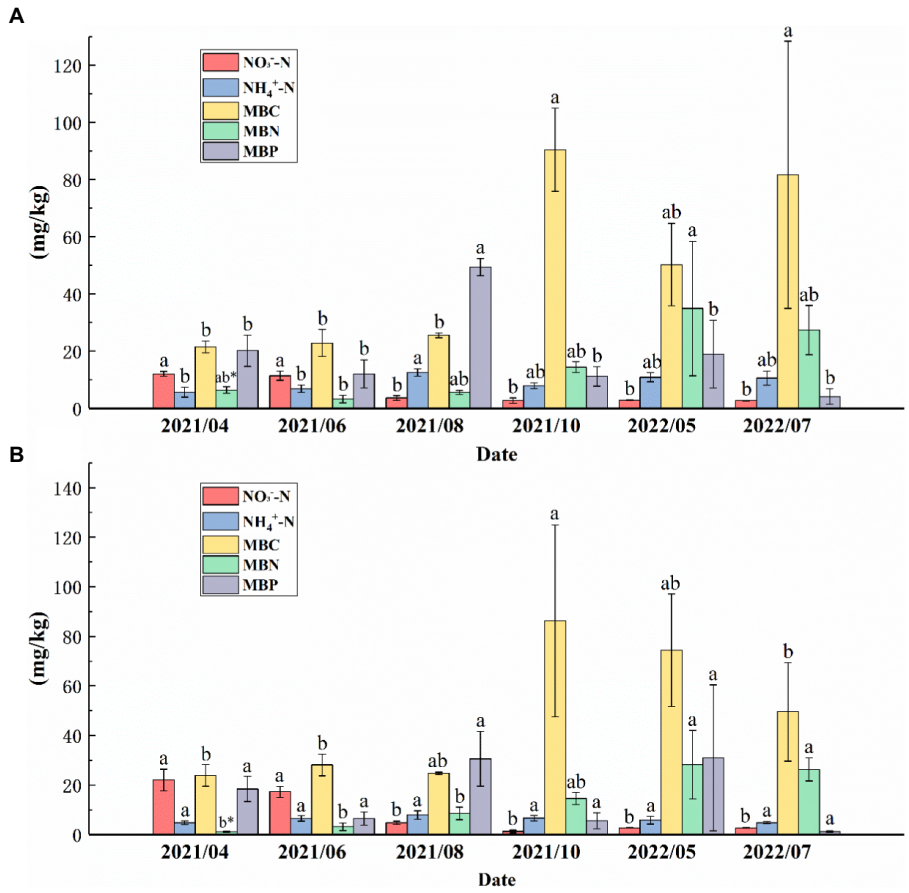

FIGURE 5
NH_4^+--N, NO_3^---N, microbial biomass carbon (MBC), microbial biomass nitrogen (MBN), and microbial biomass phosphorus (MBP) contents in the **(A)** topsoil and **(B)** subsoil from April 2021 to July 2022. Different letters indicate significant differences between months for the same variable (p <0.05). * indicates that the same variable in the same month is significantly different in different soil layers (p <0.01).

TABLE 2 Peroxidase (PER), polyphenol oxidase (PPO), β-1,4-glucosidase (βG), and cellobiohydrolase (CBH) activities in the topsoil (0–30cm) and subsoil (30–100cm) from April 2021 to July 2022.

Site	Soil depth	PER (mg H_2O_2·g^{-1})	PPO (nmol·g-1·h^{-1})	βG (nmol·g-1·h^{-1})	CBH (nmol·g-1·h^{-1})
April-21	Topsoil	4.28 ± 0.05a	3687.34 ± 163.80a	181.65 ± 25.41b**	38.01 ± 13.33a**
June-21		3.97 ± 0.13a	3340.60 ± 76.59b	122.77 ± 14.06bc**	18.96 ± 4.66ab**
August-21		3.68 ± 0.40a	20.50 ± 1.20d	2.34 ± 0.35c**	0.18 ± 0.03c**
October-21		3.41 ± 0.29ab	476.30 ± 52.40c	73.92 ± 11.07c	16.01 ± 4.00bc
May-22		2.78 ± 0.37b	479.42 ± 52.89c	291.16 ± 42.54a	26.13 ± 2.42ab
July-22		2.28 ± 0.36b	496.76 ± 48.71c	199.42 ± 43.04b	28.75 ± 2.15ab*
April-21	Subsoil	4.10 ± 0.20a	2632.48 ± 219.10b	11.69 ± 2.86d**	9.79 ± 8.52b**
June-21		4.03 ± 0.25ab	3335.98 ± 156.34a	23.08 ± 9.38 cd**	1.62 ± 1.25b**
August-21		3.69 ± 0.12ab	16.84 ± 1.08d	0.31 ± 0.03d**	0.02 ± 0.01b**
October-21		3.21 ± 0.22ab	507.90 ± 49.44c	74.68 ± 11.48c	11.11 ± 4.84ab
May-22		3.23 ± 0.48ab	485.6 ± 41.14c	248.73 ± 20.69a	22.93 ± 2.45a
July-22		3.15 ± 0.50b	480.1 ± 63.26c	202.42 ± 39.42b	21.80 ± 0.49ab*

The data are expressed as the mean values ± SEs. Different letters indicate that the same variable differs significantly from month to month (P <0.05).
* indicates that the same variable in the same month is significantly different in different soil layers (p <0.05). ** indicates that the same variable in the same month is significantly different in different soil layers (p <0.01).

(Melillo et al., 2018). When the T_S is low, the activities of some critical enzymes that control R_S decrease, resulting in a lower R_S rate. On the monthly scale, with increasing T_S, the R_S rate starts to increase in April, reaches a maximum value in July, and then gradually decreases to a

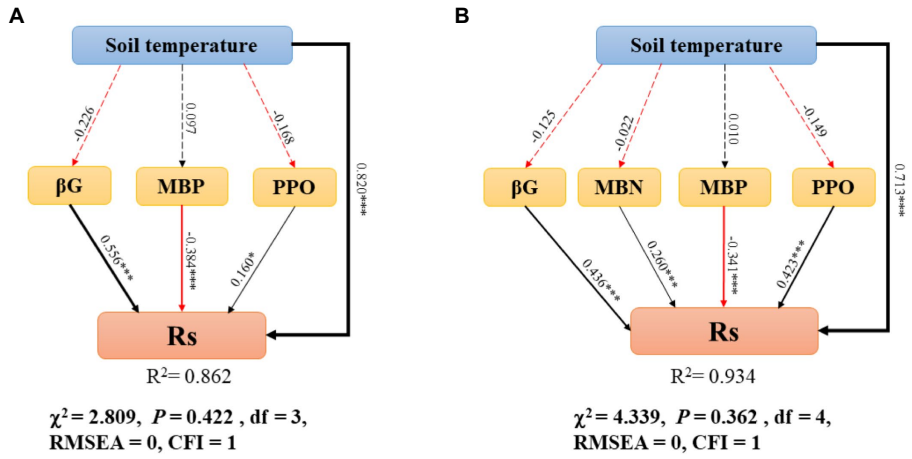

FIGURE 6
Structural equation model describes the relationship between variables and R_S in the topsoil **(A)** and whole soil **(B)**. R_S, soil respiration; MBN, microbial biomass nitrogen; MBP, microbial biomass phosphorus; PPO, polyphenol oxidase; βG, β-1,4-glucosidase; soil temperature (T_S). Arrows represent the assumed direction of causation. The width of arrow is proportional to the path coefficient. The red and black solid lines represent negative and positive pathways, respectively. Insignificant pathways are indicated by grey dashed lines. The importance of the variables is reflected by standardized path coefficients. R^2 reflects the proportion of variance explained for all variables in the model. The significance levels are as follows: *p <0.05, **p <0.01, and ***p <0.001.

lower value in October, which is consistent with the results of Tong et al. (2021). Our results differ from the results of Wen et al. (2018). A possible explanation for this phenomenon is the sensitivity of the research site to climate warming, resulting in a significantly higher rate of temperature change than in the other areas (Cao et al., 2016), thereby increasing the T_S to a maximum at an earlier time and leading to an increase in the R_S rate. The temperature sensitivity (Q_{10}) of R_S is often used as an important parameter to measure the feedback of R_S to global warming (Hu et al., 2013). During the whole study period, there was a significant statistical relationship between the R_S rate and T_S ($p < 0.01$; Figure 4), and the fitting effect between the R_S rate and T_S also had some explanatory significance ($R^2 = 0.2654$). Increased temperature stimulates R_S because climate warming may enhance the activity of soil microorganisms and promote soil organic C and litter decomposition, which partly explains why the R_S rate in summer is significantly higher than that in spring and autumn (Figure 3). Our findings suggest that a sustained increase in temperature may lead to greater soil C loss; that is, climate warming reduces soil C sinks.

M_S has been identified in previous studies as a major factor affecting R_S, especially after drought rewetting events stimulate R_S (Hu et al., 2019). Our results show that M_S is significantly negatively correlated with R_S (Supplementary Figure S4), proving that M_S limits CO_2 emissions from soil in a shorter period, which is different from the results of Yu et al. (2021). There may be several reasons for this: first, higher M_S inhibits the CO_2 transportation process from the atmosphere to the soil (Yan et al., 2018). During the study period, the M_S variation range was 92.44% ~42.20%, especially in summer and autumn, and the M_S remained at a high level (Figure 2B). It has been suggested in previous studies that under anoxic conditions, soil organic carbon (SOC) may be more persistent (Li et al., 2021), resulting in a decrease in R_S rate. Second, differences in SOC and microbial communities that decompose specific soil SOC lead to different relationships between M_S and R_S (Yan et al., 2018). Third, in this study, M_S may not be the main factor affecting the R_S rate because R_S is often regulated by multiple factors (Duan et al., 2021). For example, soil salinity and R_S show a negative correlation. When in a salt-stress environment, the activities of plant roots and soil microorganisms are severely affected (Song et al., 2021).

The correlations between T_S, M_S, and R_S demonstrate that T_S and M_S data are useful for optimizing microbial decomposition models, which facilitates soil microbial activity prediction much better in the context of future climate change.

4.2. Physical and chemical properties in different soil layers

Most previous studies have focused on the topsoil physicochemical properties (Liu et al., 2021). In this study, there were significant differences in the TP, AK, and SOM contents of different soil layers; TP was higher in the subsoil, and AK and SOM were higher in the topsoil (Table 1). The soil physicochemical properties changed with increasing soil depth, and our results are consistent with the results of Rahman et al. (2022). Microbial secretions can significantly affect soil potassium availability (Zorb et al., 2014), and factors such as microbial abundance and activity determine the pathway of soil litter conversion into SOM (Witzgall et al., 2021). In addition, plant roots and soil microbial communities can also dissolve P in the soil (Yang et al., 2021). Litter and most of the plant roots in the study site are concentrated in the topsoil. As shown in Figure 7, the microbial enzyme activity in the topsoil is higher than that in the subsoil, which proves that the microorganisms in the surface soil may be more active. Therefore, the AK and SOM contents were significantly higher than those in the subsoil, and the TP content was significantly lower than that in the subsoil. C and N cycle and nutrient turnover in soil are carried out by microorganisms through substrate (organic matter and litter) decomposition. In recent years, microbial decomposition models have been commonly used to explore the role of soil microorganisms in the coupled C and N cycle (Wang et al., 2014; Buchkowski et al., 2015). Our results can provide a reference for describing C, N, and P stocks and stoichiometry as well as soil nutrient distribution patterns in Loess Plateau soils and provide initial response data for soil microbial decomposition models.

4.3. Effects of soil microbial biomass and enzyme activity on R_S

The soil microbial biomass can regulate microbial biochemical processes and nutrient cycling and affect soil physical and chemical properties, which in turn affects soil quality (He et al., 2003). MBC is often considered to be a crucial factor affecting R_S, reflecting the ability of microorganisms to utilize SOC (Zeng et al., 2018). We found that, whether in the subsoil or topsoil, the MBC content showed a gradually increasing trend, and the MBC in May 2022 was significantly higher than in the other 3 months (Figure 5). We found that the trend of R_S was out of sync with that of the MBC. R_S decreased to a minimum value in autumn 2021, but the MBC reached a peak value in 2021. Our multiple stepwise regression results demonstrate that MBC is not a crucial factor affecting R_S (Supplementary Tables S1, S2). The reason for this phenomenon may be due to the decrease in the use efficiency of microorganisms. Microbial carbon use efficiency (CUE) refers to the distribution ratio between the MBC produced by organic matter catabolism and the C allocated by microorganisms for aerobic respiration (Schimel et al., 2022). The results of Manzoni et al. demonstrated that high temperature reduces the CUE of microorganisms (Manzoni et al., 2012) because the increase in T_S results in less C being allocated for microbial growth, which in turn reduces the ability of microbes to decompose organic resources to mitigate ecosystem C loss (Allison et al., 2010). During the growing season, T_S gradually increased, and microbes probably allocated more C for R_S than for MBC.

According to the results of the SEM, in addition to T_S, βG and PPO also significantly influenced R_S. Soil enzymes and microorganisms are involved in regulating the transformation of various organic matter and material circulation processes. Enzyme activity can be used as an indicator of microbial activity and plays a crucial role in decomposing organic compounds (Boerner R. E. J. et al., 2005). Previous studies have demonstrated that βG could participate in the decomposition of cellulose in litter (Caldwell, 2005). Litter is the most important source of organic matter input to the soil, and it can influence R_S by affecting the amount of labile C in the soil (Zhang et al., 2020). Therefore, βG has a significant positive effect on R_S. In addition, PPO can promote the accumulation of SOC by depolymerizing or aggregating lignin molecules and phenolic compounds in the soil (KIRK et al., 1987), thus positively influencing R_S.

Our results suggest that T_S, microbial biomass, and enzyme activity may be the main factors influencing soil microbial activity, which has important scientific implications for constructing microbial decomposition models that predict soil microbial activity under climate change in the future. To better understand the relationship between soil dynamics and C emissions, it will be necessary to incorporate climate data as well as R_S and microbial parameters into microbial decomposition models, which will be important for soil conservation and reducing soil C loss in the Loess Plateau.

5. Conclusion

We examined the soil physical and chemical properties at different depths in the Ziwuling Mountains, Loess Plateau, China, and conducted a soil observation experiment to record the temporal and spatial dynamic changes in the soil microbial characteristics in this area. Our results prove that R_S in the Ziwuling area has obvious diurnal and seasonal variations and that the R_S rate is significantly correlated with T_S and M_S. The strong effect of temperature on R_S leads to increased CO_2 emissions from the soil to the atmosphere, which in turn leads to greater

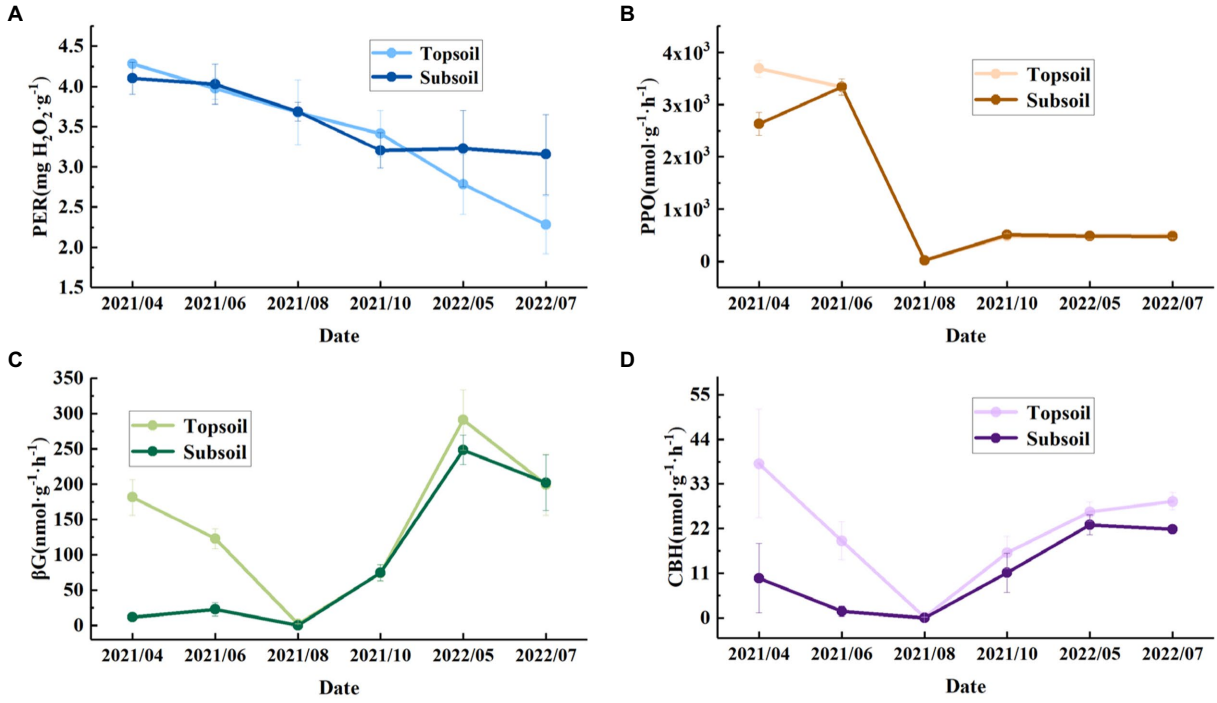

FIGURE 7
Monthly variations in enzyme activities in the topsoil (0–30cm) and subsoil (30–100cm) from April 2021 to July 2022. **(A)** PER, peroxidase. **(B)** PPO, polyphenol oxidase. **(C)** βG, β-1,4-glucosidase. **(D)** CBH, cellobiohydrolase.

forest soil C loss. Our study reveals the main factors affecting R_S, in order to better understand and predict changes in soil carbon dynamics in the future, incorporating T_S, MBN, MBP, βG, and PPO data into microbial decomposition models is necessary.

Data availability statement

The original contributions presented in the study are included in the article/Supplementary material, further inquiries can be directed to the corresponding author.

Author contributions

KW conceived the idea and plotted the figures. RQ and GL conducted field sampling and sample determination. MY, GW, and CP conducted the statistical analysis. RQ and KW wrote the first draft of the manuscript. All authors contributed substantially to revisions, intellectual input and assistance to this study, and manuscript preparation.

Funding

This research was supported in part by the National Natural Science Foundation of China (NSFC) (grant no. 41901059), Natural Science Foundation of Shaanxi Provincial Department (grant no. 2020JQ-593), and China Scholarship Council (CSC) (grant no: 202006970003).

Acknowledgments

We are grateful to Dong Hu, JiaYi Zhong, and JinHan Li for their help in soil sampling and data analysis.

Conflict of interest

The authors declare that the research was conducted in the absence of any commercial or financial relationships that could be construed as a potential conflict of interest.

Publisher's note

All claims expressed in this article are solely those of the authors and do not necessarily represent those of their affiliated organizations, or those of the publisher, the editors and the reviewers. Any product that may be evaluated in this article, or claim that may be made by its manufacturer, is not guaranteed or endorsed by the publisher.

Supplementary material

The Supplementary Material for this article can be found online at: https://www.frontiersin.org/articles/10.3389/fmicb.2023.1105723/full#supplementary-material

References

Abs, E., Leman, H., and Ferriere, R. (2020). A multi-scale eco-evolutionary model of cooperation reveals how microbial adaptation influences soil decomposition. *Commun. Biol.* 3:520. doi: 10.1038/s42003-020-01198-4

Allison, S. D., Wallenstein, M., and Bradford, M. A. J. N. G. (2010). Soil-carbon response to warming dependent on microbial physiology Nature Geoscience 3, 336–340. doi: 10.1038/ngeo846,

Bach, C. E., Warnock, D. D., Van Horn, D. J., Weintraub, M. N., Sinsabaugh, R. L., Allison, S. D., et al. (2013). Measuring phenol oxidase and peroxidase activities with pyrogallol, l-DOPA, and ABTS: effect of assay conditions and soil type. *Soil Biol. Biochem.* 67, 183–191. doi: 10.1016/j.soilbio.2013.08.022

Barberan, A., McGuire, K. L., Wolf, J. A., Jones, F. A., Wright, S. J., Turner, B. L., et al. (2015). Relating belowground microbial composition to the taxonomic, phylogenetic, and functional trait distributions of trees in a tropical forest. *Ecol. Lett.* 18, 1397–1405. doi: 10.1111/ele.12536

Boerner, R., Brinkman, J., and Smith, A. (2005). Seasonal variations in enzyme activity and organic carbon in soil of a burned and unburned hardwood forest. *Soil Biol. Biochem.* 37, 1419–1426. doi: 10.1016/j.soilbio.2004.12.012

Boerner, R. E. J., Brinkman, J. A., and Smith, A. (2005). Seasonal variations in enzyme activity and organic carbon in soil of a burned and unburned hardwood forest. *Soil Biol. Biochem.* 37, 1419–1426. doi: 10.1016/j.soilbio.2004.12.012

Bot, A., and Bernites, J. J. J. O. G. (2005). The importance of soil organic matter. *Journal of Geology*. 117, 241–262. doi: 10.1086/597364

Bradstreet, R. B. (1965). Distillation and determination of nitrogen - ScienceDirect Kjeldahl method for organic nitrogen. *Science Direct*. 147–168. Available at https://www.elsevier.com/books/the-kjeldahl-method-for-organic-nitrogen/bradstreet/978-1-4832-3298-0

Buchkowski, R. W., Schmitz, O. J. B., and Ecology, M. J. (2015). Microbial stoichiometry overrides biomass as a regulator of soil carbon and nitrogen cycling. *Ecology*. 96, 1139–1149. doi: 10.1890/14-1327.1,

Burns, R. G., DeForest, J. L., Marxsen, J., Sinsabaugh, R. L., Stromberger, M. E., Wallenstein, M. D., et al. (2013). Soil enzymes in a changing environment: current knowledge and future directions. *Soil Biol. Biochem.* 58, 216–234. doi: 10.1016/j.soilbio.2012.11.009

Cade-Menun, B. J., and Lavkulich, L. M. (1997). A comparison of methods to determine total, organic, and available phosphorus in forest soils. *Commun. Soil Sci. Plant Anal.* Taylor & Francis Inc. 28, 651–663. doi: 10.1080/00103629709369818

Caldwell, B. A. (2005). Enzyme activities as a component of soil biodiversity: a review. *Pedobiologia* 49, 637–644. doi: 10.1016/j.pedobi.2005.06.003

Cao, L., Zhu, Y., Tang, G., Yuan, F., and Yan, Z. J. I. J. O. C. (2016). *Climatic warming in China according to a homogenized data set from 2419 stations*, Wiley. 4384–4392.

Cardoso, E.J.B.N., Bini, D., Miyauchi, M.Y.H., Santos, C.A.D., Alves, P.R.L., Paula, A.M.D., et al. (2013). *Soil health: Looking for suitable indicators: What should be considered to assess the effects of use and management on soil health?* Univ Sao Paulo, Esalq.

Chai, Y., Yue, M., Liu, X., Guo, Y., Wang, M., Xu, J., et al. (2016). Patterns of taxonomic, phylogenetic diversity during a long-term succession of forest on the loess plateau, China: insights into assembly process. *Sci. Rep.* 6:27087. doi: 10.1038/srep27087

Chander, K., Goyal, S., Nandal, D. P., Kapoor, K. K. J. B., and Soils, F.o., (1998). Soil organic matter, microbial biomass and enzyme activities in a tropical agroforestry system. *Biology and Fertility of Soils*. 27, 168–172. doi: 10.1007/s003740050416,

Chen, Y. S., Hou, M. T., Dan, M. A., Han, X. H., Zhang, R. Y., and Zhang, X. Z. (2018). Determination of Total phosphorus in soil by alkali fusion-Mo-Sb anti spectrophotometric method. *China Stand.* 4,193–196. Avilable at: http://en.cnki.com.cn/Article_en/CJFDTotal-ZGBZ2018S1041.htm

Davidson, E. A., Janssens, I. A., and Luo, Y. (2006). On the variability of respiration in terrestrial ecosystems: moving beyond Q 10. *Glob. Chang. Biol.* 12, 154–164. doi: 10.1111/j.1365-2486.2005.01065.x

Duan, L., Liu, T., Ma, L., Lei, H., and Singh, V. P. (2021). Analysis of soil respiration and influencing factors in a semiarid dune-meadow cascade ecosystem. *Sci. Total Environ.* 796:148993. doi: 10.1016/j.scitotenv.2021.148993

Eivazi, F., and Tabatabai, M. (1988). Glucosidases and galactosidases in soils. Soil biol. Biochem. 20, 601-606. *Soil Biol. Biochem.* 20, 601–606. doi: 10.1016/0038-0717(88)90141-1

Friedlingstein, P., Cox, P., Betts, R., Bopp, L., Bloh, W. V., Brovkin, V., et al. (2006). Climate–Carbon cycle feedback analysis: Results from the C4MIP model intercomparison. *Journal of Climate* 19, 3337.

Fierer, N., Wood, S. A., and Bueno de Mesquita, C. P. (2021). How microbes can, and cannot, be used to assess soil health. *Soil Biol. Biochem.* 153:8111. doi: 10.1016/j.soilbio.2020.108111

Fu, B., Wang, S., Liu, Y., Liu, J., Liang, W., Miao, C. J. A. R. O. E., et al. (2016). Hydrogeomorphic ecosystem responses to natural and anthropogenic changes in the Loess Plateau of China. *Annual Review of Earth & Planetary Sciences*. 45, 223–243. doi: 10.1146/annurev-earth-063016-020552

Green, D. M., and Oleksyszyn, M. J. S. S. S. O. A. J. (2002). Enzyme activities and carbon dioxide flux in a Sonoran. *Des. Urban Ecosyst.* 66, 2002–2008. doi: 10.2136/sssaj2002.2002

Guo, X., Gao, Q., Yuan, M., Wang, G., Zhou, X., Feng, J., et al. (2020). Gene-informed decomposition model predicts lower soil carbon loss due to persistent microbial adaptation to warming. *Nat. Commun.* 11:4897. doi: 10.1038/s41467-020-18706-z

Hanson, P. J., Edwards, N. T., Garten, C. T., and Andrews, J. A. (2000). Separating root and soil microbial contributions to soil respiration: a review of methods and observations. Biogeochemistry 48: 115-146. *Biogeochemistry* 48, 115–146. doi: 10.1023/A:1006244819642

He, Z. L., Yang, X. E., Baligar, V. C., and Calvert, D. V. (2003). *Microbiological and biochemical indexing systems for assessing quality of acid soils*, Academic Press Inc. 89–138.

Hou, Q. Q., Pei, T. T., Chen, Y., Ji, Z. X., and Xie, B. P. J. Y. Y. S. T. X. B. T. J. O. A. E. Z. S. T. X. X. H. Zhongguo ke xue yuan Shenyang ying yong sheng tai yan jiu suo zhu ban (2021). Variations of drought and its trend in the Loess Plateau from 1986 to 2019. *Chinese Journal of Applied Ecology*. 32, 649–660. doi: 10.13287/j.1001-9332.202102.012

Hu, L. T., and Bentler, P. M. (1999). Cutoff criteria for fit indexes in covariance structure analysis: conventional criteria versus new alternatives. *Struct. Equ. Model.* 6, 1–55. doi: 10.1080/10705519909540118

Hu, Z., Cui, H., Chen, S., Shen, S., Li, H., Yang, Y., et al. (2013). Soil respiration and N2O flux response to UV-B radiation and straw incorporation in a soybean–winter wheat rotation. *System* 224:1394. doi: 10.1007/s11270-012-1394-z

Hu, Z., Towfiqul Islam, A. R. M., Chen, S., Hu, B., Shen, S., Wu, Y., et al. (2019). Effects of warming and reduced precipitation on soil respiration and N2O fluxes from winter wheat-soybean cropping systems. *Geoderma* 337, 956–964. doi: 10.1016/j.geoderma.2018.10.047

Jansson, J. K., and Hofmockel, K. S. (2020). Soil microbiomes and climate change. *Nat. Rev. Microbiol.* 18, 35–46. doi: 10.1038/s41579-019-0265-7

Jenkinson, D. S., and Ladd, J. N. J. S. B. (1981). Microbial biomass in soil. *Meas. Turnover*:5.

Ji, C., Luo, Y., Jan, V., Hungate, B. A., Cao, J., Zhou, X., et al. (2018). A keystone microbial enzyme for nitrogen control of soil carbon storage. *Science Advances* 4, eaaq1689.

Kang, D., Guo, Y., Ren, C., Zhao, F., Feng, Y., Han, X., et al. (2014). Population structure and spatial pattern of main tree species in secondary *Betula platyphylla* forest in Ziwuling Mountains China. *Sci. Rep.* 4:6873. doi: 10.1038/srep06873

Kirk, T. K., Farrell, , and Microbiol, R. J. A. R. (1987). *Enzymatic combustion - the microbial-degradation of lignin*, Annual Reviews: Copernicus Gesellschaft Mbh vol. 41, 465–505.

Laganière, J., Paré, D., Bergeron, Y., and Chen, H. Y. H. (2012). The effect of boreal forest composition on soil respiration is mediated through variations in soil temperature and C quality. *Soil Biol. Biochem.* 53, 18–27. doi: 10.1016/j.soilbio.2012.04.024

Li, Y., Shahbaz, M., Zhu, Z., Deng, Y., Tong, Y., Chen, L., et al. (2021). Oxygen availability determines key regulators in soil organic carbon mineralization in paddy soils. *Soil Biol. Biochem.* 153:8106. doi: 10.1016/j.soilbio.2020.108106

Liu, D., Fang, Y., Tu, Y., and Pan, Y. (2014). Chemical method for nitrogen isotopic analysis of ammonium at natural abundance. *Anal. Chem.* 86, 3787–3792. doi: 10.1021/ac403756u

Liu, M., Li, X., Zhu, R., Chen, N., Ding, L., and Chen, C. (2021). Vegetation richness, species identity and soil nutrients drive the shifts in soil bacterial communities during restoration process. *Environ. Microbiol. Rep.* 13, 411–424. doi: 10.1111/1758-2229.12913

Lucas, R. W., Casper, B. B., Jackson, J. K., and Balser, T. C. (2007). Soil microbial communities and extracellular enzyme activity in the New Jersey pinelands. *Soil Biol. Biochem.* 39, 2508–2519. doi: 10.1016/j.soilbio.2007.05.008

Mahajan, G. R., Das, B., Manivannan, S., Manjunath, B. L., Verma, R. R., Desai, S., et al. (2021). *Soil and water conservation measures improve soil carbon sequestration and soil quality under cashews*, Irtces. *36*, 190–206 doi: 10.1016/j.ijsrc.2020.07.009.

Manzoni, S., Taylor, P., Richter, A., Porporato, A., and Agren, G. I. (2012). Environmental and stoichiometric controls on microbial carbon-use efficiency in soils. *New Phytol.* 196, 79–91. doi: 10.1111/j.1469-8137.2012.04225.x

Marland, G. (1983). Relationship between global fossil-fuel consumption and the concentration of carbon dioxide in the atmosphere. *Part.* 1, 1–133.

Melillo, J. M., Frey, S. D., Deangelis, K. M., Werner, W. J., Bernard, M. J., Bowles, , et al. (2018). Long-term pattern and magnitude of soil carbon feedback to the climate system in a warming world *Science*. 2, 101–105. doi: 10.1126/science.aan2874

Piao, S., Ciais, P., Huang, Y., Shen, Z., Peng, S., Li, J., et al. (2010a). The impacts of climate change on water resources and agriculture in China. *Nature*. 467, 43–51. doi: 10.1038/nature07944

Piao, S., Fang, J., Ciais, P., Peylin, P., Huang, Y., Sitch, S., et al. (2010b). The carbon balance of terrestrial ecosystems in China. *Nature*. 458, 1009–1013. doi: 10.1038/nature07944

Rahman, M., Zhang, K., Wang, Y., Ahmad, B., Ahmad, A., Zhang, Z., et al. (2022). Variations in soil physico-chemical properties, soil stocks, and soil stoichiometry under different soil layers, the major forest region Liupan Mountains of Northwest China. *Braz. J. Biol.* 84:e256565. doi: 10.1590/1519-6984.256565

Schimel, J., Weintraub, M. N., and Moorhead, D. (2022). Estimating microbial carbon use efficiency in soil: isotope-based and enzyme-based methods measure fundamentally different aspects of microbial resource use. *Soil Biol. Biochem.* 169:108677. doi: 10.1016/j.soilbio.2022.108677

Schlesinger, W. H., and Andrews, J. A. J. B. (2000). Soil respiration and the global carbon cycle. *Biogeochemistry*. 48, 7–20.

Schloter, M., Dilly, O., and Munch, J. C. J. A. E. (2003). Environment indicators for evaluating soil quality. *Agriculture Ecosystems & Environment*. 98, 255–262. doi: 10.1016/S0167-8809(03)00085-9,

Sicardi, M., Garcia-Prechac, F., and Frioni, L. (2004). Soil microbial indicators sensitive to land use conversion from pastures to commercial Eucalyptus grandis (hill ex maiden) plantations in Uruguay. *Appl. Soil Ecol.* 27, 125–133. doi: 10.1016/j.apsoil.2004.05.004

Sinsabaugh, R. L., Antibus, R. K., Linkins, A. E., Mcclaugherty, C. A., Rayburn, L., Repert, D., et al. (1992). Wood decomposition over a first-order watershed: Mass loss as a function of lignocellulase activity. *Soil Biology & Biochemistry*. 24, 743–749. doi: 10.1016/0038-0717(92)90248-V,

Sinsabaugh, R. L., Lauber, C. L., Weintraub, M. N., Ahmed, B., Allison, S. D., Crenshaw, C., et al. (2008). Stoichiometry of soil enzyme activity at global scale. *Ecol. Lett.* 11, 1252–1264. doi: 10.1111/j.1461-0248.2008.01245.x

Song, X., Zhu, Y., and Chen, W. (2021). Dynamics of the soil respiration response to soil reclamation in a coastal wetland. *Sci. Rep.* 11:2911. doi: 10.1038/s41598-021-82376-0

Tabachnick, B. G., and Fidell, L. S. (2007). *Using multivariate statistics*. 5th Edn. Lippincott Williams & Wilkins

Tollefson, J. J. N. (2021). *IPCC climate report: Earth is warmer than it's been in 125,000 years*. Nature Portfolio. 596.

Tong, D., Li, Z., Xiao, H., Nie, X., Liu, C., and Zhou, M. (2021). How do soil microbes exert impact on soil respiration and its temperature sensitivity? *Environ. Microbiol.* 23, 3048–3058. doi: 10.1111/1462-2920.15520

Vance, E. D., and Brookes, P. C. (1987). "Measurement of microbial biomass in soil" in *Chemical analysis in environmental research*. (Rowland: Abbots Ripton, Institute of Terrestrial Ecology).

Vile, D., Shipley, B., and Garnier, E. (2006). A structural equation model to integrate changes in functional strategies during old-field succession. *Ecology* 87, 504–517. doi: 10.1890/05-0822

Voigt, C., Lamprecht, R. E., Marushchak, M. E., Lind, S. E., Novakovskiy, A., Aurela, M., et al. (2016). Warming of subarctic tundra increases emissions of all three important greenhouse gases – carbon dioxide, methane, and nitrous oxide. *Global Change Biology*.

Wang, X. (2010). Comparison of methods for determining alkali-hydrolyzed nitrogen in soil. *J. Beijing Norm. Univ. Nat. Sci.* 46, 76–78. http://en.cnki.com.cn/article_en/cjfdtotal-bsdz201001021.htm

Wang, Y. P., Chen, B. C., Wieder, W.R., Leite, M., and Luo, Y. Q. J. B. (2014). *Oscillatory behavior of two non-linear microbial models of soil carbon decomposition*. 11. Copernicus Gesellschaft Mbh.

Wang, G., Huang, W., Zhou, G., Mayes, M. A., and Zhou, J. (2020). Modeling the processes of soil moisture in regulating microbial and carbon-nitrogen cycling. *J. Hydrol.* 585:124777. doi: 10.1016/j.jhydrol.2020.124777

Wang, G., Jagadamma, S., Mayes, M. A., Schadt, C. W., Steinweg, J. M., Gu, L., et al. (2015). Microbial dormancy improves development and experimental validation of ecosystem model. *ISME J.* 9, 226–237. doi: 10.1038/ismej.2014.120

Wang, X., Luo, X., Jia, H., and Zheng, H. (2018). Dynamic characteristics of soil respiration in Yellow River Delta wetlands China. *Physics and chemistry of the earth*. 103, 11–18. doi: 10.1016/j.pce.2017.06.008,

Wang, J., Song, B., Ma, F., Tian, D., Li, Y., Yan, T., et al. (2019). *Nitrogen addition reduces soil respiration but increases the relative contribution of heterotrophic component in an alpine meadow running head: A rising r h /r s ratio along with n addition gradient*.

Wang, C., Yang, J., and Zhang, Q. (2006). Soil respiration in six temperate forests in China. *Glob. Chang. Biol.* 12, 2103–2114. doi: 10.1111/j.1365-2486.2006.01234.x

Wen, L., Jinlan, W., Xiaojiao, Z., Shangli, S., and Wenxia, C. (2018). Effect of degradation and rebuilding of artificial grasslands on soil respiration and carbon and nitrogen pools on an alpine meadow of the Qinghai-Tibetan plateau. *Ecol. Eng.* 111, 134–142. doi: 10.1016/j.ecoleng.2017.10.013

Wieder, W. R., Cleveland, C. C., Smith, W. K., and Todd-Brown, K. J. N. G. (2015). Future productivity and carbon storage limited by terrestrial nutrient availability. Nature Geoscience. 8, 441–444. doi: 10.1038/ngeo2413,

Witzgall, K., Vidal, A., Schubert, D. I., Hoschen, C., Schweizer, S. A., Buegger, F., et al. (2021). Particulate organic matter as a functional soil component for persistent soil organic carbon. *Nat. Commun.* 12:4115. doi: 10.1038/s41467-021-24192-8

Wood, T. M., and Bhat, K. M. (1988). "Methods for measuring cellulase activities" in *Methods in enzymology* (United States: Academic Press), 87–112.

Yan, Z., Bond-Lamberty, B., Todd-Brown, K. E., Bailey, V. L., Li, S., Liu, C., et al. (2018). A moisture function of soil heterotrophic respiration that incorporates microscale processes. Nature. *Communications* 9:4971. doi: 10.1038/s41467-018-04971-6

Yang, F., Sui, L., Tang, C., Li, J., Cheng, K., and Xue, Q. (2021). Sustainable advances on phosphorus utilization in soil via addition of biochar and humic substances. *Sci. Total Environ.* 768:145106. doi: 10.1016/j.scitotenv.2021.145106

Yu, H., Liu, X., Ma, Q., Yin, Z., Wang, Y., Xu, Z., et al. (2021). Climatic warming enhances soil respiration resilience in an arid ecosystem. *Sci. Total Environ.* 756:144005. doi: 10.1016/j.scitotenv.2020.144005

Yu, Y., Zhao, W., Martinez-Murillo, J. F., and Pereira, P. (2020). Loess plateau: from degradation to restoration. *Sci. Total Environ.* 738:140206. doi: 10.1016/j.scitotenv.2020.140206

Zanati, M. R., Guirguis, M. A., and Saber, M. S. M. (1973). Biological and chemical determination of available potassium in soil. Zentralblatt für Bakteriologie, Parasitenkunde, Infektionskrankheiten und hygiene. *Zweite Naturwissenschaftliche Abteilung: Allgemeine, Landwirtschaftliche und Technische Mikrobiologie* 128, 572–577. doi: 10.1016/s0044-4057(73)80079-6

Zeng, W., Chen, J., Liu, H., and Wang, W. (2018). Soil respiration and its autotrophic and heterotrophic components in response to nitrogen addition among different degraded temperate grasslands. *Soil Biol. Biochem.* 124, 255–265. doi: 10.1016/j.soilbio.2018.06.019

Zhang, H., Wang, E., Zhou, D., Luo, Z., and Zhang, Z. (2016). Rising soil temperature in China and its potential ecological impact. *Sci. Rep.* 6:35530. doi: 10.1038/srep35530

Zhang, Y., Zhao, J., Xu, J., Chai, Y., Liu, P., Quan, J., et al. (2022). Effects of water availability on the relationships between hydraulic and economic traits in the *Quercus wutaishanica* forests. *Front. Plant Sci.* 13:902509. doi: 10.3389/fpls.2022.902509

Zhang, Y., Zou, J., Meng, D., Dang, S., Zhou, J., Osborne, B., et al. (2020). Effect of soil microorganisms and labile C availability on soil respiration in response to litter inputs in forest ecosystems: a meta-analysis. *Ecol. Evol.* 10, 13602–13612. doi: 10.1002/ece3.6965

Zhou, T., Shi, P., Hui, D., and Luo, Y. (2009). Global pattern of temperature sensitivity of soil heterotrophic respiration (Q10) and its implications for carbon-climate feedback. Journal of geophysical research. *Biogeosciences* 114:850. doi: 10.1029/2008jg000850

Zhu, C., Zhang, Z., Wang, H., Wang, J., and Yang, S. (2020). Assessing soil organic matter content in a coal mining area through spectral variables of different numbers of dimensions. *Sensors* 20:1795. doi: 10.3390/s20061795

Zorb, C., Senbayram, M., and Peiter, E. (2014). Potassium in agriculture--status and perspectives. *J. Plant Physiol.* 171, 656–669. doi: 10.1016/j.jplph.2013.08.008

frontiers | Frontiers in Microbiology

TYPE Original Research
PUBLISHED 17 March 2023
DOI 10.3389/fmicb.2023.1127179

OPEN ACCESS

EDITED BY
Upendra Kumar,
National Rice Research Institute (ICAR),
India

REVIEWED BY
Rui Liu,
China Agricultural University,
China
M. Manjunath,
Central Research Institute for Dryland Agriculture (ICAR),
India

*CORRESPONDENCE
Weixin Ding
✉ wxding@issas.ac.cn

SPECIALTY SECTION
This article was submitted to Terrestrial Microbiology, a section of the journal Frontiers in Microbiology

RECEIVED 19 December 2022
ACCEPTED 27 February 2023
PUBLISHED 17 March 2023

CITATION
Xie L, Liu D, Chen Z, Niu Y, Meng L and Ding W (2023) Non-native *Brachiaria humidicola* with biological nitrification inhibition capacity stimulates *in situ* grassland N_2O emissions.
Front. Microbiol. 14:1127179.
doi: 10.3389/fmicb.2023.1127179

Non-native *Brachiaria humidicola* with biological nitrification inhibition capacity stimulates *in situ* grassland N_2O emissions

Lu Xie[1,2], Deyan Liu[1], Zengming Chen[1], Yuhui Niu[1], Lei Meng[3] and Weixin Ding[1]*

[1]State Key Laboratory of Soil and Sustainable Agriculture, Institute of Soil Science, Chinese Academy of Sciences, Nanjing, China, [2]University of Chinese Academy of Sciences, Beijing, China, [3]College of Tropical Crops, Hainan University, Haikou, China

Introduction: *Brachiaria humidicola*, a tropical grass, could release root exudates with biological nitrification inhibition (BNI) capacity and reduce soil nitrous oxide (N_2O) emissions from grasslands. However, evidence of the reduction effect *in situ* in tropical grasslands in China is lacking.

Methods: To evaluate the potential effects of *B. humidicola* on soil N_2O emissions, a 2-year (2015–2017) field experiment was established in a Latosol and included eight treatments, consisting of two pastures, non-native *B. humidicola* and a native grass, *Eremochloa ophiuroide*, with four nitrogen (N) application rates. The annual urea application rates were 0, 150, 300, and 450 kg N ha^{-1}.

Results: The average 2-year *E. ophiuroides* biomass with and without N fertilization were 9.07–11.45 and 7.34 t ha^{-1}, respectively, and corresponding values for *B. humidicola* increased to 31.97–39.07 and 29.54 t ha^{-1}, respectively. The N-use efficiencies under *E. ophiuroide* and *B. humidicola* cultivation were 9.3–12.0 and 35.5–39.4%, respectively. Annual N_2O emissions in the *E. ophiuroides* and *B. humidicola* fields were 1.37 and 2.83 kg N_2O-N ha^{-1}, respectively, under no N fertilization, and 1.54–3.46 and 4.30–7.19 kg N_2O-Nha^{-1}, respectively, under N fertilization.

Discussions: According to the results, *B. humidicola* cultivation increased soil N_2O emissions, especially under N fertilization. This is because *B. humidicola* exhibited the more effective stimulation effect on N_2O production *via* denitrification primarily due to increased soil organic carbon and exudates than the inhibition effect on N_2O production *via* autotrophic nitrification. Annual yield-scaled N_2O emissions in the *B. humidicola* treatment were 93.02–183.12 mg N_2O-N kg^{-1} biomass, which were significantly lower than those in the *E. ophiuroides* treatment. Overall, our results suggest that cultivation of the non-native grass, *B. humidicola* with BNI capacity, increased soil N_2O emissions, while decreasing yield-scaled N_2O emissions, when compared with native grass cultivation.

KEYWORDS

biological nitrification inhibition, *Brachiaria humidicola*, denitrification, N_2O emissions, yield-scaled N_2O emission

1. Introduction

Nitrous oxide (N_2O) is a potent greenhouse gas with a significant 100-year global warming potential that is 265 times higher than that of carbon dioxide on a per-molecule basis (IPCC, 2013). In addition, N_2O depletes stratospheric ozone, which protects the earth from biologically damaging ultraviolet radiation (Ravishankara et al., 2009). Notably, the concentration of

atmospheric N_2O has increased from 270 ppb during the pre-industrial era to 335.55 ppb in 2022, with an average annual increase rate of 0.90 ppb over the last 2 decades (Lan et al., 2022). Agriculture reportedly emitted approximately 4.1 Tg N_2O-N $year^{-1}$, accounting for approximately 66% of total global anthropogenic N_2O emissions (UNEP, 2013). Using the dynamic land ecosystem model, Dangal et al. (2019) estimated that the net N_2O emission from the global grasslands was 2.2 Tg N_2O-N $year^{-1}$, which was responsible for 54% of the total agricultural N_2O emissions.

To meet the increasing food demands, nitrogen (N) fertilizer and agricultural land are growing substantially (Foley et al., 2011). The global synthetic N fertilizer consumption has increased from 12 to 112 Tg N while that has risen from 0.8 to 24 Tg N in China during the 1961–2020.[1] However, the N-use efficiency (NUE) in China was only 28–35%, which is much lower than the global average (Liu et al., 2013; Han et al., 2015; Zhang et al., 2015).The heavy reliance of N fertilizers in agriculture has contributed to the stimulation of nitrifier activity and the trend toward high-nitrifying soil environments (Poudel et al., 2002; Bellamy et al., 2005).

Nitrification is closely related to N utilization and loss, and has become a key process to improve NUE and reduce N pollution (Subbarao et al., 2006; Beeckman et al., 2018). Nitrification is a microbes-driven process of oxidizing ammonia (NH_3) to nitrite and further to nitrate (NO_3^-) and producing N_2O as a byproduct (Stein, 2020). The NO_3^- produced during nitrification serves as a substrate and denitrification further reduces NO_3^- to dinitrogen and produces N_2O as an intermediate product (Coskun et al., 2017a). Nitrification inhibitors can depress the activities of nitrifiers in soil, thereby delaying NH_3 oxidation and reducing N_2O emissions and NO_3^- production (Rodgers, 1986; Coskun et al., 2017b). To date, a few synthetic nitrification-inhibiting compounds have been efficiently adopted in the field, such as nitrapyrin, dicyandiamide, and 3,4-dimethyl pyrazole phosphate (Weiske et al., 2001; Zerulla et al., 2001; Niu et al., 2018). Meta-analysis revealed that the combination application of nitrification inhibitors and urea reduced NO_3^- leaching by 48% and N_2O emissions by 44% (Burzaco et al., 2014), and increased crop yields by 7.5% and NUE by 12.9% (Abalos et al., 2014a). However, synthetic nitrification inhibitors have certain limitations such as low cost-effectiveness, application challenges, poor biological stability, and environmental pollution risks (Subbarao et al., 2012; Coskun et al., 2017b; Wang et al., 2021).

Natural compounds with biological nitrification inhibition (BNI) have been found from litters, root exudates, tissue extracts, and rhizosphere of plants such as grasses, trees, and crops (Wang et al., 2021), including methyl 3-(4 hydroxyphenyl) propionate (MHPP), sorgoleone and sakuranetin from sorghum (Subbarao et al., 2013), 1,9-decanediol from rice (Sun et al., 2016) and brachialactone from *Brachiaria humidicola* grass (Subbarao et al., 2009). Some root-secreted biological nitrification inhibitors (BNIs) like sorgoleone, sakuranetin, and brachialactone as well as linolenic acid and linoleic acid found in *B. humidicola* can inhibit both ammonia mono-oxygenase and hydroxylamine oxidoreductase activities (Coskun et al., 2017b), while 1,9-decanediol and MHPP only inhibits activity of ammonia mono-oxygenase (Zakir et al., 2008; Nardi et al., 2013, 2020; Sun et al., 2016; Lu et al., 2019). Up to date, the functional validation of the BNIs is mainly performed in the pure culture system of a single strain *Nitrosomonas europaea*, and the effect in the complicated soil system remains to be tested (Subbarao et al., 2015). For example, sakuranetin isolated from sorghum shows a strong inhibitory activity *in vitro*-cultural bioassay but losses the inhibitory effect in soil-assay (Subbarao et al., 2013). Gopalakrishnan et al. (2009) found that the inhibition effect of BNIs is affected by soil type, and the BNIs derived from *B. humidicola* in Cambisol can inhibit 90% nitrification with comparable effects to dicyandiamide (50 mg kg^{-1} soil), but are less effective in Andosol during the 60-day incubation.

Forage grasses with biological nitrification inhibition (BNI) capacity exhibit approximately 2-fold greater productivity than those lacking such capacity in nutrient-limited ecosystems, based on an estimate of a newly developed model (Lata et al., 1999; Boudsocq et al., 2009). The *B. humidicola*, reportedly exhibits the strongest BNI function among tropical grasses reduces the NH_3 oxidation rate and N_2O emissions significantly during a 3-year field experiment, when compared with soybean-planted or plant-free soils (Subbarao et al., 2009). During a short-term (29 days) monitoring period in Colombia, cumulative N_2O emissions from a *B. humidicola* cv. Tully field was decreased by approximately 60% when compared with that in a *Brachiaria* hybrid cv. Mulato field under bovine urine amendment (Byrnes et al., 2017). In contrast, no significant effect on N_2O emissions of the two forage genotypes was observed under cattle dung amendment in the same experimental site (Lombardi et al., 2022).

Latosol is a most widely distributed soil and covers 51.26% of the total area in Hainan Province, China. In the present study, a 2-year field experiment was conducted in a Latosol cultivated with *B. humidicola* and a native grass species, *Eremochloa ophiuroides*. We hypothesized that *in situ* N_2O emissions from grasslands under cultivation with *Brachiaria* with higher BNI capacity are lower than in those cultivated with *Eremochloa*. The objectives of the present study were: (1) to determine whether the N_2O emissions from a *B. humidicola* field are lower than those from an *E. ophiuroides* field in tropical Hainan Province, China; and (2) to evaluate the mitigation effects of *B. humidicola* on yield-scaled N_2O emissions under the different N application rates. We also established an incubation with soils from the field experiment using a ^{15}N tracing technique to evaluate the influence of *B. humidicola* on the N transformation process rates and N_2O production rates *via* nitrification and denitrification (Xie et al., 2022).

2. Materials and methods

2.1. Study site

The field site was located in Danzhou, Hainan Province, China (109°29′ E, 19°30′ N). The region is characterized by a tropical monsoon climate, with a rainy season from May to October, and a dry season from November to April. The mean annual temperature and precipitation are 23.1°C and 1,823 mm, respectively. The soil is derived from granite and classified as a Latosol, with a sandy loam texture. Latosol is a most widely distributed soil in Hainan Province. The properties of surface soil (0–20 cm) prior to the field experiment are shown in Table 1.

1 https://www.ifastat.org/databases/graph/1

TABLE 1 Soil properties before field experiment.

BD (g cm^{-3})	Soil pH	SOC (g C kg^{-1})	TN (g N kg^{-1})	NH_4^+-N (mg N kg^{-1})	NO_3^--N (mg N kg^{-1})	Available P (mg P kg^{-1})	Available K (mg K kg^{-1})
1.29 ± 0.18	5.42 ± 0.02	5.70 ± 0.05	0.27 ± 0.01	0.22 ± 0.06	6.03 ± 0.17	20.76 ± 1.06	76.00 ± 3.45

Means ± standard errors ($n = 3$). BD, soil bulk density; SOC, soil organic carbon; TN, total soil nitrogen; Available P, available phosphorus; and Available K, available potassium.

TABLE 2 Specific dates of field management during the 2-year field experiment.

Year	Planting	Basal fertilization	Top-dressing fertilization	Harvest
2015–2016	15 August	15 Aug. 2015	15 Apr. 2016	14 April 2016; 27 Aug. 2016
2016–2017	-	28 Aug. 2016	13 Mar. 2017; 9 June 2017	12 Mar. 2017; 8 June 2017; 1 Sept. 2017

2.2. Experimental design

A field experiment was established in August 2015 and included eight treatments, consisting of two pastures, *Brachiaria humidicola* CIAT679 and *Eremochloa ophiuroides*, with four N application rates. The annual urea application rates were 0, 150, 300, and 450 kg N ha^{-1}, which were designated as BCK, BN1, BN2, and BN3, respectively, for *B. humidicola*, and ECK, EN1, EN2, and EN3, respectively, for *E. ophiuroides*. The plots measured 3 m × 4 m. The treatments, which had three replicates, were set up based on a randomized complete block design. During the first season from August 2015 to August 2016, 60 and 40% of urea was applied as basal fertilizer and top-dressing fertilizer, respectively, in the fertilized treatments. In the second season from August 2016 to August 2017, urea was added with three splits: 40% as basal fertilizer, and 30% as top-dressing fertilizer on 13 March and 9 June 2017, respectively. Calcium superphosphate (150 kg P_2O_5 ha^{-1}) and potassium chloride (105 kg K_2O ha^{-1}) were applied as basal fertilizer. All the fertilizers were dissolved in water and uniformly spread into the soil. Harvested plant samples were oven-dried at 60°C to a constant weight, and then ground to less than 0.2 mm for analysis. Field management practices were similar to local practices and standardized at all plots. Specific dates are listed in Table 2.

2.3. Nitrous oxide flux measurement

Nitrous oxide fluxes were measured using the static chamber method. Before grass planting, a stainless steel chamber with a rectangular base (50 cm × 50 cm × 15 cm) and a 5-cm groove around the upper edge was permanently fit 10 cm into the soil. During gas sampling, a stainless chamber (50 cm × 50 cm × 50 cm) was inserted into the groove, which was filled with water to ensure airtightness. The chamber was covered with reflective film and foam to minimize air temperature change inside the chamber. A rubber plug with a mercury thermometer was fit tightly into the hole on the top of the chamber for use in measuring the chamber temperature while gas sampling. Two vents welded with stainless tubes were punched on top of the chamber, one connected to a rubber tube with a three-way stopcock for gas collection, and another one for ensuring air pressure equilibrium inside and outside the chamber. Gas samples were obtained once every other day during 1 week after each fertilization and once a week during the other period. Sampling was conducted between 7:00 am and 12:00 pm to minimize diurnal variation. Four gas samples were extracted from the chamber at 0, 10, 20, and 30 min after chamber closure using airtight plastic syringes and instantly injected into 20-ml pre-evacuated vials fitted with butyl rubber stoppers. The N_2O concentrations were analyzed using a gas chromatograph (GC; Agilent 7890, Agilent Technologies, Santa Clara, CA, United States) equipped with a ^{63}Ni electron capture detector and a thermal conductivity detector. The N_2O fluxes were calculated using the following equation (Niu et al., 2018):

$$F = \rho \times (V / S) \times (\Delta C / \Delta t) \times [273 / (273 + T)]$$

where F is the flux in N_2O (μg N_2O-N m^{-2} h^{-1}); ρ is the density of N_2O at 0°C and 760 mm Hg (kg m^{-3}); V is the effective volume of the chamber (m^3); S is the soil area covered by the chamber (m^2); $\Delta C/\Delta t$ is the rate of N_2O concentration increase in the chamber (ppbv N_2O-N h^{-1}); and, T is mean air temperature inside the chamber during sampling (°C).

2.4. Auxiliary variables measurement

Soil temperature was measured at 5 cm depth using a geothermometer. Soil water content was measured at three different positions in each plot with time domain reflectometry (TDR) probes and expressed as water-filled pore space (WFPS, %) as follows (Niu et al., 2018):

$$\text{WFPS} = \text{volumetric water content} / \text{total soil porosity}$$

where total soil porosity = 1 - (soil bulk density/2.65), 2.65 being the soil particle density (g cm^{-3}).

Surface (0–20 cm) soil samples were collected at five different positions in each plot fortnightly using a stainless steel soil sampler and thoroughly mixed to form a composite sample. The samples were taken to the laboratory immediately and stored at −20°C before analysis. Soil exchangeable ammonium-N (NH_4^+-N) and nitrate-N (NO_3^--N) were extracted with 2 M KCl (soil/KCl solution ratio of 1:5) by agitating for 1 h on a rotary shaker, and the concentrations were measured using a colorimetric method on a segmented flow analyzer (Skalar, The Netherlands; Chen et al., 2014). Dissolved organic C (DOC) was extracted with deionized water at a soil water ratio of 1:5, which was shaken for 0.5 h, followed by centrifugation for 15 min at

2,300 × *g* and filtration (<0.45 μm). Subsequently, the DOC was analyzed using the combustion oxidation nondispersive infrared absorption method on a TOC analyzer (vario TOC Cube, Elementar, Hanau, Germany).

Soil samples were collected after the end of the field experiments. Soil pH was determined from soil-water suspensions (1:2.5 v/v) using a pH meter (SevenCompact, Mettler Toledo, Swiss). Soil organic C (SOC) was measured using the wet oxidation-redox titration method (Walkley and Black, 1934). Total N content in soil and plant was determined using an elemental analyzer (Vario MAX, Elementar, Germany). Soil available P was extracted with 0.05 M HCl and 0.025 M H_2SO_4, and determined using the molybdenum blue colorimetric method (Ye et al., 2019). Available K was extracted with ammonium acetate and analyzed using a flame photometer (Lu, 2000).

2.5. Data calculation and statistical analysis

Annual cumulative N_2O emissions (E_{N2O}, kg N_2O-N ha^{-1}) were calculated using the following equation (Chen et al., 2014):

$$E_{N2O} = \sum_{i=0}^{n} \left(f_i + f_{i+1}\right) / 2 \times \left(t_{i+1} - t_i\right) \times 24 \times 10^{-5}$$

where f is the N_2O flux (μg N_2O-N m^{-2} h^{-1}); i is the ith measurement; ($t_{i+1} - t_i$) is the interval between the i th and the ($i+1$) th measurement time (d); n is the total number of measurements; and 24×10^{-5} was used for unit conversion.

The N_2O emission factor of applied fertilizer N (EF, %) was calculated using the following equation:

$$EF = \left(E_{fertilizer} - E_{control}\right) / N_{applied}$$

where $E_{fertilizer}$ and $E_{control}$ are the cumulative N_2O emissions from the fertilized and control treatments, respectively; and $N_{applied}$ is the amount of fertilizer N applied to the corresponding treatment.

The yield-scaled N_2O emission (mg N_2O-N kg^{-1} biomass) was computed using the following equation (Venterea et al., 2011):

$$Yield\text{-}scaled\ N_2O = E_{N2O} / yield$$

where E_{N2O} is the annual cumulative N_2O emissions (kg N_2O-N ha^{-1}); and yield is the amount of grass biomass harvested annually (kg ha^{-1}).

Fertilizer N-use efficiency (NUE, %) was calculated as follows:

$$NUE = \left(N_{fertilizer} - N_{control}\right) / N_{applied}$$

where $N_{fertilizer}$ and $N_{control}$ are the amount of N uptake in aboveground biomass (kg N ha^{-1}) in the fertilized and control treatments, respectively; and $N_{applied}$ is the amount of the N applied to the corresponding treatment (kg N ha^{-1}).

Significant differences among treatments were evaluated using one-way ANOVA followed by the Duncan test at $p < 0.05$. Spearman's correlation analysis was used to determine the relationships between N_2O flux and soil WFPS, soil inorganic N, soil dissolved organic C, and air temperature. All statistical analyses were performed using IBM SPSS Statistics 26 for Windows (IBM corp., Armonk, NY, United States).

3. Results

3.1. Soil characteristics

After 2 years of grass cultivation, soil pH in all the treatments increased when compared with that in the pre-treatment soil (Table 3). The maximum soil pH was observed in the ECK treatment without N fertilization, and soil pH decreased with an increase in N application rate in both grasslands. SOC increased by 17.5–22.8% under *B. humidicola* cultivation and only by 5.8–15.1% under *E. ophiuroides*, when compared with the pre-treatment soil. Cultivation of both pastures promoted soil N accumulation significantly ($p < 0.05$); however, there were no significant differences in soil N accumulation among treatments under different N application rates (Table 3).

3.2. Grass yield

The biomass of *B. humidicola* ranged from 29.54 to 31.37 t ha^{-1} in the BCK treatment, which was 3.1–6.0-fold that of *E. ophiuroide* during the two seasons (Table 4). The N application increased biomass yield of *B. humidicola* by 11.3–25.8% ($p < 0.05$) but did not increase the biomass yield of *E. ophiuroides*, during the first season. During the 2016–2017 season, however, the biomass of both grasses was enhanced with N fertilization, and increased with an increase in the N application rate ($p < 0.05$).

The amounts of N uptake by *B. humidicola* under no N fertilization were 220.08 and 188.74 kg N ha^{-1} during the 2015–2016 and 2016–2017 seasons, respectively, and decreased to 44.22 and 69.82 kg N ha^{-1} for *E. ophiuroide*, respectively (Table 4). The mean NUE of the N applied under *B. humidicola* was 19.5–29.5% during the 2015–2016 season and increased to 47.9–59.2% during the 2016–2017 season, which was significantly higher than that under *E. ophiuroides* during both seasons.

3.3. Soil and environmental variables

Air temperature (AT) ranged from 5.4 to 32.6°C, with an average of 24.8°C over the 2-year measurement period, and there was no apparent difference between two growth seasons (Figure 1). Soil temperature (ST) at 5 cm depth ranged from 13.7 to 34.8°C, a trend similar to that of AT (ST = 0.758AT + 7.062, $R^2 = 0.42$, $p < 0.01$). Mean rainfall was 2,341 and 2,373 mm during the 2015–2016 and 2016–2017 seasons, respectively. Precipitation mainly occurred in the rainy season, from May to October, accounting for 87% of the total annual precipitation. Soil moisture fluctuated from 5.1 to 58.3% WFPS, and the mean WFPS in all the treatments was 33.5–38.3%, with no significant differences among treatments.

Soil NH_4^+-N concentration peaks occurred approximately 1 week after each fertilization, and decreased to a constant level 40 days later

TABLE 3 Soil properties before and after 2 years of *Brachiaria humidicola* and *Eremochloa ophiuroides* cultivation.

Treatment	Soil pH	SOC (g C kg^{-1})	TN (g N kg^{-1})	DOC (mg C kg^{-1})
Pre-soil	5.42 ± 0.02d	5.70 ± 0.05b	0.27 ± 0.01b	115.87 ± 7.39d
BCK	6.37 ± 0.17a	6.70 ± 0.19ab	0.52 ± 0.03a	161.45 ± 3.70b
BN1	6.41 ± 0.27a	6.78 ± 0.65ab	0.55 ± 0.02a	151.48 ± 1.95bc
BN2	5.75 ± 0.05bcd	6.89 ± 0.10a	0.55 ± 0.02a	142.71 ± 8.68c
BN3	5.60 ± 0.07 cd	7.00 ± 0.30a	0.58 ± 0.04a	145.40 ± 0.66c
ECK	6.49 ± 0.16a	6.03 ± 0.00ab	0.51 ± 0.01a	160.15 ± 3.53bc
EN1	6.06 ± 0.10abc	6.51 ± 0.48ab	0.59 ± 0.05a	147.11 ± 8.22c
EN2	6.19 ± 0.15ab	6.56 ± 0.08ab	0.57 ± 0.04a	156.53 ± 1.79bc
EN3	5.74 ± 0.16bcd	6.48 ± 0.38ab	0.55 ± 0.04a	179.84 ± 6.56a

Means ± standard errors ($n = 3$). BCK, no nitrogen application for *B. humidicola*; BN1, nitrogen application at 150 kg N ha^{-1} for *B. humidicola*; BN2, nitrogen application at 300 kg N ha^{-1} for *B. humidicola*; BN3, nitrogen application at 450 kg N ha^{-1} for *B. humidicola*; ECK, no nitrogen application for *E. ophiuroides*; BN1, nitrogen application at 150 kg N ha^{-1} for *E. ophiuroides*; EN2, nitrogen application at 300 kg N ha^{-1} for *E. ophiuroides*; EN3, nitrogen application at 450 kg N ha^{-1} for *E. ophiuroides*. Pre-soil, soil prior to field experiment; SOC, soil organic carbon; TN, total soil nitrogen; DOC, dissolved organic carbon. Different letters within the same columns indicate significant differences between treatments ($p < 0.05$).

TABLE 4 Yield, nitrogen uptake, and nitrogen use efficiency of *Brachiaria humidicola* and *Eremochloa ophiuroides* during two growth seasons.

Treatment	2015–2016			2016–2017			Mean		
	Yield (t ha^{-1})	N uptake (kg N ha^{-1})	NUE (%)	Yield (t ha^{-1})	N uptake (kg N ha^{-1})	NUE (%)	Yield (t ha^{-1})	N uptake (kg N ha^{-1})	NUE (%)
BCK	31.37 ± 0.30c	220.08 ± 8.57b	–	29.54 ± 0.14d	188.74 ± 17.65d	–	30.45 ± 0.21c	204.41 ± 11.96d	–
BN1	34.91 ± 2.05b	249.37 ± 10.77b	19.5 ± 6.1ab	31.92 ± 0.62c	277.47 ± 9.81c	59.2 ± 5.3a	33.41 ± 0.81b	263.42 ± 5.76c	39.3 ± 5.5a
BN2	38.72 ± 0.73a	308.59 ± 23.54a	29.5 ± 10.6a	37.01 ± 0.76b	336.02 ± 5.84b	49.1 ± 6.5a	37.87 ± 0.73a	322.3 ± 13.79b	39.3 ± 8.4a
BN3	39.47 ± 0.60a	324.02 ± 12.00a	23.1 ± 0.8ab	39.07 ± 0.46a	404.07 ± 7.22a	47.9 ± 3.5a	39.27 ± 0.43a	364.05 ± 5.74a	35.5 ± 1.4a
ECK	5.24 ± 0.51d	44.22 ± 2.25c	–	9.44 ± 0.15 g	69.82 ± 1.63 g	–	7.34 ± 0.31f	57.02 ± 1.12f	–
EN1	7.47 ± 0.34d	59.90 ± 3.33c	10.5 ± 3.0b	10.66 ± 0.82 g	90.08 ± 1.59 fg	13.5 ± 0.3b	9.07 ± 0.58e	74.99 ± 2.45f	12.0 ± 1.4b
EN2	6.50 ± 0.19d	63.11 ± 4.27c	6.3 ± 1.5b	12.77 ± 0.44f	106.68 ± 2.88f	12.3 ± 0.7b	9.63 ± 0.31e	84.9 ± 1.18ef	9.3 ± 0.5b
EN3	7.74 ± 0.61d	72.15 ± 2.99c	6.2 ± 1.1b	15.15 ± 0.18e	138.07 ± 7.95e	15.2 ± 2.1b	11.45 ± 0.22d	105.11 ± 2.48e	10.7 ± 0.6b

Means ± standard errors ($n = 3$). BCK, no nitrogen application for *B. humidicola*; BN1, nitrogen application at 150 kg N ha^{-1} for *B. humidicola*; BN2, nitrogen application at 300 kg N ha^{-1} for *B. humidicola*; BN3, nitrogen application at 450 kg N ha^{-1} for *B. humidicola*; ECK, no nitrogen application for *E. ophiuroides*; BN1, nitrogen application at 150 kg N ha^{-1} for *E. ophiuroides*; EN2, nitrogen application at 300 kg N ha^{-1} for *E. ophiuroides*; EN3, nitrogen application at 450 kg N ha^{-1} for *E. ophiuroides*. Yield, grass aboveground biomass; N uptake, the amount of N uptake in aboveground biomass; NUE, nitrogen use efficiency. Different letters in the same column indicate significant differences between treatments ($p < 0.05$).

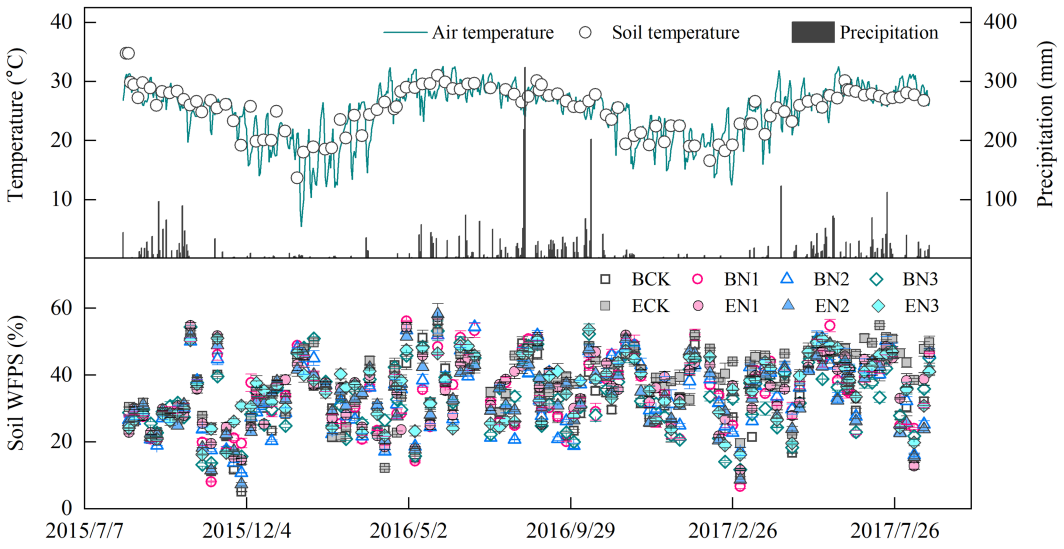

FIGURE 1
Temporal variation in precipitation, air temperature, and soil temperature at 5cm depth, and water-filled pore space (WFPS). Vertical bars denote the standard errors of the mean ($n = 3$).

(Figure 2A). The mean soil NH_4^+-N concentrations under the BCK and ECK treatments were 4.60 and 4.05 mg N kg^{-1}, respectively and increased to 10.46–14.93 and 10.09–15.91 mg N kg^{-1} in the BN and EN treatments, respectively, increasing with increases in the N application rate. Mean soil NH_4^+-N concentrations were not significantly different between the *B. humidicola* and *E. ophiuroides* fields under similar N application rates. Soil NO_3^--N concentrations in the BCK and ECK treatments were on average 3.21 and 2.59 mg N kg^{-1}, respectively (Figure 2B). Under N fertilization, mean soil NO_3^--N concentrations increased to 5.61, 6.02, and 8.42 mg N kg^{-1} in the BN1, BN2, and BN3 treatments, respectively, which were higher than the corresponding values under *E. ophiuroides* cultivation, excluding BN2 ($p < 0.05$).

3.4. Nitrous oxide emissions

Nitrous oxide flux peaks emerged after each fertilization, and increased with an increase in the N application rates. The highest flux was 544.60 μg N_2O-N m^{-2} h^{-1} in the BN3 treatment on 31 August 2016, which was 3-fold that in the EN3 treatment (Figure 3). During

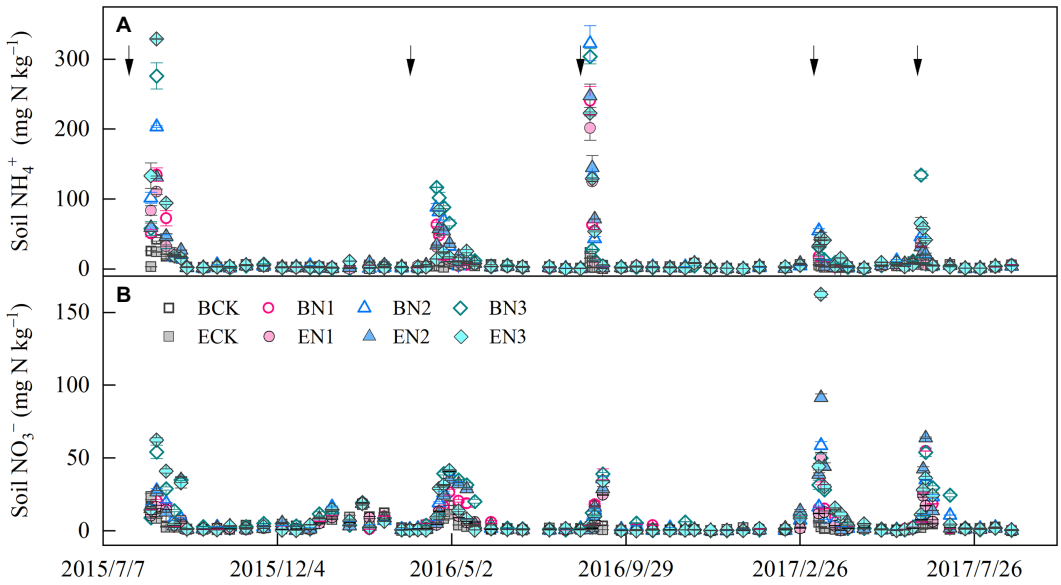

FIGURE 2
Soil ammonium **(A)** and nitrate **(B)** concentration dynamics in the 0–20-cm layer. Vertical bars denote the standard errors of the mean (n=3). The solid arrows indicate the N fertilization time.

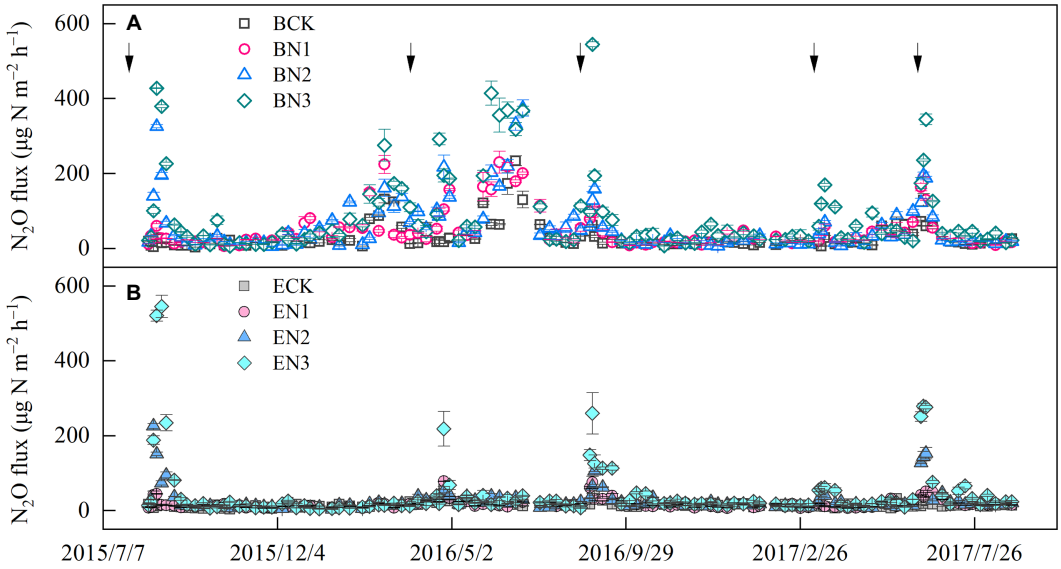

FIGURE 3
Temporal variation in nitrous oxide (N_2O) flux in *Brachiaria humidicola* **(A)** and *Eremochloa ophiuroides* **(B)** soil. Solid line arrows indicate the timing of fertilizer application. Vertical bars denote the standard errors of the mean (n=3). The solid arrows indicate the nitrogen (N) fertilization time.

TABLE 5 Correlation between nitrous oxide (N_2O) flux and soil moisture (WFPS), ammonium-nitrogen (NH_4^+-N), nitrate-nitrogen (NO_3^--N), inorganic nitrogen (NH_4^+-N plus NO_3^--N), and air temperature (AT).

Treatment	WFPS	NH_4^+-N	NO_3^--N	Inorganic N	AT
BCK	0.232*	0.348**	0.166	0.339**	0.289**
BN1	0.224*	0.325**	0.310**	0.390**	0.224*
BN2	0.193*	0.335**	0.264**	0.363**	0.415**
BN3	0.245**	0.290**	0.360**	0.370**	0.238*
ECK	0.148	0.113	−0.043	0.030	0.188*
EN1	0.171	0.290**	0.131	0.248**	0.445**
EN2	0.208*	0.411**	0.259**	0.358**	0.504**
EN3	0.200*	0.457**	0.246**	0.379**	0.475**

*$p < 0.05$, **$p < 0.01$. BCK, no nitrogen application for *B. humidicola*; BN1, nitrogen application at 150 kg N ha^{-1} for *B. humidicola*; BN2, nitrogen application at 300 kg N ha^{-1} for *B. humidicola*; BN3, nitrogen application at 450 kg N ha^{-1} for *B. humidicola*; ECK, no nitrogen application for *E. ophiuroides*; BN1, nitrogen application at 150 kg N ha^{-1} for *E. ophiuroides*; EN2, nitrogen application at 300 kg N ha^{-1} for *E. ophiuroides*; and EN3, nitrogen application at 450 kg N ha^{-1} for *E. ophiuroides*.

the 2016–2017 season, the peak flux in the BN3 treatments (344.60 μg N_2O-N m^{-2} h^{-1}) was also observed on 20 June 2017, which, however, was only 1.2-fold greater than that in the EN3 treatment. The N_2O fluxes were significantly ($p < 0.01$) correlated with soil moisture, NH_4^+-N, NO_3^--N, and air temperature (Table 5).

Annual N_2O emissions in the *B. humidicola* fields were higher than those in the *E. ophiuroides* fields, regardless of N fertilization rate ($p < 0.05$; Figure 4A). They were also greater during the first (2015–2016) season than during the second (2016–2017) season in the case of *B. humidicola* but not in the case of *E. ophiuroides*. Annual N_2O emissions in the *B. humidicola* fields under BCK were 3.64 and 2.02 kg N_2O-N ha^{-1} during the 2015–2016 and 2016–2017 season, respectively, with an average of 2.83 kg N_2O-N ha^{-1}. Under N fertilization, annual N_2O emissions from the *B. humidicola* field increased to 5.72–9.54 and 2.88–4.84 kg N_2O-N ha^{-1} during the 2015–2016 and 2016–2017 season, respectively. In the *E. ophiuroides* field, N_2O emissions under no N fertilization (ECK) were 1.38 and 1.35 kg N_2O-N ha^{-1} during the 2015–2016 and 2016–2017 seasons, respectively, and increased to 1.43–3.28 and 1.65–3.64 kg N_2O-N ha^{-1} under N fertilization, respectively. The annual N_2O emissions increased linearly with an increase in the N application rate in the *B. humidicola* fields ($E_{N2O} = 0.0092\ N_{applied} + 2.76$, $R^2 = 0.97$); conversely, they exhibited exponential correlations with the N application rate in the *E. ophiuroides* fields ($E_{N2O} = 1.24e^{0.021Napplied}$, $R^2 = 0.95$).

The N_2O emission factor (EF) of the N applied ranged from 0.74 to 0.98% for *B. humidicola*, and decreased to 0.11–0.47% for *E. ophiuroides* over the 2 years (Figure 4B). The EF increased with an increase in the N application rate only under *E. ophiuroides* cultivation.

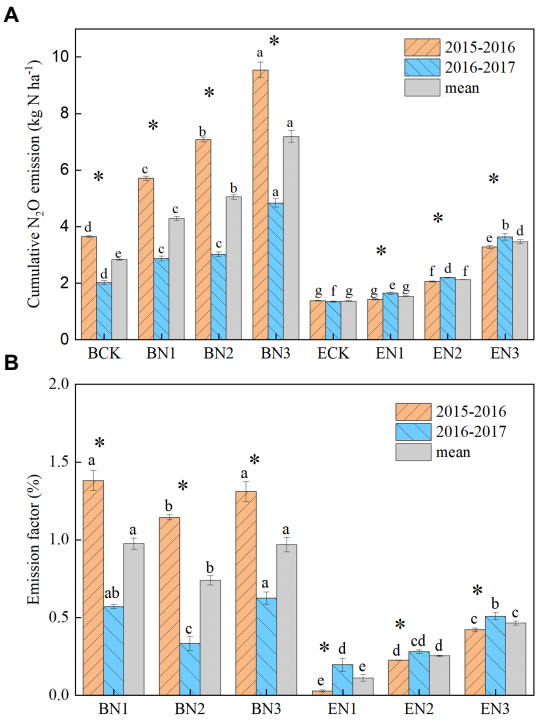

FIGURE 4
Annual soil nitrous oxide (N_2O) emission **(A)** and emission factor of the fertilizer nitrogen applied **(B)** in the *Brachiaria humidicola* and *Eremochloa ophiuroides* fields. Vertical bars denote the standard errors of the mean (n=3). Different letters indicate significant differences between treatments for the same measurement year and mean at p<0.05. *indicates the significant difference between 2years for the same treatment at p<0.05.

3.5. Yield-scaled nitrous oxide emissions

The mean yield-scaled N_2O emissions in the BCK and ECK treatments were 95 and 206 mg N_2O-N kg^{-1} biomass, respectively, over the 2 years (Figure 5). Under N fertilization, they increased to 128, 132, and 183 mg N_2O-N kg^{-1} biomass in the BN1, BN2, and BN3 treatments, respectively, which were significantly lower than the corresponding values in the EN treatments by 26.76–46.04%. The reduction increased with an increase in the N application rate.

4. Discussion

Annual N_2O emissions from this tropical grassland varied from 1.35 to 9.54 kg N_2O-N ha^{-1}, which was within the 0–29.1 kg N_2O-N ha^{-1} range in grasslands as reported previously (Mosier et al., 1996; Wolf et al., 2010; Merbold et al., 2014; Luo et al., 2017). Out of expectation, N_2O emissions from the *B. humidicola* field were

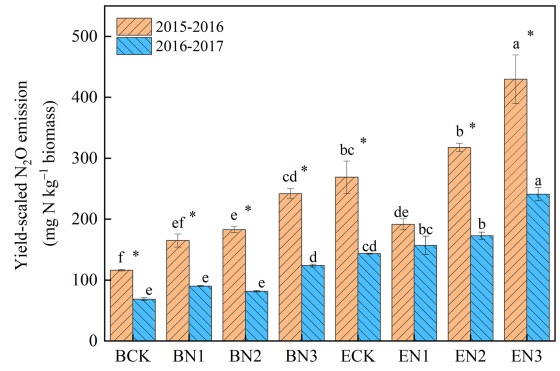

FIGURE 5
Yield-scaled N_2O emissions from the *Brachiaria humidicola* and *Eremochloa ophiuroides* field. Vertical bars denote the standard errors of the mean (n=3). Different letters indicate the significant differences between treatments for the same measurement year and for mean at p<0.05. *indicates the significant difference between two measurement years for the same treatment at p<0.05.

1.3–2.6-fold higher than those from the *E. ophiuroides* field under N fertilization. Additionally, the N_2O emission factor of the N applied was increased to 0.74–0.98% under *B. humidicola* from 0.11–0.47% under *E. ophiuroides*. Our results suggest that cultivation of exotic, tropical forage grass *B. humidicola* with BNI capacity by replacing native *E. ophiuroides* stimulated N_2O emission. To our knowledge, this is the first study to find the stimulation effect of *B. humidicola* on N_2O emissions in the field when compared with the native grass. Apparently, more field studies are required to evaluate the impact of plants with BNI capacity on N_2O emissions at the ecosystem and global scale, as suggested by Lata et al. (2022).

Previous study suggested that *Brachiaria* genotype with high BNI capacity reduced almost 50% of N_2O emission when compared with soybean or plant-free soils (Subbarao et al., 2009). Byrnes et al. (2017) reported that *B. humidicola* cv. Tully with high BNI capacity reduced approximately 60% of N_2O emissions in the field when compared with the *Brachiaria* hybrid cv. Mulato having low BNI capacity during the 29-day monitoring period. Planting *B. humidicola* with high BNI capacity reduced soil N_2O emissions by 18.3% when compared with *B. humidicola* with low BNI capacity in a 21-day pot experiment (Teutscherová et al., 2022). The active substances with BNI capacity, such as methyl-p-coumarate, methyl ferulate, and brachialactone, have been identified from exudates of *B. humidicola* (Gopalakrishnan et al., 2009; Subbarao et al., 2009). Brachialactone can simultaneously block the enzymatic pathways of ammonia monooxygenase and hydroxylamino oxidoreductase (Subbarao et al., 2009). The inhibitory potential reportedly increases with an increase in grass root density (Subbarao et al., 2007; Boudsocq et al., 2009). Subbarao et al. (2009) estimated that *B. humidicola* roots can potentially release 2.6×10^6–7.5×10^6 ATU (allylthiourea units) ha^{-1} day^{-1} BNI activity in the South American savannas, which is equivalent to the application of 6.2–18 kg ha^{-1} nitrapyrin based on 1 ATU being equal to 0.6 μg of nitrapyrin. Karwat et al. (2017) demonstrated that *B. humidicola,* like dicyandiamide, significantly suppresses soil nitrification potential. In a previous study, using the ^{15}N tracing incubation with soils collected from the *B. humidicola* and *E. ophiuroides* plots at the field experiment end, we found that *B. humidicola* decreased the autotrophic nitrification rate and N_2O production rate *via* nitrification by 27.3 and 14.7%, respectively when compared with *E. ophiuroides* (Xie et al., 2022). This indicated that in the test soil, *B. humidicola* efficiently inhibited nitrification and N_2O production *via* nitrification.

Subbarao et al. (2009) observed that cultivation of *B. humidicola* reduced the abundance of both ammonia-oxidizing archaea (AOA) and bacteria (AOB) in a Vertisol with pH 7.40 when compared with soil cultivated with soybean. Hink et al. (2018) further reported that although both AOA and AOB were capable of N_2O production under high NH_4^+-N concentrations, the contribution of AOB was greater in a soil with pH 6.50. In the test acid soil with pH 5.42, it is likely that both AOA and AOB participated in NH_3 oxidation and N_2O production. Further investigations are required to determine the relative importance of AOA and AOB in N_2O production, and the suppression effects of *B. humidicola* on AOA and AOB activity (Nuñez et al., 2018).

Byrnes et al. (2017) suggested that by increasing N uptake, *B. humidicola* with high BNI capacity more efficiently decreased soil NO_3^--N availability and potential denitrification than *B. humidicola* with low BNI capacity, thereby reducing N_2O emissions. Abalos et al. (2014b) reported that mixed cultivation of *Folium perennial* L. and *Poi trivialize* L. decreased soil NO_3^--N concentrations and consequent N_2O emissions when compared with either monoculture at an N application rate of 60 kg N ha^{-1}. They suggested that the trends were attributed to *L. perennial* taking up N using the "scale strategy" by increasing root biomass, and *P. trivialize* absorbing N *via* the "precision strategy" by providing access to N hotspots that were not emptied by *L. perennial*. In the present study, although *B. humid cola* cultivation increased N uptake, N_2O emissions were positively correlated with pasture yield and N uptake, indicating that increased N uptake by *B. humid cola* did not reduce N_2O emissions. In the present study, the mean soil NO_3^--N concentration under N fertilization ranged from 5.60 mg N kg^{-1} in the BN1 treatment to 8.45 mg N kg^{-1} in the BN3 treatment, which was higher than the 5 mg N kg^{-1} threshold for occurrence of denitrification (Dobbie and Smith, 2003), and indicated that although *B. humid cola* efficiently increased N uptake and partially inhibited nitrification, soil NO_3^--N under N fertilization was still higher than the threshold value for denitrification in the test field.

Using ^{15}N paired incubation ($^{15}NH_4NO_3$ and $NH_4{}^{15}NO_3$), we found that the N_2O production rate during denitrification in the *B. humid cola* soil increased by 7.7-fold when compared with the *E. ophiuroides* soil and the contribution of denitrification to N_2O emissions sharply enhanced from 9.7% in the *E. ophiuroides* soil to 47.1% (Xie et al., 2022). In the present study, *B. humidicola* biomass was 3–6-fold greater than that of *E. ophiuroides* and SOC was more efficiently increased under *B. humidicola*. Horrocks et al. (2019) also observed that 1-year cultivation of *B. humidicola* increases SOC content and improves aggregate stability in Colombia. Fisher et al. (1994) and Amézquita et al. (2004) attributed the SOC enhancement to rapid accumulation of *B. humidicola* roots and exudates. Plant reportedly release as much as 40% of net photosynthetic C into the rhizosphere (Marschner, 2011), which in turn provides more labile C substrates for denitrifiers (Wu et al., 2017). Enhanced SOC at least exhibits two stimulation effects on denitrification. Firstly, enhanced SOC promotes the formation of anaerobic microsites for denitrification by stimulating

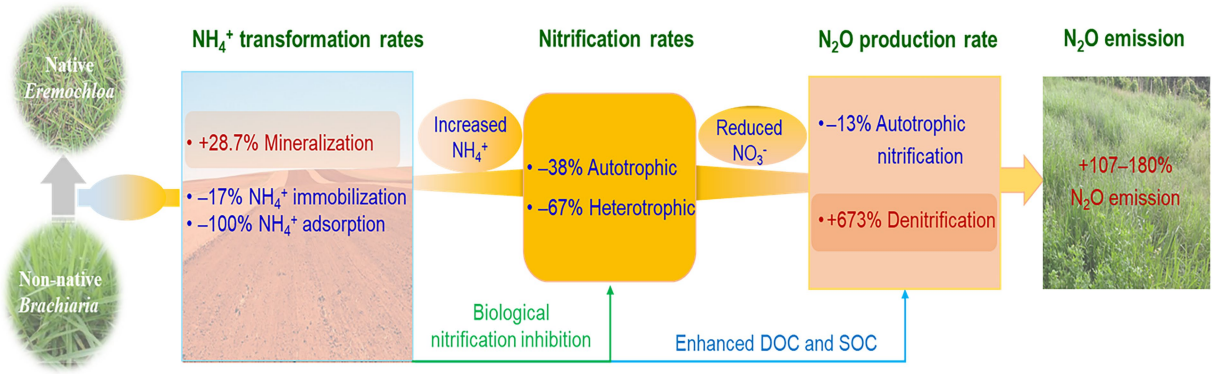

FIGURE 6
Schematic diagram showing how *Brachiaria humidicola* cultivation stimulated the nitrous oxide (N_2O) emission in the study grassland. Nitrogen transformation rates and N_2O production rates *via* autotrophic nitrification and denitrification are cited from Xie et al. (2022).

aggregation (Bollmann and Conrad, 2004). Secondly, increased organic C availability reduces the soil moisture threshold for the occurrence of denitrification (Rochette et al., 2000; Van Groenigen et al., 2004; Chantigny et al., 2013) resulting in increased denitrification potentials. Our results indicate that cultivation of exotic *B. humidicola* with a much higher biomass compared with *E. ophiuroides* stimulated N_2O production during denitrification by providing more organic C, which in turn masked N_2O reduction by inhibiting nitrification, thereby enhancing N_2O emissions.

Comparing yield-scaled N_2O emissions has been suggested to be an effective way of evaluating the tradeoff between production and environmental impacts and determining the economic feasibility of N_2O emission mitigation methods (van Groenigen et al., 2010; Grassini and Cassman, 2012). In the present study, yield-scaled N_2O emissions from *B. humidicola* field with and without N fertilization during two seasons were 128.80–183.02 and 93.02 g N kg^{-1} biomass, respectively, which were significantly lower than the corresponding values under *E. ophiuroides* cultivation (171.07–221.62 and 186.93 g N kg^{-1} biomass, respectively). In addition, we observed interannual shifts in yield-scaled N_2O emissions in both grasslands, which was primarily driven by changes in annual N_2O emission in *B. humidicola* fields, whereas they were driven by changes in biomass yield in *E. ophiuroides* fields. The lower yield-scaled N_2O emissions under *B. humidicola* cultivation compared with under *E. ophiuroides* indicated that although *B. humidicola* increased annual N_2O emissions, it was more environmentally friendly based on its higher forage productivity and NUE.

5. Conclusion

In the present study, *B. humidicola* exhibited higher yields and NUE, and in contrast and unexpectedly, induced higher soil N_2O emissions when compared with *E. ophiuroides*. Although cultivation of *B. humidicola* with high BNI capacity reduced N_2O production rate *via* nitrification, however, it more efficiently enhanced N_2O production rate than *E. ophiuroides via* denitrification due to increased SOC and exudate concentrations, thereby increasing N_2O emissions (Figure 6). When compared with under *E. ophiuroides*, however, the lower yield-scaled N_2O emissions under *B. humidicola* cultivation indicated that although *B. humidicola* increased annual N_2O emissions, it was more environmentally friendly based on its higher forage productivity and NUE.

Data availability statement

The original contributions presented in the study are included in the article/supplementary material, further inquiries can be directed to the corresponding author.

Author contributions

WD and DL: conceptualization. LX, YN, and DL: field experiment. LX and ZC: data analysis. LX, WD, and LM: writing. WD: funding acquisition. All authors contributed to the article and approved the submitted version.

Funding

This work was financially supported from the National Natural Science Foundation of China (41730753, 41977049 and 42077029), the International Partnership Program of Chinese Academy of Sciences (151432KYSB20200001), and International Atomic Energy Agency coordinated research project (D15020).

Acknowledgments

We would like to gratefully acknowledge the Hainan University Danzhou Campus for providing the study site and assistance in field experiment. And special thanks to Fang Yage for the collaboration in field work.

Conflict of interest

The authors declare that the research was conducted in the absence of any commercial or financial relationships that could be construed as a potential conflict of interest.

Publisher's note

References

Abalos, D., De Deyn, G. B., Kuyper, T. W., and van Groenigen, J. W. (2014b). Plant species identity surpasses species richness as a key driver of N_2O emissions from grassland. *Glob. Chang. Biol.* 20, 265–275. doi: 10.1111/gcb.12350

Abalos, D., Jeffery, S., Sanz-Cobena, A., Guardia, G., and Vallejo, A. (2014a). Meta-analysis of the effect of urease and nitrification inhibitors on crop productivity and nitrogen use efficiency. *Agric. Ecosyst. Environ.* 189, 136–144. doi: 10.1016/j.agee.2014.03.036

Amézquita, E., Thomas, R. J., Rao, I. M., Molina, D. L., and Hoyos, P. (2004). Use of deep-rooted tropical pastures to build-up an arable layer through improved soil properties of an Oxisol in the Eastern Plains (llanos Orientales) of Colombia. *Agric. Ecosyst. Environ.* 103, 269–277. doi: 10.1016/j.agee.2003.12.017

Beeckman, F., Motte, H., and Beeckman, T. (2018). Nitrification in agricultural soils: impact, actors and mitigation. *Curr. Opin. Biotechnol.* 50, 166–173. doi: 10.1016/j.copbio.2018.01.014

Bellamy, P. H., Loveland, P. J., Bradley, R. I., Lark, R. M., and Kirk, G. J. D. (2005). Carbon losses from all soils across England and Wales 1978–2003. *Nature* 437, 245–248. doi: 10.1038/nature04038

Bollmann, A., and Conrad, R. (2004). Influence of O_2 availability on NO and N_2O release by nitrification and denitrification in soils. *Glob. Chang. Biol.* 4, 387–396. doi: 10.1046/j.1365-2486.1998.00161.x

Boudsocq, S., Lata, J. C., Mathieu, J., Abbadie, L., and Barot, S. (2009). Modelling approach to analyse the effects of nitrification inhibition on primary production. *Funct. Ecol.* 23, 220–230. doi: 10.1111/j.1365-2435.2008.01476.x

Burzaco, J. P., Ciampitti, I. A., and Vyn, T. J. (2014). Nitrapyrin impacts on maize yield and nitrogen use efficiency with spring-applied nitrogen: field studies vs. meta-analysis comparison. *Agron. J.* 106, 753–760. doi: 10.2134/agronj2013.0043

Byrnes, R. C., Nùñez, J., Arenas, L., Rao, I., Trujillo, C., Alvarez, C., et al. (2017). Biological nitrification inhibition by *Brachiaria* grasses mitigates soil nitrous oxide emissions from bovine urine patches. *Soil Biol. Biochem.* 107, 156–163. doi: 10.1016/j.soilbio.2016.12.029

Chantigny, M. H., Pelster, D. E., Perron, M. H., Rochette, P., Angers, D. A., Parent, L. É., et al. (2013). Nitrous oxide emissions from clayey soils amended with paper sludges and biosolids of separated pig slurry. *J. Environ. Qual.* 42, 30–39. doi: 10.2134/jeq2012.0196

Chen, Z., Ding, W., Luo, Y., Yu, H., Xu, Y., Müller, C., et al. (2014). Nitrous oxide emissions from cultivated black soil: a case study in Northeast China and global estimates using empirical model. *Glob. Biogeochem. Cy.* 28, 1311–1326. doi: 10.1002/2014GB004871

Coskun, D., Britto, D. T., Shi, W., and Kronzucker, H. J. (2017a). Nitrogen transformations in modern agriculture and the role of biological nitrification inhibition. *Nat. Plants* 3:17074. doi: 10.1038/nplants.2017.74

Coskun, D., Britto, D. T., Shi, W., and Kronzucker, H. J. (2017b). How plant root exudates shape the nitrogen cycle. *Trends Plant Sci.* 22, 661–673. doi: 10.1016/j.tplants.2017.05.004

Dangal, S. R. S., Tian, H., Xu, R., Chang, J., Canadell, J. G., Ciais, P., et al. (2019). Global nitrous oxide emissions from pasturelands and rangelands: magnitude, spatiotemporal patterns, and attribution. *Glob. Biogeochem. Cy.* 33, 200–222. doi: 10.1029/2018GB006091

Dobbie, K. E., and Smith, K. A. (2003). Impact of different forms of N fertilizer on N_2O emissions from intensive grassland. *Nutr. Cycl. Agroecosyst.* 67, 37–46. doi: 10.1023/A:1025119512447

Fisher, M. J., Rao, I. M., Ayarza, M. A., Lascano, C. E., Sanz, J. I., Thomas, R. J., et al. (1994). Carbon storage by introduced deep-rooted grasses in the south American savannas. *Nature* 371, 236–238. doi: 10.1038/371236a0

Foley, J. A., Ramankutty, N., Brauman, K. A., Cassidy, E. S., Gerber, J. S., Johnston, M., et al. (2011). Solutions for a cultivated planet. *Nature* 478, 337–342. doi: 10.1038/nature10452

Gopalakrishnan, S., Watanabe, T., Pearse, S. J., Ito, O., Hossain, A. K. M., and Subbarao, G. V. (2009). Biological nitrification inhibition by Brachiaria humidicola roots varies with soil type and inhibits nitrifying bacteria, but not other major soil microorganisms. *Soil Sci. Plant Nutr.* 55, 725–733. doi: 10.1111/j.1747-0765.2009.00398.x

Grassini, P., and Cassman, K. G. (2012). High-yield maize with large net energy yield and small global warming intensity. *Proc. Natl. Acad. Sci. U. S. A.* 109, 1074–1079. doi: 10.1073/pnas.1201296109

Han, M., Okamoto, M., Beatty, P. H., Rothstein, S. J., and Good, A. G. (2015). The genetics of nitrogen use efficiency in crop plants. *Annu. Rev. Genet.* 49, 269–289. doi: 10.1146/annurev-genet-112414-055037

Hink, L., Gubry-Rangin, C., Nicol, G. W., and Prosser, J. I. (2018). The consequences of niche and physiological differentiation of archaeal and bacterial ammonia oxidisers for nitrous oxide emissions. *ISME J.* 12, 1084–1093. doi: 10.1038/s41396-017-0025-5

Horrocks, C. A., Arango, J., Arevalo, A., Nuñez, J., Cardoso, J. A., and Dungait, J. A. J. (2019). Smart forage selection could significantly improve soil health in the tropics. *Sci. Total Environ.* 688, 609–621. doi: 10.1016/j.scitotenv.2019.06.152

IPCC (2013). Climate change 2013: The physical science basis. Contribution of working group I to the fifth assessment report of the intergovernmental panel on climate change. Cambridge University.

Karwat, H., Moreta, D., Arango, J., Núñez, J., Rao, I., Rincón, Á., et al. (2017). Residual effect of BNI by Brachiaria humidicola pasture on nitrogen recovery and grain yield of subsequent maize. *Plant Soil* 420, 389–406. doi: 10.1007/s11104-017-3381-z

Lan, X., Thoning, K.W., and Dlugokencky, E.J. (2022). Trends in globally-averaged CH4, N2O, and SF6 determined from NOAA global monitoring laboratory measurements. Version 2023–2001.

Lata, J. C., Durand, J., Lensi, R., and Abbadie, L. (1999). Stable coexistence of contrasted nitrification statuses in a wet tropical savanna ecosystem. *Funct. Ecol.* 13, 762–768. doi: 10.1046/j.1365-2435.1999.00380.x

Lata, J. C. C., Le Roux, X., Koffi, K. F., Ye, L., Srikanthasamy, T., Konare, S., et al. (2022). The causes of the selection of biological nitrification inhibition (BNI) in relation to ecosystem functioning and a research agenda to explore them. *Biol. Fertil. Soils* 58, 207–224. doi: 10.1007/s00374-022-01630-3

Liu, X., Zhang, Y., Han, W., Tang, A., Shen, J., Cui, Z., et al. (2013). Enhanced nitrogen deposition over China. *Nature* 494, 459–462. doi: 10.1038/nature11917

Lombardi, B., Loaiza, S., Trujillo, C., Arevalo, A., Vázquez, E., Arango, J., et al. (2022). Greenhouse gas emissions from cattle dung depositions in two Urochloa forage fields with contrasting biological nitrification inhibition (BNI) capacity. *Geoderma* 406:115516. doi: 10.1016/j.geoderma.2021.115516

Lu, R. (2000). *Analytical Methods for Soil and Agro-Chemistry*. Beijing: China Agricultural Science and Technology Press

Lu, Y. F., Zhang, X. N., Jiang, J. F., Kronzucker, H. J., Shen, W. S., and Shi, W. M. (2019). Effects of the biological nitrification inhibitor 1,9-decanediol on nitrification and ammonia oxidizers in three agricultural soils. *Soil Biol. Biochem.* 129, 48–59. doi: 10.1016/j.soilbio.2018.11.008

Luo, J., Wyatt, J., van der Weerden, T. J., Thomas, S. M., de Klein, C. A. M., Li, Y., et al. (2017). Potential hotspot areas of nitrous oxide emissions from grazed pastoral dairy farm systems. *Adv. Agron.* 145, 205–268. doi: 10.1016/bs.agron.2017.05.006

Marschner, P. (2011). *Marschner's Mineral Nutrition of Higher Plants* (*3rd Edn*). London, UK: Elsevier, 651

Merbold, L., Eugster, W., Stieger, J., Zahniser, M., Nelson, D., and Buchmann, N. (2014). Greenhouse gas budget (CO_2, CH_4 and N_2O) of intensively managed grassland following restoration. *Glob. Chang. Biol.* 20, 1913–1928. doi: 10.1111/gcb.12518

Mosier, A. R., Duxbury, J. M., Freney, J. R., Heinemeyer, O., and Minami, K. (1996). Nitrous oxide emissions from agricultural fields: assessment, measurement and mitigation. *Plant Soil* 181, 95–108. doi: 10.1007/BF00011296

Nardi, P., Akutsu, M., Pariasca-Tanaka, J., and Wissuwa, M. (2013). Effect of methyl 3-4-hydroxyphenyl propionate, a sorghum root exudate, on N dynamic, potential nitrification activity and abundance of ammonia-oxidizing bacteria and archaea. *Plant Soil* 367, 627–637. doi: 10.1007/s11104-012-1494-y

Nardi, P., Laanbroek, H. J., Nicol, G. W., Renella, G., Cardinale, M., Pietramellara, G., et al. (2020). Biological nitrification inhibition in the rhizosphere: determining interactions and impact on microbially mediated processes and potential applications. *FEMS Microbiol. Rev.* 44, 874–908. doi: 10.1093/femsre/fuaa037

Niu, Y., Luo, J., Liu, D., Müller, C., Zaman, M., Lindsey, S., et al. (2018). Effect of biochar and nitrapyrin on nitrous oxide and nitric oxide emissions from a sandy loam soil cropped to maize. *Biol. Fertil. Soils* 54, 645–658. doi: 10.1007/s00374-018-1289-2

Nuñez, J., Arevalo, A., Karwat, H., Egenolf, K., Miles, J., Chirinda, N., et al. (2018). Biological nitrification inhibition activity in a soil-grown biparental population of the forage grass, *Brachiaria humidicola*. *Plant Soil* 426, 401–411. doi: 10.1007/s11104-018-3626-5

Poudel, D. D., Horwath, W. R., Lanini, W. T., Temple, S. R., and Van Bruggen, A. H. C. (2002). Comparison of soil N availability and leaching potential, crop yields and weeds in organic, low-input and conventional farming systems in northern California. *Agric. Ecosyst. Environ.* 90, 125–137. doi: 10.1016/S0167-8809(01)00196-7

Ravishankara, A. R., Daniel, J. S., and Portmann, R. W. (2009). Nitrous oxide (N_2O): the dominant ozone-depleting substance emitted in the 21st century. *Science* 326, 123–125. doi: 10.1126/science.1176985

Rochette, P., van Bochove, E., Prévost, D., Angers, D. A., Coté, D., and Bertrand, N. (2000). Soil carbon and nitrogen dynamics following application of pig slurry for the 19th consecutive year. II. Nitrous oxide fluxes and mineral nitrogen. *Soil Sci. Soc. Am. J.* 64, 1396–1403. doi: 10.2136/sssaj2000.6441396x

Rodgers, G. A. (1986). Nitrification inhibitors in agriculture. *J. Environ. Sci. Health Part A* 21, 701–722. doi: 10.1080/10934528609375320

Stein, L. Y. (2020). The long-term relationship between microbial metabolism and greenhouse gases. *Trends Microbiol.* 28, 500–511. doi: 10.1016/j.tim.2020.01.006

Subbarao, G. V., Ito, O., Sahrawat, K. L., Berry, W. L., Nakahara, K., Ishikawa, T., et al. (2006). Scope and strategies for regulation of nitrification in agricultural systems - challenges and opportunities. *Crit. Rev. Plant Sci.* 25, 303–335. doi: 10.1080/07352680600794232

Subbarao, G. V., Nakahara, K., Hurtado, M. P., Ono, H., Moreta, D. E., Salcedo, A. F., et al. (2009). Evidence for biological nitrification inhibition in *Brachiaria* pastures. *Proc. Natl. Acad. Sci. U. S. A.* 106, 17302–17307. doi: 10.1073/pnas.0903694106

Subbarao, G. V., Nakahara, K., Ishikawa, T., Ono, H., Yoshida, M., Yoshihashi, T., et al. (2013). Biological nitrification inhibition (BNI) activity in sorghum and its characterization. *Plant Soil* 366, 243–259. doi: 10.1007/s11104-012-1419-9

Subbarao, G. V., Rondon, M., Ito, O., Ishikawa, T., Rao, I. M., Nakahara, K., et al. (2007). Biological nitrification inhibition (BNI) - is it a widespread phenomenon? *Plant Soil* 294, 5–18. doi: 10.1007/s11104-006-9159-3

Subbarao, G. V., Sahrawat, K. L., Nakahara, K., Ishikawa, T., Kishii, M., Rao, I. M., et al. (2012). Biological nitrification inhibition-a novel strategy to regulate nitrification in agricultural systems. *Adv. Agron.* 114, 249–301. doi: 10.1016/B978-0-12-394275-3.00001-8

Subbarao, G. V., Yoshihashi, T., Worthington, M., Nakahara, K., Ando, Y., Sahrawat, K. L., et al. (2015). Suppression of soil nitrification by plants. *Plant Sci.* 233, 155–164. doi: 10.1016/j.plantsci.2015.01.012

Sun, L., Lu, Y. F., Yu, F. W., Kronzucker, H. J., and Shi, W. M. (2016). Biological nitrification inhibition by rice root exudates and its relationship with nitrogen-use efficiency. *New Phytol.* 212, 646–656. doi: 10.1111/nph.14057

Teutscherová, N., Vázquez, E., Trubač, J., Villegas, D. M., Subbarao, G. V., Pulleman, M., et al. (2022). Gross N transformation rates in soil system with contrasting Urochloa genotypes do not confirm the relevance of BNI as previously assessed in vitro. *Biol. Fertil. Soils* 58, 321–331. doi: 10.1007/s00374-021-01610-z

UNEP (2013). Drawing down N2O to protect climate and the ozone layer.

Van Groenigen, J. W., Kasper, G. J., Velthof, G. L., Van Den Pol-Van Dasselaar, A., and Kuikman, P. J. (2004). Nitrous oxide emissions from silage maize fields under different mineral nitrogen fertilizer and slurry applications. *Plant Soil* 263, 101–111. doi: 10.1023/B:PLSO.0000047729.43185.46

van Groenigen, J. W., Velthof, G. L., Oenema, O., Van Groenigen, K. J., and Van Kessel, C. (2010). Towards an agronomic assessment of N_2O emissions: a case study for arable crops. *Eur. J. Soil Sci.* 61, 903–913. doi: 10.1111/j.1365-2389.2009.01217.x

Venterea, R. T., Bijesh, M., and Dolan, M. S. (2011). Fertilizer source and tillage effects on yield-scaled nitrous oxide emissions in a corn cropping system. *J. Environ. Qual.* 40, 1521–1531. doi: 10.2134/jeq2011.0039

Walkley, A., and Black, I. A. (1934). An examination of Degtjareff method for determining soil organic matter and a proposed modification of the chromic acid titration method. *Soil Sci.* 37, 29–38. doi: 10.1097/00010694-193401000-00003

Wang, X., Bai, J., Xie, T., Wang, W., Zhang, G., Yin, S., et al. (2021). Effects of biological nitrification inhibitors on nitrogen use efficiency and greenhouse gas emissions in agricultural soils: a review. *Ecotoxicol. Environ. Saf.* 220:112338. doi: 10.1016/j.ecoenv.2021.112338

Weiske, A., Benckiser, G., and Ottow, J. C. G. (2001). Effect of the new nitrification inhibitor DMPP in comparison to DCD on nitrous oxide (N_2O) emissions and methane (CH4) oxidation during 3 years of repeated applications in field experiments. *Nutr. Cycl. Agroecosyst.* 60, 57–64. doi: 10.1023/a:1012669500547

Wolf, B., Zheng, X., Brüggemann, N., Chen, W., Dannenmann, M., Han, X., et al. (2010). Grazing-induced reduction of natural nitrous oxide release from continental steppe. *Nature* 464, 881–884. doi: 10.1038/nature08931

Wu, D., Senbayram, M., Well, R., Brüggemann, N., Pfeiffer, B., Loick, N., et al. (2017). Nitrification inhibitors mitigate N_2O emissions more effectively under straw-induced conditions favoring denitrification. *Soil Biol. Biochem.* 104, 197–207. doi: 10.1016/j.soilbio.2016.10.022

Xie, L., Liu, D., Müller, C., Jansen-Willems, A., Chen, Z., Niu, Y., et al. (2022). *Brachiaria humidicola* cultivation enhances soil nitrous oxide emissions from tropical grassland by promoting the denitrification potential: a ^{15}N tracing study. *Agriculture* 12:1940. doi: 10.3390/agriculture12111940

Ye, G., Lin, Y., Liu, D., Chen, Z., Luo, J., Bolan, N., et al. (2019). Long-term application of manure over plant residues mitigates acidification, builds soil organic carbon and shifts prokaryotic diversity in acidic Ultisols. *Appl. Soil Ecol.* 133, 24–33. doi: 10.1016/j.apsoil.2018.09.008

Zakir, H. A. K. M. K. M. A. K. M., Subbarao, G. V. V., Pearse, S. J. J., Gopalakrishnan, S., Ito, O., Ishikawa, T., et al. (2008). Detection, isolation and characterization of a root-exuded compound, methyl 3-(4-hydroxyphenyl) propionate, responsible for biological nitrification inhibition by sorghum (Sorghum bicolor). *New Phytol.* 180, 442–451. doi: 10.1111/j.1469-8137.2008.02576.x

Zerulla, W., Barth, T., Dressel, J., Erhardt, K., von Locquenghien, K. H., Pasda, G., et al. (2001). 3, 4-Dimethylpyrazole phosphate (DMPP)–a new nitrification inhibitor for agriculture and horticulture. *Biol. Fertil. Soils* 34, 79–84. doi: 10.1007/s003740100380

Zhang, X., Davidson, E. A., Mauzerall, D. L., Searchinger, T. D., Dumas, P., and Shen, Y. (2015). Managing nitrogen for sustainable development. *Nature* 528, 51–59. doi: 10.1038/nature15743

frontiers | Frontiers in Microbiology

TYPE Original Research
PUBLISHED 21 July 2023
DOI 10.3389/fmicb.2023.1130298

OPEN ACCESS

EDITED BY
Huan Zhong,
Nanjing University, China

REVIEWED BY
Yucheng Wu,
Institute of Soil Science, Chinese Academy of Sciences (CAS), China
Xi-En Long,
Nantong University, China
Yongping Kou,
Chengdu Institute of Biology, Chinese Academy of Sciences (CAS), China

*CORRESPONDENCE
Jiahua Guo
✉ jiahua_guo@nwu.edu.cn
Baoli Zhu
✉ baoli.zhu@isa.ac.cn

RECEIVED 23 December 2022
ACCEPTED 23 June 2023
PUBLISHED 21 July 2023

CITATION
Han L, Qin H, Wang J, Yao D, Zhang L, Guo J and Zhu B (2023) Immediate response of paddy soil microbial community and structure to moisture changes and nitrogen fertilizer application.
Front. Microbiol. 14:1130298.
doi: 10.3389/fmicb.2023.1130298

Immediate response of paddy soil microbial community and structure to moisture changes and nitrogen fertilizer application

Linrong Han[1,2], Hongling Qin[2], Jingyuan Wang[2,3], Dongliang Yao[3,4], Leyan Zhang[2,3], Jiahua Guo[1]*and Baoli Zhu[2]*

[1]Shaanxi Key Laboratory of Earth Surface System and Environmental Carrying Capacity, College of Urban and Environmental Sciences, Northwest University, Xi'an, China, [2]Key Laboratory of Agro-Ecological Processes in Subtropical Region, Institute of Subtropical Agriculture, Chinese Academy of Sciences, Changsha, China, [3]College of Resources and Environment, Hunan Agricultural University, Changsha, China, [4]College of Biodiversity, Conservation Southwest Forestry University, Kunming, China

Water and fertilizer managements are the most common practices to maximize crop yields, and their long-term impact on soil microbial communities has been extensively studied. However, the initial response of microbes to fertilization and soil moisture changes remains unclear. In this study, the immediate effects of nitrogen (N)-fertilizer application and moisture levels on microbial community of paddy soils were investigated through controlled incubation experiments. Amplicon sequencing results revealed that moisture had a stronger influence on the abundance and community composition of total soil bacteria, as well as ammonia oxidizing-archaea (AOA) and -bacteria (AOB). Conversely, fertilizer application noticeably reduced the connectivity and complexity of the total bacteria network, and increasing moisture slightly exacerbated these effects. NH_4^+-N content emerged as a significant driving force for changes in the structure of the total bacteria and AOB communities, while NO_3^--N content played more important role in driving shifts in AOA composition. These findings indicate that the initial responses of microbial communities, including abundance and composition, and network differ under water and fertilizer managements. By providing a snapshot of microbial community structure following short-term N-fertilizer and water treatments, this study contributes to a better understanding of how soil microbes respond to long-term agriculture managements.

KEYWORDS

paddy soil, fertilization, moisture levels, microbial community, AOA, AOB, network analysis

1. Introduction

Water and nutrients availability are two critical factors that limit global crop productivity. Chemical fertilizer application has been one of the most important practices of modern agriculture (Soman et al., 2017; Chen et al., 2019; Li G. C. et al., 2021). Fertilization enhances soil fertility by increasing nutrient levels. However, current estimates suggest that the efficiency of fertilizer use is relatively low, with only 40%–50% of the applied nitrogen (N)-fertilizer being utilized by crops (Bijay-Singh and Craswell, 2021). Overfertilization not only depletes resources but also gives rise to various environmental issues, including water pollution, soil degradation,

greenhouse gas emissions, and loss of biodiversity (Francioli et al., 2016).

Microorganisms, as an integral component of the soil ecosystem, play a crucial role in maintaining soil quality and functions, and they are highly sensitive to changes in soil conditions (Li et al., 2016; Pan et al., 2016; Chen et al., 2017; Banerjee et al., 2018). Microorganisms drive the biogeochemical cycles of soil carbon and nitrogen, thus regulating the size of the soil carbon pool and the emissions of greenhouse gases like methane and N_2O into the atmosphere (Chai et al., 2019). Different agriculture management practices influence soil microbial communities through various mechanisms (Liang et al., 2012). For instance, manure application improves soil texture and organic matter content, thereby stimulating the growth and activity of soil microorganisms (Gomiero et al., 2011; Tang et al., 2019). In addition to benefiting crop yield, fertilization also provides nutrients and substrates for soil microbes (Feng et al., 2015; Yu et al., 2019). Soil moisture directly or indirectly affects microbial activities by regulating oxygen concentration and nutrient availability (Drenovsky et al., 2004; Pan et al., 2016). Furthermore, the presence of free water connecting soil particles can facilitate the mobility of nutrient and microbial cell, thereby shaping the structure of the soil microbial community (Zhou et al., 2002; Yuan et al., 2016).

Both fertilizer application and water content play crucial roles in sustaining crop productivity. However, their impact on soil microbial community structure and associated ecosystem function is not always positive. For instance, the addition of fertilizer can stimulate microbial activity, leading to the decomposition of organic matter and denitrification, which can result in soil carbon loss and the emission of greenhouse gases (Canarini et al., 2016; Bastida et al., 2017; Tian et al., 2017).

Moisture levels and the availability of N-compounds are considered important factors in regulating the communities of nitrifying and denitrifying microbes (Qin et al., 2021; Liu et al., 2022), whose activities determine soil N_2O emission fluxes (Wang et al., 2019; Jia et al., 2021). Interestingly, the highest N_2O emissions are often observed at different moisture levels, suggesting that microbial communities in diverse environments respond differently to the same factor. This response is influenced by synergistic interactions with other elements such as soil type, vegetation and historical conditions (e.g., Liu et al., 2018; Qin et al., 2020).

Contrasting responses in nitrification rates and denitrification enzyme activities to moisture and N-fertilizer addition have been reported in grassland soils from China and Australia (Long et al., 2017). Additionally, a microcosm simulation study highlighted the legacy effects of soil moisture on microbial community structure and the transcription of genes encoding key enzymes involved in N-cycling (Banerjee et al., 2016). In the Three Gorges Reservoir environment, ammonia oxidizing archaea (AOA) have been suggested to be more adaptive than ammonia oxidation bacteria (AOB) to water level fluctuations, while AOB have shown greater competitiveness than AOA in riparian soils of the Miyun Reservoir in Beijing (Wang et al., 2016; Liu et al., 2018).

The effects of agricultural practices on soil microbial communities and their activities are intricate, often requiring long-term implementation to observe significant changes. For instance, changes in microbial diversity have been captured after decades of organic framing (Hartmann et al., 2015) or reduced tillage (Tyler, 2019). However, microbial community changes are dynamic and exhibit spatiotemporal heterogeneity. Therefore, snapshots taken after long-term treatments provide limited insight into how microbes initiate their responses and adapt to these conditions. Additionally, the initial response of microbial communities to specific soil conditions remains unclear.

In this study, we aimed to investigate the responses of soil microbial communities and key ammonia-oxidizing microbes to short-term changes in moisture levels, represented by different water filled pore space (WFPS) values, and nitrogen fertilization, through high-throughput 16S rRNA and *amoA* genes sequencing. The abundance, community structure and network connections of total bacteria and ammonia-oxidizing microbes were scrutinized to address two primary objectives: (1) understanding how the soil bacterial community responds to short-term N-fertilization and water treatments, and (2) examining the combined effects of moisture levels and fertilization on the indigenous microbial community.

2. Materials and methods

2.1. Soil sample preparation

Paddy soil samples were collected from the National Agroecological Research Station (111°26′ E, 28°55′ N, altitude: 92.2–125.3 m) in Taoyuan, Hunan Province, China. The region is characterized by a subtropical humid monsoon climate, with an average annual temperature of 16.5°C, an average annual precipitation of 1,448 mm, an average daily sunshine duration of 15 h and 13 min, and an annual frost-free period of 283 days. Soil samples (0–20 cm) were collected, sieved (<2 mm), and stored. The soil is silty clay, developed from red clay, comprising 31.1% clay (<0.002 mm), 53.0% silt (0.002–0.05 mm), and 15.9% sand (0.05–2.00 mm). The other main soil properties were as follows: pH, 5.06; Soil Organic Matter, 34.73 g kg^{-1}; Total Phosphorus, 0.66 g kg^{-1}; Total N, 2.22 g kg^{-1}; Total Potassium, 11.76 g kg^{-1} (Qin et al., 2020).

2.2. Experimental design

In order to initiate the activity of microorganisms, the soil was pre-incubated for 2 days under dark conditions at 25°C, with 25% WFPS. Then microcosm culture experiments were set up in 1000 mL glass jars, each with 200 g (dry weight) preconditioned soil and was covered with a film to facilitate gas exchange. Two fertilization conditions, with nitrogen-fertilizer (NF) and without (CK) were prepared. For the NF treatment, NH_4NO_3 was applied at 720 μg N/g dry soil, which was equivalent to 200 kg N/ha on a surface area basis (200 g soils possess a surface area of 72 cm^2). For each treatment, five soil moisture levels, namely, 25%, 50%, 75%, 100%, and 125% WFPS were maintained, as previously described (Qin et al., 2020). All microcosms were incubated at 25°C for 96 h.

2.3. DNA extraction

At the end of incubation, 0.5 g of soil samples were used for DNA extraction as previously described (Qin et al., 2020), DNA quality and concentration were measured using a spectrophotometer (NanoDrop

ND-1000; ThermoFisher Scientific, Germany). For each incubation, three extractions were performed, and the DNA were pooled and stored at −80°C for further analysis.

2.4. PCR amplification

The AOA *amoA* gene, AOB *amoA* gene, and 16S rRNA gene sequences were amplified from soil DNA by PCR. A 25 μL PCR reaction contained 30 mM Tris-HCl (pH 8.3), 50 mM potassium chloride, 1.5 mM magnesium chloride, 10 μg bovine serum albumin, 200 μM of each deoxyribonucleoside triphosphate, 1.5 U of Taq DNA polymerase, 25 ng soil DNA and respective primers. Deionized water instead of DNA was used as a negative control. AOA, AOB *amoA* genes were amplified using Arch-amoA 23F (5′-ATGGTCTGGCTWAGACG-3′) and Arch-amoA 616R (5′-GGGGTTTCTACTGGTGGT-3′); amoA-1F (5′-GGGG TTTCTACTGGTGGT-3′) and amoA-2R (5′-CCCCTCKGSAAAGCCTTCTTC-3′), respectively; and for 16S rRNA the primer pair 1369F (5′-CGGTGAATACGTTCYCGG-3′) and 1492R (5′-GGWTACCTTGTTACGACT-3′) was used (Sahan and Muyzer, 2008). The amplification conditions for amoA genes were as follows: 95°C for 5 min, followed by 40 cycles: 94°C for 45 s, 60°C for 1 min, 72°C for 1 min; and a final extension at 72°C for 10 min. The PCR procedure for 16S rRNA was the same, except the annealing temperature was 54°C.

2.5. qPCR

qPCR was performed using ABI7900HT (Applied Biosystems, Foster City, CA, United States). qPCR was performed by the SYBR Green method. 16S rRNA-1369F/1492R was used to quantify total bacteria abundance, using Arch-*amoA* 23F/A616R and amoA-1F/2R for AOA and AOB, respectively (Rotthauwe et al., 1997; Tourna et al., 2008). Plasmids containing the target fragments diluted in 10 x series were used to make qPCR standard curves. The reaction systems are all 10 μ L, including:5 μL 2× SYBR green mix II (TaKaRa Biotechnology Co. Ltd., Dalian, China), 1 μL (10 μM) of forward and reverse primers, 0.2 μL 50× Rox Reference Dye (TaKaRa Biotechnology Co. Ltd., Dalian, China), 5 ng DNA template and deionized water.

The 16S rRNA qPCR procedure was as follows: 95°C pre-denaturation for 30 s; followed by 40 cycles of 95°C denaturation for 5 s, 60°C annealing for 30 s, 72°C extension for 30 s; and then a final extension at 72°C for 1 min. The AOA and AOB *amoA* gene qPCR procedures were the same, except that the annealing temperature was 53°C and 55°C, respectively. Deionized water instead of soil DNA was used as a negative control to determine DNA contamination (Vestergaard et al., 2017). Three parallels were done for each sample. The results were required to have an amplification efficiency greater than 95%, $R^2 > 0.999$, and a single peak for the melting curve.

2.6. AOA, AOB *amoA* gene and total 16S rRNA amplicon sequencing

The PCR processing, sequencing, and analysis of Illumina MiSeq sequencing data were performed as described in Qin et al. (2020). PCR mixtures contained 4 μL of 5× TransStart FastPfu buffer, 0.8 μL of forward primer (5 μM), 0.8 μL of reverse primer (5 μM), 2 μL of 2.5 mM dNTPs, 10 ng of template DNA and filled up to 20 μL with ddH_2O (TransGen, Beijing, China). PCR products were purified using AxyPrep DNA purification kit (Axygen Bio, United States), and were pooled in equimolar. Paired-end sequencing was performed on the Illumina Miseq platform (Illumina, San Diego, United States) at Shanghai Majorbio BioPharm Technology Co., Ltd., Shanghai. Raw FASTQ files were demultiplexed and quality filtered using QIIME2-2021.4. Barcodes were trimmed, low quality and chimeric sequences were deleted. All samples were normalized to a similar sequencing depth using MOTHUR. Operational clustering of taxonomic units (OTUs) was performed using UPARSE v7.1, based on a cut-off of 97% similarity (Yang et al., 2018). Taxonomic classification was using RDP and FunGene-amoA database for 16S rRNA and amoA sequences, respectively. Representative sequences of each OTU were analyzed using NCBI BLAST to further validate their taxonomy.

2.7. Network analysis

Co-occurrence network analyses were performed to explore how nitrogen fertilization and moisture treatments affect the co-occurrence patterns of microbial communities. Interaction networks were constructed using CoNet v1.1.1 in Cytoscape v.3.6.1 based on the Pearson and Spearman correlation values, mutual information similarity, and Bray–Curtis and Kullback–Leibler dissimilarity measures. All networks were visualized using the Fruchterman–Reingold layout with 9,999 permutations and implemented in Gephi. Global network properties such as average path length, average clustering coefficient, and positive and negative correlation of links are calculated.

2.8. Statistical analysis

Analysis of variance (ANOVA) was run in SPSS v. 18.0 and used to test the significant effects of moisture and fertilization treatments on soil physiochemical properties, microbial gene abundance and diversity. The copy numbers of all functional genes were log-transformed, and the normality of all data was checked before ANOVA. Principal co-ordinates analysis (PCoA) was used to assess the similarities between the community composition of AOA, AOB and total bacteria. Redundancy analysis (RDA) was used to evaluate the effect of soil properties (exchangeable NH_4^+-N, NO_3^--N, and DOC) on the community composition of AOA, AOB and total bacteria. ANOSIM (analysis of similarities) based on the Bray–Curtis distances of OTUs was used to measure the effects of moisture, fertilization, and their interactions on the community composition of AOA, AOB and total bacteria. PCoA, RDA and ANOSIM analysis were performed using R statistical software.

3. Results

3.1. Soil characteristics

N-fertilizer application clearly increased inorganic N content in the NF treatments, in which nitrate concentrations significantly

dropped with the increasing WFPS, and was undetectable in the 125% WFPS incubations, indicating a higher nitrate-consuming activity in higher moisture soils. Nitrate concentration was very low in all CK incubations, regardless the WFPS levels. Ammonium concentration peaked at moderate moisture level of 75% and 50% WFPS for the CK and NF incubations, respectively. However, if treating ammonium in the CK incubations as indigenous background and deducting it from corresponding NF incubations, the remaining ammonium (net NH_4^+) in NF incubations showed a decreasing trend along increasing WFPS levels, suggesting a possible active net ammonium consumption under higher moisture conditions (Table 1). DOC level in both treatments was similar under low moisture condition (25% and 50% WFPS), and it significantly increased when moisture was high (100% and 125% WFPS), especially in these of the CK treatment (Table 1).

3.2. Soil microbial abundance and diversity

Compared to diversity, the abundance of soil bacteria was more sensitive to water management, but not to N-fertilizer application (Table 2). For total bacteria, the abundance, Shannon index and PD index were affected by moisture levels. The total bacteria abundance was the lowest at 25% WFPS, while the Shannon and PD indexes were the lowest at 125% WFPS, irrespective of fertilization. For AOA and AOB communities, water management only affected their abundance, but not Shannon and PD index. AOB was always more abundant than AOA in all treatments (Figure 1). Fertilizer application had significant effect on total bacteria diversity, and decreased their Shannon index, especially under higher moisture conditions.

3.3. Soil bacterial community composition

Under 25% and 125% WFPS, the respective microbial composition on phylum level remained very similar between the CK and NF treatments. While under other WFPS conditions, fertilization significantly enhanced the relative abundance of *Firmicutes*, mainly at the expense of *Proteobacteria* abundance loss, when compared to the non-fertilized incubations (Figure 2A). The most dominant bacteria phyla were *Firmicutes*, *Proteobacteria*, *Actinobacteria*, *Chloroflexi*, *Planctomycetes*, *Acidobacteria*, and *Verrucomicrobia* (Figure 2A). The shift of relative abundance and composition of ammonia-oxidizing microorganisms at the OTU level appeared to be more responsive to water content changes (Figures 2B,C).

ANOSIM analysis indicated that both fertilization and water content had a significant effect on total bacteria community ($p < 0.05$), while their influence on AOA and AOB was less significant (Table 3). PCoA analysis showed that the total bacterial community of most incubations were separated between treatments of fertilization and non-fertilized controls (Figure 3A). The NF and CK treatments at 50%–100% WFPS were mostly grouped into respective clusters, albeit the microbial communities of both treatments at 25% and 125% WFPS were loosely distributed, indicating that "extreme" moisture conditions exerted additional influence on the bacterial community composition (Figure 3A). While, the communities of ammonia-oxidizing microorganisms could not be clearly divided between fertilization and non-fertilization treatments, nor among different WFPS levels, presumably due to the relatively slow growth rate of ammonia oxidizing microbes (Figures 3B,C). RDA analysis indicated that NO_3^-, NH_4^+ and DOC played an important role in shaping the community structure of total bacteria, AOA and AOB. Among them, the content of NO_3^--N had a greater effect on AOA, and NH_4^+-N had the largest effect on total bacteria and AOB (Figure 4; Table 4).

3.4. Network analysis

Microbial network analyses showed that fertilizer application reduced the connectivity and complexity of total bacterial networks (Figure 5; Table 5). Compared to the CK treatments, the average number of nodes and edges decreased by 45.37% and 75.84%, respectively. Higher WFPS levels led to stronger decrease in the network density and clustering coefficients in NF than in CK treatment, suggesting that increasing moisture aggravated the effects of fertilization on the complexity of bacterial networks. The modularity pattern also changed with fertilization and high moisture. In the non-fertilized incubations with relatively low WFPS, two large modules were formed, each containing a number of OTUs with relatively high connectivity (Figure 5A). And all dominant phyla were represented by well-connected OTUs approximately according to their relative abundances, suggesting a rather stable microbial community was maintained. Increasing moisture or nitrogen fertilization diminished modularity, with fewer nodes forming modules. And Firmicutes, or Chloroflexi and Planctomycetes became the respective dominant taxa with well-connected OTUs (Figures 5B,C). Under simultaneous N-fertilization and high moisture, the microbial network did not form clear modules, and highly connected nodes were mostly Firmicutes.

TABLE 1 Physicochemical properties of soil under different WFPS and fertilization treatments.

WFPS	NO_3^--N (mg/kg)		NH_4^+-N (mg/kg)		DOC (mg/kg)	
	CK	NF	CK	NF	CK	NF
25%	$0.85 \pm 0.17_a$	$343.65 \pm 42.23_a$	$74.43 \pm 2.93_e$	$388.71 \pm 26.48_{bc}$	$350.22 \pm 32.18_b$	$317.32 \pm 30.5_b$
50%	$0.49 \pm 0.03_b$	$324.74 \pm 12.13_a$	$135.53 \pm 2.72_b$	$432.14 \pm 11.27_a$	$311.2 \pm 20.9_b$	$293.79 \pm 26.38_b$
75%	—	$131.96 \pm 62.42_b$	$142.93 \pm 3.11_a$	$410.97 \pm 13.41_{ab}$	$334.23 \pm 20.92_b$	$405.42 \pm 44.45_a$
100%	—	$20.85 \pm 29.6_c$	$127.05 \pm 4.94_c$	$372.79 \pm 35.81_{cd}$	$624.04 \pm 17.32_a$	$458.62 \pm 53.18_a$
125%	—	—	$96.05 \pm 6.34_d$	$344.1 \pm 27.42_d$	$624.14 \pm 65.11_a$	$439.14 \pm 45.42_a$

Data in the table are mean ± standard deviation; different lowercase letters indicate significant differences between treatments for the same indicator ($P < 0.05$). CK, non-fertilized soil samples; NF, soil samples received nitrogen fertilization.

TABLE 2 Differences in the abundance and diversity indices of 16S rRNA, AOA and AOB affected by fertilization and water treatments.

Treatment			DF	SS	MS	F	*P*-value
Gene abundance	16S rRNA	Water	4	2.22	0.56	116.10	$P < 0.001$
		Fertilizer	1	<0.01	<0.01	0.85	$P = 0.45$
		Water × Fertilizer	4	0.33	0.08	18.43	$P < 0.001$
	AOA amoA	Water	4	0.96	0.24	119.00	$P < 0.001$
		Fertilizer	1	<0.01	0.01	1.78	$P = 0.31$
		Water × Fertilizer	4	0.31	0.08	16.71	$P < 0.001$
	AOB amoA	Water	4	0.06	0.02	4.82	$P = 0.03$
		Fertilizer	1	0.09	0.09	11.61	$P = 0.08$
		Water × Fertilizer	4	0.07	0.02	1.57	$P = 0.28$
Shannon index	16S rRNA	Water	4	5.92	1.48	32.61	$P < 0.001$
		Fertilizer	1	2.12	2.12	23.09	$P = 0.04$
		Water × Fertilizer	4	2.14	0.53	31.71	$P < 0.001$
	AOA amoA	Water	4	0.01	<0.01	0.20	$P = 0.93$
		Fertilizer	1	0.11	0.11	5.44	$P = 0.14$
		Water × Fertilizer	4	0.18	0.05	1.56	$P = 0.28$
	AOB amoA	Water	4	0.04	0.01	1.93	$P = 0.20$
		Fertilizer	1	0.01	<0.01	1.09	$P = 0.41$
		Water	4	0.03	<0.01	1.68	$P = 0.25$
PD index	16S rRNA	Fertilizer	4	1315.00	328.80	18.38	$P < 0.001$
		Water × Fertilizer	1	31.14	31.14	0.68	$P = 0.50$
		Water	4	56.13	14.03	2.05	$P = 0.18$
	AOA amoA	Fertilizer	4	71.16	17.79	0.68	$P = 0.63$
		Water × Fertilizer	1	13.46	13.46	7.16	$P = 0.16$
		Water	4	134.20	33.55	2.14	$P = 0.17$
	AOB amoA	Fertilizer	4	<0.01	<0.01	0.50	$P = 0.74$
		Water × Fertilizer	1	<0.01	<0.01	3.00	$P = 0.23$
		Water	4	<0.01	<0.01	0.50	$P = 0.74$

4. Discussion

Soil microbial communities play an essential role in various ecological processes, including nutrient cycling, organic matter turnover, greenhouse gas emission, and soil fertility and structure maintenance. Nitrogen compounds and moisture are considered key factors shaping bacterial community in soils (Wang S. et al., 2018; Wang R. et al., 2018). However, common agricultural practices aimed at maximizing crop productivity, such as fertilization, can introduce excessive nitrogen into agroecosystems, and may have adverse ecological effects. Excessive nitrogen supply may reduce soil microbial biomass, alter microbial diversity, community structure and enzyme activity (Wang et al., 2023). Therefore, understanding how soil microbial communities respond to nitrogen fertilization and moisture fluctuations is crucial for developing sustainable agricultural practices. While several studies have examined the long-term impact of nitrogen addition on soil microbial diversity and richness in different environments, the results have been inconsistent (Fierer and Jackson, 2006; Jing et al., 2015). Investigating the immediate changes in microbial communities following short-term nitrogen fertilization and moisture variations can provide insights into the microbial response processes under long-term agricultural management.

In this study, NH_4NO_3 was provided as the nitrogen fertilizer, introducing both nitrate and ammonium to the NF treatments. However, after 96 h incubation, nitrate concentration in the NF incubations decreased with increasing WFPS and became undetectable under 125% WFPS. The "net NH_4^+" in the NF treatments also showed a decreasing trend with higher WFPS levels (Table 1), indicating a higher consumption rate of both nitrate and ammonium under increased moisture conditions. Rice paddies are well known nitrogen cycling hotspots, and denitrification and anammox are likely the main processes responsible for nitrate and ammonium consumption, especially under high WFPS levels (Zhu et al., 2011). Ammonium was available in significant concentrations, which likely supported a higher abundance of AOB compared to AOA in all incubations (Figure 1). AOA are more dominant in oligotrophic environments, while AOB tend to dominate in eutrophic habitats (Jung et al., 2022). Among the AOA OTUs, OTU276, OTU278 and OTU279 were consistently abundant in almost all incubations, while OTU323 was the most dominant AOB (Figure 2B). These OTUs had

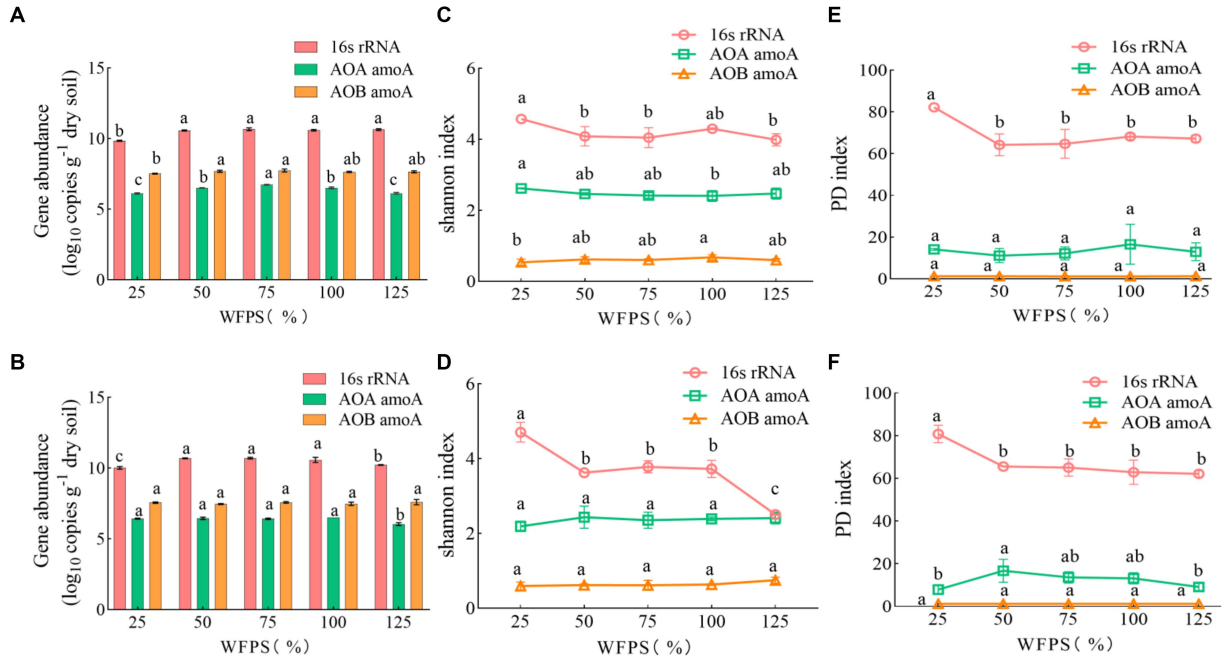

FIGURE 1
The abundance and diversity index of soil microbes under different WFPS and fertilization treatment conditions. Data are presented as mean and standard error (n =3). Data labeled by different letters indicate significant differences (p <0.05). **(A,C,E)** None-fertilized soil samples (CK); **(B,D,F)** Soil samples received nitrogen fertilization (NF).

their closest cultured relatives as *Nitrososphaera viennensis* EN76 and *Nitrosospira lacus* (Tourna et al., 2011; Urakawa et al., 2015), with *amoA* sequence similarities below 80 and 86%, respectively. Hence, the AOA and AOB OTUs identified in this study were mostly uncultured, indicating a vast unexplored diversity of ammonia-oxidizing microbes in agriculture ecosystems. The abundance and composition of AOA and AOB shifted after the short-term incubation, but it remains unclear if these microbes directly contributed to the removal of 'net NH_4^+', particularly under higher WFPS conditions that were anoxic. Future studies should conduct a comprehensive analysis of the rates of different N-cycling processes, including the recently discovered oxygenic denitrification and nitrate-driven anaerobic methane oxidation (Zhu et al., 2020), to better understand their differential responses to N addition.

Soil moisture levels have been identified as a significant factor influencing soil microbial composition and activity (Shi et al., 2018). Adequate moisture levels can promote microbial growth and metabolic activities (Francioli et al., 2016; Yang et al., 2019). In our study, the microbial diversity and abundance responded differently to short-term fertilization and water management. Our results showed that total soil bacteria abundance was more responsive to water content than to fertilization (Table 2). This suggests that microbial growth was generally more strongly influenced by water content than nitrogen addition in the short-term incubation. This could be because the paddy soil was not N-limited, since there was sufficient residual ammonium present (Table 1). However, fertilization did increase bacteria diversity, likely due to the introduction of nitrate, which serves as a favorable electron acceptor for microbial respiration.

Firmicutes were the most dominant bacteria, especially in the NF treatments with higher WFPS (Figure 2). In the CK treatment with saturated moisture (125% WFPS), the relative abundance of Firmicutes (84.2%) was significantly higher than in other CK incubations (approximately 40%). This indicates a favorable response of Firmicutes to nitrogen addition and high moisture, consistent with previous findings (e.g., Supramaniam et al., 2016). Many Firmicutes are capable of forming spores, which confer high resistance to environmental stresses and enable quick response to substrate availability, making them one of the most common microbes in soils (Filippidou et al., 2016; Donhauser et al., 2021). Proteobacteria were abundant only in the CK treatments with moderate moisture levels (50%, 75%, and 100% WFPS). Interestingly, the relative abundance of Acidobacteria, Actinobacteria, Chloroflexi, and Planctomycetes was significant in both the CK and NF treatments with the lowest moisture (25% WFPS) but diminished in all other higher moisture incubations (Figure 2A). This indicates the influence of water management on soil microbial community structure. Acidobacteria and Chloroflexi members are often considered oligotrophs, and several studies have reported a decrease in their abundance with increasing concentrations of NO_3^--N and NH_4^+-N (Zhou et al., 2015; Wang R. et al., 2018) and higher water content (Zhalnina et al., 2015; Zhou et al., 2015; Li H. et al., 2021). However, some long-term field studies have found had no significant effect of water content on soil bacterial communities (Zhang et al., 2021), possibly because there was sufficient time for the local microbial community to recover from and adapt to moisture changes (Azarbad et al., 2020). These inconsistent findings highlight the need to study the immediate responses of microbes to environmental changes.

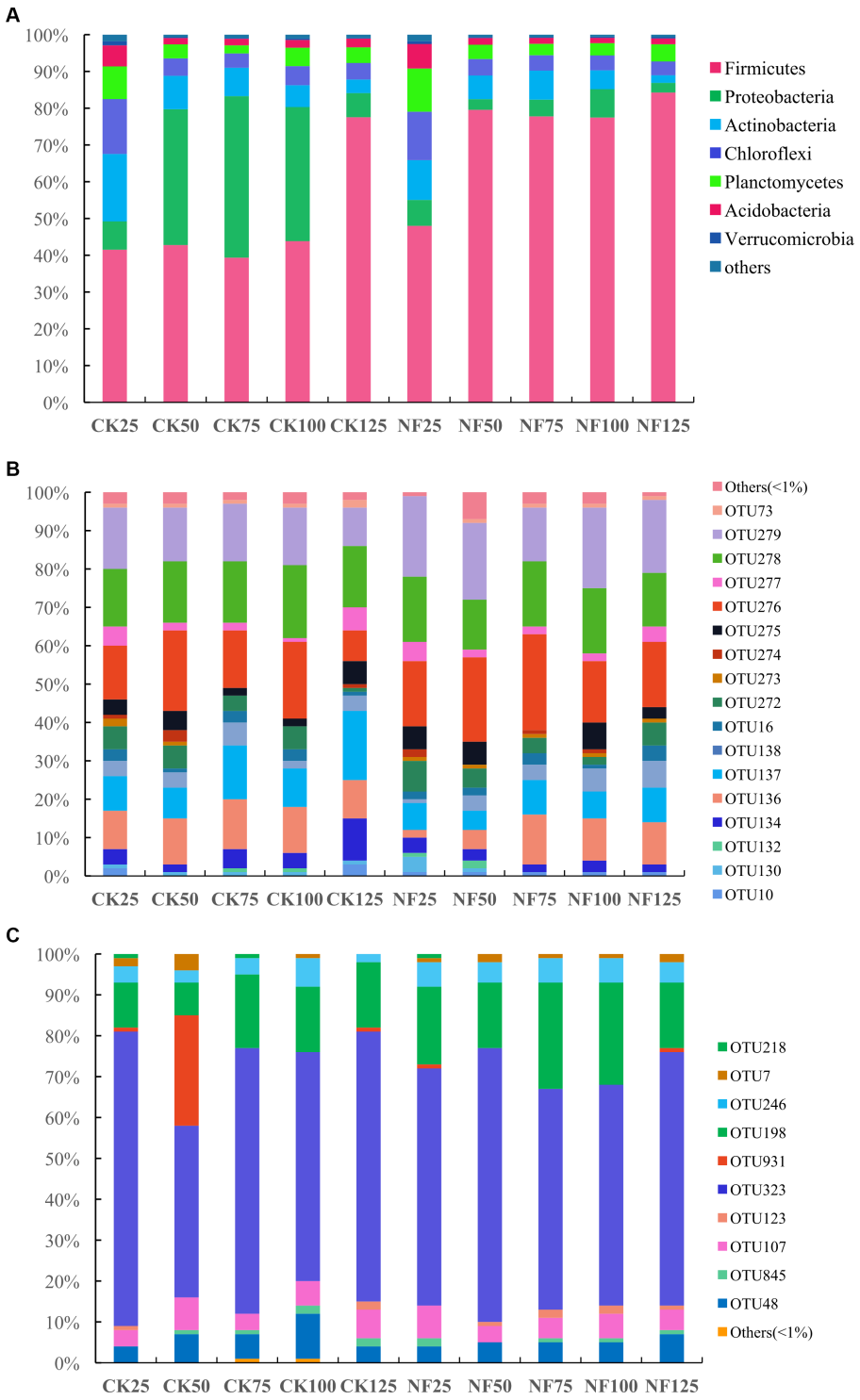

FIGURE 2
Relative abundance of soil microbes at the phylum (total bacteria) or OTU (AOA and AOB) level. CK, none-fertilized soil samples; NF, soil samples with nitrogen-fertilization; 25, 50, 75, 100, and 125 indicate the respective WFPS levels: 25%, 50%, 75%, 100%, and 125%. **(A)** total bacteria; **(B)** AOA; and **(C)** AOB.

In the present study, after a four-day incubation, it was observed that bacterial community structure, rather than total bacterial abundance, showed a stronger response to fertilization. Nitrogen fertilization has been demonstrated to be a significant factor in shaping soil microbial community (Yuan et al., 2015; Wu et al., 2021; Jin et al., 2022), probably by providing substrates and energy sources for indigenous microbes or due to nutrients imbalances resulting from a pulse input of N (Eo and Park, 2016). The bacterial abundance

TABLE 3 Intergroup similarity analysis (ANOSIM) of the fertilization and water content treatments.

ANOSIM		Statistic (R)	Pr	R^2	*P*
16S rRNA	Fertilization	0.188	0.006	0.747	0.004
	Water	0.614	0.001	0.558	0.001
AOA	Fertilization	−0.019	0.285	0.152	0.649
	Water	0.034	0.023	0.070	0.143
AOB	Fertilization	0.031	0.31	0.155	0.235
	Water	0.123	0.003	0.133	0.015

Statistic R value, the closer to 1, the greater the difference between groups than the difference within each group; R^2, the greater the value, the higher degree of explanation; Pr, <0.05 indicates high confidence in this test. *P*, significant difference.

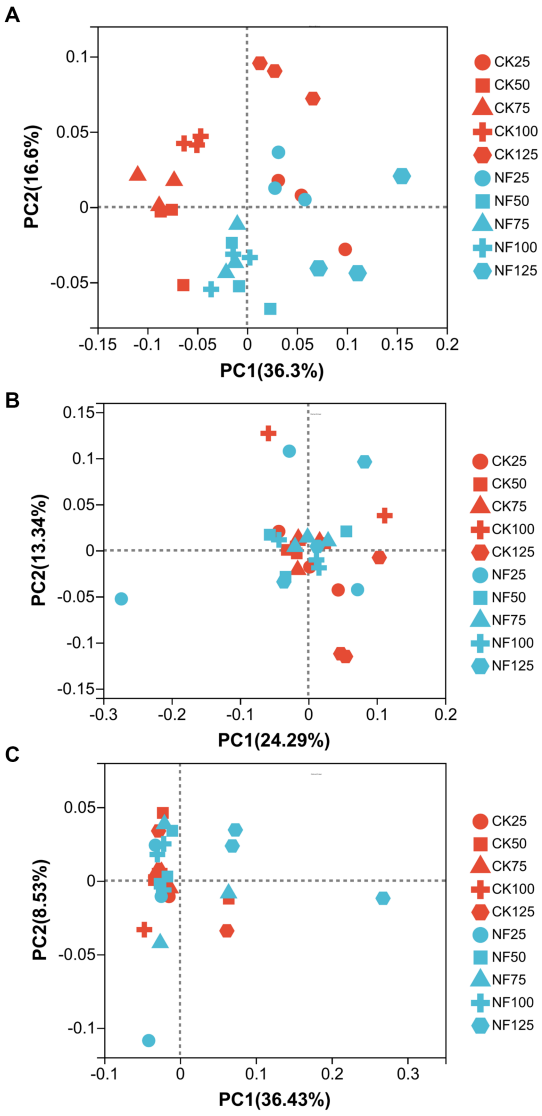

FIGURE 3
Principal coordinate analysis (PCoA) of the bacterial community structure. CK, soil samples with no N application; NF, soil samples with N-fertilization; 25, 50, 75, 100, and 125 represent WFPS level is 25%, 50%, 75%, 100%, 125%. **(A)** Total bacteria; **(B)** AOA; **(C)** AOB.

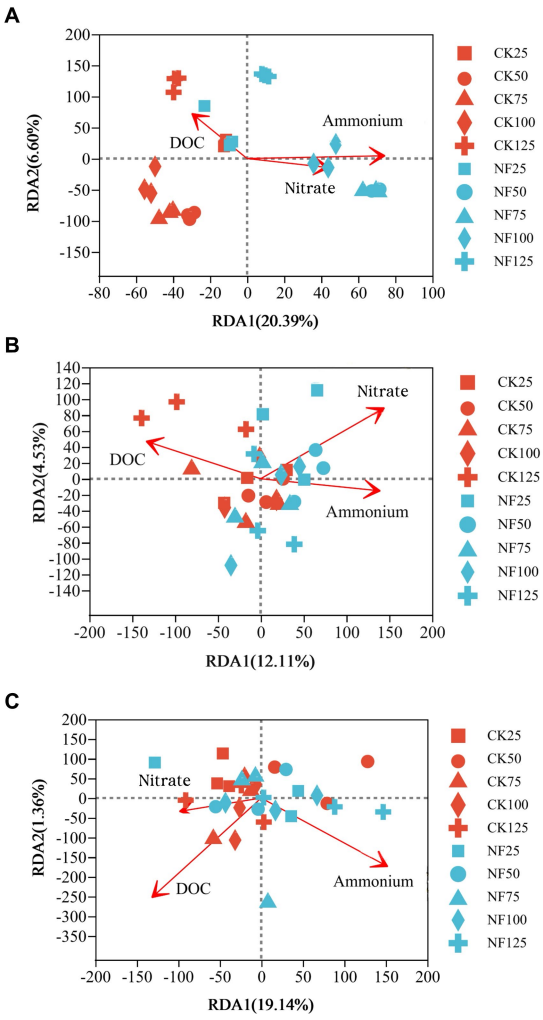

FIGURE 4
Redundancy analysis (RDA) of the effect of soil characteristics on the microbial community composition. CK, soil samples with no nitrogen application; NF, soil samples with nitrogen application; 25, 50, 75, 100, 125 represent WFPS level is 25%, 50%, 75%, 100%, 125%. **(A)** Total bacteria; **(B)** AOA; **(C)** AOB.

remained relatively stable after the 96-h incubation, which is consistent with the fact that soil bacteria generally have very slow growth rates, with a doubling time being over 100 days (Harris and Paul, 1994). Nevertheless, the shift in microbial community indicates a differential response among distinct groups of microbes. In long-term fertilizer treatments, both the structure and abundance of soil bacterial communities can also be influenced by indirect environmental changes, such as soil acidification resulting from nitrification (Zhou et al., 2015; Wang et al., 2016; Lin et al., 2020). However, some studies suggest that soil parent material plays a key role in shaping agricultural soil bacterial communities from a long-term perspective (Sheng et al., 2023).

The number of nodes, edges and average clustering coefficients decreased in the microbial networks of the NF treatment and higher moisture incubations, and the interaction pattern among soil microbes also shifted (Table 5). In the non-fertilized treatment, increasing moisture reduced the ratio of negative interactions, which represent

microbial competition and are considered important for stabilizing microbial communities and their ecological services (van der Heijden et al., 2010; Hoek et al., 2016). These results indicated that both fertilization and higher water content rapidly reduced the complexity and stability of soil bacterial communities. Based on the degree of each node, key taxa identified in the microbial network mostly belonged to Firmicutes, Proteobacteria, Actinobacteria, Chloroflexi and Planctomycetes, indicating their crucial role in paddy soils under fertilization and water management. In recent years, the construction of microbial network has become increasingly popular for high-throughput sequencing data analysis and been helpful in uncovering interactions from complex datasets (Deng et al., 2012; Faust and Raes, 2012). However, it should be noted that the inference of biotic interactions from the cooccurrence or absence of sequences may not always reliable, and conclusions should be drawn with caution (Faust, 2021).

5. Conclusion

The composition and abundance of soil bacteria and ammonia-oxidizing microorganisms in paddy fields demonstrated varying degrees of response to fertilization and moisture, with a higher sensitivity to changes in water content levels. The impact of fertilization on the stability and complexity of bacteria networks was evident and slightly exacerbated by elevated moisture. Changes in the

TABLE 4 Redundancy analysis (RDA) of the effect of different soil characteristics on microbial community composition.

RDA analyze		RD^1	RD^2	R^2	*P*
16S rRNA	Nitrite	0.998	−0.059	0.234	0.028
	Ammonium	0.998	0.064	0.696	0.001
	DOC	−0.780	0.626	0.270	0.020
AOA	Nitrite	0.856	0.518	0.470	0.001
	Ammonium	1.000	0.005	0.293	0.003
	DOC	−0.977	0.211	0.282	0.014
AOB	Nitrite	−0.599	−0.801	0.037	0.595
	Ammonium	0.903	−0.430	0.063	0.430
	DOC	0.885	−0.466	0.042	0.573

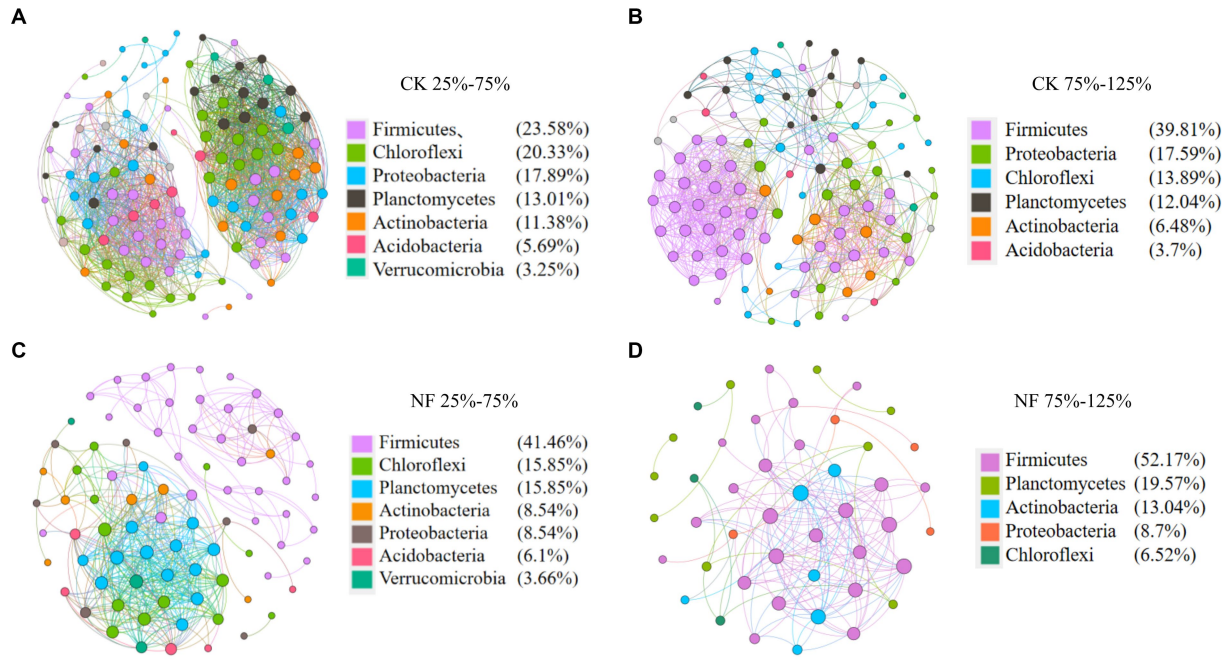

FIGURE 5
Co-occurrence analysis of total bacteria. Nodes are colored according to microbial taxonomy (phylum), edges indicate correlations among nodes. CK, none-fertilized soil samples; NF, soil samples received N-fertilization; 25, 50, 75, 100, 125 indicate respective WFPS level is 25%, 50%, 75%, 100%, 125%. **(A)** CK 25%–75%; **(B)** CK 75%–125%; **(C)** NF25%–75%; **(D)** NF 75%–125%.

TABLE 5 Node-level topological features of the co-occurrence network of fertilization and non-fertilized treatments grouped by moisture levels.

16S rRNA	CK 25%–75%	CK 75%-125%	NF 25%–75%	NF 75%-125%
Number of nods	123	108	82	46
Number of edges	1,634	764	458	155
Number of positive correlations	77.42%	85.08%	97.51%	81.29%
Number of negative correlations	22.58%	14.92%	2.49%	18.71%
Average degree	26.57	14.15	11.18	6.74
Network diameter	8	9	4	6
Average clustering coefficient	0.77	0.64	0.73	0.61
Average path distance	3.78	3.64	1.80	2.36
Network density	0.22	0.13	0.14	0.15

CK, soil samples with no nitrogen application; NF, soil samples with nitrogen-fertilization; WFPS level is used to divide low moisture (25%–75%) and high moisture (75%–125%) conditions.

total bacteria and AOB community showed significant correlations with NH_4^+-N content, while NO_3^--N content played a crucial role in driving changes in the AOA community structure. Studying the initial changes in microbial community composition and structure in response to water and fertilizer applications can provide valuable insights into how soil microbes adapt to long-term agricultural practices, thus aiding in the development of more sustainable agricultural approaches.

Data availability statement

The original contributions presented in the study are included in the article/supplementary material, further inquiries can be directed to the corresponding authors.

Author contributions

LH, HQ, JW, DY, and LZ carried out the experiments. HQ, LH, BZ, and JG did sequencing and data analysis. LH, HQ, JG, and BZ wrote the manuscript. All authors contributed to the article and approved the submitted version.

Funding

The research was supported by the National Key Research and Development Program of China (2021YFD1901203), the National Natural Science Foundation of China (project no. 42177104), and the National Ecosystem Science Data Center (no. NESDC20210204).

Conflict of interest

The authors declare that the research was conducted in the absence of any commercial or financial relationships that could be construed as a potential conflict of interest.

Publisher's note

All claims expressed in this article are solely those of the authors and do not necessarily represent those of their affiliated organizations, or those of the publisher, the editors and the reviewers. Any product that may be evaluated in this article, or claim that may be made by its manufacturer, is not guaranteed or endorsed by the publisher.

References

Azarbad, H., Tremblay, J., Giard-Laliberté, C., Bainard, L. D., and Yergeau, E. (2020). Four decades of soil water stress history together with host genotype constrain the response of the wheat microbiome to soil moisture. *FEMS Microbiol. Ecol.* 96:fiaa098. doi: 10.1093/femsec/fiaa098

Banerjee, S., Helgason, B., Wang, L., Winsley, T., Ferrari, B. C., and Siciliano, S. D. (2016). Legacy effects of soil moisture on microbial community structure and N2O emissions. *Soil Biol. Biochem.* 95, 40–50. doi: 10.1016/j.soilbio.2015.12.004

Banerjee, S., Schlaeppi, K., and van der Heijden, M. G. A. (2018). Keystone taxa as drivers of microbiome structure and functioning. *Nat. Rev. Microbiol.* 16, 567–576. doi: 10.1038/s41579-018-0024-1

Bastida, F., Torres, I. F., Hernández, T., and García, C. (2017). The impacts of organic amendments: do they confer stability against drought on the soil microbial community? *Soil Biol. Biochem.* 113, 173–183. doi: 10.1016/j.soilbio.2017.06.012

Bijay-Singh, C. E., and Craswell, E. (2021). Fertilizers and nitrate pollution of surface and ground water: an increasingly pervasive global problem. *SN Appl. Sci.* 3:518. doi: 10.1007/s42452-021-04521-8

Canarini, A., Carrillo, Y., Mariotte, P., Ingram, L., and Dijkstra, F. A. (2016). Soil microbial community resistance to drought and links to C stabilization in an Australian grassland. *Soil Biol. Biochem.* 103, 171–180. doi: 10.1016/j.soilbio.2016.08.024

Chai, R., Ye, X., Ma, C., Wang, Q., Tu, R., Zhang, L., et al. (2019). Greenhouse gas emissions from synthetic nitrogen manufacture and fertilization for main upland crops in China. *Carbon Balance Manag.* 14:20. doi: 10.1186/s13021-019-0133-9

Chen, J. H., Chen, D., Xu, Q. F., Fuhrmann, J. J., Li, L. Q., Pan, G. X., et al. (2019). Organic carbon quality, composition of main microbial groups, enzyme activities, and temperature sensitivity of soil respiration of an acid paddy soil treated with biochar. *Biol. Fertil. Soils* 55, 185–197. doi: 10.1007/s00374-018-1333-2

Chen, Z. M., Wang, H., Liu, X., Zhao, X., Lu, D., Zhou, J., et al. (2017). Changes in soil microbial community and organic carbon fractions under short-term straw return in a rice-wheat cropping system. *Soil Tillage Res.* 165, 121–127. doi: 10.1016/j.still.2016.07.018

Deng, Y., Jiang, Y. H., Yang, Y., He, Z., Luo, F., Zhou, J., et al. (2012). Molecular ecological network analyses. *Bioinformatics* 13:113. doi: 10.1186/1471-2105-13-113

Donhauser, J., Qi, W., Bergk-Pinto, B., and Frey, B. (2021). High temperatures enhance the microbial genetic potential to recycle C and N from necromass in high-mountain soils. *Glob. Chang. Biol.* 27, 1365–1386. doi: 10.1111/gcb.15492

Drenovsky, R. E., Vo, D., Graham, K. J., and Scow, K. M. (2004). Soil water content and organic carbon availability are major determinants of soil microbial community composition. *Microb. Ecol.* 48, 424–430. doi: 10.1007/s00248-003-1063-2

Eo, J., and Park, K. C. (2016). Long-term effects of imbalanced fertilization on the composition and diversity of soil bacterial community. *Agric. Ecosyst. Environ.* 231, 176–182. doi: 10.1016/j.agee.2016.06.039

Faust, K. (2021). Open challenges for microbial network construction and analysis. *ISME J.* 15, 3111–3118. doi: 10.1038/s41396-021-01027-4

Faust, K., and Raes, J. (2012). Microbial interactions: from networks to models. *Nat. Rev. Microbiol.* 10, 538–550. doi: 10.1038/nrmicro2832

Feng, Y. Z., Chen, R., Hu, J., Zhao, F., Wang, J., Chu, H., et al. (2015). *Bacillus asahii* comes to the fore in organic manure fertilized alkaline soils. *Soil Biol. Biochem.* 81, 186–194. doi: 10.1016/j.soilbio.2014.11.021

Fierer, N., and Jackson, R. B. (2006). The diversity and biogeography of soil bacterial communities. *PNAS* 103, 626–631. doi: 10.1073/pnas.0507535103

Filippidou, S., Wunderlin, T., Junier, T., Jeanneret, N., Dorador, C., Molina, V., et al. (2016). Combination of extreme environmental conditions favor the prevalence of endospore-forming firmicutes. *Front. Microbiol.* 7:1707. doi: 10.3389/fmicb.2016.01707

Francioli, D., Schulz, E., Lentendu, G., Wubet, T., Buscot, F., and Reitz, T. (2016). Mineral vs. organic amendments: microbial community structure, activity and abundance of agriculturally relevant microbes are driven by long-term fertilization strategies. *Front. Microbiol.* 14:1446. doi: 10.3389/fmicb.2016.01446

Gomiero, T., Pimentel, D., and Paoletti, M. G. (2011). Environmental impact of different agricultural management practices: conventional vs. Organic agriculture. *Crit. Rev. Plant Sci.* 30, 95–124. doi: 10.1080/07352689.2011.554355

Harris, D., and Paul, E. A. (1994). Measurement of bacterial growth rates in soil. *Appl. Soil Ecol.* 1, 277–290. doi: 10.1016/0929-1393(94)90005-1

Hartmann, M., Frey, B., Mayer, J., Maeder, P., and Widmer, F. (2015). Distinct soil microbial diversity under long-term organic and conventional farming. *ISME J.* 9, 1177–1194. doi: 10.1038/ismej.2014.210

Hoek, T. A., Axelrod, K., Biancalani, T., Yurtsev, E. A., Liu, J., and Gore, J. (2016). Resource availability modulates the cooperative and competitive nature of a microbial cross feeding mutualism. *PLoS Biol.* 14:e1002540. doi: 10.1371/journal.pbio.1002540

Jia, M., Gao, Z., Gu, H., Zhao, C., Liu, M., Liu, F., et al. (2021). Effects of precipitation change and nitrogen addition on the composition, diversity, and molecular ecological network of soil bacterial communities in a desert steppe[J]. *PLoS One* 16:e0248194. doi: 10.1371/journal.pone.0248194

Jin, Y., Chen, Z., He, Y., White, J. F., and Li, C. (2022). Effects of achnatherum inebrians ecotypes and endophyte status on plant growth, plant nutrient, soil fertility and soil microbial community. *Soil Sci. Soc. Am. J.* 86, 1028–1042. doi: 10.1002/saj2.20420

Jing, X., Sanders, N. J., Shi, Y., Chu, H., Classen, A. T., Zhao, K., et al. (2015). The links between ecosystem multifunctionality and above- and belowground biodiversity are mediated by climate. *Nat. Commun.* 6:8159. doi: 10.1038/ncomms9159

Jung, M. Y., Sedlacek, C. J., Kits, K. D., Mueller, A. J., Rhee, S. K., Hink, L., et al. (2022). Ammonia-oxidizing archaea possess a wide range of cellular ammonia affinities. *ISME J.* 16, 272–283. doi: 10.1038/s41396-021-01064-z

Li, G. C., Niu, W., Sun, J., Zhang, W., Zhang, E., and Wang, J. (2021). Soil moisture and nitrogen content influence wheat yield through their effects on the root system and soil bacterial diversity under drip irrigation. *Land Degrad. Dev.* 32, 3062–3076. doi: 10.1002/ldr.3967

Li, H., Wang, H., Jia, B., Li, D., Fang, Q., and Li, R. (2021). Irrigation has a higher impact on soil bacterial abundance, diversity and composition than nitrogen fertilization. *Sci. Rep.* 11:6. doi: 10.1038/s41598-021-96234-6

Li, H., Xu, Z. W., Yang, S., Li, X. B., Top, E. M., Wang, R. Z., et al. (2016). Responses of soil bacterial communities to nitrogen deposition and precipitation increment are closely linked with above ground community variation. *Microb. Ecol.* 71, 974–989. doi: 10.1007/s00248-016-0730-z

Liang, Q., Chen, H., Gong, Y., Fan, M., Yang, H., Lal, R., et al. (2012). Effects of 15 years of manure and inorganic fertilizers on soil organic carbon fractions in a wheat-maize system in the North China plain. *Nutr. Cycl. Agroecosyst.* 92, 21–33. doi: 10.1007/s10705-011-9469-6

Lin, Y. X., Ye, G., Ding, W., Hu, H. W., Zheng, Y., Fan, J., et al. (2020). Niche differentiation of comammox Nitrospira and canonical ammonia oxidizers in soil aggregate fractions following 27-year fertilizations. *Agric. Ecosyst. Environ.* 304:107147. doi: 10.1016/j.agee.2020.107147

Liu, Y., Liu, J., Yao, P., Ge, T., Qiao, Y., Zhao, M., et al. (2018). Distribution patterns of ammonia-oxidizing archaea and bacteria in sediments of the eastern China marginal seas. *Syst. Appl. Microbiol.* 41, 658–668. doi: 10.1016/j.syapm.2018.08.008

Liu, H., Zheng, X., Li, Y., Yu, J., Ding, H., Sveen, T. R., et al. (2022). Soil moisture determines nitrous oxide emission and uptake. *Sci. Total Environ.* 822:153566. doi: 10.1016/j.scitotenv.2022.153566

Long, X., Shen, J., Wang, J., Zhang, L., Di, H., and He, J. (2017). Contrasting response of two grassland soils to N addition and moisture levels: N_2O emission and functional gene abundance. *J. Soil. Sediment.* 17, 384–392. doi: 10.1007/s11368-016-1559-2

Pan, F. X., Li, Y. Y., Chapman, S. J., and Yao, H. (2016). Effect of rice straw application on microbial community and activity in paddy soil under different water status [J]. *Environ. Sci. Pollut. Res.* 23, 5941–5948. doi: 10.1007/s11356-015-5832-5

Qin, H., Wang, D., Xing, X., Tang, Y., Wei, X., Chen, X., et al. (2021). A few key nirK- and nosZ-denitrifier taxa play a dominant role in moisture-enhanced N_2O emissions in acidic paddy soil. *Geoderma* 385:114917. doi: 10.1016/j.geoderma.2020.114917

Qin, H., Xing, X., Tang, Y., Zhu, B., Wei, X., Chen, X., et al. (2020). Soil moisture and activity of nitrite- and nitrous oxide-reducing microbes enhanced nitrous oxide emissions in fallow paddy soils. *Biol. Fertil. Soils* 56, 53–67. doi: 10.1007/s00374-019-01403-5

Rotthauwe, J. H., Witzel, K. P., and Liesack, W. (1997). The ammonia monooxygenase structural gene amoA as a functional marker: molecular fine-scale analysis of natural ammonia-oxidizing populations. *Appl. Environ. Microbiol.* 63, 4704–4712. doi: 10.1128/aem.63.12.4704-4712.1997

Sahan, E., and Muyzer, G. (2008). Diversity and spatio-temporal distribution of ammonia-oxidizing archaea and bacteria in sediments of the Westerschelde estuary. *FEMS Microbiol. Ecol.* 64, 175–186. doi: 10.1111/j.1574-6941.2008.00462.x

Sheng, R., Xu, H., Xing, X., Zhang, W., Hou, H., Qin, H., et al. (2023). The role of inherited characteristics from parent materials in shaping bacterial communities in agricultural soils. *Geoderma* 433:116455. doi: 10.1016/j.geoderma.2023.116455

Shi, L., Zhang, H., Liu, T., Mao, P., Zhang, W., Shao, Y., et al. (2018). An increase in precipitation exacerbates negative effects of nitrogen deposition on soil cations and soil microbial communities in a temperate forest. *Environ. Pollut.* 235, 293–301. doi: 10.1016/j.envpol.2017.12.083

Soman, C., Li, D. F., Wander, M. M., and Kent, A. D. (2017). Long-term fertilizer and crop-rotation treatments differently affect soil bacterial community structure. *Plant and Soil* 413, 145–159. doi: 10.1007/s11104-016-3083-y

Supramaniam, Y., Chong, C. W., Silvaraj, S., and Tan, K. P. (2016). Effect of short term variation in temperature and water content on the bacterial community in a tropical soil. *Appl. Soil Ecol.* 107, 279–289. doi: 10.1016/j.apsoil.2016.07.003

Tang, H. M., Xiao, X. P., Li, C., Tang, W. G., Cheng, K. K., Wang, K., et al. (2019). Effects of rhizosphere and long-term fertilization practices on the activity and community structure of denitrifiers under double-cropping rice field. *Commun. Soil Sci. Plant Anal.* 50, 682–697. doi: 10.1080/00103624.2019.1589480

Tian, J. H., Wei, K., Condron, L. M., Chen, Z. H., Xu, Z. W., Feng, J., et al. (2017). Effects of elevated nitrogen and precipitation on soil organic nitrogen fractions and nitrogen-mineralizing enzymes in semi-arid steppe and abandoned cropland. *Plant and Soil* 417:6. doi: 10.1007/s11104-017-3253-6

Tourna, M., Freitag, T. E., Nicol, G. W., and Prosser, J. I. (2008). Growth, activity and temperature responses of ammonia-oxidizing archaea and bacteria in soil microcosms. *Environ. Microbiol.* 10, 1357–1364. doi: 10.1111/j.1462-2920.2007.01563.x

Tourna, M., Stieglmeier, M., Spang, A., Koenneke, M., Schintlmeister, A., Urich, T., et al. (2011). Nitrososphaera viennensis, an ammonia oxidizing archaeon from soil. *PNAS* 108, 8420–8425. doi: 10.1073/pnas.1013488108

Tyler, H. L. (2019). Bacteria community composition under long-term reduced tillage and no till management. *J. Appl. Microbiol.* 126, 1797–1807. doi: 10.1111/jam.14267

Urakawa, H., Garcia, J. C., Nielsen, J., Le, V. Q., Kozlowski, J. A., Stein, L. Y., et al. (2015). Nitrosospira lacus sp. nov., a psychrotolerant, ammonia-oxidizing bacterium from sandy lake sediment. *Int. J. Syst. Evol. Microbiol.* 65, 242–250. doi: 10.1099/ijs.0.070789-0

van der Heijden, M. G. A., Bardgett, R. D., and van Straalen, N. M. (2010). The unseen majority: soil microbes as drivers of plant diversity and productivity in terrestrial ecosystems. *Ecol. Lett.* 11, 296–310. doi: 10.1111/j.1461-0248.2007.01139.x

Vestergaard, G., Schulz, S., Schöler, A., and Schloter, M. (2017). Making big data smart—how to use metagenomics to understand soil quality. *Biol. Fertil. Soils* 53, 479–484. doi: 10.1007/s00374-017-1191-3

Wang, X., Feng, J., Ao, G., Qin, W., Han, M., Shen, Y., et al. (2023). Globally nitrogen addition alters soil microbial community structure, but has minor effects on soil microbial diversity and richness. *Soil Biol. Biochem.* 179:108982. doi: 10.1016/j.soilbio.2023.108982

Wang, X., Hefting, M. M., Schwark, L., and Zhu, G. (2019). Anammox and denitrification separately dominate microbial N-loss in water saturated and unsaturated soils horizons of riparian zones. *Water Res.* 162, 139–150. doi: 10.1016/j.watres.2019.06.052

Wang, S., Wang, X., Han, X., and Deng, Y. (2018). Higher precipitation strengthens the microbial interactions in semiarid grassland soils. *Glob. Ecol. Biogeogr.* 27, 570–580. doi: 10.1111/geb.12718

Wang, C., Xiao, H., Liu, J., Zhou, J., and Du, D. (2016). Insights into the effects of simulated nitrogen deposition on leaf functional traits of *Rhus Typhina*. *Pol. J. Environ. Stud.* 25, 1279–1284. doi: 10.15244/pjoes/61788

Wang, R., Xiao, Y., Lv, F., Hu, L., Wei, L., Yuan, Z., et al. (2018). Bacterial community structure and functional potential of rhizosphere soils as influenced by nitrogen addition and bacterial wilt disease under continuous sesame cropping. *Appl. Soil Ecol.* 125, 117–127. doi: 10.1016/j.apsoil.2017.12.014

Wu, Y., Liu, J., Shaaban, M., and Hu, R. (2021). Dynamics of soil n2o emissions and functional gene abundance in response to biochar application in the presence of earthworms. *Environ. Pollut.* 268:115670. doi: 10.1016/j.envpol.2020.115670

Yang, J., Chen, W., Hou, H. J., Chen, C. L., Qin, H. L., and Lv, D. Q. (2019). Difference in response of soil bacterial to soil moisture and temperature in the hilly red soil region of subtropics of southern China. *Chin J Trop Crops* 40, 609–615. doi: 10.3969/j.issn.1000-2561.2019.03.028

Yang, Y. D., Hu, Y. G., Wang, Z. M., and Zeng, Z. H. (2018). Variations of the nirS-, nirK-, and nosZ-denitrifying bacterial communities in a northern Chinese soil as

affected by different long-term irrigation regimes. *Environ. Sci. Pollut. R.* 25, 14057–14067. doi: 10.1007/s11356-018-1548-7

Yu, H. L., Ling, N., Wang, T. T., Zhu, C., Wang, Y., Wang, S. J., et al. (2019). Responses of soil biological traits and bacterial communities to nitrogen fertilization mediate maize yields across three soil types. *Soil Tillage Res.* 185, 61–69. doi: 10.1016/j.still.2018.08.017

Yuan, X., Knelman, J. E., Gasarch, E., Wang, D., Nemergut, D. R., and Seastedt, T. R. (2016). Plant community and soil chemistry responses to long-term nitrogen inputs drive changes in alpine bacterial communities. *Ecology* 97, 1543–1554. doi: 10.1890/15-1160.1

Yuan, H. C., Wu, H., Ge, T. D., Li, K. L., Wu, J. S., and Wang, J. R. (2015). Effects of long-term fertilization on bacterial and archaeal diversity and community structure within subtropical red paddy soils[J]. *Chin. J. Appl. Ecol.* 26, 1807–1813.

Zhalnina, K., Dias, R., de Quadros, P. D., Davis, R. A., Camargo, F. A., Clark, I. M., et al. (2015). Soil pH determines microbial diversity and composition in the park grass experiment. Microbiology. *Ecology* 69, 395–406. doi: 10.1007/s00248-014-0530-2

Zhang, R., Gu, J., and Wang, X. (2021). Responses of soil bacterial and fungi after 36 years fertilizer, straw cover, and irrigation management practices in Northwest China. *Soil Use Manage.* 37, 843–854. doi: 10.1111/sum.12671

Zhou, J., Guan, D., Zhou, B., Zhao, B., Ma, M., Qin, J., et al. (2015). Influence of 34-years of fertilization on bacterial communities in an intensively cultivated black soil in Northeast China. *Soil Biol. Biochem.* 90, 42–51. doi: 10.1016/j.soilbio.2015.07.005

Zhou, J., Xia, B., Treves, D. S., Wu, L. Y., Marsh, T. L., O'Neill, R. V., et al. (2002). Spatial and resource factors influencing high microbial diversity in soil. *Appl. Environ. Microbiol.* 68, 326–334. doi: 10.1128/AEM.68.1.326-334.2002

Zhu, B., Wang, Z., Kanaparthi, D., Kublik, S., Ge, T., Casper, P., et al. (2020). Long-read amplicon sequencing of nitric oxide dismutase (nod) genes reveal diverse oxygenic Denitrifiers in agricultural soils and Lake sediments. *Microb. Ecol.* 80, 243–247. doi: 10.1007/s00248-020-01482-0

Zhu, G., Wang, S., Wang, Y., Wang, C., Risgaard-Petersen, N., Jetten, M. S., et al. (2011). Anaerobic ammonia oxidation in a fertilized paddy soil. *ISME J.* 5, 1905–1912. doi: 10.1038/ismej.2011.63

Frontiers in Microbiology

Explores the habitable world and the potential of microbial life

The largest and most cited microbiology journal which advances our understanding of the role microbes play in addressing global challenges such as healthcare, food security, and climate change.

Discover the latest Research Topics

See more →

Frontiers

Avenue du Tribunal-Fédéral 34
1005 Lausanne, Switzerland
frontiersin.org

Contact us

+41 (0)21 510 17 00
frontiersin.org/about/contact